

---

Origins of salinity and salinisation processes  
in the Wybong Creek Catchment,  
New South Wales,  
Australia

A thesis by Julia Jasonsmith, submitted for the degree of  
**Doctor of Philosophy of The Australian National University**  
Research School of Earth Sciences &  
Fenner School of Environment and Society

---



**Statement**

I declare that this thesis has not been used toward the award of any other degree of any institution and to the best of my knowledge, this thesis is my own original work except where due reference is made in the text.

Julia Jasonsmith

March 12<sup>th</sup> 2010

---



## Acknowledgments

I had three main supervisors throughout this project, these being Ben Macdonald, Bear McPhail, and Sara Beavis. Ben supervised the larger project of which this thesis was part, and introduced the concept of it to me in late 2006. At this time and ever since I have continually been so inspired by Ben, and am continually reminded by his professionalism, intellect and easy going nature, as to why I chose to do this project in particular. Ben has been gracious, compassionate and easy going in difficult moments, and has provided the momentum which has enabled the work presented within this PhD to be completed in timely fashion.

Sara Beavis must set the bar for what an academic should strive to be. I wish I could find the words to express how impressed I am by Sara, by her compassion, intellect and integrity, again, in the most trying of circumstances. As a supervisor she has been beyond compare and I feel so very blessed to have known her as a friend and as a supervisor.

Bear McPhail has been my primary supervisor throughout this project and – though almost unheard of in the busy (selfish?) world of academia – has always been there to talk about *whatever* I needed to talk about, *whenever* I needed to talk about it, in the most caring and often courageous of ways. Bear has been endlessly patient throughout the writing of this thesis, despite my thought processes and my limitations diverging sometimes significantly from his own. In very trying circumstances, Bear has continually been a rock to rely on, and I hope that the thorough scrutiny he has given me and my work will be reflected in the following pages.

Ian Roach deserves special acknowledgment for all the time he has donated towards increasing my skills and knowledge on regolith and GIS. A gifted educator, I would have been very much worse off if I had not met Ian, and would not have been able to research, write and depict things the way I wanted without his very gracious efforts in educating me, for no benefit of his own.

Ben Harris, at the Hunter Central Rivers Catchment Management Authority has provided field assistance at short notice for field excursions, but more so has braved foul weather and frustrating conditions to get data downloaded and sent to me. Again I am hugely in his debt!

Others have also provided the aid which has enabled the smooth running completion of this thesis. This includes Richard Green, who has discussed certain aspects of soil chemistry with me; the Ulli Troitzch who provided the nicest of

---

environments to conduct soils and mineral research in; Mauro Davanzo and Piers Bairstow who have enabled the timely booking of vehicles; Lorna Fitsimmons who has provided very well cared for and very important field equipment – I am so grateful for your aid Lorna! Richard Reilly who provided patient tutoring in various aspects of surveying and the use of DGPS systems; Brian Harrold provided timely and thorough IT support, without which this thesis would have been handed in many months later; Ken Johnson, a real statistician in a world with few; my advisor Ian White, who sings, dances and happens to be one of the most impressive, and mind-bogglingly inspirational human beings I have ever met; Richard Cresswell who gave his objective and absolutely necessary opinions on many aspects of this study; the indispensable, ever helpful, and always lovely Maree Coldrick; and in particular, Nigel Craddy, Richard Arculus, Dick Barwick, Ken Campbell, Ross Taylor, Ann Felton, and Keith Crooke have been important people whom I have talked to in times of strife and caffeine deprivation, and I am eternally grateful for their easy going company. I don't think there are words to describe how fortunate I am to all these people who, while not central to my needs in writing and researching this thesis, have been so very important to its completion.

Matt Lenahan, Luke Wallace, Sarah Tynan, Sophie Lewis, Andy Myers, Fern Beavis, Merinda Nash, Jenna Wallace, Nicolá Darinogogue, and of course the wonderful Kyle Horner have provided the fun, inspiration, advice and sounding boards without which I would have been absolutely miserable for the last three years.

My Twin sister Adelaide has always provided the self-esteem for me when the times have been really tough, and I am so grateful for her unending and unconditional love. Words cannot really describe how and why Margus has helped me throughout the writing of this thesis, except that by simply being there, Margus has made me, my life and my thesis better. My dear Aunty Rhona has been supportive in all aspects of my life, as have Aunts Sharon and Kate, and my “other” parents Reg and Shirls. My dear old Mum and Dad have always been excited about my research, and have provided interest, enthusiasm, love, support and encouragement – quite simply I would not have been a scientist without them.

Finally, the wonderful, interesting and observant farmers of the Wybong valley have bought back poignant, happy memories of country hospitality. Many of farmers I met and talked to, had an extraordinary, intimate, decades long knowledge of the land which has been critically important for me weigh my short term study against. In particular Dudley Googe has been so interested and open and allowed me to put in piezometers all over the show, with never any hesitation if it would help me in the

---

pursuit of answers. Few people would say yes to great big trucks rolling onto their property's and digging big holes at a moments notice, yet alone drop everything to take the hole-diggers on a tour of their property, but Dudley did and I am so impressed and grateful. Similarly in the final stages of this thesis, Percy and Robin Rayne, and Tracey and Scott Anshaw, allowed me to place piezometers in their property's and like other farmers of Wybong Valley, were always kind and interested and helpful.

My sincere thanks go to Ian Cartwright and Michael Rosen, who provided detailed and and very constructive feedback on an early manuscript drawn from work presented in Chapter Two. I thank the two anonymous reviewers of a paper drawn from work presented in Chapter Five, accepted in the Australian Journal of Earth Sciences (Salinisation processes in a sub-catchment of Wybong Creek, New South Wales, Australia). A paper from this chapter also was also presented at the Groundwater in the Sydney Basin symposium, with helpful discussion provided by Jerzy Jankowski. This work was supported by ARC Linkage grant number LP05060743. Scholarship funding was provided by The Australian National University Faculty of Science and Research School of Earth Sciences, with project funding and support also provided by Hunter Central Rivers Catchment Management Authority and the New South Wales Office of Water.

Thankyou all so much!!

Jubes ☺



**Abstract**

The Wybong Creek catchment is located in the upper Hunter Valley of New South Wales, Australia, and contains award winning beef and wine producing operations. Solute concentrations in Wybong Creek are often too high for irrigation use, however, with previous research showing that the saline and Na-Cl dominated water discharged from Wybong Creek decreases water quality in both the Goulburn and Hunter Rivers into which it flows. This study therefore aimed at identifying the source of solutes to the Wybong Creek catchment and the processes which cause salinisation of surface water, soil (regolith) and groundwater.

Surface water was sampled at ten sites along Wybong Creek over three years, while groundwater was sampled from most of the bores and piezometers occurring in the Wybong Creek valley. Surface and groundwater in the upper catchment were dominated by Na-Mg-HCO<sub>3</sub>. Ratios of <sup>87</sup>Sr/<sup>86</sup>Sr and cation/HCO<sub>3</sub> indicated these facies were due to silicate weathering of the Liverpool Ranges, with localised groundwater bodies recharging in the Liverpool Ranges and discharging in the upper Wybong Creek valley. Wybong Creek became saline, and Na-Mg-Cl dominated in the mid-catchment area, with salinity doubling between the 55 and 60 km sample sites on some dates. Changes in surface water chemistry occurred independently of surface water input from tributaries, with abrupt salinity increases within a pool between these sites attributed to groundwater input via fractures beneath the Creek. One of two salt scalds in the Wybong Creek catchment also occurs adjacent to this stretch of river. A field site was established at the mid-catchment locality of Manobalai, therefore, in order to constrain the relationship between surface water, regolith and groundwater salinity.

Ten piezometers were established at Manobalai, including three piezometer nests. Most regolith at Manobalai was found to be non-saline, including that within the salt scald, with the most saline and Na-Cl dominated regolith samples occurring in some of the most moist and coarse sandy/gravel layers. Groundwater sampled from piezometers installed in the holes drilled for regolith samples had salinities up to 20 times higher than the regolith on a per weight basis, and were similarly dominated by Na-Cl. A lack of carbonate and sulfate minerals within the soils and no indication of Ca-Mg/HCO<sub>3</sub>-SO<sub>4</sub> dominated facies within alluvial soil solutions indicated groundwater did not evolve from rainwater to Na-Cl dominated facies while infiltrating the regolith.

Groundwater samples from Manobalai were instead found to be amongst the most fresh and the most saline within the Wybong Creek catchment, and changed salinity

---

---

abruptly down-gradient along a transect. Groundwater flow occurred through fractures in the Narrabeen Group sandstones and conglomerates, with vertical groundwater flow via fractures causing abrupt changes in salinity. Ratios of Na/Cl, Cl/Br and  $^{87}\text{Sr}/^{86}\text{Sr}$  indicated saline groundwater at Manobalai and in the lower catchment was influenced by a marine endmember and halite dissolution. A poor relationship between salinity and  $\delta^{18}\text{O}$  indicated this marine endmember was not evapoconcentrated rainwater. The occurrence of saline surface and groundwater in the Wybong Creek catchment was instead attributed to discharge from the regional groundwater system occurring in the Wittingham Coal Measures, with the abrupt increases in salinity at Manobalai indicating mixing between local, intermediate and/or regional groundwater systems. Salinity is likely to function similarly to this in the rest of the Hunter Valley also. The occurrence of salinity in both the Hunter River and Wybong Creek catchments is a naturally occurring phenomenon with salinity mitigation difficult due to the regional extent of the saline groundwater systems. Living with salt strategies are therefore recommended, such as limiting irrigation using both saline and fresh water and continuing with restrictions on saline discharge from coal mines.

**Table of contents**

	<i>Page</i>
Title page	i
Statement of authorship	iii
Acknowledgements	v
Abstract	ix
Table of Contents	xi
List of figures	xii
List of tables	xv
List of equations	xvii
Chapter One – Introduction	1
Chapter Two – Identification of solute sources to Wybung Creek	13
Introduction	15
Methods	17
Results and discussion	23
Conclusions	46
Chapter Three – Aquifers and groundwater bodies	49
Introduction	51
Methods	57
Results and discussion	62
Conclusions	82
Chapter Four – Surface and groundwater geochemistry	85
Introduction	87
Methods	89
Results and discussion	91
Conclusions	107
Chapter Five – Causes of salinity at Manobalai	111
Introduction	113
Methods	116
Results and discussion	125
Conclusions	148
Chapter Six – Hydrology and hydrogeology of Manobalai	151
Introduction	153
Materials and methods	155
Results and discussion	162
Conclusions	184
Chapter Seven – Conclusions	187
References	197
Appendix for Chapter Two	213
Appendix for Chapter Three	229
Appendix for Chapter Five	249
Appendix for Chapter Six	263

**List of figures**

	<i>Page</i>
Chapter One – Introduction	1
Figure 1.1. Location of the Hunter and Wyong catchments	6
Chapter Two – Identification of solute sources to Wybong Creek	13
Figure 2.1. Surface water sampling sites in Wybong Creek	18
Figure 2.2. Salinity increase down Wybong Creek	24
Figure 2.3. Major cations and anions in Wybong Creek	25
Figure 2.4. Hourly EC in Wybong Creek during Aug., Sept., and Nov. 07 at the 60 km sample site	30
Figure 2.5. EC, gravity and temperature relationships at the 60 and 72 km sample sites during Sept. 07	32
Figure 2.6. FFT of EC, temperature, and gravity in Sept. 07	33
Figure 2.7. FFT of EC, temperature, and gravity in Nov. 09	34
Figure 2.8. EC and water height at the 60 and 72 km sample sites	36
Figure 2.9. EC increases between the 55 and 60 km sample points	37
Figure 2.10. $\delta^{18}\text{O}$ and $\delta^2\text{H}$ of Wybong Creek surface water samples	42
Figure 2.11. Saturation indices for major soluble minerals	44
Figure 2.12. EC as a function of discharge in Wybong Creek	46
Chapter Three – Aquifers and groundwater bodies	49
Figure 3.1. Groundwater sampling locations	59
Figure 3.2. Cross-sections of the Wybong Creek catchment	63
Figure 3.3. Data collection points for the geological transect	64
Figure 3.4. Geology of the Wybong Creek catchment	67
Figure 3.5. Stiff diagrams of water sampled in 2006 and 2007	69
Figure 3.6. Stiff diagrams of water sampled in 2008 and 2009	70
Figure 3.7. Dendrogram of groundwater groups	71
Figure 3.8. Canonical and PCA plots of groundwater samples	73
Figure 3.9. Uncorrected $^{14}\text{C}$ dates of select groundwater samples	78
Chapter Four – Surface and groundwater chemistry	85
Figure 4.1. Groundwater sampling locations	90
Figure 4.2. $^{87}\text{Sr}/^{86}\text{Sr}$ in Wybong Creek surface and groundwater	92
Figure 4.3. Ca+Mg+Na+K/HCO <sub>3</sub> in water samples	94
Figure 4.4. Saturation indices for calcite and dolomite	94
Figure 4.5. $\delta^{35}\text{S}$ , Br/Cl and Na/Cl in water samples	96
Figure 4.6. $\delta^{18}\text{O}$ and $\delta^2\text{H}$ of Wybong catchment water samples	98
Figure 4.7. Mg/Na and Ca/Na in water samples	100
Figure 4.8. Piper diagram of groundwater samples from piezometers	101
Figure 4.9. Two component mixing curves of Sr vs $^{87}\text{Sr}/^{86}\text{Sr}$	103
Figure 4.10. Two component mixing curves of $^{87}\text{Sr}/^{86}\text{Sr}$ vs Na/Cl, Sr/Na and Sr/Cl	104
Figure 4.11. Conceptual model of groundwater systems in the Wybong Creek catchment	107

	<i>Page</i>
Chapter Five – Causes of salinity at Manobalai	111
Figure 5.1. Location of Manobalai within Wybong and the Hunter Valley	114
Figure 5.2. Geology of the Manobalai field site	117
Figure 5.3. Soil landscape series of the Wybong Creek catchment	118
Figure 5.4. The erosion gully sampled for pedogenic carbonate	119
Figure 5.5. Regolith landform map of Manobalai	126
Figure 5.6. Cross-sections of select cores sampled from Manobalai	129
Figure 5.7. EC <sub>1:5</sub> and total moisture at Sites One to Three	131
Figure 5.8. EC <sub>1:5</sub> and total moisture at Sites Four to Seven	132
Figure 5.9. EC <sub>1:5</sub> and total moisture at Site Seven	133
Figure 5.10. Soil salinity as a function of pH	135
Figure 5.11. Major cation and anion concentrations in Manobalai soil cores from Sites Two – Four	137
Figure 5.12. Major cation and anion concentrations in Manobalai soil cores from Site Six	138
Figure 5.13. Stiff diagrams of groundwater chemistry at Manobalai	141
Figure 5.14. Molar Na/Cl in Manobalai groundwater samples	142
Figure 5.15. $\delta^2\text{H}$ as a function of $\delta^{18}\text{O}$ for Manobalai groundwater	143
Figure 5.16. Conceptual model of salinisation at Manobalai	147
Chapter Six – Hydrology and hydrogeology of Manobalai	151
Figure 6.1. Geology of the Manobalai field site	156
Figure 6.2. Differenced groundwater height at Manobalai	162
Figure 6.3. Differenced groundwater height at Sites One – Five	165
Figure 6.4. Relationships between EC at the 60 km sample site, gravity, and groundwater height at Site Eight	167
Figure 6.5. Relationships between EC at the 60 km sample site, temperature, and groundwater height at Site Eight	168
Figure 6.6. Groundwater height in response to precipitation at Hannah's and Sites One – Two	169
Figure 6.7. Groundwater height in response to precipitation at Sites Three, Four, Six and Eight	170
Figure 6.8. Hydraulic head at Manobalai sample sites on different dates	173
Figure 6.9. $^{87}\text{Sr}/^{86}\text{Sr}$ vs Cl (mmol L <sup>-1</sup> ); and (b) $^{87}\text{Sr}/^{86}\text{Sr}$ versus $\delta^{18}\text{O}$ for groundwater sampled from Manobalai	176
Figure 6.10. Temporal variation in EC at Sites Six and Eight	178
Figure 6.11. Relationship between gravity, Wybong Creek salinity and groundwater height at Sites Six and Eight	182
Figure 6.12. Relationship between gravity, Wybong Creek salinity, Wybong Creek depth, Wybong Creek temperature and air pressure	183
Appendix for Chapter Five	249
Figure A5.1. Aeromagnetic survey of the Manobalai field site	251

	<i>Page</i>
Figure A5.2. Spectra from XRD analysis of 0.0 – 0.5 m at Site Two	260
Figure A5.3. Spectra from XRD analysis of 0.5 – 1.0 m at Site Two	260
Figure A5.4. Spectra from XRD analysis of 4.0 – 4.5 m at Site Two	261
Figure A5.5. Spectra from XRD analysis of 15.0 – 16.0 m at Site Two	261
Figure A5.6 SEM of the Site Two Deep subsample representing a depth of 0.0 – 0.5 m	262
Appendix for Chapter Six	263
Figure A6.1. Slug test analyses for Manobalai sites on 14/07/2008	265
Figure A6.2. Slug test analyses Manobalai sites on 18/01/2009	266
Figure A6.3. Slug test analyses for Manobalai sites on 18/01/2009	267
Figure A6.4. Spectral analyses of relationships between hydraulic head, gravity and air pressure at Site Eight	273

## List of tables

	<i>Page</i>
Chapter Two – Identification of solute sources to Wybong Creek	13
Table 2.1. Monthly precipitation, evaporation at Scone	27
Table 2.2. Discharge and salt flux from Wybong Creek	28
Table 2.3. Aeolian salt accession to Wybong Creek catchment	29
Table 2.4. Major cations and anions in the salt pool	38
Table 2.5. Evapotranspiration changes in the Wybong Creek catchment	39
Table 2.6. Percent increase in salinity due to evaporation	41
Table 2.7. Molal ion ratios in Wybong Creek	43
Chapter Three – Aquifers and groundwater bodies	49
Table 3.1. Borehole data for sampled bores	65
Table 3.2. Loading results for PCA and canonical analyses	72
Table 3.3. Groundwater bodies in the Wybong Creek catchment	75
Chapter Four – Surface and groundwater geochemistry	87
Table 4.1. $^{87}\text{Sr}/^{86}\text{Sr}$ of possible Sr sources to the Wybong Creek catchment	93
Table 4.2. $\delta^{34}\text{S}$ of possible S sources	97
Table 4.3. Ca and Mg concentrations resulting from cation exchange	102
Table 4.4. Parameters for an optimised saline endmember	105
Chapter Five – Causes of salinity at Manobalai	111
Table 5.1. Parameters describing bored and piezometers installed at Manobalai	121
Table 5.2. Regolith landforms at Manobalai	127
Table 5.3. Chemistry of select Manobalai soil samples	134
Table 5.4. Minerals occurring in select samples from Site Two	136
Table 5.5. Rain and groundwater chemistry of the Manobalai site	140
Table 5.6. $\delta^{13}\text{C}$ and $^{14}\text{C}$ dates for erosion gully soil samples	144
Chapter Six – Hydrology and hydrogeology of Manobalai	151
Table 6.1. Parameters for bores and piezometers at the Manobalai field site	157
Table 6.2. Flow at surface water sample sites	160
Table 6.3. Parameters for modelling groundwater flux from Manobalai	160
Table 6.4. Parameters for modelling groundwater flux changes in response to fluctuating hydraulic head	162
Table 6.5. Hydraulic conductivity for piezometers at Manobalai	172
Table 6.6. Groundwater chemistry at Manobalai	175
Table 6.7. Measured and modelled increases in solute concentration in Wybong Creek due to groundwater flux from Manobalai	181

	<i>Page</i>
<b>Appendix for Chapter Two</b>	213
Table A2.1. Cation detection limit and concentrations in surface water blanks	215
Table A2.2. Anion detection limit and concentrations in surface water blanks	216
Table A2.3. Water quality in Wybong Creek surface water sample sites, tributaries and rainwater	217
Table A2.4. Cation concentrations in Wybong Creek surface water sample sites, tributaries and rainwater	220
Table A2.5. Anion concentrations in Wybong Creek surface water sample sites, tributaries and rainwater	224
Table A2.6. Parameters used to calculate evapoconcentration	227
Table A2.7. Isotope data for Wybong Creek surface water samples and isotopes	228
<b>Appendix for Chapter Three</b>	229
Table A3.1. Cation detection limit and concentrations in groundwater blanks	231
Table A3.2. Anion detection limit and concentrations in groundwater water blanks	232
Table A3.3. Water quality data for Wybong Creek groundwater samples	233
Table A3.4. Anion concentrations for Wybong Creek groundwater samples	237
Table A3.5. Cation concentrations for Wybong Creek groundwater samples	241
Table A3.6. Isotope concentrations for Wybong Creek groundwater samples	245
<b>Appendix for Chapter Five</b>	249
Table A5.1. Soil quality parameters for Manobalai regolith cores	252
Table A5.2. Cation and anion concentrations in 1:5 soil-water extracts	256
Table A5.3. Percent weight cation and anion concentration in 1:5 soil-water extracts	258
<b>Appendix for Chapter Six</b>	263
Table A6.1. Hydraulic conductivity measured on the 14 <sup>th</sup> – 17 <sup>th</sup> July 2008	270
Table A6.2. Hydraulic conductivity measured on the 17 <sup>th</sup> – 21 <sup>st</sup> January 2008	271
Table A6.3. Hydraulic conductivity measured on the 14 <sup>th</sup> May 2009	272
Table A6.4. Correlation coefficients for the relationship between rainfall and groundwater height at Site Two Shallow	274
Table A6.5. Correlation coefficients for the relationship between rainfall and groundwater height at Site Two Deep	275

## List of equations

	<i>Page</i>
Chapter Two – Identification of solute sources to Wybong Creek	13
Eq. 2.1. Charge balances	21
Eq. 2.2. Effects of evaporation on volume	23
Eq. 2.3. Effects of evaporation on solute concentration	23
Chapter Four – Surface and groundwater geochemistry	87
Eq. 4.1. Sources of Mg and Ca to groundwater	89
Eq. 4.2. Quantification of the effects of cation exchange	91
Eq. 4.3. Model for two-component mixing of ions	91
Eq. 4.4. Model for two-component mixing of $^{87}\text{Sr}/^{86}\text{Sr}$	91
Eq. 4.5. Cation exchange reactions	99
Chapter Five – Causes of salinity at Manobalai	111
Eq. 5.1. Total soil moisture	122
Eq. 5.2. Exchangeable sodium percentage	124
Chapter Six – Hydrology and hydrogeology of Manobalai	151
Eq. 6.1. Hydraulic conductivity using the Bouwer and Rice method	158
Eq. 6.2. $\ln Re/Rw$ for fully penetrating piezometers	158
Eq. 6.3. $\ln Re/Rw$ for partially penetrating piezometers	159
Eq. 6.4. Increase in solute concentration as a result of groundwater flux to Wybong Creek	159
Eq. 6.5. Groundwater discharge to Wybong Creek	151
Eq. 6.6. Increase in solute concentration as a result of groundwater flux to Wybong Creek	162
Appendix for Chapter Five	249
Eq. A5.1. Soil solute concentrations as a function of soil weight	251
Appendix for Chapter Six	263
Eq. A6.1. Cl load delivered from eastern and western aquifers	268
Eq. A6.2. Solute flux from eastern and western aquifers	268
Eq. A6.3. Increase in salt load to Wybong Creek as a result of groundwater flux	268
Eq. A6.4. Specific discharge ( $V_D$ ) to Wybong Creek	268
Eq. A6.5. Groundwater discharge ( $Q$ ) to Wybong Creek	269
Eq. A6.6. Specific discharge ( $V_D$ ) Discharge to Wybong Creek	269
Eq. A6.7. Hydraulic conductivity necessary for delivered flux	269

---

Origins of salinity and salinisation processes  
in the Wybong Creek Catchment,  
New South Wales,  
Australia

A thesis by Julia Jasonsmith, submitted for the degree of  
**Doctor of Philosophy of The Australian National University**  
Research School of Earth Sciences &  
Fenner School of Environment and Society

---



**Statement**

I declare that this thesis has not been used toward the award of any other degree of any institution and to the best of my knowledge, this thesis is my own original work except where due reference is made in the text.

Julia Jasonsmith

March 12<sup>th</sup> 2010

---



## Acknowledgments

I had three main supervisors throughout this project, these being Ben Macdonald, Bear McPhail, and Sara Beavis. Ben supervised the larger project of which this thesis was part, and introduced the concept of it to me in late 2006. At this time and ever since I have continually been so inspired by Ben, and am continually reminded by his professionalism, intellect and easy going nature, as to why I chose to do this project in particular. Ben has been gracious, compassionate and easy going in difficult moments, and has provided the momentum which has enabled the work presented within this PhD to be completed in timely fashion.

Sara Beavis must set the bar for what an academic should strive to be. I wish I could find the words to express how impressed I am by Sara, by her compassion, intellect and integrity, again, in the most trying of circumstances. As a supervisor she has been beyond compare and I feel so very blessed to have known her as a friend and as a supervisor.

Bear McPhail has been my primary supervisor throughout this project and – though almost unheard of in the busy (selfish?) world of academia – has always been there to talk about *whatever* I needed to talk about, *whenever* I needed to talk about it, in the most caring and often courageous of ways. Bear has been endlessly patient throughout the writing of this thesis, despite my thought processes and my limitations diverging sometimes significantly from his own. In very trying circumstances, Bear has continually been a rock to rely on, and I hope that the thorough scrutiny he has given me and my work will be reflected in the following pages.

Ian Roach deserves special acknowledgment for all the time he has donated towards increasing my skills and knowledge on regolith and GIS. A gifted educator, I would have been very much worse off if I had not met Ian, and would not have been able to research, write and depict things the way I wanted without his very gracious efforts in educating me, for no benefit of his own.

Ben Harris, at the Hunter Central Rivers Catchment Management Authority has provided field assistance at short notice for field excursions, but more so has braved foul weather and frustrating conditions to get data downloaded and sent to me. Again I am hugely in his debt!

Others have also provided the aid which has enabled the smooth running completion of this thesis. This includes Richard Green, who has discussed certain aspects of soil chemistry with me; the Ulli Troitzch who provided the nicest of

---

environments to conduct soils and mineral research in; Mauro Davanzo and Piers Bairstow who have enabled the timely booking of vehicles; Lorna Fitsimmons who has provided very well cared for and very important field equipment – I am so grateful for your aid Lorna! Richard Reilly who provided patient tutoring in various aspects of surveying and the use of DGPS systems; Brian Harrold provided timely and thorough IT support, without which this thesis would have been handed in many months later; Ken Johnson, a real statistician in a world with few; my advisor Ian White, who sings, dances and happens to be one of the most impressive, and mind-bogglingly inspirational human beings I have ever met; Richard Cresswell who gave his objective and absolutely necessary opinions on many aspects of this study; the indispensable, ever helpful, and always lovely Maree Coldrick; and in particular, Nigel Craddy, Richard Arculus, Dick Barwick, Ken Campbell, Ross Taylor, Ann Felton, and Keith Crooke have been important people whom I have talked to in times of strife and caffeine deprivation, and I am eternally grateful for their easy going company. I don't think there are words to describe how fortunate I am to all these people who, while not central to my needs in writing and researching this thesis, have been so very important to its completion.

Matt Lenahan, Luke Wallace, Sarah Tynan, Sophie Lewis, Andy Myers, Fern Beavis, Merinda Nash, Jenna Wallace, Nicolá Darinogogue, and of course the wonderful Kyle Horner have provided the fun, inspiration, advice and sounding boards without which I would have been absolutely miserable for the last three years.

My Twin sister Adelaide has always provided the self-esteem for me when the times have been really tough, and I am so grateful for her unending and unconditional love. Words cannot really describe how and why Margus has helped me throughout the writing of this thesis, except that by simply being there, Margus has made me, my life and my thesis better. My dear Aunty Rhona has been supportive in all aspects of my life, as have Aunts Sharon and Kate, and my “other” parents Reg and Shirls. My dear old Mum and Dad have always been excited about my research, and have provided interest, enthusiasm, love, support and encouragement – quite simply I would not have been a scientist without them.

Finally, the wonderful, interesting and observant farmers of the Wybong valley have bought back poignant, happy memories of country hospitality. Many of farmers I met and talked to, had an extraordinary, intimate, decades long knowledge of the land which has been critically important for me weigh my short term study against. In particular Dudley Googe has been so interested and open and allowed me to put in piezometers all over the show, with never any hesitation if it would help me in the

---

pursuit of answers. Few people would say yes to great big trucks rolling onto their property's and digging big holes at a moments notice, yet alone drop everything to take the hole-diggers on a tour of their property, but Dudley did and I am so impressed and grateful. Similarly in the final stages of this thesis, Percy and Robin Rayne, and Tracey and Scott Anshaw, allowed me to place piezometers in their property's and like other farmers of Wybong Valley, were always kind and interested and helpful.

My sincere thanks go to Ian Cartwright and Michael Rosen, who provided detailed and and very constructive feedback on an early manuscript drawn from work presented in Chapter Two. I thank the two anonymous reviewers of a paper drawn from work presented in Chapter Five, accepted in the Australian Journal of Earth Sciences (Salinisation processes in a sub-catchment of Wybong Creek, New South Wales, Australia). A paper from this chapter also was also presented at the Groundwater in the Sydney Basin symposium, with helpful discussion provided by Jerzy Jankowski. This work was supported by ARC Linkage grant number LP05060743. Scholarship funding was provided by The Australian National University Faculty of Science and Research School of Earth Sciences, with project funding and support also provided by Hunter Central Rivers Catchment Management Authority and the New South Wales Office of Water.

Thankyou all so much!!

Jubes ☺



**Abstract**

The Wybong Creek catchment is located in the upper Hunter Valley of New South Wales, Australia, and contains award winning beef and wine producing operations. Solute concentrations in Wybong Creek are often too high for irrigation use, however, with previous research showing that the saline and Na-Cl dominated water discharged from Wybong Creek decreases water quality in both the Goulburn and Hunter Rivers into which it flows. This study therefore aimed at identifying the source of solutes to the Wybong Creek catchment and the processes which cause salinisation of surface water, soil (regolith) and groundwater.

Surface water was sampled at ten sites along Wybong Creek over three years, while groundwater was sampled from most of the bores and piezometers occurring in the Wybong Creek valley. Surface and groundwater in the upper catchment were dominated by Na-Mg-HCO<sub>3</sub>. Ratios of <sup>87</sup>Sr/<sup>86</sup>Sr and cation/HCO<sub>3</sub> indicated these facies were due to silicate weathering of the Liverpool Ranges, with localised groundwater bodies recharging in the Liverpool Ranges and discharging in the upper Wybong Creek valley. Wybong Creek became saline, and Na-Mg-Cl dominated in the mid-catchment area, with salinity doubling between the 55 and 60 km sample sites on some dates. Changes in surface water chemistry occurred independently of surface water input from tributaries, with abrupt salinity increases within a pool between these sites attributed to groundwater input via fractures beneath the Creek. One of two salt scalds in the Wybong Creek catchment also occurs adjacent to this stretch of river. A field site was established at the mid-catchment locality of Manobalai, therefore, in order to constrain the relationship between surface water, regolith and groundwater salinity.

Ten piezometers were established at Manobalai, including three piezometer nests. Most regolith at Manobalai was found to be non-saline, including that within the salt scald, with the most saline and Na-Cl dominated regolith samples occurring in some of the most moist and coarse sandy/gravel layers. Groundwater sampled from piezometers installed in the holes drilled for regolith samples had salinities up to 20 times higher than the regolith on a per weight basis, and were similarly dominated by Na-Cl. A lack of carbonate and sulfate minerals within the soils and no indication of Ca-Mg/HCO<sub>3</sub>-SO<sub>4</sub> dominated facies within alluvial soil solutions indicated groundwater did not evolve from rainwater to Na-Cl dominated facies while infiltrating the regolith.

Groundwater samples from Manobalai were instead found to be amongst the most fresh and the most saline within the Wybong Creek catchment, and changed salinity

---

---

abruptly down-gradient along a transect. Groundwater flow occurred through fractures in the Narrabeen Group sandstones and conglomerates, with vertical groundwater flow via fractures causing abrupt changes in salinity. Ratios of Na/Cl, Cl/Br and  $^{87}\text{Sr}/^{86}\text{Sr}$  indicated saline groundwater at Manobalai and in the lower catchment was influenced by a marine endmember and halite dissolution. A poor relationship between salinity and  $\delta^{18}\text{O}$  indicated this marine endmember was not evapoconcentrated rainwater. The occurrence of saline surface and groundwater in the Wybong Creek catchment was instead attributed to discharge from the regional groundwater system occurring in the Wittingham Coal Measures, with the abrupt increases in salinity at Manobalai indicating mixing between local, intermediate and/or regional groundwater systems. Salinity is likely to function similarly to this in the rest of the Hunter Valley also. The occurrence of salinity in both the Hunter River and Wybong Creek catchments is a naturally occurring phenomenon with salinity mitigation difficult due to the regional extent of the saline groundwater systems. Living with salt strategies are therefore recommended, such as limiting irrigation using both saline and fresh water and continuing with restrictions on saline discharge from coal mines.

**Table of contents**

	<i>Page</i>
Title page	i
Statement of authorship	iii
Acknowledgements	v
Abstract	ix
Table of Contents	xi
List of figures	xii
List of tables	xv
List of equations	xvii
Chapter One – Introduction	1
Chapter Two – Identification of solute sources to Wybung Creek	13
Introduction	15
Methods	17
Results and discussion	23
Conclusions	46
Chapter Three – Aquifers and groundwater bodies	49
Introduction	51
Methods	57
Results and discussion	62
Conclusions	82
Chapter Four – Surface and groundwater geochemistry	85
Introduction	87
Methods	89
Results and discussion	91
Conclusions	107
Chapter Five – Causes of salinity at Manobalai	111
Introduction	113
Methods	116
Results and discussion	125
Conclusions	148
Chapter Six – Hydrology and hydrogeology of Manobalai	151
Introduction	153
Materials and methods	155
Results and discussion	162
Conclusions	184
Chapter Seven – Conclusions	187
References	197
Appendix for Chapter Two	213
Appendix for Chapter Three	229
Appendix for Chapter Five	249
Appendix for Chapter Six	263

**List of figures**

	<i>Page</i>
Chapter One – Introduction	1
Figure 1.1. Location of the Hunter and Wyong catchments	6
Chapter Two – Identification of solute sources to Wybong Creek	13
Figure 2.1. Surface water sampling sites in Wybong Creek	18
Figure 2.2. Salinity increase down Wybong Creek	24
Figure 2.3. Major cations and anions in Wybong Creek	25
Figure 2.4. Hourly EC in Wybong Creek during Aug., Sept., and Nov. 07 at the 60 km sample site	30
Figure 2.5. EC, gravity and temperature relationships at the 60 and 72 km sample sites during Sept. 07	32
Figure 2.6. FFT of EC, temperature, and gravity in Sept. 07	33
Figure 2.7. FFT of EC, temperature, and gravity in Nov. 09	34
Figure 2.8. EC and water height at the 60 and 72 km sample sites	36
Figure 2.9. EC increases between the 55 and 60 km sample points	37
Figure 2.10. $\delta^{18}\text{O}$ and $\delta^2\text{H}$ of Wybong Creek surface water samples	42
Figure 2.11. Saturation indices for major soluble minerals	44
Figure 2.12. EC as a function of discharge in Wybong Creek	46
Chapter Three – Aquifers and groundwater bodies	49
Figure 3.1. Groundwater sampling locations	59
Figure 3.2. Cross-sections of the Wybong Creek catchment	63
Figure 3.3. Data collection points for the geological transect	64
Figure 3.4. Geology of the Wybong Creek catchment	67
Figure 3.5. Stiff diagrams of water sampled in 2006 and 2007	69
Figure 3.6. Stiff diagrams of water sampled in 2008 and 2009	70
Figure 3.7. Dendrogram of groundwater groups	71
Figure 3.8. Canonical and PCA plots of groundwater samples	73
Figure 3.9. Uncorrected $^{14}\text{C}$ dates of select groundwater samples	78
Chapter Four – Surface and groundwater chemistry	85
Figure 4.1. Groundwater sampling locations	90
Figure 4.2. $^{87}\text{Sr}/^{86}\text{Sr}$ in Wybong Creek surface and groundwater	92
Figure 4.3. Ca+Mg+Na+K/HCO <sub>3</sub> in water samples	94
Figure 4.4. Saturation indices for calcite and dolomite	94
Figure 4.5. $\delta^{35}\text{S}$ , Br/Cl and Na/Cl in water samples	96
Figure 4.6. $\delta^{18}\text{O}$ and $\delta^2\text{H}$ of Wybong catchment water samples	98
Figure 4.7. Mg/Na and Ca/Na in water samples	100
Figure 4.8. Piper diagram of groundwater samples from piezometers	101
Figure 4.9. Two component mixing curves of Sr vs $^{87}\text{Sr}/^{86}\text{Sr}$	103
Figure 4.10. Two component mixing curves of $^{87}\text{Sr}/^{86}\text{Sr}$ vs Na/Cl, Sr/Na and Sr/Cl	104
Figure 4.11. Conceptual model of groundwater systems in the Wybong Creek catchment	107

	<i>Page</i>
Chapter Five – Causes of salinity at Manobalai	111
Figure 5.1. Location of Manobalai within Wybong and the Hunter Valley	114
Figure 5.2. Geology of the Manobalai field site	117
Figure 5.3. Soil landscape series of the Wybong Creek catchment	118
Figure 5.4. The erosion gully sampled for pedogenic carbonate	119
Figure 5.5. Regolith landform map of Manobalai	126
Figure 5.6. Cross-sections of select cores sampled from Manobalai	129
Figure 5.7. EC <sub>1:5</sub> and total moisture at Sites One to Three	131
Figure 5.8. EC <sub>1:5</sub> and total moisture at Sites Four to Seven	132
Figure 5.9. EC <sub>1:5</sub> and total moisture at Site Seven	133
Figure 5.10. Soil salinity as a function of pH	135
Figure 5.11. Major cation and anion concentrations in Manobalai soil cores from Sites Two – Four	137
Figure 5.12. Major cation and anion concentrations in Manobalai soil cores from Site Six	138
Figure 5.13. Stiff diagrams of groundwater chemistry at Manobalai	141
Figure 5.14. Molar Na/Cl in Manobalai groundwater samples	142
Figure 5.15. $\delta^2\text{H}$ as a function of $\delta^{18}\text{O}$ for Manobalai groundwater	143
Figure 5.16. Conceptual model of salinisation at Manobalai	147
Chapter Six – Hydrology and hydrogeology of Manobalai	151
Figure 6.1. Geology of the Manobalai field site	156
Figure 6.2. Differenced groundwater height at Manobalai	162
Figure 6.3. Differenced groundwater height at Sites One – Five	165
Figure 6.4. Relationships between EC at the 60 km sample site, gravity, and groundwater height at Site Eight	167
Figure 6.5. Relationships between EC at the 60 km sample site, temperature, and groundwater height at Site Eight	168
Figure 6.6. Groundwater height in response to precipitation at Hannah's and Sites One – Two	169
Figure 6.7. Groundwater height in response to precipitation at Sites Three, Four, Six and Eight	170
Figure 6.8. Hydraulic head at Manobalai sample sites on different dates	173
Figure 6.9. $^{87}\text{Sr}/^{86}\text{Sr}$ vs Cl (mmol L <sup>-1</sup> ); and (b) $^{87}\text{Sr}/^{86}\text{Sr}$ versus $\delta^{18}\text{O}$ for groundwater sampled from Manobalai	176
Figure 6.10. Temporal variation in EC at Sites Six and Eight	178
Figure 6.11. Relationship between gravity, Wybong Creek salinity and groundwater height at Sites Six and Eight	182
Figure 6.12. Relationship between gravity, Wybong Creek salinity, Wybong Creek depth, Wybong Creek temperature and air pressure	183
Appendix for Chapter Five	249
Figure A5.1. Aeromagnetic survey of the Manobalai field site	251

	<i>Page</i>
Figure A5.2. Spectra from XRD analysis of 0.0 – 0.5 m at Site Two	260
Figure A5.3. Spectra from XRD analysis of 0.5 – 1.0 m at Site Two	260
Figure A5.4. Spectra from XRD analysis of 4.0 – 4.5 m at Site Two	261
Figure A5.5. Spectra from XRD analysis of 15.0 – 16.0 m at Site Two	261
Figure A5.6 SEM of the Site Two Deep subsample representing a depth of 0.0 – 0.5 m	262
Appendix for Chapter Six	263
Figure A6.1. Slug test analyses for Manobalai sites on 14/07/2008	265
Figure A6.2. Slug test analyses Manobalai sites on 18/01/2009	266
Figure A6.3. Slug test analyses for Manobalai sites on 18/01/2009	267
Figure A6.4. Spectral analyses of relationships between hydraulic head, gravity and air pressure at Site Eight	273

## List of tables

	<i>Page</i>
Chapter Two – Identification of solute sources to Wybong Creek	13
Table 2.1. Monthly precipitation, evaporation at Scone	27
Table 2.2. Discharge and salt flux from Wybong Creek	28
Table 2.3. Aeolian salt accession to Wybong Creek catchment	29
Table 2.4. Major cations and anions in the salt pool	38
Table 2.5. Evapotranspiration changes in the Wybong Creek catchment	39
Table 2.6. Percent increase in salinity due to evaporation	41
Table 2.7. Molal ion ratios in Wybong Creek	43
Chapter Three – Aquifers and groundwater bodies	49
Table 3.1. Borehole data for sampled bores	65
Table 3.2. Loading results for PCA and canonical analyses	72
Table 3.3. Groundwater bodies in the Wybong Creek catchment	75
Chapter Four – Surface and groundwater geochemistry	87
Table 4.1. $^{87}\text{Sr}/^{86}\text{Sr}$ of possible Sr sources to the Wybong Creek catchment	93
Table 4.2. $\delta^{34}\text{S}$ of possible S sources	97
Table 4.3. Ca and Mg concentrations resulting from cation exchange	102
Table 4.4. Parameters for an optimised saline endmember	105
Chapter Five – Causes of salinity at Manobalai	111
Table 5.1. Parameters describing bored and piezometers installed at Manobalai	121
Table 5.2. Regolith landforms at Manobalai	127
Table 5.3. Chemistry of select Manobalai soil samples	134
Table 5.4. Minerals occurring in select samples from Site Two	136
Table 5.5. Rain and groundwater chemistry of the Manobalai site	140
Table 5.6. $\delta^{13}\text{C}$ and $^{14}\text{C}$ dates for erosion gully soil samples	144
Chapter Six – Hydrology and hydrogeology of Manobalai	151
Table 6.1. Parameters for bores and piezometers at the Manobalai field site	157
Table 6.2. Flow at surface water sample sites	160
Table 6.3. Parameters for modelling groundwater flux from Manobalai	160
Table 6.4. Parameters for modelling groundwater flux changes in response to fluctuating hydraulic head	162
Table 6.5. Hydraulic conductivity for piezometers at Manobalai	172
Table 6.6. Groundwater chemistry at Manobalai	175
Table 6.7. Measured and modelled increases in solute concentration in Wybong Creek due to groundwater flux from Manobalai	181

	<i>Page</i>
<b>Appendix for Chapter Two</b>	213
Table A2.1. Cation detection limit and concentrations in surface water blanks	215
Table A2.2. Anion detection limit and concentrations in surface water blanks	216
Table A2.3. Water quality in Wybong Creek surface water sample sites, tributaries and rainwater	217
Table A2.4. Cation concentrations in Wybong Creek surface water sample sites, tributaries and rainwater	220
Table A2.5. Anion concentrations in Wybong Creek surface water sample sites, tributaries and rainwater	224
Table A2.6. Parameters used to calculate evapoconcentration	227
Table A2.7. Isotope data for Wybong Creek surface water samples and isotopes	228
<b>Appendix for Chapter Three</b>	229
Table A3.1. Cation detection limit and concentrations in groundwater blanks	231
Table A3.2. Anion detection limit and concentrations in groundwater water blanks	232
Table A3.3. Water quality data for Wybong Creek groundwater samples	233
Table A3.4. Anion concentrations for Wybong Creek groundwater samples	237
Table A3.5. Cation concentrations for Wybong Creek groundwater samples	241
Table A3.6. Isotope concentrations for Wybong Creek groundwater samples	245
<b>Appendix for Chapter Five</b>	249
Table A5.1. Soil quality parameters for Manobalai regolith cores	252
Table A5.2. Cation and anion concentrations in 1:5 soil-water extracts	256
Table A5.3. Percent weight cation and anion concentration in 1:5 soil-water extracts	258
<b>Appendix for Chapter Six</b>	263
Table A6.1. Hydraulic conductivity measured on the 14 <sup>th</sup> – 17 <sup>th</sup> July 2008	270
Table A6.2. Hydraulic conductivity measured on the 17 <sup>th</sup> – 21 <sup>st</sup> January 2008	271
Table A6.3. Hydraulic conductivity measured on the 14 <sup>th</sup> May 2009	272
Table A6.4. Correlation coefficients for the relationship between rainfall and groundwater height at Site Two Shallow	274
Table A6.5. Correlation coefficients for the relationship between rainfall and groundwater height at Site Two Deep	275

## List of equations

	<i>Page</i>
Chapter Two – Identification of solute sources to Wybong Creek	13
Eq. 2.1. Charge balances	21
Eq. 2.2. Effects of evaporation on volume	23
Eq. 2.3. Effects of evaporation on solute concentration	23
Chapter Four – Surface and groundwater geochemistry	87
Eq. 4.1. Sources of Mg and Ca to groundwater	89
Eq. 4.2. Quantification of the effects of cation exchange	91
Eq. 4.3. Model for two-component mixing of ions	91
Eq. 4.4. Model for two-component mixing of $^{87}\text{Sr}/^{86}\text{Sr}$	91
Eq. 4.5. Cation exchange reactions	99
Chapter Five – Causes of salinity at Manobalai	111
Eq. 5.1. Total soil moisture	122
Eq. 5.2. Exchangeable sodium percentage	124
Chapter Six – Hydrology and hydrogeology of Manobalai	151
Eq. 6.1. Hydraulic conductivity using the Bouwer and Rice method	158
Eq. 6.2. $\ln Re/Rw$ for fully penetrating piezometers	158
Eq. 6.3. $\ln Re/Rw$ for partially penetrating piezometers	159
Eq. 6.4. Increase in solute concentration as a result of groundwater flux to Wybong Creek	159
Eq. 6.5. Groundwater discharge to Wybong Creek	151
Eq. 6.6. Increase in solute concentration as a result of groundwater flux to Wybong Creek	162
Appendix for Chapter Five	249
Eq. A5.1. Soil solute concentrations as a function of soil weight	251
Appendix for Chapter Six	263
Eq. A6.1. Cl load delivered from eastern and western aquifers	268
Eq. A6.2. Solute flux from eastern and western aquifers	268
Eq. A6.3. Increase in salt load to Wybong Creek as a result of groundwater flux	268
Eq. A6.4. Specific discharge ( $V_D$ ) to Wybong Creek	268
Eq. A6.5. Groundwater discharge ( $Q$ ) to Wybong Creek	269
Eq. A6.6. Specific discharge ( $V_D$ ) Discharge to Wybong Creek	269
Eq. A6.7. Hydraulic conductivity necessary for delivered flux	269



---

# **Chapter One**

## Introduction



## 1. Background - Salt and salinity

Salts are cations and anions produced by the acid-base reactions which occur during chemical weathering (Jones and Atkins 2002). The amount of dissolved salt (i.e. solutes) in the soil and water is approximated by the measurement of electrical conductivity (EC) or measured precisely by quantifying solute concentrations. Water and soils are defined as being saline when solute concentrations are at levels which inhibit plant growth (Rhoades 1996; Salama *et al.* 1998; Essington 2004; Rose 2004), with salinisation being the increasing of solute/salt concentrations in soil and/or water (Williams 1999; 2001). Water is defined as fresh when total dissolved solid (TDS) concentrations are below 500 mg L<sup>-1</sup>; brackish with concentrations between 500 and 5000 mg L<sup>-1</sup>; saline with concentrations above 5000 mg L<sup>-1</sup>; and as brines when concentrations are above 45 000 mg L<sup>-1</sup> (Rhoades *et al.* 1992). Soil salinity is defined differently depending on the method of analysis, with soils being saline when the percent weight of Na and Cl is above 0.2 % (Northcote and Skene 1972), or when five parts water extracted from one part soil has an EC of over 1500 µS cm<sup>-1</sup> (Charman and Murphy 2000). The percent of exchangeable Na (ESP) on soil exchange sites is also a measure of salinity, with ESP salinity thresholds depending on the salinity of the soil solution (Ayers and Westcot 1994).

Salinisation has resulted in land degradation and a loss of productivity since the rise of human civilisation. The Sumer people were the first human civilisation, for example, with collapse of this society occurring due to catastrophic decreases in grain harvests due to salinisation (Jacobsen and Adams 1958). Loss of productivity and ecosystem integrity has continued into modern times, with salinisation resulting in tree die-back, invasion of ecosystems by foreign salt tolerant plants, decreased productivity, destruction of soil structure, and damage to buildings and infrastructure (Cartwright *et al.* 2004; Rose 2004). These effects are largely restricted to arid and semi-arid parts of the world which have insufficient rainfall to flush salts from the soil. As the most arid inhabited continent in the world, 33 to 42 % of soils in Australia are estimated to be salt affected (Northcote and Skene 1972). This damage costs \$145 million in lost agricultural production, infrastructure damage and salinity mitigation annually (Ruprecht and Schofield 1991; AGDA and AGDEH 2007). Salinisation is therefore a risk to ecosystem, economic and agricultural productivity, with the prevention of further salinisation an important part of sustainable land-use practice.

---

There are two forms of salinisation, with these differing in the mechanism by which they occur. Primary salinity is a natural phenomenon in arid and semi-arid environments and closed basins, with examples including Salt Lake in the USA, the Dead Sea in the Middle East, the Dry Valleys of Antarctica, and Lake Eyre in central Australia (Matsubaya *et al.* 1979; Jankowski and Jacobson 1989; Essington 2004; Rose 2004). Secondary salinity is instead caused by human disturbance to the hydrological cycle (e.g., Sharma 1984; Hart *et al.* 1990; Greenwood *et al.* 1992; Salama *et al.* 1999; Peck and Hatton 2003). Dryland salinity is a type of secondary salinity whereby hydrological changes caused by humans are the result of deforestation. This leads to increases in the quantity of water recharging aquifers and reduces the quantity of groundwater removed from aquifers by evapotranspiration, with the Australian definition of groundwater including both the vadose water within unconsolidated materials such as soil, as well as the water occurring within rocks (Eggleton 2001). The increase in groundwater recharge leads to increases in groundwater height. Salt stores occurring within the regolith in arid to semi-arid areas and regions with deeply weathered geology may then be dissolved by rising groundwater, causing salinisation of regolith and surface water when solutes are brought to the Earth's surface (Pigram 1986; Bradd *et al.* 1997; George *et al.* 1999; Hoey *et al.* 2002; Knight *et al.* 2002; Robins 2004). Irrigation of crops and/or fodder causes similar changes to the hydrological cycle and also allows for the evapoconcentration of solutes at the Earth's surface (e.g., Hart *et al.* 1990; Salama *et al.* 1999; Peck and Hatton 2003). Such evapoconcentration occurs when groundwater heights rise to within five meters of the regolith surface, where it is exposed to evaporation through capillary rise (Summerell *et al.* 2006).

### **1.1. Salinity in Australia**

The geology of arid and semi-arid regions in Australia plays a role in their susceptibility to both primary and secondary salinity (Gibbs 1970; Jobbágy and Jackson 2001; Summerell *et al.* 2006). Many parts of Australia, for example, have been subject to rock weathering over extensive geological time scales. This has resulted in landforms of low relief which are covered in regolith, with regolith being the product of sedimentary, aeolian, and rock weathering processes, rather than soil which is formed by pedogenic processes (Eggleton 2001). The extensive weathering of Australia has also resulted in a relatively clay rich regolith. The poor drainage that results from low relief and high clay contents increases water residence times (MacKenzie *et al.* 2004;

---

Summerell *et al.* 2006), and inhibits percolation (Northcote and Skene 1972). Water received in these highly weathered landscapes then has little propensity to percolate into and wash salts through the regolith, causing salt concentrations to increase.

Climate also plays a key role in the salinisation of Australian catchments, with evaporation exceeding rainfall in many areas. Water which is received as rainfall with low solute concentrations (i.e. 0.1 – 30 µg Cl L<sup>-1</sup>; Keywood *et al.* 1997) can evapoconcentrate to form playa brines with TDS concentrations of more than 300 000 mg L<sup>-1</sup> in central Australia (Jankowski and Jacobson 1989; Herczeg *et al.* 2001). Dust blown in from central Australia is then deposited in a number of catchments in south-eastern Australia (Acworth *et al.* 1997; Cattle *et al.* 2002), with salt stores building due to inadequate rainfall. Salt stores are also formed in areas with high evaporation and where salts have been occluded during the process of evapotranspiration (Salama *et al.* 1993). Low rainfall is, therefore, well correlated to the formation of salt stores in regolith, with secondary salinity occurring in all arid to semi-arid areas across Australia (Summerell *et al.* 2006; AGDA and AGDEH 2007).

New South Wales is a state in the south-east of Australia and has an area of 803 131 km<sup>2</sup> or 80 313 100 ha (Figure 1.1; ABS 2006). Of this area, 181 000 ha was estimated as being salinised or at high risk of salinisation in the period 1998-2000 by Robins (2004). This number has been revised down in more recent studies. A maximum salinised area of 62 372 ha, for example, is estimated in the Murray-Darling Basin, with this catchment comprising almost all the salinised land in New South Wales (New South Wales Department of Environment, Climate Change, and Water 2009). The Hunter River catchment is one of the larger and more agriculturally important valleys in New South Wales and eastern Australia (Robinson and Helyar 1996). Approximately 25 000 ha of land within the Hunter Catchment is affected by salinisation. High levels of salinity in the regolith, groundwater and tributaries of the Hunter River are identified as major management issues (Kellett *et al.* 1987; Beale *et al.* 2000), with at least one vineyard (Rosemount at Hollydeen) closing due to salinity induced vine mortality. The identification of solute sources and salinity mitigation measures are required in order to prevent further salinisation and ensure continuing productivity and sustainable land-use in this important agricultural area.

## 1.2. Salinity in the Hunter River Catchment

The Goulburn River is located in the western reaches of the 22 000 km<sup>2</sup> Hunter River catchment (Figure 1.1). Empirical studies have shown that nearly a third of the

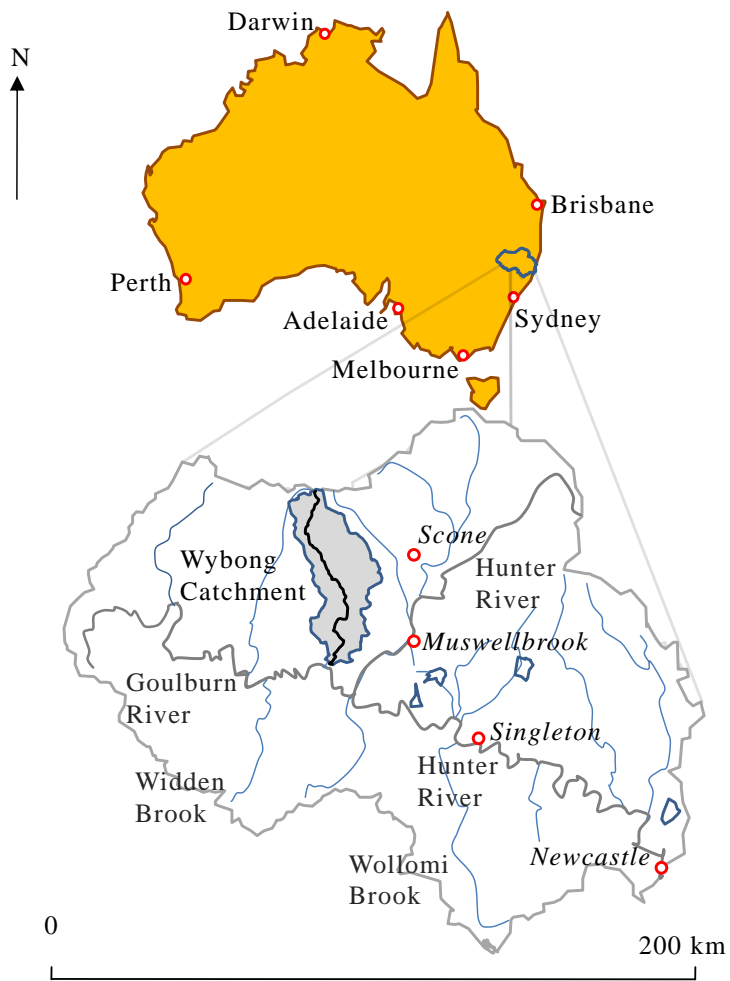


Figure 1.1 The location of the Hunter River catchment within Australia. The Goulburn River and the Hunter River are drawn in grey, with other tributaries shown in blue. The Wybong Creek catchment is illustrated in grey.

total salt load in the Hunter River is sourced from the Goulburn River (Beale *et al.* 2000; HCR CMA 2002; Beale *et al.* 2004), which delivers between 50 600 and 91 000 t of salt to the Hunter River every year (Bembrick 1993 in: Raine 2000). Salt concentrations in the Goulburn River often exceed recommended guidelines for the irrigation of crops (ANZECC and ARMCANZ 2001), with a significant proportion of these salts and especially Na and Cl sourced from a tributary called Wybong Creek (Kellett *et al.* 1987). Salt scalds occur in a number of places within the upper Hunter, including the mid-lower Wybong Creek catchment, the lower Widden catchment, and isolated areas around Scone. A study on surface and groundwater interactions has been undertaken in the Widden Brook (Sommerville *et al.* 2006), a subcatchment of the Goulburn and Hunter Rivers, with regional hydrogeochemical studies undertaken in the upper Hunter Valley (Kellett *et al.* 1987; Creelman 1994). Detailed studies of surface and groundwater interactions specifically relating to salinity have not been undertaken

in the Wybong Creek catchment, however, despite this being identified as the main source of solutes to the upper Hunter River.

### 1.2.1. Salt sources in the Hunter Valley

Salinity outbreaks in the Hunter catchment could be linked to dryland salinity, with the Hunter catchment being cleared for timber in the 19<sup>th</sup> and 20<sup>th</sup> centuries to increase grazable land and for lumber (Abbott and Glengarry 1880; Albrecht 2000). Increased river permanency resulted from this land-clearing, likely due to the increase in groundwater recharge and discharge caused by decreased evapotranspiration (Abbot and Glengarry 1880). The increased groundwater recharge may have caused the dissolution of salts from the upper layers of the regolith and the discharge of saline groundwater, with this process occurring in the Namoi catchment just north of the Hunter catchment (Ringose-Voase *et al.* 2003). Increases in groundwater heights are difficult to detect in the Hunter Valley, however, due to a paucity of groundwater monitoring data in the catchment (Beale *et al.* 2000).

Geology could also be linked to salinity in the upper Hunter, with both rock type and geological structures playing a role. The Goulburn River is incised into marine influenced (i.e. Wittingham) and deltaic (i.e. Newcastle) Permian Coal Measures in its lower reaches. These coals are identified as being the source of salinity to the Goulburn and Wybong catchments, with the weathering of coal seams and silicate minerals in tuffaceous inter-seam beds identified as causing saline Na-Cl dominated water (Kellett *et al.* 1987). Groundwater fluxes from major fault zones associated with these coal measures are identified as the primary source of salinity in the Hunter Valley (Beale *et al.* 2000), especially during periods of low rainfall (where evaporation causes increased solute concentrations and dilution by rainwater is minimised).

Electrical conductivities of up to 50 500  $\mu\text{s cm}^{-1}$  were found in a Wybong Creek tributary (Big Flat Creek; Umwelt Environmental Consultants 2006), with this level of salinity similar to those seen in the sea. Geological reports commissioned by Centennial Coal identified the Newcastle Coal Measures (formerly the Wollombi Coal Measures) as the source of solutes to Wybong Creek (Umwelt Environmental Consultants 2006). The Newcastle Coal Measures were deposited in a freshwater environment (Kellett *et al.* 1987; Kramer *et al.* 2001), however, with both these and the deeper Wittingham Coal Measures presumably exposed to water-rock interaction and leaching of solutes since the Permian. Observations can link both human change to the hydrological cycle and groundwater discharge from the Permian Coal Measures to salinisation in the

Wybong catchment, with empirical evidence required in order to isolate which, if not both of these, is the source of salinity.

### **1.2.2. Surface and groundwaters in the Wybong Creek catchment**

The Wybong Creek catchment has been identified as a priority saline sub-catchment of the Hunter river for detailed study by the New South Wales Department of Energy Climate Change and Water (NSW DECCW), and the Hunter Central Rivers Catchment Management Authority (HCR CMA). This was due to both the salinity of the Creek itself (median salinity of  $1455 \mu\text{S cm}^{-1}$ ) and the significant salt loads discharged from the Creek into the Goulburn River (Beale *et al.* 2000). A number of possible causes of soil and surface water salinisation occur in Australia which may also be related to salinity in the Wybong Creek catchment, including dryland salinity (Rengasamy and Olsson 1991; Albrecht 2000), irrigation using saline groundwaters (Bradd *et al.* 1997; Healthy Rivers Commission 2002), climate regime (Creelman 1994), and groundwater discharge from saline Permian strata via faults and fractures (Kellett *et al.* 1987; Beale *et al.* 2000; Robins 2004).

### **1.3. Scope of this research**

Data and research is required in order to give empirical evidence for salinity sources within the Wybong Creek catchment. Further research is also required in order to better understand the roles that hydrology, soil (regolith) chemistry, climate and geology play in catchment salinity. The aim of this thesis is, therefore, to contribute knowledge on the subject of catchment salinisation, using salinity in the Wybong Creek catchment as a basis for this research. This aim is met by outlining where salts are arising in the Wybong Creek catchment and which processes are controlling salt dynamics and transport into Wybong Creek. Interactions between surface waters, groundwaters, and regolith are therefore a significant component of the thesis, with different aspects of salinity within these three media addressed by meeting more specific aims in each of the five chapters.

This study was designed to meet research objectives by sampling, measuring, and analysing field parameters at a catchment scale, due to laboratory studies and models often having limited accuracy when extrapolated to field sites due to oversimplification of complex environmental conditions (e.g., Stonestrom *et al.* 1998; Sandberg *et al.* 2002; Peck and Hatton 2003; Evans *et al.* 2006). Extrapolation of findings to catchments with a similar geophysical nature was anticipated as part of thesis outcomes.

The chapters in this thesis are presented in manuscript format for ease of publication, with this leading to a degree of repetition which is minimised as much as possible. Ions are denoted throughout the thesis without any indication of valency (i.e. Cl rather than  $\text{Cl}^-$ ), with no consistency within the literature as to the denotation of charge when discussing ions.

### **1.3.1. Chapter Two – Identification of solute sources to Wybong Creek**

The aim of Chapter Two was to investigate solute sources and hydrological processes affecting solute concentrations in Wybong Creek. This aim was met by addressing the following objectives:

1. To characterise the distribution of solutes and salinity in Wybong Creek;
2. To estimate the influence of aeolian deposition on the Wybong Creek catchment;
3. To estimate the change in the quantity of evapotranspiration in the Wybong Creek catchment as a result of deforestation;
4. To estimate the influence of evaporation on solute concentrations in Wybong Creek;
5. To determine the influence of groundwater discharge on Wybong Creek; and
6. To estimate the influence of mineral precipitation on solute concentrations in Wybong Creek.

### **1.3.2. Chapter Three – Aquifers and groundwater bodies in the Wybong Creek catchment**

The aim of this chapter was to understand the extent and interconnectedness of groundwater bodies or systems within the Wybong Creek catchment and the aquifers in which they occur. This aim was met by addressing the following objectives:

1. To create geological cross-sections of the Wybong Creek catchment;
2. To isolate formations which are acting as aquifers within the Wybong Creek catchment;
3. To place groundwater samples into groups which represent groundwater bodies; and
4. To identify the local, intermediate and regional groundwater systems occurring in the catchment.

### **1.3.3. Chapter Four – Surface and groundwater geochemistry**

The aim of Chapter Four was to identify the source of solutes to surface and groundwater in the Wybong Creek catchment. This was achieved by meeting the following objectives:

1. To identify chemical weathering reactions occurring along groundwater flow paths;
2. To identify the affects of cation exchange on solute concentrations in groundwater bodies; and
3. To identify the affects of evaporation on solute concentrations in groundwater bodies.

### **1.3.4. Chapter Five – Causes of salinity at the Manobalai field site**

The aim of Chapter Five was to deduce whether solutes in the saline groundwater discharged into Wybong Creek in the mid-catchment area was sourced from salt stores within the regolith or occurred in a saline groundwater body discharging from a deeper formation. The following objectives were addressed:

1. To characterise regolith chemistry according to sample depth, landform, and texture;
2. To identify minerals acting as sources of solutes to the regolith and groundwater;
3. To identify geomorphological factors controlling salt occurrence in the area; and
4. To correlate solute occurrence within the regolith to either aeolian deposition or groundwater.

### **1.3.5. Chapter Six – The hydrology and hydrogeology of Manobalai**

The aim of Chapter Six was to understand groundwater movements at the Manobalai field site. The following objectives were considered in order to meet this aim:

1. To describe groundwater systems at the Manobalai field site;
2. To isolate factors controlling hydraulic head at Manobalai;
3. To identify groundwater connectivity within the Manobalai area; and
4. To identify whether a relationship occurs between changes in Wybong Creek salinity and groundwater discharge from Manobalai.

**1.3.6. Chapter Seven – Conclusions: Salt origins and salinisation processes in the Wybong Creek Catchment**

Chapter Seven summarises the conclusions of previous chapters, in order to identify the source of solutes in the Wybong Creek catchment and the processes by which these solutes are leading to salinisation of surface water, groundwater and soil. Salinity mitigation and management strategies, limitations of this study, and avenues for future research are identified.



---

## **Chapter Two**

Identification of solute sources to  
Wybong Creek



## 1. Introduction

Saline rivers are a serious problem to water users, not only because they are unable to be used for drinking purposes, but because of the detrimental affect saline water has on soils and its toxicity to plants (e.g. Rhoades *et al.* 1992). The aridity of many Australian catchments makes them particularly vulnerable to salinisation due to evapoconcentration of solute containing waters and the immobilisation of salts within the regolith (e.g., Eugster and Jones 1979; Allison *et al.* 1990; Chivas *et al.* 1991). Australian rivers draining salinised catchments have electrical conductivities (EC) from as low as  $302 \mu\text{S cm}^{-1}$  in Narrabri Creek, which drains the Liverpool Plains, to as high as  $1200 \mu\text{S cm}^{-1}$  in the South Creek, Sydney (NSW DWE 2009). The Murray River has been the subject of a number salinity studies, and has salinities of  $668 \pm 230 \mu\text{S cm}^{-1}$  near its mouth (GEMS/Water 2004). Previous hydrogeochemical studies in the upper Hunter Valley indicated solute concentrations in a minor tributary of the Hunter, the Wybong Creek, at levels which decreased water quality in the Hunter River (Kellett *et al.* 1987; Creelman 1994). Electrical conductivity within Wybong Creek has exceeded  $3000 \mu\text{S cm}^{-1}$  a number of times in the last fifty years (NSW DWE 2009), with the irrigation of vineyards using surface water causing vine mortality within the catchment. In addition, the highly saline water which discharged from the Creek at times necessitates limiting the Hunter River for irrigation use further downstream, with the saline water discharged from Wybong Creek threatening both sustainable farming and economic productivity in this important agricultural region. This research therefore aimed at identifying the source of solutes to Wybong Creek by investigating chemical changes along the flow path of the river, with surficial processes affecting salinity such as evaporation and evapotranspiration also investigated.

Rain and dust are the main source of salts and/or nutrients to a number of well studied salinised catchments in Australia (Mazor and George 1992; Jones *et al.* 1994; Herczeg *et al.* 2001), and non-salinised catchments around the world (Graustein and Armstrong 1983; Miller *et al.* 1993). Rainwater acquires solutes from the oceans during cloud formation (Appelo and Postma 2005), while salts are also entrained with dust that is deflated from arid regions (Abuduwaili *et al.* 2008). Salts deposited with rainfall and dust can be immobilised within the regolith and stored in arid and semi-arid regions for millennia (Salama *et al.* 1993b; Summerell *et al.* 2006), becoming a source of solutes to catchments when a change in hydrology occurs. Annual solute fluxes from rivers which are in excess of annual aeolian deposits on catchments, are used to indicate mobilisation of aeolian salt stores (e.g. Salama 1993b; Jolly *et al.* 2001; Poulsen *et al.* 2006).

---

Groundwater transports solutes to surface water and regolith (e.g., Ruprecht and Schofield 1991a; Salama *et al.* 1999), with abrupt salinity increases in rivers such as the Murray, in southern Australia, occurring as a result of groundwater discharge (MDBA 2009). Groundwater salinity in Australia often arises due to the process of dryland salinisation, whereby a decrease in evapotranspiration is caused by deforestation (e.g., Coram *et al.* 2001). This in turn causes an increase in groundwater recharge and water tables, and may result in the dissolution of salts stored within the regolith. This dryland salinity is a major cause of salinisation, causing increases to surface water salinity in many parts of Australia (Salama *et al.* 1993b; Jolly *et al.* 2001; Summerell *et al.* 2006), with saline water defined as containing solutes at concentrations greater than 500 mg L<sup>-1</sup> (Rhoades *et al.* 1992).

A number of processes affect solute concentrations and proportions within rivers independent of solute sources that may occur. These processes include evapoconcentration, dilution (Gibbs 1970; Herczeg *et al.* 1993), and mineral precipitation (Eugster and Hardie 1975). Sodium and Cl increasingly dominate water chemistry with increasing distance from a river's headwaters, for example, with this due to less soluble ions such as Ca, SO<sub>4</sub>, Mg and HCO<sub>3</sub> precipitating out of solution. The precipitation of carbonate causes the Ca-HCO<sub>3</sub> dominated headwaters and Na-Cl dominated river mouths characteristic of many rivers (e.g., Gibbs 1970; Eugster and Hardie 1975). Changes to the proportions of ions may be also due to groundwater discharge, with ion ratios and saturation indices useful for the detection of such discharge.

## **1.2. Aims**

The aim of this chapter was to investigate solute sources and hydrological processes affecting solute concentrations in Wybong Creek. This aim was met by addressing the following objectives:

1. To characterise the distribution of solutes and salinity in Wybong Creek;
2. To estimate the influence of aeolian deposition on the Wybong Creek catchment;
3. To estimate the change in the quantity of evapotranspiration in the Wybong Creek catchment as a result of deforestation;
4. To estimate the influence of evaporation on solute concentrations in Wybong Creek;

5. To estimate the influence of mineral precipitation on solute concentrations in Wybong Creek; and
6. To determine the influence of groundwater discharge on Wybong Creek.

### **1.3. Site description**

Wybong Creek is the last tributary of the Goulburn River, before the Goulburn in turn flows into the Hunter River (Chapter One: Figure 1.1). The upper Wybong Creek catchment drains the southern side of the Liverpool Ranges, which are an eroded remnant of the Liverpool Shield Volcano that was created in the Eocene-Miocene (Scheibner 1998). The elevation of the river drops approximately 230 m in its first 60 km as Wybong Creek moves along through pool – riffle sequences, from an elevation of approximately 500 m at its headwaters. The water course is deeply (~ 20 m) incised into the smectitic clay which makes up the Wybong floodplain in the mid-lower catchment, and is in places further incised into the Narrabeen Group sandstones and conglomerates. The valley narrows through the mid-catchment where accumulations of alluvium comprised of basalt cobbles and boulders occur. The relief below the 60 km sample point becomes flatter, with the river dropping 50 m along the next 30 km until it's confluence with the Goulburn River. Low relief dominates the lower catchment, though sandstone escarpments up to 200 m high still occur at the sides of the valley. Coloured quartzite pebbles are increasingly frequent as alluvial deposits in the lower parts of the catchment.

More rainfall is received in the catchment in the average summer (221 mm) than in the average winter (129 mm; ABM 2009), and more rainfall is received at the top of the Liverpool Ranges in the upper catchment than on the alluvial flats in the lower catchment (McMahon 1968). Rainfall in the Wybong Creek catchment during 2006 was 319 mm, less than half the mean annual rainfall of 649 mm, and was significantly below the mean rainfall until June 2007 (ABM 2009). Mean and above mean rainfall occurred from June 2007. Mean maximum summer (January) temperatures are 31 °C, while mean winter (July) temperatures are 16.3 °C.

## **2. Materials and methods**

Sample collection and analyses are outlined first within the Materials and Methods section, followed by the collection of time-series data, flow measurements, calculation of hydrological parameters and aeolian deposition, and time-series analyses.

---

## 2.1. Sample collection

Surface water samples were collected from ten easily accessible locations along the length of Wybong Creek, with sample sites located at regular intervals (Figure 2.1). Sampling occurred on three dates during the low flow conditions of 2001-2007: the 21<sup>st</sup>-22<sup>nd</sup> April; the 21-23<sup>rd</sup> July 2006; and the 1<sup>st</sup> June 2007. Average rainfall and higher flow conditions occurred in the catchment from mid-2007 onwards, with surface water samples collected on the 5<sup>th</sup>-7<sup>th</sup> July 2007; and the 17-18<sup>th</sup> June 2008. Samples were collected from the centre of the channel at one third of the total depth below the Creek's surface, except at the 87 km site where water depth necessitated collection from the edge of the Creek. Rainwater samples were collected 13 km south of the catchment (Denman) on the 14<sup>th</sup> of June 2007, and 18<sup>th</sup> of July 2008, with all other rainwater samples collected 20 km west of Wybong Creek (Muswellbrook) during 2008.

## 2.2. Sample analyses

Water quality parameters were measured on unfiltered water samples at the time of sampling using Orion Gel-Filled pH and Eh electrodes and pH and Eh meters. An Orion DuraProbe™ 4-electrode conductivity cell and conductivity meter was used to measure electrical conductivity (EC). The EC cell and meter was calibrated in the field using Thermo Orion Application Solution ( $1413 \mu\text{S cm}^{-1}$ ), while the Eh meter and

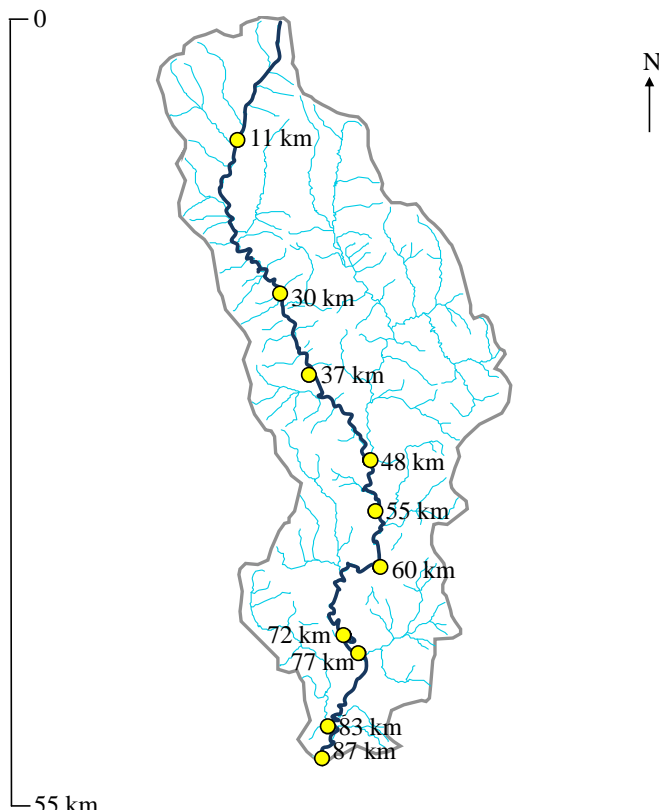


Figure 2.1. Wybong Creek surface water sampling sites.

electrode were calibrated using Thermo Orion ORP standard solution. The pH meters were calibrated using LabChem pH buffer solutions at pH 4, 7, and 10. All meters were regularly calibrated and checked against standard solutions in the field.

Bicarbonate concentrations were determined on filtered samples by HCl titration using an Hach digital titrator, and methyl orange indicator (Franson 2005), with the exception of a number of rainwater samples which were at times collected independent of field work. Water samples collected for cation, anion, and isotope analyses were filtered in the field using 0.45 µm Millipore® nitrocellulose filters, and collected in new or HNO<sub>3</sub> acid-washed 250 mL polyethylene bottles and/or 50 mL Falcon tubes. Samples for cation and <sup>87</sup>Sr/<sup>86</sup>Sr analyses were acidified using 2 mL 50 % Merck ultra-pure HNO<sub>3</sub>. Blanks made up of milli-Q water were prepared in the same way as samples for cation and anion analyses at the time of sampling.

### **2.2.1. Cation, anion and isotope analyses**

Reactive ions were analysed in the field using a Hach spectrophotometer and methods 8146, 1, 10-Phenanthroline for Fe<sup>2+</sup>; method 10209 phosphomolybdate for PO<sub>4</sub><sup>2-</sup>; cadmium reduction for NO<sub>3</sub><sup>2-</sup>; and BaCl for SO<sub>4</sub><sup>2-</sup> (Hach Company 2009).

Samples collected for ion analyses during 2006 and 2009 were sent to the Centre for Coastal Biogeochemistry, Southern Cross University, with Ben Macdonald collecting samples in 2006. Samples for ion analyses collected in 2007 – 2008 were sent to the Department of Water and Energy Water Environmental Laboratory, New South Wales, for analyses. Ion Chromatography (IC) was used to analyse anions while cations were analysed using Inductively Coupled Plasma – Mass Spectrometers (ICP-MS) and Inductively Coupled Plasma – Atomic Emission Spectrometers (ICP-AES).

Modelling of saturation indices was conducted in PHREEQC Interactive version 2.13.2.1727 using the PHREEQC.dat database.

### **2.2.2. Oxygen and hydrogen isotopes**

Select samples were analysed for O and H isotopes by Claudia Kietel and Hillary Stuart-Williams at the Research School of Biological Sciences, The Australian National University. The stable isotopes of O and H were measured using a Micromass Isoprime CF-IRMS (Continuous-Flow Isotope-Ratio Mass Spectrometer). Oxygen isotope ratios of the water were determined by equilibration with CO<sub>2</sub>. Water volumes measuring 250 µL were pipetted into screw top glass vials. A mixture of air and 5 % CO<sub>2</sub> was then gently flowed into the remaining spaces and screw tops with a PTFE lined, butyl rubber septum immediately fitted. The sealed samples were then stood in the mass

---

spectrometer room and held at a constant temperature of 0.5 °C for approximately 48 hours. Samples of standard waters with values spanning the anticipated analytical values were similarly treated. Two needles were inserted through septums (He carrier gas in and out) at the end of this period. Samples were then carried through a magnesium perchlorate moisture scrubber and a Porapak QS GC column which separated the CO<sub>2</sub> from the other gases in the helium carrier stream using a loop valve. The δ<sup>18</sup>O of CO<sub>2</sub> was then measured in the mass spectrometer with values normalised against a reference gas pulse. The analysed values of O in CO<sub>2</sub> were equilibrated with standard waters at the end of the run, in order that a slope and offset could be calculated to correct the analytical results to the Vienna Standard Mean Ocean Water (VSMOW) scale.

Hydrogen isotope values were calculated using the chromium method in which water is reduced on hot Cr metal to liberate <sup>2</sup>H. Water samples measuring 0.9 µL aliquots were pipetted into Sn cups, sealed immediately using crimping pliers, and placed in an AS200 autosampler. The sampler sat atop a furnace which maintained a Cr-packed quartz column at 1000 °C, with a Ni crucible on top of the Cr to catch the excess Sn, and a He carrier flowing down through the column. The Cr in the column was used to bind the O in the water as chromium oxide and release the <sup>2</sup>H to the column in the He carrier. The carrier gas was passed through a magnesium perchlorate scrubber to dry and then through a Porapak QS GC column to separate the H from traces of other gases and shape the peak. The gas then flowed into the mass spectrometer through a capillary system, with it's ratios then determined. Each sample peak was placed between a large and a small reference pulse, permitting normalisation of the results and calculation of the H<sup>3+</sup> correction. Each sample was typically run two or three times so that memory effects from one sample to the next were minimised. The slope and offset for the standard waters was determined finally and the results all corrected to the VSMOW scale. Precision for the δ<sup>18</sup>O runs was between 0.06 and 0.1 ‰, and for the δ<sup>2</sup>H was between 0.3 and 0.6 ‰ (C. Kietel, Pers. Comm., 2009).

#### **2.2.4. Quality assurance**

Sample contamination was monitored by creating blanks in the field using milli-Q water. Traces of Cd, Al, Ba, Zn, Ca, Mg, K, Si, Na, and Sr were found in many blanks (Appendix Two: Table A2.1). Zn contamination from suncream was likely to have contributed significantly to overall Zn concentration in blanks collected in July 2007, with the Zn concentration in blanks subtracted from sample concentrations to correct for

this. Anions were below detection limits (BDL) in all blanks (Appendix Two: Table A2.2).

The quality of cation and anion analyses were monitored using charge balances (Eq. 2.1):

$$\% \text{difference} = 100 \frac{\sum \text{cations} - \sum \text{anions}}{\sum \text{cations} + \sum \text{anions}} \quad (2.1)$$

where cation and anion concentrations were in meq L<sup>-1</sup>. The majority of charge balance differences were below 10 % (Appendix Two: Table A2.3). Rainwater and blanks were not measured for HCO<sub>3</sub> in the field, accounting for the large charge balance differences seen for these samples. The 11 km samples collected on 21/07/2006 and 18/07/2008 had charge balances of -18.4 % and -20.0 % respectively. A major cation was unlikely the cause of the charge imbalances as all major and many minor and trace elements were included in analyses, with the poor charge balance therefore caused by inaccurate HCO<sub>3</sub> measurement (which contributed most of the negativity). These samples were included in analyses though HCO<sub>3</sub> may have been over-estimated.

### 2.3. Time-series data

Hydrolab MiniSonde 5 instruments were installed at the 60 km sample site in the lower catchment and the 37 km sample site in the upper catchment from December 2006 (Figure 2.1). Datasonde installation involved drilling holes on the downstream side of a concrete bridge buttress in the centre of stream flow, and bolting a slotted steel pipe onto the buttress. The datasonde was suspended within the steel pipe by wire from the steel cap. Datasondes were equipped with pH, EC, water depth, and temperature sensors, and were calibrated monthly using Thermo Orion Application Solutions (1413 and 12 880 µS cm<sup>-1</sup>) and LabChem pH buffer solutions at pH 4, 7, and 10. Depth was calibrated to air pressure while temperature remained uncalibrated. The 37 km datasonde was removed at the end of August 2007, while the 60 km datasonde recorded data until the end of July 2009.

### 2.4. Flow measurements

Flow was measured at sampling sites along Wybong Creek using a hand-held Ott C2 '10.150' small current flow meter, whereby flow and depth was measured at 0.5 – 1.0 m increments across Wybong Creek. Hourly and mean daily flow measurements were also recorded by the Yarraman Gauge (Station 210040), located at the 72 km sample site (Figure 2.1; NSW DWE 2008).

### **2.4.1. Solute fluxes**

The salt load discharged from the catchment by Wybong Creek was calculated using daily flow and EC data from the Yarraman gauging station (210040; NSW DWE 2008). Electrical conductivity was multiplied by 0.67 to give TDS in mg L<sup>-1</sup> (Rayment and Higginson 1992), with this conversion factor checked against known EC to TDS ratios at the site. Missing data occurred on a number of dates, with mean EC and discharge values from the three weeks before the missing data used to fill these dates.

## **2.5. Hydrological analyses**

A number of climate stations measuring a small number of parameters are available within the Wybong Creek catchment. Climate data from the Scone SCS climate station, located within 20 km of the upper catchment, was instead used throughout this thesis. This was due to the Scone SCS station conducting measurements of all the parameters necessary for calculations over a long (>50 years) time period and having a similar (e.g. 640 mm at Bunnan versus 648 mm at Scone SCS) annual rainfall as the Wybong climate stations (ABM 2009).

The potential evapotranspiration for the catchment was calculated using a derivation of the Penman equation specific to south-eastern Australia (Meyer 1999). Changes in the quantity of water evapotranspirated from the catchment due deforestation were calculated based on a change from 100 % Eucalyptus dominated woodland, to 10 % cropland, 74 % grassland, and 16 % Eucalypt forest. Crop area statistics were taken from Beale *et al.* (2004), with the difference between remaining woodland and cropping calculated as the area of grassland. The climate aridity index was calculated using methods described by the Food and Agriculture Organisation of the United Nations (1989), whereby rainfall was divided by the potential evapotranspiration.

### **2.5.1. Aeolian deposition**

The mass of solutes deposited on the catchment with rainfall was calculated by multiplying the annual rainfall received at the Scone SCS weather station by the Wybong Creek catchment area (800 km<sup>2</sup>) and by the mean solute concentration in rainwater samples collected in this study (ABM 2009). This calculation was based on the assumption that the mean rainfall received over the entire Wybong Creek catchment is analogous to that received at the Scone SCS weather station. In the absence of wet-only and dry-only rain gauges, an approximation of dust deposition was made based on methods described by Appelo and Postma (2005). Dry deposition was estimated using

the ratio of Na to Cl in seawater (0.86) multiplied by Na concentration in Wybong rainwater, which gave the proportion of solutes sourced from rainwater and the proportion sourced from dust.

### 2.5.2. Evapoconcentration

The effects of evaporation on surface water were calculated using Eq. 2.2,

$$\% V = \frac{100}{(f)} \times \left( \left( \frac{d}{v} \right) \times \frac{86\ 400s}{day} \times E \times W \times \frac{1000L}{m^3} \right) \quad (2.2)$$

where  $\% V$  is the percent change in volume of Wybong Creek per day due to evaporation; flow is  $f$  ( $L\ day^{-1}$ ) at the sampling site;  $d$  (m) is the distance the water had travelled from the previous site as measured using MapInfo Professional 8.0 Geographical Information System (2005);  $v$  is the velocity ( $m\ s^{-1}$ ) of water measured at the sampling site; and 86 400 is the number of seconds in a day. Pan evaporation is  $E$  ( $m\ day^{-1}$ ); specific to each month (ABM 2009); and  $W$  is the width of Wybong Creek (m). The change in solute concentration due to volume decrease was then calculated (Eq. 2.3):

$$\% C = \% V \times C \quad (2.3)$$

where  $\% C$  is the change in solute concentration at the surface water sampling site;  $\% V$  is the decrease in volume between sites as calculated in Eq. 2.2; and  $C$  is the solute concentration (TDS,  $mg\ L^{-1}$ ) at the surface water sampling site.

## 2.6. Time-series analyses

Time-series data of EC and temperature were collected from the two Hydrolab MiniSonde 5 instruments installed at the 37 km and 60 km sample sites, and from the gauging station at the 72 km sample site (Section 2.3 – 2.4). Hourly air pressure data was collected from the Australian Bureau of Meteorology (2009) and theoretical tide data was calculated using the Tsoft program (Van Camp and Vauterin 2005). Fast Fourier transforms (FFTs) of these data were conducted using Tsoft, with spectral analyses conducted using MATLAB 7.4 (2007).

## 3. Results and discussion

A general discussion on the chemistry of Wybong Creek is presented first in the following results and discussion, followed by possible solute sources to the river and processes causing changes to solute concentrations. Raw data for the following results and discussion can be found in Appendix for Chapter Two (Tables A2.3 – A2.5), with time-series data compiled on the accompanying DVD.

### 3.1 Wybong Creek salinity

Salinity in Wybong Creek was initially assessed by measuring electrical conductivity (EC), which increased from  $517 - 807 \mu\text{S cm}^{-1}$  at the first sampling site to between  $740 - 1143 \mu\text{S cm}^{-1}$  at the 55 km sampling site, a rate of between  $1 - 70 \mu\text{S cm}^{-1} \text{ km}^{-1}$  (Figure 2.2). Electrical conductivity more than doubled between the 55 km and the 60 km site during drought conditions. Electrical conductivity continued to increase by  $60 - 378 \mu\text{S cm}^{-1}/\text{km}$  downstream of the 60 km sampling site during drought conditions, with increases of  $1 - 49 \mu\text{S cm}^{-1}$  after drought conditions eased post

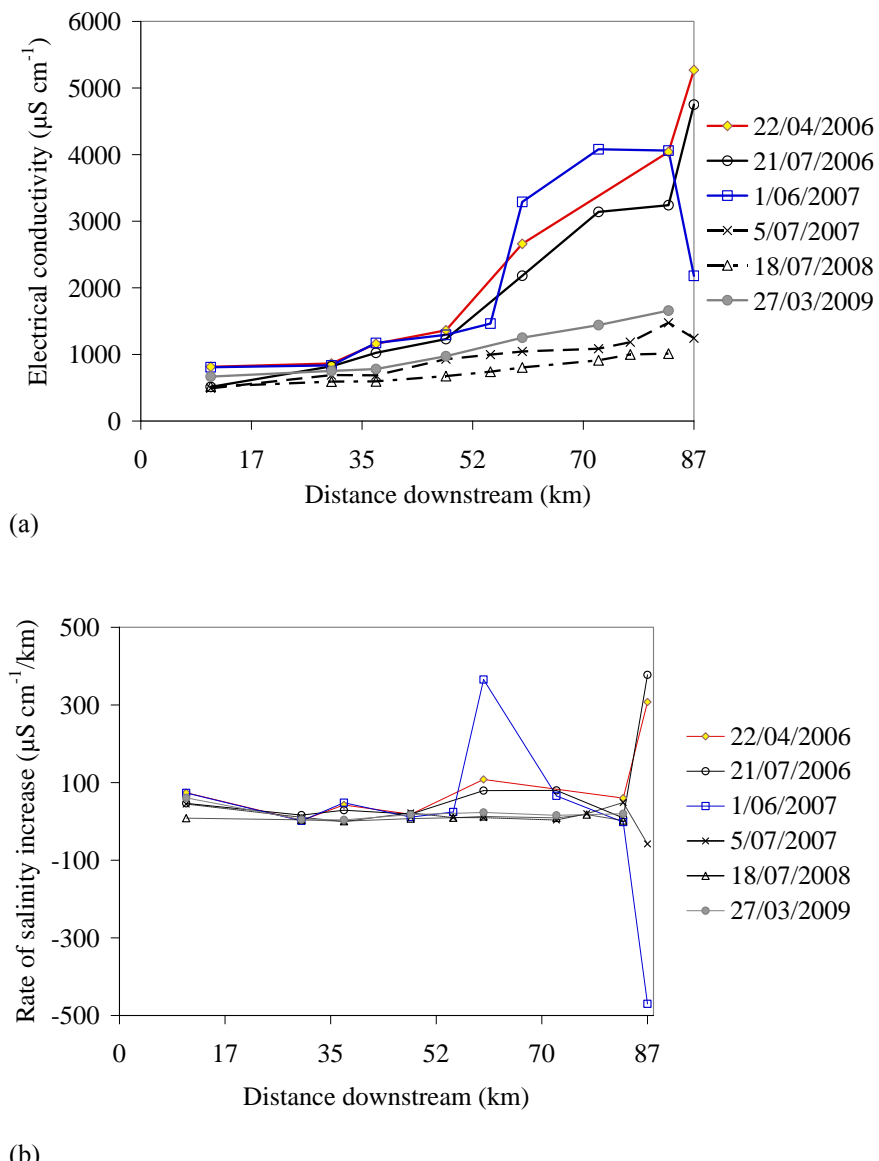


Figure 2.2. (a) Salinity ( $\mu\text{S cm}^{-1}$ ) at surface water sampling sites on different sample dates (DD/MM/YYYY); and (b) rate of salinity increase as a function of distance down Wybong Creek (km) on different sampling dates. Distances were calculated using the Geographic Information System (GIS) MapInfo.

June 2007. Decreases in salinity occurred in the last 15 km of Wybong Creek on some sampling occasions post June 2007, presumably due to dilution by the Goulburn River which was similar in elevation to the last one kilometre of Wybong Creek.

The gradual increase in salinity in the upper 55 km of Wybong Creek occurred in water dominated by Na, Mg, and HCO<sub>3</sub> (Figure 2.3). From 60 km down to the 90 km sampling point one kilometre above the Goulburn River, saline water was dominated by Na, Mg and Cl. A transition zone occurred mid-catchment between the 48 km to the 55 km sample sites, where Cl concentrations increased and Cl and HCO<sub>3</sub> were codominant anions. This increase in Cl concentration corresponded to the increase in overall salinity as measured by EC.

### 3.2. Causes of salinity and salinisation processes in Wybong Creek

The source of solutes and the means by which some solutes dominate surface water chemistry can be elucidated using hydrochemical data. Solute sources include aeolian deposition and groundwater discharge, with mineral precipitation, and evapoconcentration processes by which solute proportions increase and/or change relative to each other. Solute sources and the means by which solutes come to change proportion will be discussed separately in the following results and discussion.

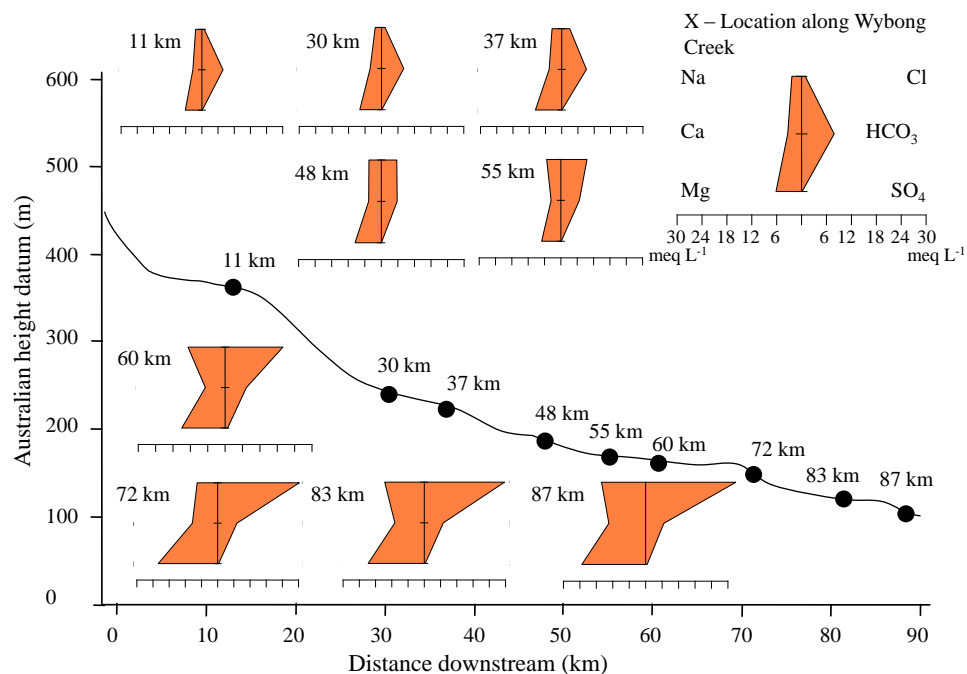


Figure 2.3. Mean major cation and anion concentrations ( $\text{meq L}^{-1}$ ) at surface water sampling sites in Wybong Creek during the low flow (drought) conditions of 2006 – June 2007. Elevations are in Australian height datum (m) on the y-axis, with distance along the river channel (km) on the x-axis.

### 3.2.1. Sources of salinity

Solutes arrive in catchments through aeolian accession. Solutes acquired through aeolian accession, which includes both salts dissolved in rainwater and entrained with dust, may then be mobilised by surface or groundwater within a catchment.

Groundwater may acquire solutes apart from aeolian sources, with aeolian accession and groundwater discharge discussed separately in the following sections.

#### 3.2.1.1. Aeolian accession

Rain contains solutes from the oceans where it forms and is the main source of solutes to a number of Australian catchments (e.g. Salama 1999; Jolly *et al.* 2001), with areas receiving winter dominated rainfall the most prone to salinisation (Bradd *et al.* 2007). Rainfall is summer dominated in the Wybong Creek and is often observed in the form of thunderstorms. Evaporation is highest in the summer months and exceeds rainfall for the entire year (Table 2.1). The mean annual salt deposition on the Wybong catchment was calculated based on the six rainwater samples collected during this study (Table 2.2), which included one rainwater sample collected during the initial hours of the extreme rainfall event of June 6<sup>th</sup> 2007, where more than 300 mm fell on some parts of the Hunter Catchment (ABM 2009). The low solute concentrations of this rainfall were used to calculate the minimum deposition on the catchment ( $0.4 \text{ t km}^{-2} \text{ yr}^{-1}$ ), which were also based on the minimum amount of rainfall received on the catchment according to meteorological records (ABM 2009). The maximum deposition on the catchment was  $23.2 \text{ t km}^{-2} \text{ yr}^{-1}$ , based on calculations using maximum solute concentrations seen in rainwater samples and the maximum annual rainfall. The mean solute deposition on the catchment, based on mean solute concentrations in six rainwater samples and mean rainfall received at Scone SCS, was instead  $5.65 \text{ t km}^{-2}$ , or  $0.06 \text{ t ha}^{-1}$ .

Data presented by the NSW EPA (1994) on rainwater chemistry in the upper Hunter Valley and climate data from Scone (SCS) climate station were used to attain another estimate of salt deposition on the catchment. These results indicated that deposition was  $21.1 \text{ t km}^{-2} \text{ yr}^{-1}$  or  $0.2 \text{ t ha}^{-1} \text{ yr}^{-1}$  in 1987. Salt deposition in the western Hunter catchment has been measured at  $4 \text{ t km}^{-2} \text{ yr}^{-1}$  (Beale *et al.* 2000), while mean aeolian accession in the Murray – Darling catchment is approximately  $5 \text{ t km}^{-2} \text{ yr}^{-1}$  (Herczeg *et al.* 2001). These values were within the ranges calculated using data collected in this study. The quantity of salt acquired via rainfall in the Wybong Creek catchment is typical of other areas within the Hunter and in the neighbouring Murray-Darling Basin

---

Table 2.1. Monthly evaporation ( $E$ , mm) as measured by a Class A evaporation pan, and monthly precipitation ( $P$ , mm) at the Scone SCS meteorological station (ABM 2009).

	Jan	Feb	Mar	Apr	May	Jun	Jul	Aug	Sep	Oct	Nov	Dec	Ann
Mean $P$ (1952 – 2008) (mm)	87	77	52	40	48	45	36	39	36	60	60	69	648
2006 $P$ (mm)	30	41	7	61	4	20	23	6	30	3	74	21	319
2007 $P$ (mm)	33	35	82	20	35	210	8	49	4	35	165	110	785
2008 $P$ (mm)	36	111	11	41	14	79	47	53	72	50	73	75	663
Mean $E$ (1952 – 2008) (mm)	217	175	155	108	68	48	56	84	117	458	183	220	1589
$P-E$	-130.3	-97.95	-103.5	-68.3	-20.7	-3.3	-19.9	-44.5	-77.5	-98.2	-123.2	-151.4	-941

Table 2.2. Discharge ( $Q$ , ML yr $^{-1}$ ) and salt flux ( $S$ , t TDS yr $^{-1}$ ) from, and salt deposition (t TDS yr $^{-1}$ ) on the Wybong Creek catchment during three years of sample collection for this study. Output to input ratios reflect aeolian deposition on the catchment versus discharge in surface water.

	$Q$ (ML yr $^{-1}$ )	$S$ (t TDS yr $^{-1}$ )	Deposition (t TDS yr $^{-1}$ )	Output:Input
2006	77	170	2229	0.08
2007	11100	18700	5485	3.41
2008	28513	16100	4632	3.48
Total (2006-2008)			12345	
Mean (2006-2008)			4115	

catchment; however, the summer dominated rainfall received in the catchment is not typical of other regions suffering dryland salinity. Further data acquisition is necessary in order to better constrain salt deposition on the catchment, however, which should include integration of different rainfall quantities across the catchment and rainwater sample collection across all seasons and over a number of years.

Salts are known to accumulate in catchments during drought periods and across geological time before being flushed into river systems when increased rainfall and/or recharge occurs (e.g., Ruprecht and Schofield 1991a; Summerell *et al.* 2006). This typically results in more salt fluxed from the system (output) than is received via rainfall (input) within catchments suffering dryland salinity. Salt fluxes from the Wybong Creek catchment were 170 – 18 700 t yr $^{-1}$ , with mean salt deposition on the catchment 4115 yr $^{-1}$  for 2006 – 2008 (Table 2.2). Aeolian salt accession can account for the entire flux of solutes during 2006, where 2059 t of aeolian salt was stored in the catchment and 170 t removed. More than 3.4 times as much salt was removed as was received in 2007, with 3.5 times as much removed as was received in 2008. Output:input ratios in catchments suffering dryland salinity range in value from 1.2 – 5.1 in the Murray catchment (Jolly *et al.* 2001); from 5.3 in the Lemon Catchment (Ruprecht and Schofield 1991a) up to 425 in the Cuballing catchment of Western Australia (Salama *et al.* 1993b); and between 5.5 and 15.1 in the Mount Loft Ranges in South Australia (Poulsen *et al.* 2006). Output to input ratios within the Wybong Creek catchment were, therefore, not atypical of those in other catchments which suffer from dryland salinity.

Rainwater solutes may originate from dust or from oceanic sources (e.g., Salama 1999; Abudauwaili 2008). Calculations based on the proportion of Na and Cl in Wybong rainwater relative to seawater indicated that up to 92 % of the solutes measured in the rainwater were from marine sources, with a mean of 50 % of salts in rainwater sourced from dust and from marine sources (Table 2.3). Calculations indicated 100 % of the solutes were from dust in some samples, however, this is unrealistic and was likely

Table 2.3. Na, Cl and TDS concentrations in rainwater samples collected in this study and seawater contribution to the salt concentration based on calculations described in Appelo and Postma (2005).

Site	Date (DD/MM/YYYY)	TDS (mmol L <sup>-1</sup> )	Na (mmol L <sup>-1</sup> )	Cl (mmol L <sup>-1</sup> )	Contribution from seawater (mmol Na L <sup>-1</sup> )	Dust contribution (%)
Denman	06/06/2007	0.06	0.029	0.011	0.00	100
	07/06/2007	0.01	0.002	0.011	0.00	100
Muswellbrook	03/09/2007	0.18	0.026	0.014	0.01	53
	22/12/2007	0.32	0.029	0.011	0.00	100
	19/01/2008	0.49	0.033	0.033	0.03	12
Wybong	21/07/2008	0.06	0.014	0.017	0.02	-5
Mean		0.21	0.043	0.016	0.02	50

due to the low salt concentration in rainwater causing calculation errors (Appelo and Postma 2005). Aeolian pollution has been investigated within the Hunter Valley on a number of occasions, due to the presence of the Bayswater power station, located within 30 km of the lower Wybong catchment (e.g., SPCC 1987; Bridgman 1998). These studies showed sulfur aerosols sourced from the Bayswater power station were an important source of dust to the upper Hunter Valley, with these also a likely source of solutes to the rainwater samples collected for this study. This pollution was not an important contributor of salt to Wybong Creek, however, as sulfur made up only a small proportion of the total anion concentration measured in the river (Figure 2.3).

### 3.2.1.2. Groundwater discharge

Regular increases and decreases in EC occurred at the 60 and 72 km sampling sites, where EC, temperature, water height, and pH were recorded on an hourly basis. Instruments at both sites were calibrated regularly and contained temperature compensation mechanisms, with the effects of temperature on EC measurements discounted as a cause of EC fluctuations. Electrical conductivity increased sharply during the first two weeks of September 2007, with irregular diurnal EC oscillations occurring at the 60 and 72 km sampling sites (Figure 2.4). From September 14<sup>th</sup> diurnal fluctuations became more regular, with a daily range of between 37-58 µS cm<sup>-1</sup>. Peaks occurred at the 72 km sampling site 14 hours after those at 60 km sampling site. Fluctuations occurred at both sites in October 2007 also (data not presented) though only at the 60 km sampling point and only on some days in November 2007 (Figure 2.4). Fluctuations in EC were around 350 µS cm<sup>-1</sup> at the 60 km sampling point from the 11<sup>th</sup> to the 21<sup>st</sup> of November, with peaks occurring between 6 pm and midnight and troughs between 10 am and 2 pm. Though peaks did not occur at the 72 km sample

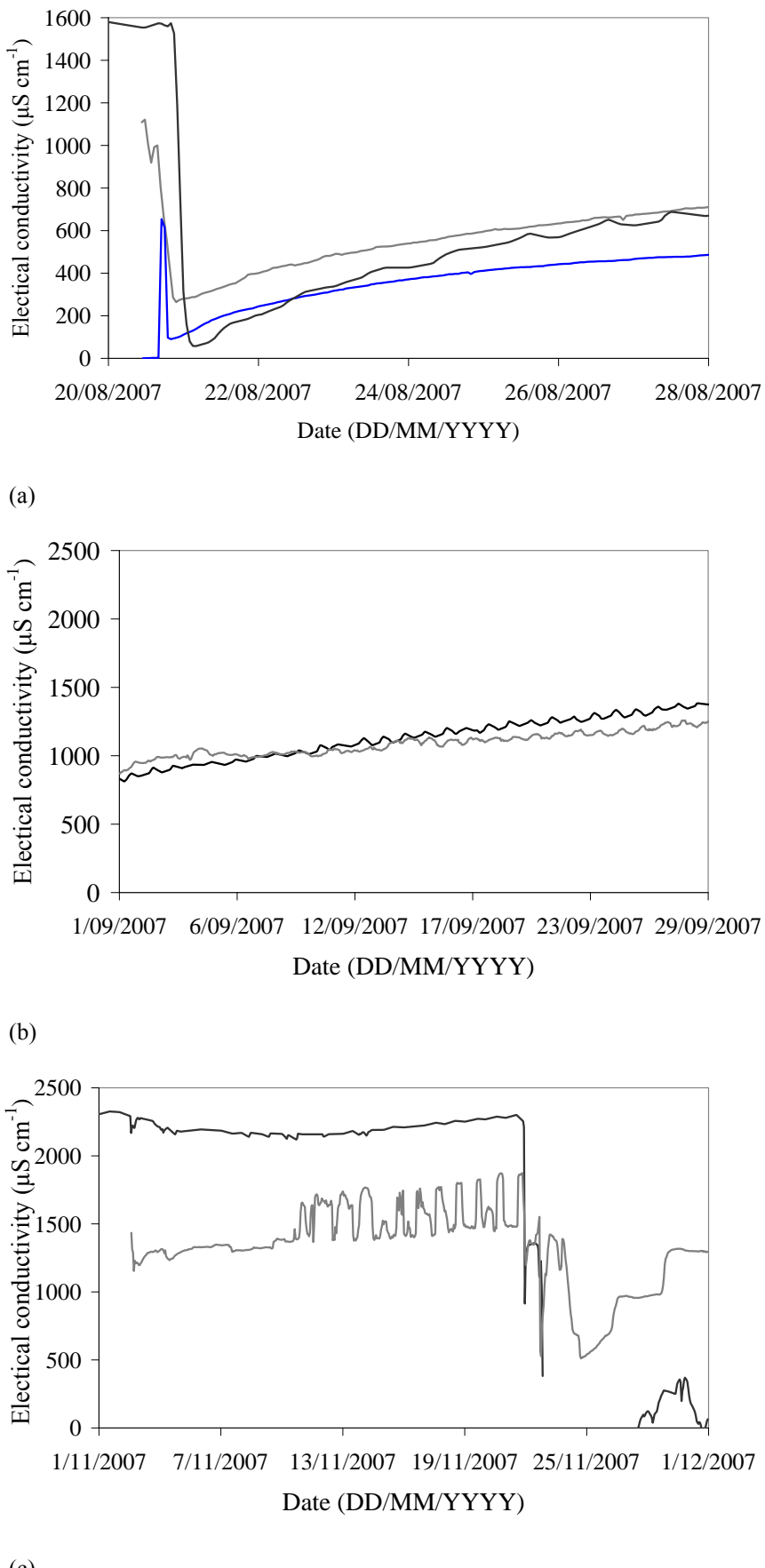


Figure 2.4. Electrical conductivity ( $\mu\text{S cm}^{-1}$ ) recordings of Wybong Creek at the 37 (—), 60 (—), and 72 km (—) sampling sites, during (a) August 2007; (b) September 2007; and (c) November 2007.

point, EC increased until 2 pm – 7 pm, and levelled out during the night before increasing again. Electrical conductivity fluctuations occurred at the 72 km sample site from the 20<sup>th</sup> to the 28<sup>th</sup> August 2007, but contrastingly did not occur at the 60 km sample site, nor at the 37 km sample site where another instrument was briefly installed.

The regular fluctuations in EC were not related to evapoconcentration as indicated by peaks occurring late in the day and at different times of the day at different sites. Detectable fluctuations in pH were not seen, with changes in pH within instrument error (0.1). Diel changes in a number of water quality parameters have been noted by a number of authors, and have been attributed to variations in dissolved oxygen and pH; Mn and Fe redox reactions in the hyporheic zone; solar influence on pH and temperature; changes in groundwater use; and the evapotranspiration and respiration cycles of aquatic and riparian vegetation (Wetzel 2001; Gandy *et al.* 2007). The Creek is incised into Widden Brook Conglomerate at both sites, with shallow sediment and the absence of organic sediments indicating that chemical reactions within the sediment were unlikely to cause EC fluctuations in Wybong Creek. Manganese and Fe did not occur in measurable concentrations at this site, also limiting the possibility that these elements could cause such significant fluctuations in EC (Table A2.4). A change in EC may be expected as a result of photosynthetic reactions in plants and biotic respiration. Minimal riparian vegetation remains along Wybong Creek, however, limiting the effects photosynthesis could possibly have had on surface water EC.

Faulty temperature compensation and/or a relationship between temperature and salinity was investigated as causing fluctuations to EC using time-series analyses. The trend of increasing salinity and temperature was removed from the data using fast Fourier transformation, in order that trends could be examined more accurately (Shumway 1988). Peaks in salinity occurred after temperature peaks at the 60 km sample site, indicating that peaks were real rather than due to failure of EC-temperature compensation mechanisms within the instruments (Figure 2.5). Temperature and salinity were better correlated at the 72 km sample site, though similar periodicity of both EC and temperature spectra occurred at both sites (Figures 2.6 – 2.7). The lag between temperature and EC indicated an indirect relationship, though cross-spectral analyses indicated high coherence between the two, especially at the 72 km sample site. Groundwater heights may fluctuate with temperature, with increases in groundwater heights occurring when groundwater becomes warmer (Rose 2004). Changes in hydraulic gradient which occur as a result of these fluctuations may have possibly caused increased fluxes of groundwater to the creek which occur slightly after

---

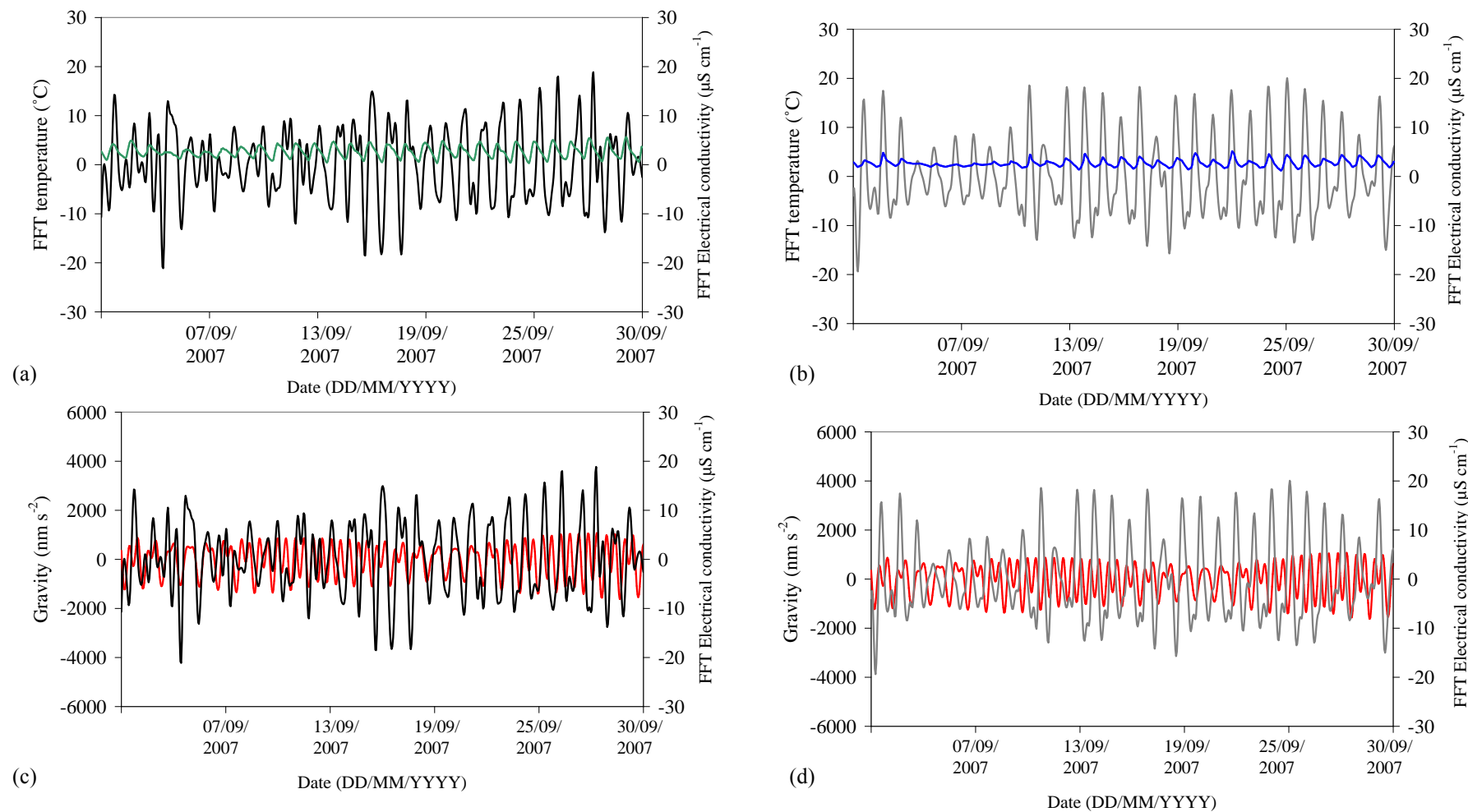


Figure 2.5. (a) Relationships between electrical conductivity (—) and temperature (—) at the 60 km site; (b) electrical conductivity (—) and temperature (—) at the 72 km sample site; (c) electrical conductivity and theoretical Earth tides (—) at the 60 km sample site; and (d) electrical conductivity and theoretical Earth tides at the 72 km sample site. Theoretical Earth tide data for these sites were calculated using the Tsoft package (Van Camp and Vauterin 2005).

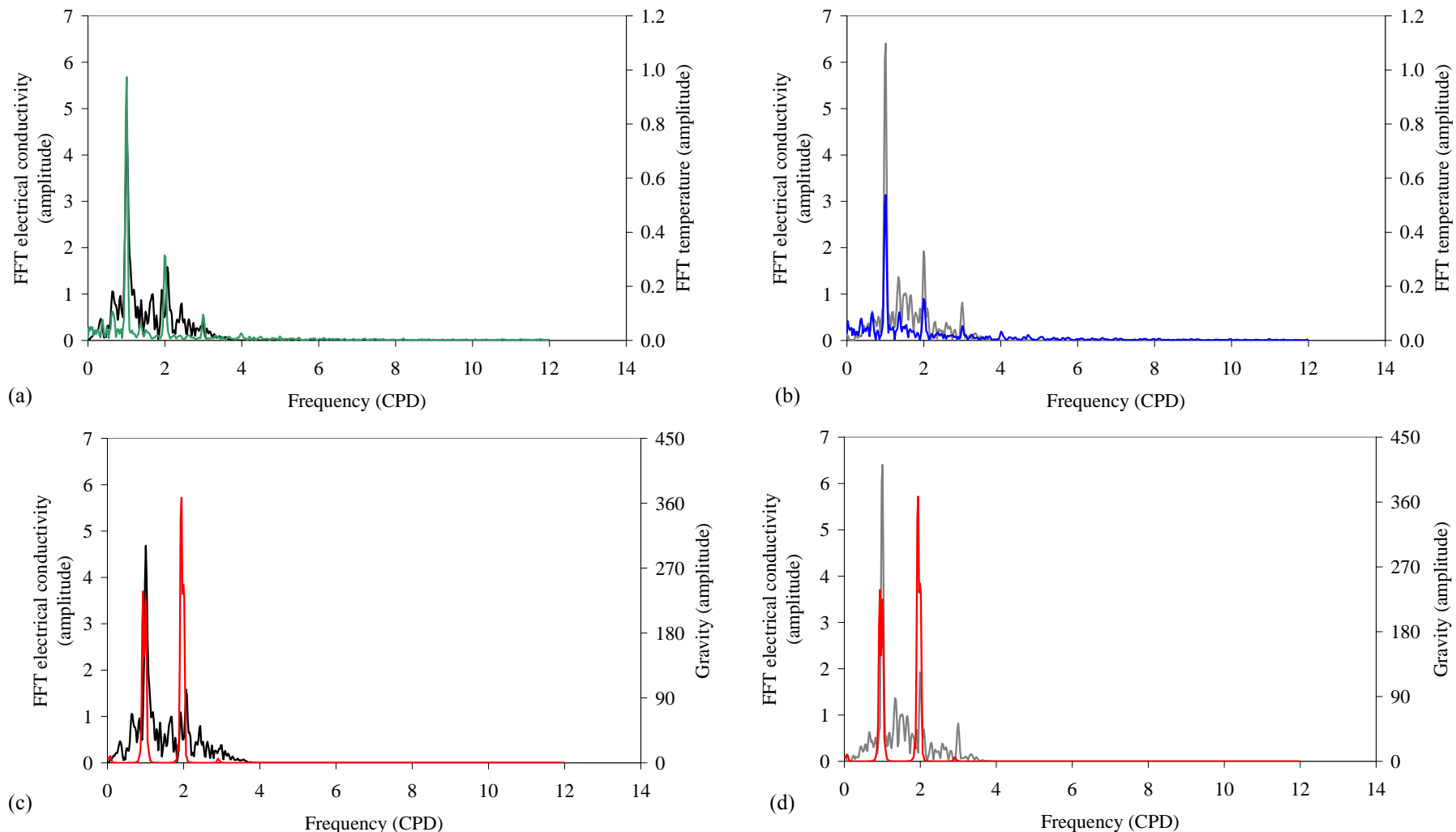


Figure 2.6.

Spectra of fast Fourier transformed (FFT) data collected in September 2007. (a) Electrical conductivity (1° y-axis; —) and temperature (2° y-axis; —) at the 60 km site; (b) electrical conductivity (1° y-axis; —) and temperature (2° y-axis; —) at the 72 km sample site; (c) electrical conductivity and theoretical Earth tides (2° y-axis; —) at the 60 km sample site; and (d) electrical conductivity and theoretical Earth tides at the 72 km sample site.

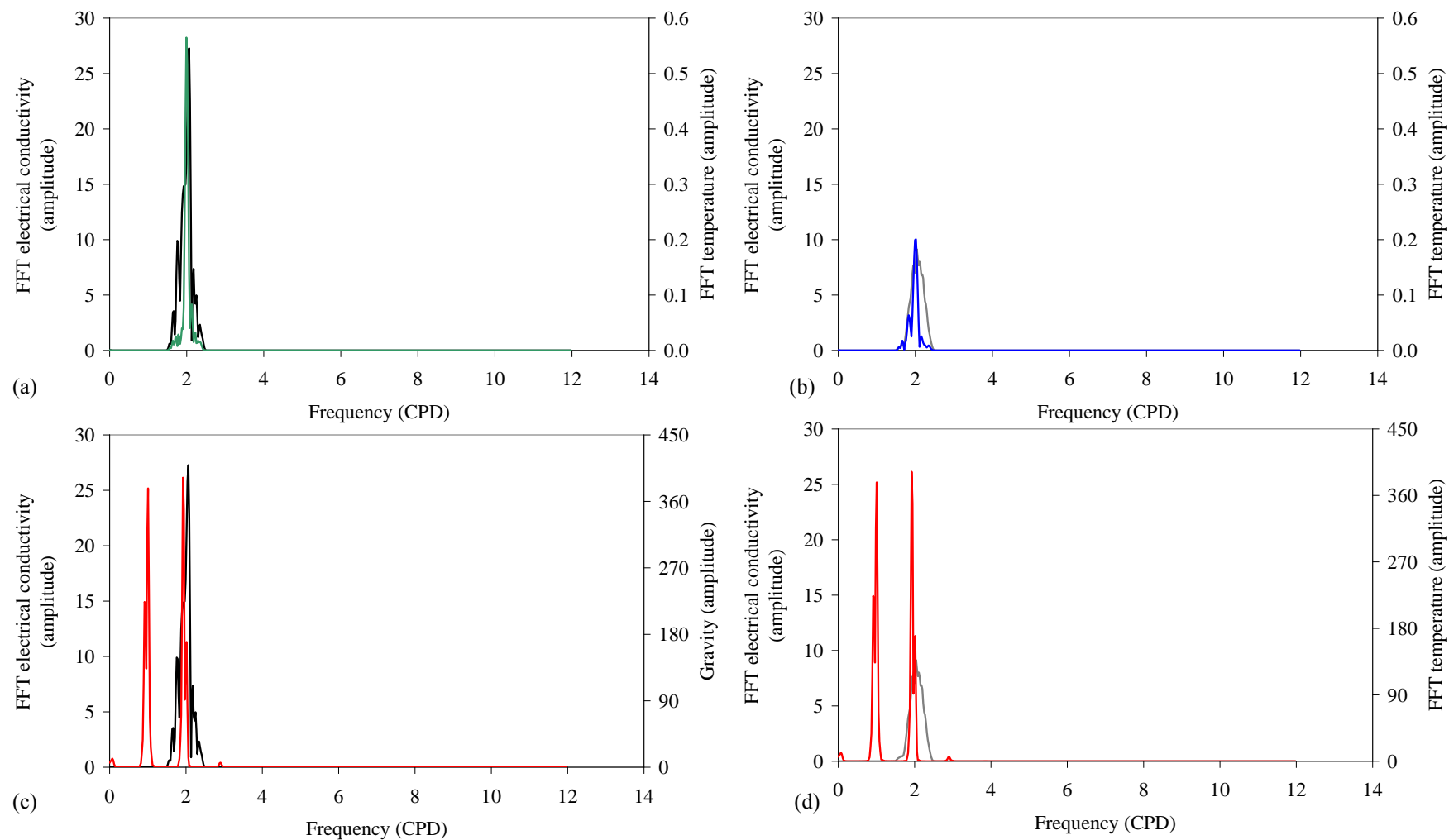


Figure 2.7.

Spectra of fast Fourier transformed (FFT) data collected in November 2007. (a) Electrical conductivity (1° y-axis;  $\text{—}$ ) and temperature (2° y-axis;  $\text{—}$ ) at the 60 km site; (b) electrical conductivity (1° y-axis;  $\text{—}$ ) and temperature (2° y-axis;  $\text{—}$ ) at the 72 km sample site; (c) electrical conductivity and theoretical Earth tides (2° y-axis;  $\text{—}$ ) at the 60 km sample site; and (d) electrical conductivity and theoretical Earth tides at the 72 km sample site.

temperature peaks. Further analyses were also conducted, in order to identify other processes which may have been causing this phenomenon.

Groundwater heights are known to increase and decrease in confined aquifers due to the elastic response of aquifer materials to loading. Trains, air pressure, and the gravitational pull of the moon are means of loading and unloading an aquifer to cause such changes in groundwater height (Domenico and Schwartz 1990). Trains do not operate in the Wybong Creek catchment, with no relationship seen between air pressure and EC. Similar periodicity was seen between EC and gravity fluctuations, however, with fluctuations in gravity causing oceanic, atmospheric and Earth tides (Figure 2.5). Earth tides occur when elastic materials at the Earth's surface are pulled towards a gravitational body (i.e. the moon or sun), with groundwater levels lowering when the gravitational pull is greatest due to decreased loading (Domenico and Schwartz 1990). Peaks in EC and gravity had similar spectra at both the 60 and 72 km sampling site. Only one peak per day is seen in EC, however, with two peaks per day seen in gravity. High coherence occurred between gravity and EC at the 72 km sample sites (Figure 2.6).

An EC and tide relationship could not have been caused by tidal intrusion of seawater (e.g., Kim *et al.* 2005), with the 60 and 72 km sample sites located at 170 m and 160 m above sea level respectively. Instead, different volumes of saline groundwater appear to be discharging from a confined aquifer adjacent to Wybong Creek in the mid-lower catchment in response to temperature, Earth tides, or some unidentified phenomenon. Water height in Wybong Creek did fluctuate, however, the signal was weak (Figure 2.8). This indicates that the influx of saline water into Wybong Creek caused changes in surface water height that were barely detectable by the instruments, and may indicate that rather than high volumes of slightly more saline water moving into Wybong Creek, smaller influxes of much more saline water occurred. The cyclical increase and decrease of EC may occur only during some months and at some sites during some months due to the effects of other phenomena, such as rainfall, groundwater recharge, and evaporation, causing groundwater heights to alter in such a way that flows into Wybong Creek changed and no longer caused EC to fluctuate, with the relative difference between groundwater and surface water salinity also likely to have an effect.

The cause of the increase in Cl and EC in the area between the 60 and 55 km sample sites was investigated by sampling EC at 10 – 500 m increments above the 60 km sample site during January 2009 (Figure 2.9). Two areas of significant groundwater

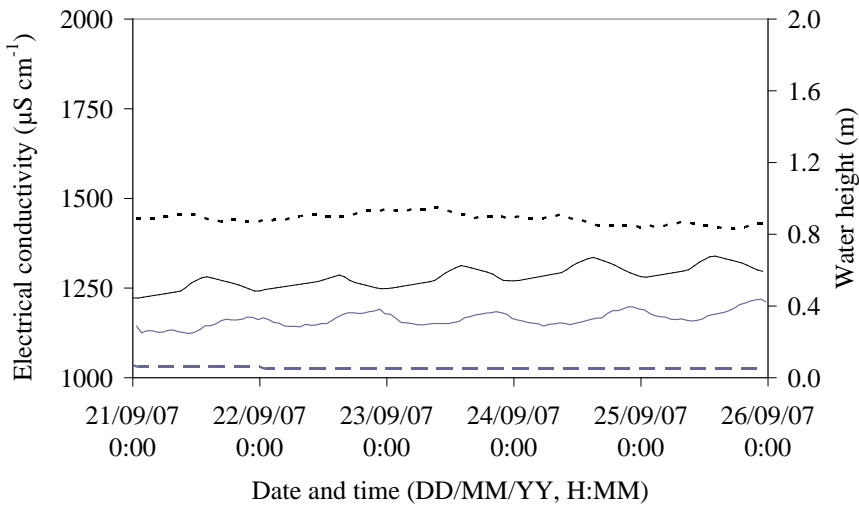


Figure 2.8. Electrical conductivity ( $\mu\text{S cm}^{-1}$ ) recordings of Wybong Creek at the 60 km sample site (—) and the 72 km sample site (—) vs water height at the 60 km sample site (--) and the 72 km sample site (- -).

input were identified. The first occurred approximately 140 m above the 60 km sample site. Wybong Creek narrowed to a pool which was 20 m long by three metres wide, with no tributaries or channels adjacent to this site though a tributary channel occurred ~15 m further upstream. Salinity in this pool increased from 1350 to 1420  $\mu\text{S cm}^{-1}$  at the surface of the pool to a maximum of 2280  $\mu\text{S cm}^{-1}$  at a depth of 1.2 m in the middle of the pool. Water flow increased from  $0.01 \text{ m}^3 \text{ s}^{-1}$  upstream of the pool to  $0.024 \text{ m}^3 \text{ s}^{-1}$  downstream of the pool, an increase of 43 %. A second spike in salinity occurred in a riffle zone 70 m above the Wybong Creek site. Salinity increased from 1480  $\mu\text{S cm}^{-1}$  to 1820  $\mu\text{S cm}^{-1}$  in 10 m, and up to 1927  $\mu\text{S cm}^{-1}$  10 m further downstream (Figure 2.9). Flow was not measured upstream and downstream of the riffle zone. The increase from the downstream end of the “Salt Pool” to the 60 km sample site, however, was  $0.06 \text{ m}^3 \text{ s}^{-1}$  – an increase of 28 %. None of these differences in salinity were found when the area was investigated again on the 15<sup>th</sup> May 2009, with only gradual increases in salinity from 1093  $\mu\text{S cm}^{-1}$  above the salt pool, to 1202  $\mu\text{S cm}^{-1}$  at the 60 km sample site.

The increase in salinity upstream of the 60 km sample site was abrupt, with salinity only increasing 64  $\mu\text{S cm}^{-1}$  in the first 4.8 km below the 55 km sample site, and then 500  $\mu\text{S cm}^{-1}$  in the last 140 m (Figure 2.9). The water moving into the Creek at the pool had similar Na/Cl ratios,  $\text{HCO}_3^-$  and major cation concentrations to the surface water above the pool, however, Cl/Br,  $\text{SO}_4^{2-}$ , Cl, and overall TDS concentrations were much higher (Table 2.4). The only source of water to the pool and riffle sequence at the

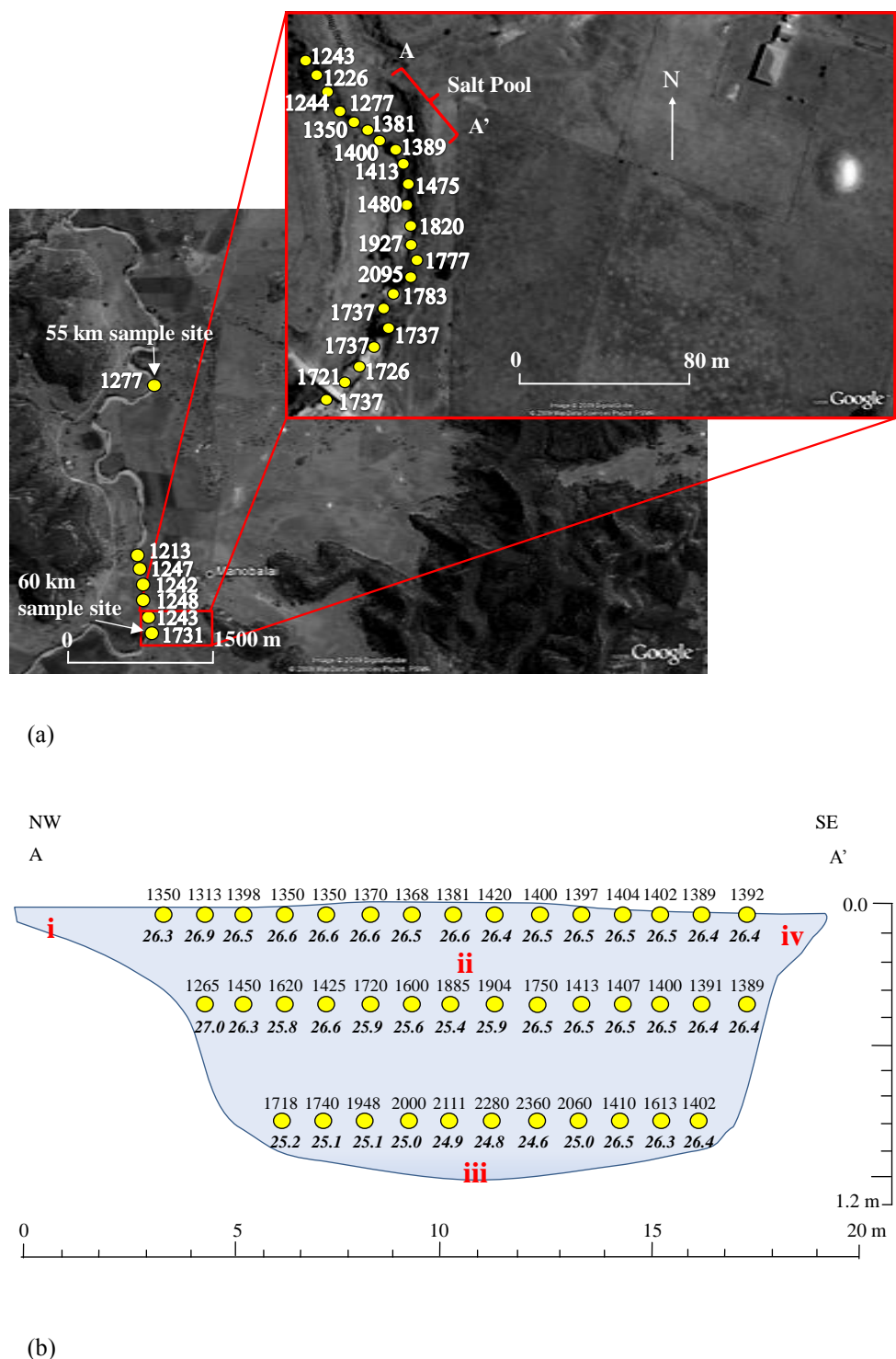


Figure 2.9. (a) Electrical conductivity ( $\mu\text{S cm}^{-1}$ ) measurements conducted between the 55 km and 60 km sample sites on the 20<sup>th</sup> of January 2009. Electrical conductivity was initially measured every 200 m, with the inset showing measurements every 10 m; (b) Electrical conductivity measurements every meter (●) within the “Salt Pool,” along the transect marked A-A’. Temperature ( $^{\circ}\text{C}$ ) measurements are presented in italics. Roman numerals indicate sample collection points for major cation and anion analyses.

60 km sample was groundwater, with Na/Cl and Cl/Br ratios indicative of water influenced by halite and seawater and/or rainwater mixing (e.g. Davies *et al.* 1998). In addition, the point source salinity increases in the pool indicated that this groundwater

Table 2.4. Major cation and anion concentrations, and molar Na/Cl and Cl/Br ratios in water samples collected from the “Salt Pool.” Sites refer to sampling points within the “Salt Pool” as depicted in Figure 2.9.

Site	TDS (mg L <sup>-1</sup> )	Ca (mg L <sup>-1</sup> )	Mg (mg L <sup>-1</sup> )	K (mg L <sup>-1</sup> )	Na (mg L <sup>-1</sup> )	Cl (mg L <sup>-1</sup> )	SO <sub>4</sub> (mg L <sup>-1</sup> )	HCO <sub>3</sub> (mg L <sup>-1</sup> )	Cl/Br (molar)	Na/Cl (molar)
i	720	25	50	2.4	39	50	8	421	552	0.8
ii	835	29	64	4.8	49	100	9	390	751	0.8
iii	939	31	68	4.2	59	130	12	404	977	0.7
iv	1134	35	82	4.0	88	190	20	390	1071	0.7

flowed into the Creek through fractures. This was corroborated by saline seeps moving into Wybong Creek from fissures in the conglomerate at the 60 km sample site, which were exposed after flooding in the catchment during June 2007.

### 3.2.2. Processes changing solute concentrations

The concentration and relative proportion of solutes to each other changes in a river system due to processes such as evapoconcentration and mineral precipitation. Changes to the amount of evapotranspiration within a catchment does not directly cause changes to solute concentrations, but causes changes to the hydrological cycle at the Earth’s surface that may then bring about a change in solute concentration. These processes will, therefore, be discussed separately in the following discussion.

#### 3.2.2.1. Evapotranspiration

Decreased evapotranspiration within arid – semi-arid catchments leads to increases in groundwater recharge, which may then cause salinisation due to an increase in groundwater discharge bringing about solute dissolution at the Earth’s surface (e.g., Ruprecht and Schofield 1991; Salama 1993b). The climate aridity index calculated for the Wybong Creek catchment was 13.3 and above in June and July, and between 0.4 and 0.8 during all other months, indicating that Wybong Creek has an arid – semi-arid climate (Table 2.5). Evapotranspiration in the Wybong Creek catchment was calculated to have decreased in all months of the year as a result of deforestation as compared to pre-European colonisation (Table 2.5). The most significant differences in evapotranspirative water use occurred during the summer months, with the difference in winter being less substantial. Climate calculations indicated that precipitation only equalled or exceeded evapotranspiration during the months of May – July, with aridity possibly leading to salt storage during the rest of the year. Evapotranspiration was highest in the summer months both before and after deforestation, in contrast to other

Table 2.5. Estimated evapotranspiration (ET, mm day<sup>-1</sup>) from the Wybung Creek catchment before and after deforestation, and climatic aridity index based on post-deforestation evapotranspiration and precipitation data from Table 2.1., where p is precipitation.

	$E_T$ (mm day <sup>-1</sup> )		Difference (mm day <sup>-1</sup> )	Climatic Aridity Index
	Pre-deforestation	Post-deforestation	(Post – pre-deforestation)	(p/ET)
Jan	4.6	4.1	0.5	0.7
Feb	5.6	5.0	0.6	0.5
Mar	5.2	4.7	0.5	0.4
Apr	3.6	3.3	0.3	0.4
May	1.7	1.5	0.2	1.0
Jun	0.1	-0.1	0.2	>13.3
Jul	0.2	0.1	0.1	13.3
Aug	1.8	1.5	0.3	0.8
Sept	3.7	3.3	0.4	0.4
Oct	5.2	4.7	0.5	0.4
Nov	5.7	5.2	0.5	0.4
Dec	6.2	5.6	0.6	0.4

studies which have found that the highest rate of evapotranspiration from Eucalyptus forests occurs in the winter months (Sharma 1984). These results were possibly due to an error in calculated evapotranspiration as opposed to actual evapotranspiration, or due to adequate water received in Wybung Creek during the summer months to sustain higher evapotranspiration rates.

Evapotranspiration calculations reflected the aridity of the Wybung Catchment, and in addition, indicated that groundwater recharge is likely to have increased due to deforestation of the Eucalyptus forests previously present. Local families in the Wybung Creek catchment undertook deforestation during the late 1800s and early 1900s, with salt scalds occurring on some mid-catchment properties for all of living memory (D. Googe, Pers. Comm.; D. Ether, Pers. Comm). Dryland salinity, whereby groundwater tables rise as a result of deforestation and decreased evapotranspiration, cannot be excluded as causal salinisation process based on these findings. Results previously presented in this

chapter indicated salt input:output ratios in the Wybung catchment were typical of those suffering dryland salinity, with salt storage and increasing groundwater tables in the regolith a plausible source of solutes in the catchment.

### 3.2.2.2. Evapoconcentration

The effect of evaporation on solute concentrations in Wybung Creek surface water was approximated using pan evaporation data, though the non-laminar river surface, shading, and other environmental factors limit the accuracy of these results. Evaporation

was calculated to have caused solute concentrations to increase by 0.6 – 9.0 % between Wybong Creek sampling sites (Table 2.6). This amounted to a total increase in TDS of 9 – 33 %, or up to  $84 \text{ mg L}^{-1}$ . The increase in solute concentrations due to evapoconcentration was 23 and 6.4 % between the 37 and 48 km sampling points during July of 2007 and 2008 respectively. This higher value relative to other surface water sampling sites was due to both the greater width of Wybong Creek at the 48 km site and a causeway structure which dammed water and lowered water velocities, with the increased evaporative exposure of Wybong Creek at this site a result of slower flow. Higher evapoconcentration was seen during summer 2009 at all sites than in the winter months of 2007 and 2008. The maximum increase in TDS concentrations due to evapoconcentration was  $271 \text{ mg L}^{-1}$ , while TDS concentrations in Wybong Creek were calculated as being  $552 - 827 \text{ mg L}^{-1}$  without the evaporation of water (Table 2.6). These calculations are almost certainly an over-estimate of actual evapoconcentration, and indicate that Wybong Creek would be amongst the most saline 15 of 193 rivers running to the New South Wales coastline (Beale *et al.* 2004), even without the effects of evaporation.

Oxygen and H isotopes were analysed on water samples collected during winter (July) 2006, in order to provide another estimate of evaporative effects on Wybong Creek. One sample from both the upper and lower catchment was on or above a local meteoric water line (LMWL) which was very approximate due to only three rainwater samples being used (Figure 2.10). One sample from both the upper and lower catchment was also on or above the Melbourne (MMWL) and global (GMWL) meteoric water lines, while one from the upper and two from the lower catchment were below the meteoric water lines. The lack of a consistent enrichment in  $^{18}\text{O}$  and  $^2\text{H}$  with increasing distance from the Wybong Creek headwaters indicates no clear trend of evaporation (Clark and Fritz 1997) affecting Wybong Creek during winter 2006, and instead indicates different inputs of unevaporated groundwater affecting Wybong Creek along different sections of the river. Samples were unfortunately not collected for O and H isotope analyses on the days for which the effects of evapoconcentration have been calculated, and not during summer when the effects of evaporation were most significant. Further analyses involving samples collected in the summer is necessary to confirm that evapoconcentration has minor effects on solute concentrations in Wybong Creek.

Table 2.6. The effects of evapoconcentration ( $E$ ) on solute concentrations ( $C$ ) in surface water sampled from Wybong Creek on different dates (DD/MM/YYYY), based on Eq. 2.2. and Eq. 2.3. N/A indicates sites at which flow was not measured on the particular date. Example step-by-step calculations are shown in Appendix for Chapter Two (Table A2.6).

Site (km)	$E$ between sites (L)				$E$ between sites (%)				$C$ increase due to $E$ (mg L <sup>-1</sup> )			$C$ increase due to $E$ (%)		
	07/07/2007	18/07/2008	27/03/2009	07/07/2007	18/07/2008	27/03/2009	07/07/2007	18/07/2008	27/03/2009	07/07/2007	18/07/2008	*27/03/2009		
11	21007	106165	22315	2.3	0.2	0.1	-	-	-	-	-	-		
30	28738	187078	234220	0.1	0.2	0.9	6.5	5.5	57	0.8	1.2	8.3		
37	N/A	29689	13975	N/A	0.0	0.1	N/A	1.4	3.7	N/A	0.3	0.6		
48	535224	584914	67275	2.6	0.7	0.2	203	34	11.0	23	6.4	1.6		
55	N/A	256249	N/A	N/A	0.3	N/A	N/A	14	N/A	N/A	2.5	N/A		
60	113960	13248	10999	0.4	0.0	0.0	30	0.8	3.0	1.7	0.14	0.3		
72	46325	85907	174495	0.1	0.1	0.7	22	4.5	61	0.9	0.7	6.8		
77	12695	4144	N/A	0.0	0.0	N/A	7.3	0.2	N/A	0.3	0.02	N/A		
83	4678	75034	253605	0.0	0.1	0.9	1.6	4.9	84	0.06	0.7	8.1		
Total C increase	-	-	-	-	-	-	271	66	222	11	9.0	21		
$C$ at 83 km sample site	-	-	-	-	-	-	823	740	1049	-	-	-		
Increase due to $E$	-	-	-	-	-	-	-	-	-	33	9	21		

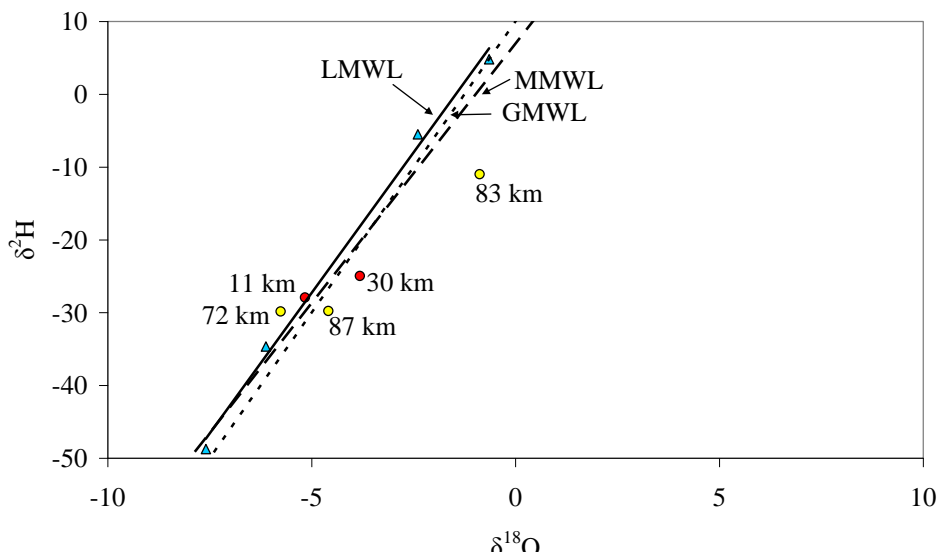


Figure 2.10.  $\delta^2\text{H}$  and  $\delta^{18}\text{O}$  data from rainwater samples ( $\blacktriangle$ ), surface water samples from the upper catchment (●), and from the lower catchment (○). The solid line indicates the approximate local meteoric water line (LMWL); the Melbourne meteoric water is indicated by the thick dashed line (MMWL line; ANSTO and CSIRO 2004); and the global meteoric water line (GMWL; Craig, 1961) is indicated by the thin dashed line.

### 3.2.2.3. Mineral precipitation

The chemical evolution of rivers through catchments is largely controlled by the dissolution and precipitation of minerals, with the precipitation of sulfate and carbonate minerals resulting in rivers being proportionally much higher in Na-Cl near their termini than at their headwaters (e.g., Gibbs 1970; Eugster and Hardie 1975). Calcite precipitates from most waters first and at low ionic strengths, with Wybong Creek saturated with high-Mg calcite for its entire length (Table 2.7; Figure 2.11), as indicated by calcite saturation indices and Mg/Ca ratios over 1.0 (Eugster and Hardie 1975; Hardie and Eugster 1970). Precipitation of calcite necessarily causes an increase in the proportion of Mg and Ca over  $\text{HCO}_3$ , or vice versa (Hardie and Eugster 1970). Ratios' of  $\text{HCO}_3/(\text{Ca}+\text{Mg})$  decreased in Wybong Creek with increasing distance downstream (Table 2.7). This indicates that carbonate precipitation likely caused Mg and Ca enrichment proportional to  $\text{HCO}_3$ , though no precipitates were obvious within the watercourse.

Bicarbonate concentrations did not increase with increasing distance downstream, however, on all sample occasions  $\text{HCO}_3/\text{Cl}$  ratios decreased significantly with increasing distance downstream, and abruptly from the mid-catchment down (Table 2.7). The increase in Cl concentration suggests a change in the geochemical environment of this area that was not entirely related to carbonate precipitation. Wybong Creek continually flowed in the mid-catchment, with the abrupt increase of Cl

Table 2.7. Molal ion ratios  $\pm$  standard deviations in Wybong Creek water samples during drought (2006 – June 6<sup>th</sup> 2007) and post drought (July 2007 – July 2008) conditions. N/A indicates absence of water at the site. BDL indicates Br concentrations below detection limit. *n* indicates the number of samples collected during particular climate conditions, with only one sample collected at the 55 km sample site during drought conditions.

Sample site (km)	Cl (mmol L <sup>-1</sup> )		HCO <sub>3</sub> (mmol L <sup>-1</sup> )		Mg/Ca (molar)		HCO <sub>3</sub> /(Ca+Mg) (molar)		HCO <sub>3</sub> /Cl (molar)		Cl/Br (molar)	
	Drought (n=4)	Post drought (n=2)	Drought (n=4)	Post drought (n=2)	Drought	Post drought	Drought	Post drought	Drought	Post drought	Drought	Post drought
11	0.9 $\pm$ 0.1	0.7 $\pm$ 0.1	7.8 $\pm$ 0.2	4.0 $\pm$ 1.5	1.8	1.5	1.6	2.0	0.253	0.171	BDL	BDL
30	1.3 $\pm$ 0.03	0.9 $\pm$ 0.9	8.1 $\pm$ 0.3	6.0 $\pm$ 0.9	1.9	1.5	1.5	2.3	0.180	0.192	BDL	BDL
37	3.0 $\pm$ 0.4	1.0 $\pm$ 0.6	9.1 $\pm$ 0.7	5.7 $\pm$ 0.2	2.1	1.6	1.4	2.3	0.087	0.156	BDL	BDL
48	5.6 $\pm$ 0.4	2.8 $\pm$ 2.0	5.7 $\pm$ 3.9	6.1 $\pm$ 0.9	2.1	1.8	1.0	2.1	0.029	0.060	1498	1012
55	9.56	5.6 $\pm$ 3.7	7.6	6.3 $\pm$ 0.7	2.0	1.9	1.3	1.8	0.708	0.032	958	1213
60	20 $\pm$ 0.4	3.7 $\pm$ 1.6	7.3 $\pm$ 0.2	5.7 $\pm$ 0.4	2.2	1.8	0.7	1.9	0.010	0.044	1709	1070
72	30 $\pm$ 9.0	4.8 $\pm$ 2.0	7.2 $\pm$ 0.1	6.0 $\pm$ 0.3	1.6	1.8	1.0	1.8	0.007	0.035	1587	1095
77	N/A	5.1 $\pm$ 1.6	N/A	5.9 $\pm$ 0.3	N/A	1.8	N/A	1.8	N/A	0.033	N/A	902
83	30 $\pm$ 6.8	5.9 $\pm$ 1.2	7.1 $\pm$ 0.3	5.3 $\pm$ 0.2	1.9	1.9	0.5	1.6	0.007	0.025	1973	1052
87	33 $\pm$ 14.1	6.2 $\pm$ 1.6	6.6 $\pm$ 1.4	5.4 $\pm$ 0.4	1.8	1.8	0.5	1.5	0.006	0.025	3155	1102

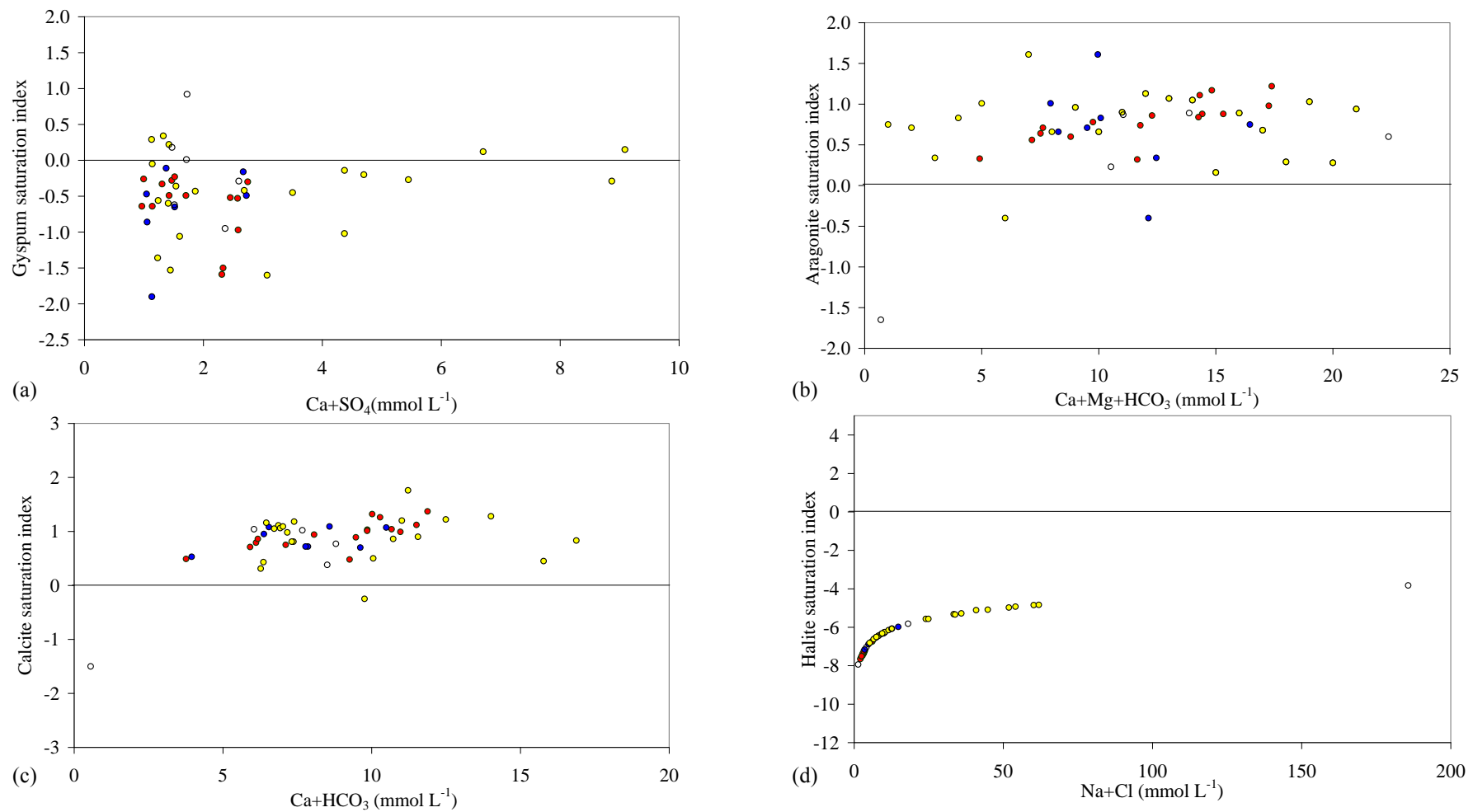


Figure 2.11. Saturation indices for major soluble minerals in Wybong Creek catchment surface water in the upper catchment (●), mid-catchment (●), lower catchment (○), and in Wybong Creek tributaries (○).

concentration indicative of significant saline water input in the mid-lower catchment area. Molar Cl/Br ratios further indicated a change in this area, where ratios of between 902 – 3155 occurred (Table 2.7). Such ratios were indicative of water which sourced Br and Cl from halite dissolution mixing as well as from precipitation or sea water (Davis *et al.* 1998). Saturation indices for surface water collected in the catchment also indicated a clear trend of increasing halite saturation in the mid-lower catchment (Figure 2.11). Results presented previously in this chapter indicated saline groundwater influenced by halite dissolution is discharged into a pool in the mid-catchment area, with the results presented here indicating groundwater similar to this brings about a change in surface water chemistry at the same place. Further research is required to corroborate these findings, however, there is reasonable evidence to conclude this groundwater gives rise the Cl dominated facies seen in the mid-lower Wybong Creek.

### 3.3 Surface water management implications

Water with salinities measured in Wybong Creek is suitable for the watering of stock, however, from the 30 km site down during drought conditions, and from the 60 km site down at all times, salinity as measured by EC was at levels which could be slightly ( $>700 \mu\text{S cm}^{-1}$ ) to severely problematic ( $>3000 \mu\text{S cm}^{-1}$ ) for irrigation (Ayers and Westcot 1994). Data from the gauging station at the 72 km sampling point indicated surface water salinity could be severely problematic for irrigation use when discharge was below  $560 \text{ ML day}^{-1}$  (Figure 2.12). Salinity was at levels which could cause slight to moderate problems for irrigation when flows were above  $560 \text{ ML day}^{-1}$ , however, salinity in Wybong Creek was often slightly to moderately problematic for irrigation independent of flow.

The Na drinking water taste threshold ( $180 \text{ mg L}^{-1}$ ) was exceeded from the 60 km sampling point down only during drought conditions (Appendix Two: Table A2.4); that for Cl ( $250 \text{ mg L}^{-1}$ ) exceeded taste thresholds from the 55 km sampling point down, also only in drought conditions (ANZECC and ARMCANZ 2000). In terms of total salinity (TDS), however, water was drinkable and of only poor – fair quality above 60 km sampling point irrespective of climate conditions. Below the 60 km sampling point, TDS often exceeded the  $1000 \text{ mg L}^{-1}$  acceptable limit for drinking water. The unsuitability of Wybong Creek for anything except the watering of stock was a reflection of its high solute concentration, with the limitation of Wybong Creek for irrigation and/or drinking water recommended except during high flow and/or flood events.

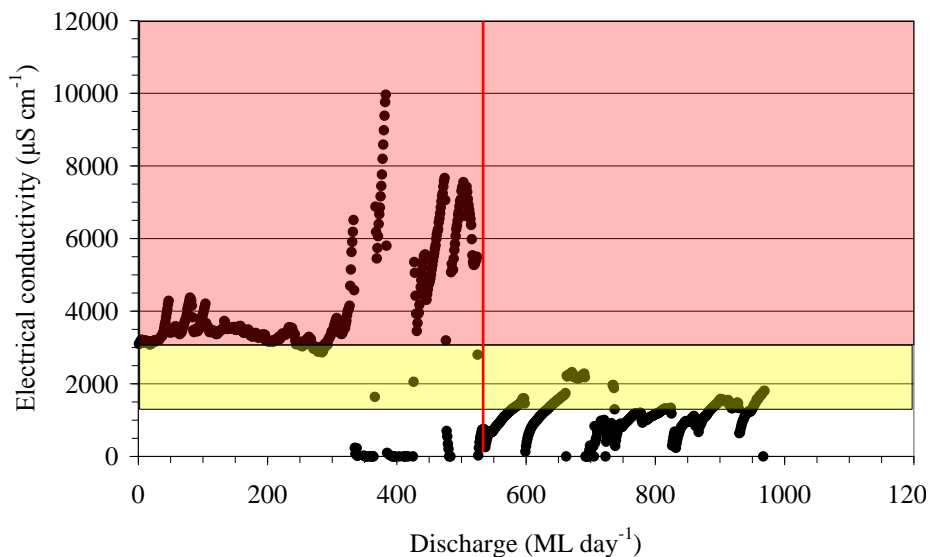


Figure 2.12. Electrical conductivity ( $\mu\text{S cm}^{-1}$ ) in Wybong Creek as a function of discharge ( $Q$ ,  $\text{ML day}^{-1}$ ), with points in the red zone indicating surface water with salinity levels which are severely problematic for irrigation; those in the yellow zone with salinity levels slightly to moderately problematic for irrigation; and those in the uncoloured zone have salinity levels which are non-problematic for irrigation.

#### 4. Conclusions

The aim of this chapter was to investigate the chemistry of Wybong Creek in order to isolate phenomena which cause this river to be anomalously salty. All stretches of Wybong Creek were dominated by the cations Na and Mg. The upper catchment was dominated by  $\text{HCO}_3^-$ , with absolute concentrations remaining similar at all Wybong Creek sampling sites.

Chloride concentrations and proportions increased with increasing river grade, though to a lesser degree after average rainfall conditions returned to the catchment post June 2007. Changes in the proportion of Na/Cl, and Cl/Br ratios indicated input from a saline, halite influenced groundwater body in the mid-lower catchment area, in addition to the changes in the proportion of Cl/ $\text{HCO}_3^-$  which were due to the precipitation of carbonate minerals. Point source increases of salinity were caused by discharge of groundwater with high Na, Cl, and TDS concentrations and high Cl/Br ratios in a “salt pool” just above the 60 km sample site. Regular fluctuations in EC occurred throughout the day during some months and indicated this or another saline groundwater body adjacent to Wybong Creek was confined, though diurnal fluctuations only affected river salinity during certain periods. The abrupt increases in salinity, element to Cl ratios, and diurnal fluctuations in EC indicated that groundwater is an important driver of salinity in Wybong Creek.

Calculations indicated evapoconcentration had a minor affect on solute concentrations in Wybong Creek, with  $\delta^{18}\text{O}$  and  $\delta^2\text{H}$  indicating evapoconcentration is not consistently increasing solute concentrations between sample sites. The solute flux from the Wybong Creek catchment in relation to aeolian deposition (i.e. output:input ratios) was typical of rivers in other catchments suffering from dryland salinity, with salt stores in such catchments built over millennia. Further evidence for dryland salinity in the catchment was indicated by a decrease in estimated evapotranspiration in the catchment which has occurred as a result of deforestation.

It is concluded that the high solute loads delivered into the Goulburn and Hunter Rivers by Wybong Creek can be sourced to groundwater influxes in the mid-lower catchment. Though aridity and decreased evapotranspiration increase the likelihood of dryland salinity being the driving cause of groundwater salinity, summer dominated rainfall received via thunderstorms may prevent substantial salt stores being built. In the absence of salt stores, saline groundwater in the mid-lower catchment may instead source solutes prior to discharging into the regolith. Research investigating the source of salinity to groundwater in this area and the degree of salt storage within the regolith is required. Additional research into the conditions which cause groundwater heights to change and to discharge at some times and not others would also be beneficial.



---

## **Chapter Three**

### Aquifers and groundwater bodies in the Wybong Creek catchment



## 1. Introduction

Aquifers and groundwater bodies are largely undescribed within the Wybong Creek catchment, despite discharging groundwater causing salinisation of surface water and soils (Chapters One and Two). Only the surficial geology is described in maps of the catchment (Glen and Beckett 1993), with no known hydrogeological maps occurring. The fractured escarpments and outcrops are known to contain groundwater, and are comprised of Narrabeen Group sandstones and conglomerates, and the Liverpool Range Volcanics. Groundwater also occurs within the quaternary alluvium which covers the valley floors. A hydrogeological report conducted at the Mangoola Coal Mine in the south-east of the catchment indicates complex vertical groundwater flow between surficial alluvium and deeper coal formations (Umwelt Environmental Consultants 2006). The sparse geological knowledge of the catchment complicates the identification of solute sources and groundwater flow paths in an area where complex flow is already likely to occur. This chapter addresses means by which flow paths and solute sources can be delineated within the Wybong Creek catchment, however, in order that salinity mitigation both within the catchment itself and the Hunter Valley further downstream can occur.

Groundwater flow within sedimentary formations is often very complex due to the highly heterogenous aquifers in which water bodies occur, with anisotropy, faults, fractures, variations in temperature, pressure, salinity, and the dipping of beds causing both vertical and horizontal components of groundwater flow (Kreitler 1989; Tóth 1995). This vertical groundwater flow limits the accuracy of piezometric surfaces in delineating groundwater flow paths (e.g., Domenico and Schwartz 1990; Mazor and Nativ 1992; Bachu 1995; Bachu and Michael 2002). The use of static water level (SWL) data from bores further limits the use of piezometric surfaces to delineate flow paths in many places, due to bores being screened into a number of water yielding units and SWLs therefore representing the sum of hydraulic potentials rather than that of a single aquifer (Mazor and Nativ 1992). Ions, ion ratios and isotopes offer a means of testing for the connectivity of groundwater bodies occurring within such aquifers, allowing for the identification of groundwater flow paths in complex sedimentary basins (Bachu 1995), such as the Sydney-Gunnedah Basin complex in which Wybong Creek occurs.

Groundwater is likely to have many solute sources within catchments, with ion and isotope concentrations varying within aquifers if groundwater flows along a number

---

of paths before being discharged into the same place. The identification of solute sources to groundwater in areas where such complex flow occurs therefore necessitates the compartmentalisation of groundwater into groups which represent groundwater bodies or systems. Local groundwater bodies or systems are those which retain solutes from infiltrating rainwater and acquire them also from the local minerals that occur in rocks, with recharge occurring at one topographic high and discharge occurring at the adjacent topographic low (e.g., Freeze and Cherry 1979; Fetter 2001). Intermediate groundwater systems instead recharge in more than one area and therefore acquire solutes from a number of spatially separate formations, while regional groundwater systems recharge at the major topographic high, acquire solutes from many formations, and discharge via many flow paths at the major topographic low. The chemistry of groundwater bodies may be therefore entirely unrelated to the aquifer within which the groundwater occurs. Placing groundwater samples into geochemical groups which represent groundwater bodies and systems, however, allows flow paths to be elucidated and the chemical evolution of groundwater to be traced in areas with complex geology and groundwater flow paths (Razack and Dazy 1990; Stuyfzand 1998). Sources of solutes to groundwater can then be identified and in some cases isolated from non-degraded water, allowing for more sustainable water supplies.

The placement of groundwater into groups which represent groundwater bodies requires visual and/or numerical analyses of groundwater samples. Visual analyses of groundwater involves diagrams such as piper and stiff plots, with these describing the four major cations (K, Ca, Mg, and Na) and three major anions ( $\text{HCO}_3$ , Cl, and  $\text{SO}_4$ ) which occur in most water bodies (e.g., Fetter 2001; Appelo and Postma 2005). Though visual diagrams describe important differences between groundwater samples, interpretation can be misleading due to subjective analyses and the small number of parameters (i.e. major ions) used to describe the data (e.g., Razack and Dazy 1990; Meng and Maynard 2001). Dominance of different groundwater bodies by similar ions is not necessarily due to a similar solute source (e.g., Dafny *et al.* 2006), for example, with  $\text{HCO}_3$  sourced from the weathering of basalts, sandstones, carbonates (Appelo and Postma 2005), and coal. Groundwater bodies with similar major ion concentrations but differing chemical origins may be identified, however, by using numerical and statistical analyses which incorporate major, minor, and isotope concentrations (Usunoff and Guzmán-Guzmán 1989; O'Shea and Jankowski 2006).

## 1.2. Aims and objectives

The aim of this chapter was to understand the extent and interconnectedness of groundwater bodies or systems within the Wybong Creek catchment and the aquifers in which they occur. This aim was met by addressing the following objectives:

1. To create geological cross-sections of the Wybong Creek catchment;
2. To isolate formations which are acting as aquifers within the Wybong Creek catchment;
3. To place groundwater samples into groups which represent groundwater bodies; and
4. To identify the local, intermediate and regional groundwater systems occurring in the catchment.

## 1.3. Background

A summary of the literature on the geology of the north-west Sydney Basin, in which Wybong Creek occurs, is covered first. The little which is known about hydrogeology in the area is then covered, followed by a review of the statistical procedures which will be used in this study.

### 1.3.1. Geological context

The Wybong Creek catchment lies within the Sydney-Gunnedah Basin complex, a sedimentary foreland basin lying between the New England Fold Belt in the north and the Lachlan Fold Belt in the south (Scheibner 1998). Publicly available geological mapping has not occurred in the Wybong Creek catchment beyond the Hunter Coalfield Regional 1:100 000 Geological Map (Glen and Beckett 1993), though detailed descriptions of the local geology do occur in an environmental impact assessment (Umwelt Environmental Consultants 2006), and two drilling reports focused on geology in the mid-Wybong Creek catchment (Leary and Brunton 2003; Brunton and Moore 2004). A brief review of the literature regarding the geology of the north-western Sydney Basin and south-eastern Gunnedah Basin is presented, therefore, in order to give context to the conditions of groundwater flow in the Wybong Creek catchment.

The basement of the Sydney-Gunnedah Basin complex in the Wybong Creek area is made up of Late Carboniferous/Early Permian rocks (Scheibner 1998). Formation of the Sydney-Gunnedah Basin began in the Late Carboniferous, where volcanic rifting produced large quantities of ignimbrites and calc-alkaline volcanics. Thermal sag and subsidence then occurred, before the Sydney Basin truly developed into a foreland basin

in the mid-Permian (Tadros 1993; Scheibner 1998). Large amounts of sedimentary material were eroded into the basin from the rising New England Fold Belt and the craton of the Lachlan Fold Belt at this time (Tadros 1993; Scheibner 1998). Thick, localised sequences of interbedded sandstones, conglomerates and coals were formed as lacustrine deposits in trough areas underlain by subsiding half-grabens. The upper-most of these Permian deposits is the Singleton Supergroup which includes the Wittingham Coal Measures, lying >300 m below the surface in the south of the Wybong Creek catchment, and 400 m below the surface in the mid-catchment (Leary and Brunton 2003; Brunton and Moore 2004). Eustatic sea rise led to marine deposition of the Denman Formation and the inundation of the Wittingham Coal Measures on which it formed (Tadros 1993; Scheibner 1998).

Large fluvial systems deposited one to two kilometres of organic and inorganic sediments and tuffs in the Sydney Basin during the Late Permian, before rapid subsidence and felsic volcanism buried these sediments (Tadros 1993; Scheibner 1998). This formed what is now known as the Newcastle Coal Measures. These coal measures lie 100 – 200 m below the surface in the mid-Wybong Creek catchment and outcrop in the southeast (Leary and Brunton 2003; Brunton and Moore 2004). Major uplift, tilting and compression of the Sydney basin occurred in the Late Permian, with coal sedimentation terminated and deep erosion of the Permian sediments occurring in the Wybong area. Alluvial fans prograding from the New England Fold Belt to the southwest produced the Narrabeen Group in the Early Triassic. This sedimentary deposition was terminated altogether in the mid-Triassic due to deformation and the formation of reverse-faults. Erosion since this period gave rise to the steep and deeply (>200 m) incised valleys seen in the catchment today, with the Quaternary alluvium within and adjacent to Wybong Creek derived from the Liverpool Range Volcanics and that further from the river channel and adjacent to the escarpments sourced from the Narrabeen Group (Kovac and Lawrie 1991).

The eastern part of the Liverpool Range forms the northern border of the Wybong Creek catchment, with the Liverpool Range being the largest lava-field province in New South Wales (Tadros 1993; Scheibner 1998). This part of the volcano is also the oldest, with K/Ar dating indicating formation in the late Eocene, around 38 – 40 Ma. The volcano is uniformly basic, with alkali olivine basalt the most common rock. Basanite, hawiiite and mugearite are also common. Plagioclase makes up 35 – 60 % of the Liverpool Range by volume, with K-feldspar rare and fluor apatite common. Mg and Na concentrations are relatively high (Schön 1985).

---

Magma intrusion caused the folding and coking of coal throughout the Sydney – Gunnedah Basin complex, with hydrated clay minerals and carbonates such as calcite currently filling fractures and cavities (Tadros 1993). Jurassic intrusions in the south of the Wybong Creek catchment are associated with the break-up of Gondwana during the Jurassic, though intrusions may also be of Tertiary age closer to the Liverpool Range. Dikes and sills have been mapped in the south-east of the Wybong Creek catchment where economic deposits of the Newcastle Coal Measures occur (Umwelt Environmental Consultants 2006).

Sparse drilling and thick alluvial cover precludes the delineation and magnitude of faults in this north-western part of the Sydney – Gunnedah Basin complex, though many cores contain thick breccia and slickensiding (Tadros 1993). Lineaments which have been interpreted as faults have been identified, however, and can be grouped into those trending north-north east and north-west, and those east-north-east and west-north west (Tadros 1993). They occur with near vertical orientation and seldom any displacement, though different structural development on either side of lineaments does take place. These lineaments have been interpreted as transfer faults, shear zones, fault zones or zones of weakness, and penetrate the lithosphere to great (though unquantified) depths. Lineaments trending north-west are associated with rift-related extension, and are expressed as mesoscale fracturing, normal faults and dykes. The north-north-east and north-western lineaments instead appear to reflect the Late Carboniferous volcanic basement underlying the basin. East-west compression of the Newcastle Coal Measures has resulted in frequent and complex faulting in the south-eastern Wybong Catchment.

### 1.3.1.1. Hydrogeological context

Regional hydrochemical studies have been conducted in the upper Hunter Valley, although hydrogeology has not been addressed specifically within the Wybong Creek catchment (Kellett *et al.* 1987; Creelman 1994). Eight hydrochemical regions with distinctive chemistry occur in the upper Hunter Valley, with these groups distinguished by canonical and principle component analyses (Kellett *et al.* 1987). Wybong Creek was placed in the TRIAS group in this study, with the low to moderate salinity of this Na-Mg-Cl-HCO<sub>3</sub> dominated group related to chemical weathering of the Triassic Narrabeen Group. The Na-Cl dominated saline groundwater of Big Flat Creek, which occurs in the south-eastern Wybong Creek catchment, was instead related to groundwater discharge from the Wittingham Coal Measures (Group WI2) and/or other units deposited or influenced by marine conditions.

Uplift and erosional unloading has lead to fracturing within the Permian Coal Measures, with groundwater flow lines in the coal measures related to faulting, fracturing, structure-jointing, thrusting and cleat directions (Creelman 1994). Halite ( $\text{NaCl}$ ), bloedite ( $\text{Na}_2\text{Mg}(\text{SO}_4)_2 \cdot 4(\text{H}_2\text{O})$ ), and thenardite ( $\text{Na}_2\text{SO}_4$ ) occur as salt efflorescences in the Wittingham Coal Measures, despite the occurrence of a regional groundwater body (Kellett *et al.* 1987). The presence of these highly soluble minerals is anomalous with the age of the 300 million year old coal measures and led Kellett *et al.* (1987) to the conclusion that groundwater was trapped within the coal measures until they were tectonically uplifted during the Tertiary, allowing molecular diffusion towards fractures to drain salts from the coal.

### **1.3.2. Statistical theory**

Statistics and numerical analyses have traditionally been the domain of psychologists and biologists (Davis 1973), however, their utilisation by hydrologists is increasingly common (e.g., Güler *et al.* 2002; McNeill *et al.* 2005; O'Shea and Jankowski 2006; Papatheodorou *et al.* 2007). The principle types of analyses useful to hydrologists are those which group samples according to their hydrochemical characteristics. Such analyses encompass both statistical (MANOVA, ANOVA, etc.) and numerical (fuzzy logic, hierarchical cluster analysis, etc.) techniques. Analyses used in this study were focused on the grouping of samples into hydrochemical groups, and were largely numerical rather than statistical. The following review is therefore relevant to these types of analyses.

#### **1.3.2.1. Factor analyses**

Factor analyses reduce data sets to those variables or samples which account for the greatest variability (Razack and Dazy 1990; Meng and Maynard 2001; Papatheodorou *et al.* 2007). Frequently used factor analyses include Q-mode analyses and R-mode analyses. All assess the relationship between groundwater samples by constructing variance-covariance matrices of a multivariate data set, before extracting eigenvalues and eigenvectors from the matrix thus produced (Davis 1973). R-mode factor analyses specifically investigate the inter-relationship between variables (ions in this case). Q-mode factor analyses instead determine the relationship between groundwater samples based on their ionic concentrations.

### 1.3.2.1.1. Principle component analyses

Principal Component Analysis (PCA) is based upon R-mode analysis and reduces the number of factors in a data set to those which describe the greatest differences between samples (Güler *et al.* 2002). It is most often used with varimax rotation in hydrochemical studies (e.g., Suk and Lee 1999; Meng and Maynard 2001; Singh *et al.* 2004; Sikdar and Chakraborty 2008). Correlation or covariance matrices are produced by PCA, with coefficients of the eigenvectors (or loadings) representing the relative contribution each factor (in this case of each ion) makes to the variation of each principle component of the test (Davis 1973). Correlation matrices are necessary if data values occur on different scales, however, covariance analyses are more useful in the case of hydrogeochemical data sets which contain significant differences in the variance of ions (i.e., when there is a large range in the concentrations of different ions). Unlike many other forms of multivariate analysis, PCA does not require the normalisation of data for reliable results.

### 1.3.2.1.2. Hierarchical cluster and discriminant analyses

Hierarchical Cluster Analyses (HCA) places samples into groups based upon their similarity. The closer samples plot to each other on a dendrogram produced by HCA the more similar they are, with Euclidean distance and Ward's method for linkage being the most frequently used means of creating dendograms in hydrogeochemical studies (e.g., Suk and Lee 1999; Güler *et al.* 2002; Singh *et al.* 2004; O'Shea and Jankowski 2006). Other methods may also be used to group similar samples in other types of cluster analyses, such as the cosine theta similarity coefficient in R-mode analysis, and the product-moment correlation coefficient used in Q-mode analyses (Meng and Maynard 2001). The dendrogram produced from HCA is projected on to two-dimensional space with the proximity of two samples reflecting their chemical rather than spatial similarity. HCA is a visual rather than statistical test, albeit utilising more data than stiff and piper diagrams (Güler *et al.* 2002).

## 2. Materials and Methods

The methods used for the analyses of O, H and Sr isotopes are described in Chapter Two (Section 2.2).

## 2.1. Sample collection

Groundwater was sampled from as many bores and piezometers as possible across the Wybong Creek catchment (Figure 3.1). Sampling occurred on three dates during the low rainfall conditions of 2001-2007: the 21<sup>st</sup>-22<sup>nd</sup> April; the 21-23<sup>rd</sup> July 2006, where samples were collected by Ben Macdonald; and the 1<sup>st</sup> June 2007. Average rainfall occurred in the catchment from mid-2007 onwards, with groundwater samples collected on the 5<sup>th</sup>-7<sup>th</sup> July 2007; the 17-18<sup>th</sup> June 2008; and the 20<sup>th</sup> January, the 14<sup>th</sup> – 15<sup>th</sup> May, and the 30<sup>th</sup> June 2009.

Bores and piezometers were purged of at least one well volume the day before sampling. Samples were then collected after groundwater had attained constant chemistry. Water quality parameters were measured on unfiltered water samples using Orion Gel-Filled pH and Eh electrodes and pH and Eh meters; an Orion DuraProbe™ 4-electrode conductivity cell and conductivity meter; and an Orion dissolved oxygen probe and dissolved oxygen meter, with instrument calibration conducted as described in Chapter Two (Section 2.2). Alkalinity was measured on filtered water in the field by titration with a Hach digital titrator, HCl and methyl orange as an indicator (Franson 2005). Rainwater samples were collected 13 km south of the catchment at Denman on June 14<sup>th</sup> 2007, and July 18<sup>th</sup> 2008. All other rainwater samples were collected 20 km west of Wybong Creek in Muswellbrook.

### 2.1.2. Sample preparation

Samples collected for isotope and ion analyses were filtered through 0.45 µm Millipore® nitrocellulose filters on site. Samples selected for anion, δ<sup>2</sup>H, δ<sup>18</sup>O, and <sup>14</sup>C analyses were stored in refrigerators prior to further laboratory preparation and/or analyses. Sample volumes of 50 mL were collected for cation and Sr isotope analyses and were acidified in the field with 2 mL 50% HNO<sub>3</sub>. Barium chloride (BaCl) was added to select samples to precipitate BaSO<sub>4</sub> for δ<sup>34</sup>S<sub>SO4</sub> analyses, with BaSO<sub>4</sub> separated from the supernatant by filtration in the laboratory. At least one blank sample was made per field trip, whereby milli-Q water was prepared for analyses as per groundwater samples.

## 2.2. Sample analyses

Sample contamination was monitored by analysing blanks created in the field, with the quality of analyses monitored using charge balances, as described in Chapter

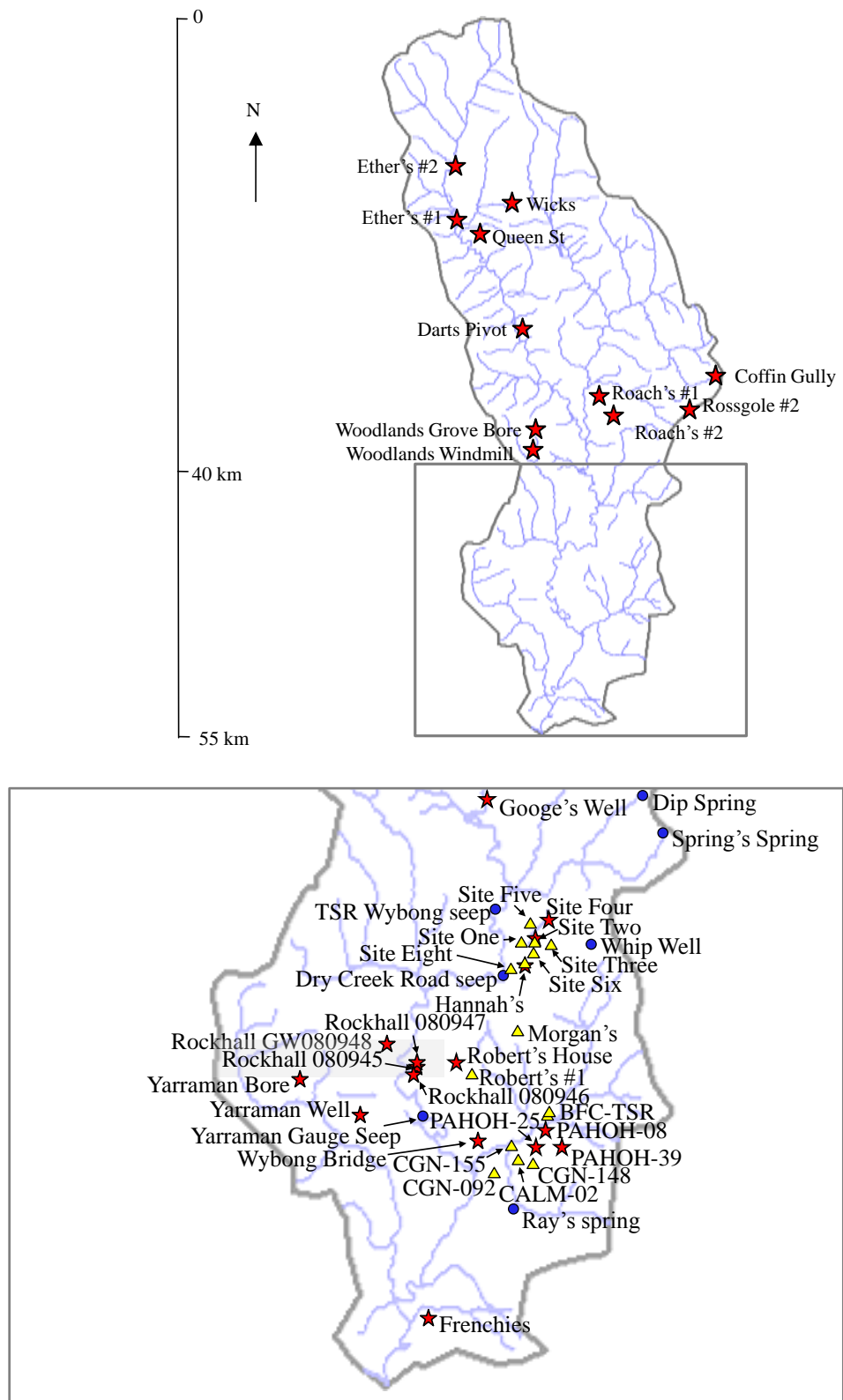


Figure 3.1. Groundwater sampling locations within the Wybong Creek catchment, including springs (●), bores (★), and piezometers (▲), where bores are screened into a number of water-yielding layers and piezometers are screened into a single layer.

Two (Section 2.2.2). Sample contamination occurred on 27/01/2009 with most contamination coming from Cl and some from Ca, Mg, Na and K (Tables A3.1 – A3.2). This contamination was ignored given the large concentration of these ions in water samples and the small error thus resulting from contamination.

The quality of analyses was monitored using charge balances (Chapter Two). Six of the 78 groundwater samples analysed for ions had charge balances exceeding 15 % (Table A3.3). Ray's Spring had a charge balance of 38.6 %, with the low ion concentration in this sample possibly causing erroneous quantification of ions.

Yarraman Bore was uncapped and was not able to be purged due to depths over 200 m, with the charge balance of -17.6 % seen for this sample possibly indicating contamination. Data presented from Yarraman Bore and Ray's Spring should be considered with these charge balances in mind. Queen St (22/07/2006), Wybong Bridge (25/04/2006), Dip Paddock Spring (22/07/2008), and Ether's #2 also had charge balances exceeding 15 %, and with all major anions and cations analysed, this was likely due to an error in the measurement of HCO<sub>3</sub> by titration in the field. Only a small decrease in the total HCO<sub>3</sub> concentration was needed to correct charge balance differences in these samples. Data was therefore uncorrected due to the small affect it had on the interpretation of results.

### **2.2.1. Cation and anion analyses**

Reactive ions were analysed in the field using a Hach spectrophotometer and method 8146, 1, 10-Phenanthroline for Fe<sup>2+</sup>; method 10209 phosphomolybdate for PO<sub>4</sub><sup>2-</sup>; cadmium reduction for NO<sub>3</sub><sup>2-</sup>; and BaCl for SO<sub>4</sub><sup>2-</sup> (Hach Company 2009). Samples collected for ion analyses during 2006 and 2009 were sent to the Centre for Coastal Biogeochemistry, Southern Cross University. Samples for ion analyses collected in 2007 – 2008 were sent to the Department of Water and Energy Water Environmental Laboratory, New South Wales, for analyses.

### **2.2.2. Strontium isotope analysis**

Select samples were analysed for <sup>87</sup>Sr/<sup>86</sup>Sr by Marc Norman at the Research School of Earth Sciences, The Australian National University. Samples were prepared for analysis by drying 10 mL of sample on a hotplate, with 1 mL of 2 M HNO<sub>3</sub> taken up for loading on Eichrom Sr-specific resin. Strontium was collected by elution with 0.05 M HNO<sub>3</sub> after eluting matrix elements using additional 2 M HNO<sub>3</sub> and 7 M HNO<sub>3</sub>. The samples were then dried with one drop of H<sub>3</sub>PO<sub>4</sub> for mass spectrometry. All of these

---

steps were conducted in a clean laboratory using distilled reagents. Strontium isotopic compositions were measured on a Finnigan MAT 261 thermal ionisation multi-collector mass spectrometer. The samples were loaded individually onto single filaments that had been outgassed under a vacuum with a four amp current. Each analysis consisted of ten blocks of 12 cycles each. The masses of  $^{84}\text{Sr}$ ,  $^{85}\text{Rb}$ ,  $^{86}\text{Sr}$ ,  $^{87}\text{Sr}$ , and  $^{88}\text{Sr}$  were measured simultaneously and corrected for mass fractionation to  $^{86}\text{Sr}/^{88}\text{Sr} = 0.1194$  (Bohlke *et al.* 2005). Corrections for  $^{87}\text{Rb}$  interferences were applied if necessary assuming  $^{85}\text{Rb}/^{87}\text{Rb} = 0.3857$  (Bohlke *et al.* 2005). The weighted mean  $^{87}\text{Sr}/^{86}\text{Sr}$  of the NBS987 isotopic standard run on this mass spectrometer during the period 2005-2009 was  $0.710221 \pm 0.000005$  (2 SE,  $n=44$ ; M. Norman, Pers. Comm., 2009).

### 2.2.3. Carbon isotope analysis

Samples were analysed for  $^{14}\text{C}$  and  $^{13}\text{C}$  at the Research School of Earth Sciences, The Australian National University. Samples were made basic using  $\sim 1\text{ mL NaOH}_{(\text{aq})}$ , with analytical grade  $\text{SrCl}_{2(\text{s})}$  then added to excess prior to analysis. The  $\text{SrCO}_3$  that precipitated out of this solution was filtered through  $0.45\text{ }\mu\text{m}$  Millipore® nitrocellulose filters and collected in 5 mL vials. Concentrations of  $^{14}\text{C}$  and  $^{13}\text{C}$  were then assessed using a National Electrostatic Corp. (NEC) Single Stage Accelerator Mass Spectrometer (SSAMS).

### 2.2.4. Sulfur isotope analysis

Select samples were analysed for  $\delta^{34}\text{S}$  at the Centre of Coastal Biogeochemistry, Southern Cross University. Tin cups containing the samples were brought to an elemental analyser (Flash EA, Thermo Fisher) coupled to a mass spectrometer for stable isotope analyses (Delta V plus, Thermo Fisher) by means of a continuous flow interface (Conflo, Thermo Fisher). Samples were combusted at  $1020\text{ }^\circ\text{C}$ , and the combustion gases passed through a matrix of tungsten alumina. Here samples were oxidized before passing through Cu wires where they were reduced. Water vapour was removed with magnesium perchlorate. The remaining gases were passed to a chromatography column to separate  $\text{SO}_2$ , before  $\text{SO}_2$  was injected into the mass spectrometer. The ratio of  $^{66}\text{SO}_2/^{64}\text{SO}_2$  was then measured against sulfanilamide standard every ten samples. The value of  $\delta^{34}\text{S}_{\text{Sulfanilamide}}$  had a standard deviation of  $20.5 \pm 0.25$  (M. Carvalho de Carvalho, Pers. Comm., 2009).

### **2.3. Statistical analyses**

Hierarchical cluster analyses was conducted on 78 groundwater samples from 49 sample sites, using the statistical software package Minitab®15 (2006). Canonical and PCA were conducted using the statistical software package GenStat Eleventh Edition (2008). Only ion concentrations were used for grouping data due to absent isotopic data skewing analyses. Ion concentrations ( $\text{mmol L}^{-1}$ ) were standardised to Cl in order to account for the possible effects of evapoconcentration.

## **3. Results and discussion**

Raw hydrochemical data for this chapter can be found in Appendix for Chapter Three (Tables A3.3 – A3.6). The  $^{14}\text{C}$  dates presented in these results and discussion are not reliable groundwater ages due the concentration of C from other sources, such as the aquifer matrix and other groundwater bodies, being unquantified (Cook 1999). Results for  $^{14}\text{C}$  are, therefore, only presented for use as a general geochemical signature and require calibration using other groundwater dating techniques if they are to be used for dating.

### **3.1 Aquifers in the Wybong Creek catchment**

Aquifers are formations which contain utilisable yields of groundwater, and may be made up of both consolidated and unconsolidated material (e.g., Fetter 2001). The assessment of which formations were acting as aquifers in the Wybong Creek catchment was undertaken by creating geological cross-sections using bore logs (Figures 3.2 – 3.3). Most bores in the catchment were drilled by private operators for stock water with a few drilled for irrigation purposes. This influenced the depth of bores in the catchment. A large proportion of bores were terminated in the Narrabeen Group, indicating that this formation acts as an important aquifer, with depths of up to 85 m on the valley floor (Figures 3.2 – 3.4; Table 3.1). Fractures in the sandstones and conglomerates of this formation are observable with the naked eye, though rock between fractures is otherwise massive. The rock is fractured and/or faulted below the surface also, with fracturing occurring at depths in excess of 300 m (Leary and Brunton 2003; Brunton and Moore 2004). Lineaments in the catchment are related to fracturing and faulting and have influenced the direction of watercourses (Figure 3.4), as indicated by aeromagnetic surveys of the mid-catchment area which show a river channel at a 90 ° angle to its paleoachannel (Leary and Brunton 2003). Groundwater is yielded from fractured layers within the rock (NSW DNR 2005), with fracture flow typical of many

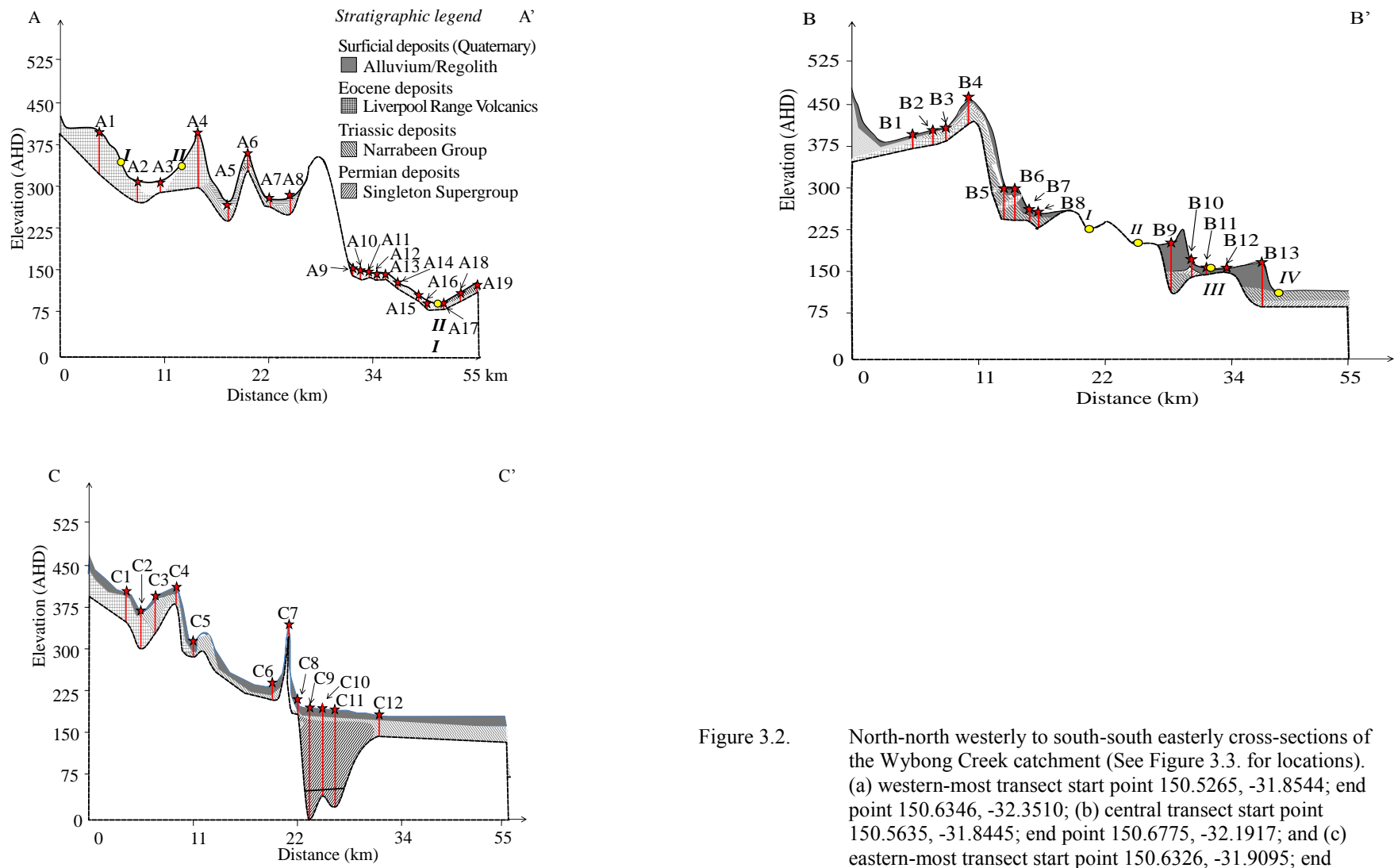


Figure 3.2. North-north westerly to south-south easterly cross-sections of the Wybong Creek catchment (See Figure 3.3. for locations). (a) western-most transect start point 150.5265, -31.8544; end point 150.6346, -32.3510; (b) central transect start point 150.5635, -31.8445; end point 150.6775, -32.1917; and (c) eastern-most transect start point 150.6326, -31.9095; end point 150.7116, -32.2723.

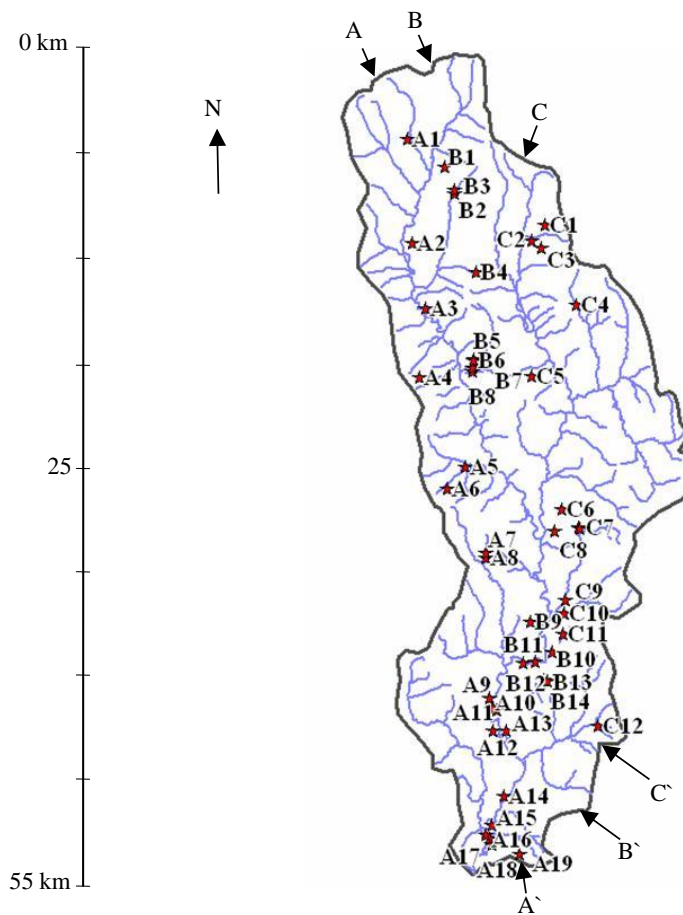


Figure 3.3. Cross-sections of the Wybong Creek catchment. Transects run from north-west-west in a south-south-easterly direction, according to the following parameters: (a) western-most transect start point 150.5265, -31.8544, end point 150.6346, -32.3510; (b) central transect, start point 150.5635, -31.8445, end point 150.6775, -32.1917; and (c) eastern-most transect, start point 150.6326, -31.9095, end point 150.7116, -32.2723.

aquifers in Australia (e.g., Acworth and Jankowski 2001; Morgan and Jankowski 2004; Tweed *et al.* 2005; Cartwright *et al.* 2007).

Bores in the mid-lower catchment were terminated in both the fractured Narrabeen Group aquifer and in alluvium which was up to 23 m deep. The alluvium in Wybong Creek is comprised of basalt-derived chocolate-brown smectitic clays adjacent to the watercourse, and of coarse gravels, sands and yellow-grey silts and clays derived from sandstones and conglomerates closer to the Narrabeen Group escarpments (Kovac and Lawrie 1991). The smectitic clay is likely to be acting as a confining layer to the alluvial aquifer adjacent to Wybong Creek and to the Narrabeen Group on the escarpments. The degree of confinement that occurs due to these smectitic clays cannot be determined without further pumping tests and/or time-series analyses of the relationship between hydraulic head and air pressure (Weight and Sonderegger 2000), with the response of many alluvial aquifers to changes in air pressure indicating

Table 3.1(a). Geographical and downhole data for bores sampled. N/A indicates information is not available. Elevation and depth in Australian height datum (AHD).

Bore number	Site	Latitude	Longitude	Elevation (AHD)	Depth (AHD)	Screened interval	Strata
GW080595	Ether's #1	-32.207635	150.343743	269	117	N/A	Basalt/Narrabeen Sandstone
No number	Ether's #2	-31.571671	150.321673	314	274	N/A	Basalt/Conglomerate
GW038293	Roach's #1	-32.824663	150.400207	215	197	204.5-203.3	Narrabeen Sandstone
GW080943	Roach's #2	-32.830726	150.395627	234	210	214.0-216.0	Shale
GW061136	Queen St	-32.214780	150.354684	300	236	248.2-236.0	Narrabeen Sandstone
No number	Darts Pivot	-32.641788	150.373609	217	N/A	N/A	N/A
GW063952	Woodlands Grove Bore	-32.102796	150.372972	230	206	210.8-210.2	N/A
No number	Woodlands Grove Windmill	-32.102721	150.372741	233	225	N/A	Alluvium
GW017391	Wicks Cuan Ck	-31.582029	150.373595	313	N/A	N/A	Basalt
GW025789	Googe's Well	-32.105331	150.395401	181	169	N/A	Alluvium
GW047877	Robert's House	-32.153288	150.418775	174	141	152.7-143.6	Alluvium
GW080434	Wybong Bridge	-32.201116	150.371688	148	131	134.0-130.6	Alluvium
GW040960	Frenchies	-32.201074	150.374355	126	112	119.0-111.5	Alluvium
GW080946	Rockhall Riverflats	-32.154682	150.383413	150	131	N/A	N/A
GW080947	Rockhall North	-32.154146	150.374229	154	94	N/A	N/A
GW080948	Rockhall Hayshed	-32.144827	150.372482	153	109	124.0-126.0	Narrabeen Sandstone
GW080945	Rockhall Old Hayshed	-32.151514	150.374853	155	130	137.0-139.0	Alluvium
GW080944	Hannah's	-32.125645	150.401485	170	140	144.0-146.0	Widden Brook Conglomerate
GW035173	Yarraman Well	-32.154482	150.374883	147	130	129.7-136.4	Alluvium
GW200417	Yarraman Bore	-32.160573	150.377766	177	-39	71.8-72.0, 44.0-43.7	Shales (Narrabeen Sandstone, Newcastle Coal Measures)
GW056645	Rossgole Bore No.2	-32.825316	150.442512	477	392	37.2-43.4	Narrabeen Sandstone
GW045179	Coffin Gully Bore	-32.758772	150.452330	430	430	55.5-64.6	Narrabeen Sandstone

Table A3.1(b). Geographical and downhole data for bores and piezometers sampled. N/A indicates information is not available. Elevation and depth are in Australian height datum (AHD).

	Site	Latitude	Longitude	Elevation (AHD)	Depth (AHD)	Screened interval	Strata
Piezo.	Robert's #1	-32.152648	150.413100	181	175	N/A	Alluvium
	Morgan's	-32.156660	150.415551	183	171	N/A	Alluvium
	BFC TSR Deep	-32.155812	150.414312	155	143	143-141	Alluvium
	BFC TSR Shallow	-32.155812	150.414312	155	147	147-145	Alluvium
	PAH-039	-32.164774	150.412269	173	145	N/A	Fassifern Seam
	PAH-025	-32.164572	150.403486	165	135	N/A	Fassifern Seam
	CGN-148	-32.164872	150.401770	158	130	N/A	Anvil Ck Alluvium
	CGN-155	-32.164501	150.406630	160	135	N/A	Anvil Ck Alluvium
	CALM-02	-32.164799	150.405912	150	142	N/A	Anvil Ck Alluvium
	CGN-092	-32.165010	150.404424	158	143	N/A	Anvil Ck Alluvium
	PAH-08	-32.161146	150.404987	161	84	N/A	Fractured sandstone
	Site One	-32.123240	150.402620	187	186	186.2-185.1	Narrabeen derived alluvium
	Site Two Shallow	-32.123650	150.403290	181	173	172.6-171.6	Narrabeen derived alluvium
	Site Two Deep	-32.123650	150.403280	181	165	164.6-164.3	Narrabeen derived alluvium
	Site Three	-32.125350	150.404910	194	188	188.3-187.3	Narrabeen derived alluvium
	Site Four	-32.122010	150.404540	189	173	173.0-172.0	Narrabeen derived alluvium
	Site Six	-32.123430	150.402640	177	166	165.5-163.5	Smectitic clay
	Site Eight Shallow	-32.131250	150.395900	165	158	158.0-159.5	Smectitic clay
	Site Eight Fractured	-32.131250	150.395900	165	156	156.0-154.5	Fractured conglomerate
Spring	"Springs Paddock" Spring	-32.102283	150.434938	467	N/A	N/A	Basalt/Conglomerate
	"Dip Paddock" Spring	-32.854070	150.425771	363	N/A	N/A	Basalt/Conglomerate
	Whip Well	-32.122931	150.414192	225	220	N/A	Sandstone Alluvium
	Dry Creek Road Seep	-32.131687	150.395644	155	N/A	N/A	Widdenbrook cong.
	Yarraman Gauge Seep	-32.167982	150.381028	144	N/A	N/A	Widdenbrook cong.
	TSR Seep	-32.114433	150.395335	179	N/A	N/A	Narrabeen sandstone
	Ray Spring	-32.161146	150.404987	160	N/A	N/A	Alluvium

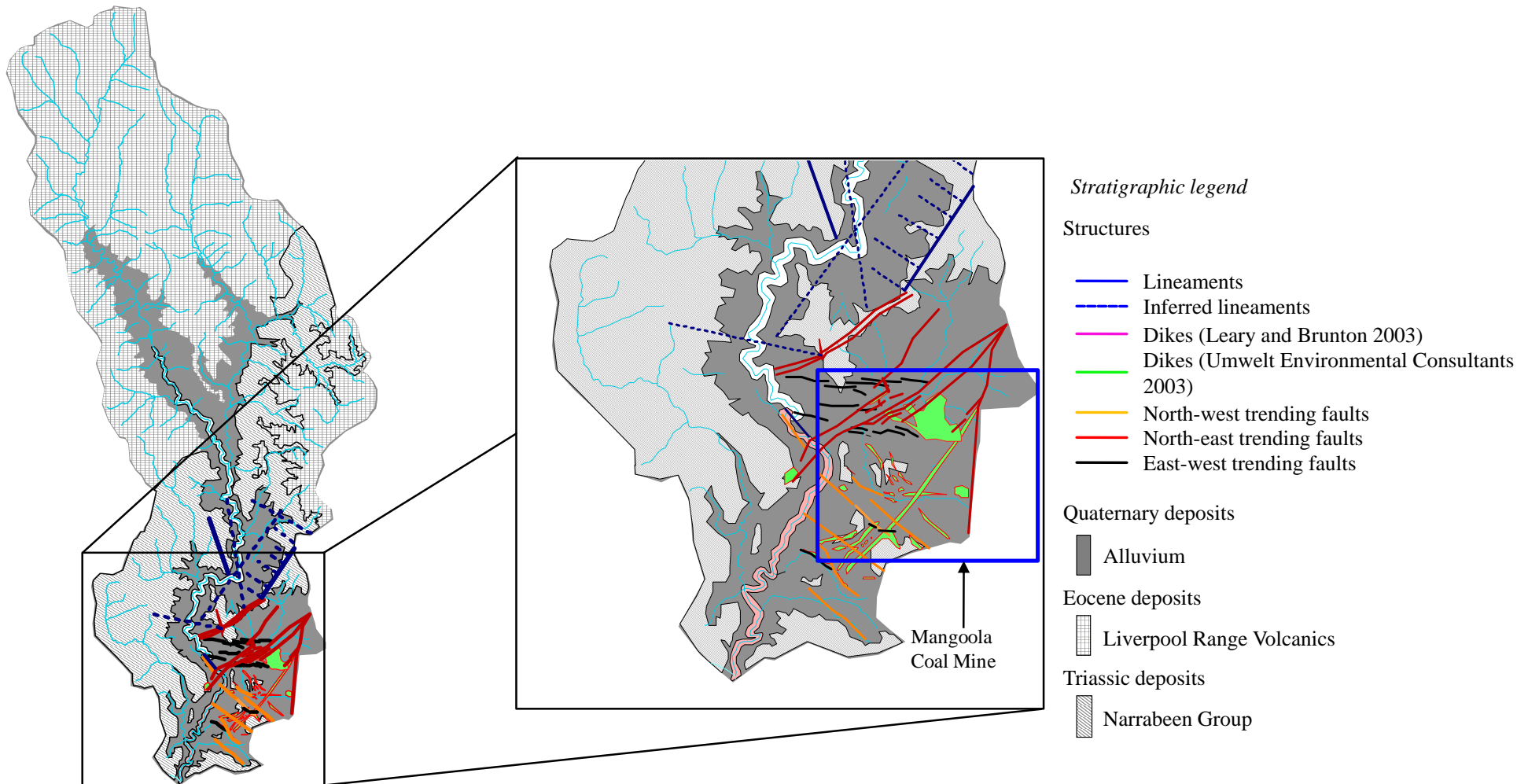


Figure 3.4. Geology of Wybong creek catchment. Figure adapted from Glen and Beckett (1993), Leary and Brunton (2003) and field observations.

confining conditions (Acworth and Brain 2008). The clay is expected to be causing some degree of confinement to both alluvial and fractured rock aquifers in the catchment. The termination of drilling within the alluvium indicates that it is another important aquifer in the Wybong Creek catchment, with groundwater in the Hunter Valley alluvium being of the lowest salinity relative to deeper formations and yielding groundwater at a rate of  $12 - 38 \text{ L s}^{-1}$  (Creelman 1994).

Regional groundwater bodies occur in the Permian Coal Measures which lie beneath the alluvium and the Narrabeen Group in the mid Wybong Creek catchment and outcrop in the southeast (Kellett *et al.* 1987). Flow in both the upper Newcastle Coal Measures and in the deeper Wittingham Coal Measures occurs along joints, thrusts cleats, faults and fractures, with flow less influenced by the configuration of the coal seams which do not have a simple layer cake formation (Creelman 1994). Groundwater from the coal aquifer is not utilised within the Wybong Creek catchment, however, presumably due to the availability of groundwater in the alluvial and fractured Narrabeen Group aquifers close to the surface.

### **3.2. Groundwater bodies**

Groundwater with similar major and minor solute and isotope concentrations can be assumed to source from the same groundwater body, with these solutes in turn having a similar source (Freeze and Cherry 1979; Green *et al.* 2006). Stiff diagrams of samples in the upper catchment were dominated by  $\text{HCO}_3^-$  while those in the lower catchment were dominated by  $\text{Cl}^-$  (Figures 3.5 – 3.6). Analyses of major and minor ions by HCA indicated groundwater samples occurred in two main groups which represented the upper and lower catchment and were distinguishable by  $\text{HCO}_3^-$  and  $\text{Cl}^-$  dominance (Figure 3.7), rather than minor and isotopic constituents. These two larger groups were partitioned into seven sub-groups according to the proportions of Na, Mg, Cl and  $\text{HCO}_3^-$ . Principle component analysis indicated that the proportions of Ba/Cl and Si/Cl were important in differentiating groundwater into groups, however, the two major groups indicated by PCA could again be separated into samples from the upper and lower catchment which were dominated by  $\text{HCO}_3^-$  and  $\text{Cl}^-$  respectively. Canonical analyses also partitioned samples in the upper and lower catchment into different groups though identified differences as occurring mostly due to Ba/Cl, Mn/Cl, and Sr/Cl (Table 3.2; Figure 3.8). Both visual and numerical analyses of groundwater solutes indicated that groundwater in the upper catchment differed from that in the lower catchment, with the

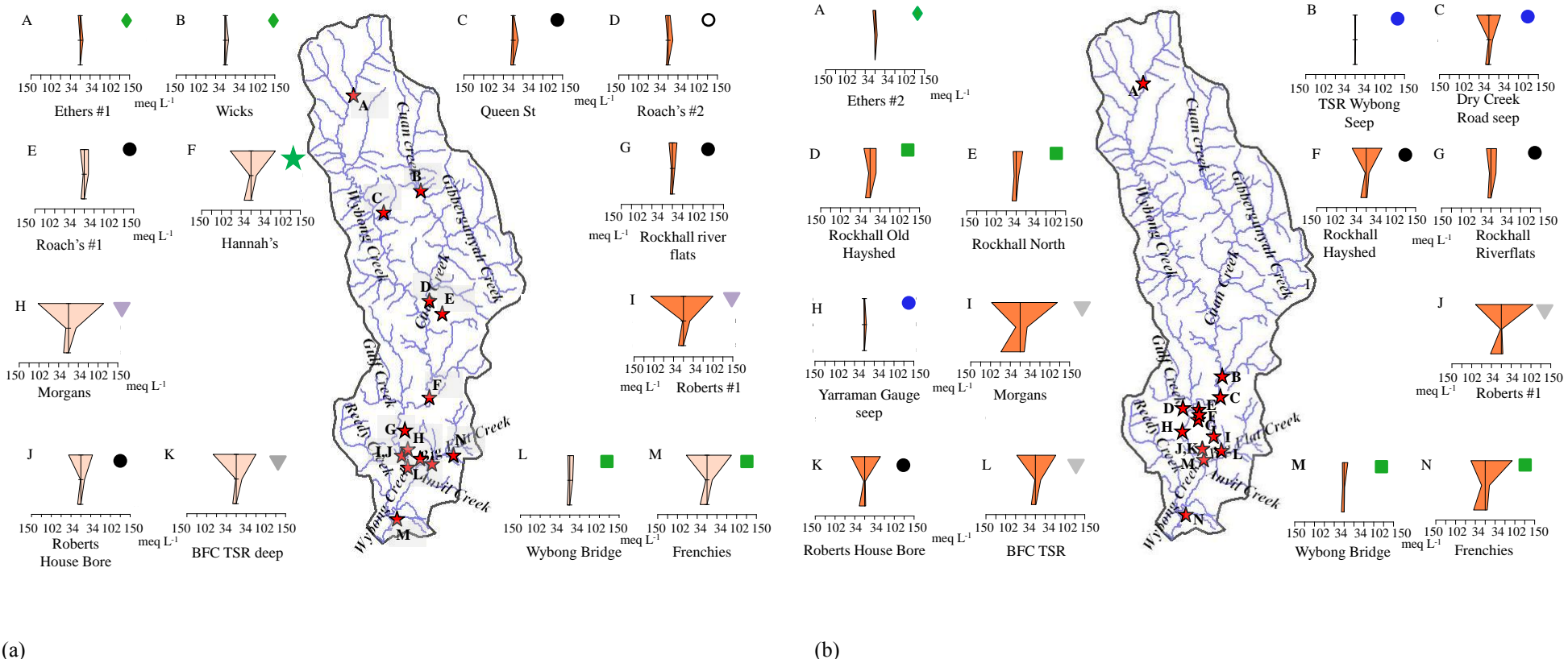


Figure 3.5. Stiff diagrams representing groundwater samples collected in (a) 2006; and (b) 2007. Symbols represent the material into which bores and piezometers were screened: Basalt (◆); sandstone (●); shale (○) conglomerate (★); clay/unconsolidated material (▼); gravel alluvium (■); and springs (●).

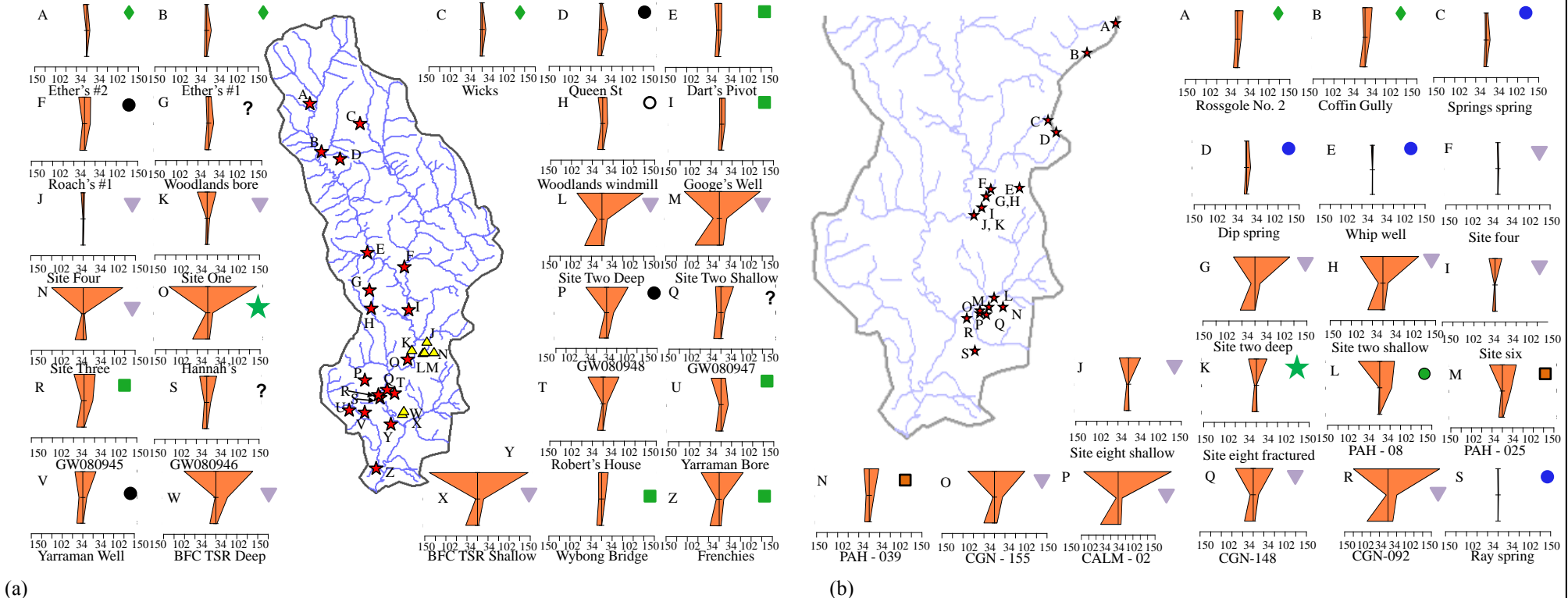


Figure 3.6. Stiff diagrams representing groundwater samples collected in (a) 2008; and (b) 2009. Symbols represent the material into which bores and piezometers were screened: Basalt (◆); sandstone (●); shale (○); conglomerate (★); clay/unconsolidated material (▽); gravel alluvium (■); springs (●); tuffaceous sandstone (□); and coal (●). Bores sunk into indeterminable strata are indicated by (?).

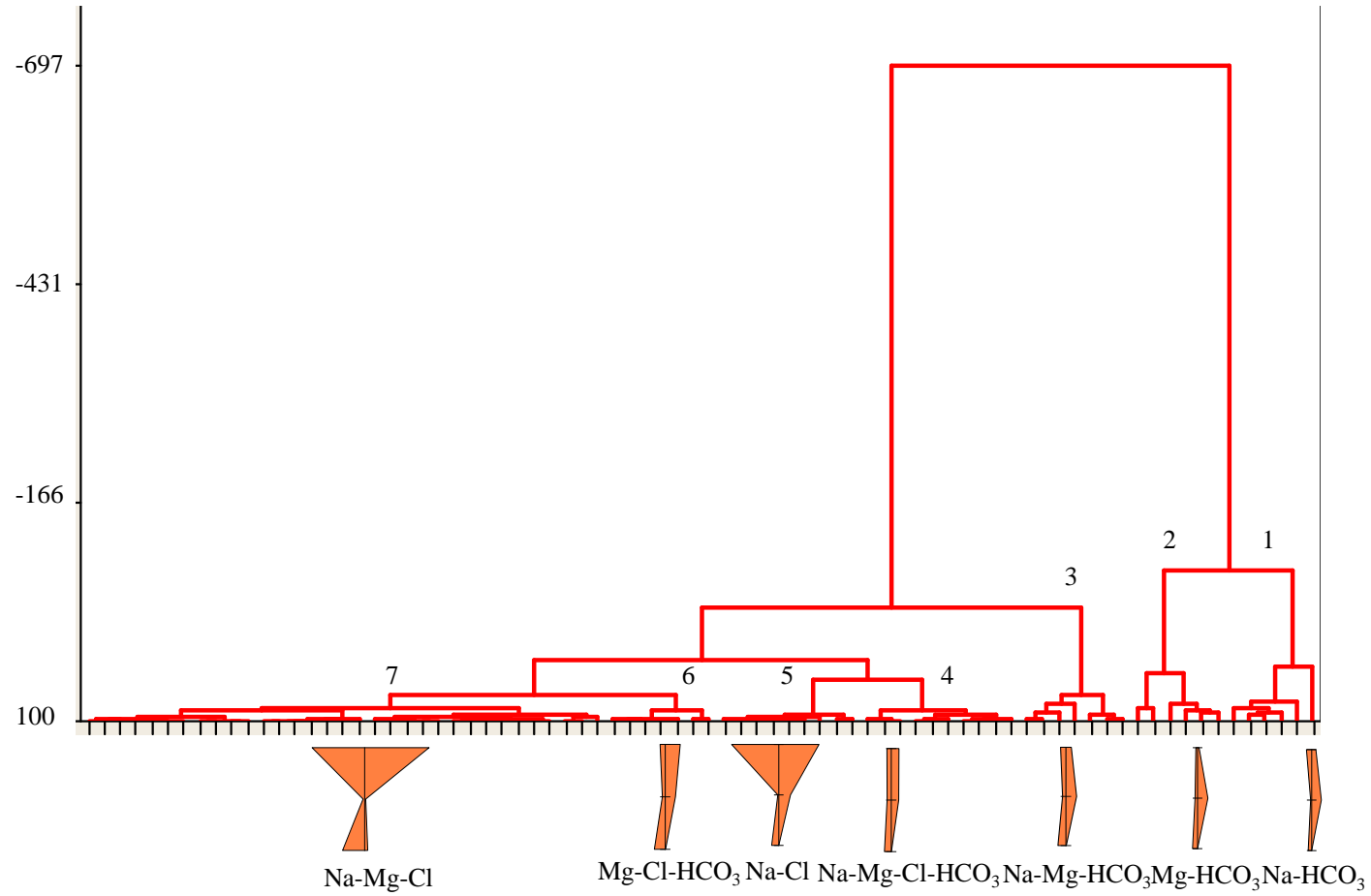


Figure 3.7. Dendrogram of groundwater samples from Wybong Creek. Hierarchical cluster analysis distance measure based on Euclidean distance, linkage rule on Ward's method. Groups are described in Table 3.3.

Table 3.2. Loadings for canonical analysis and for the first and second components of PCA based on orthogonal and varimax rotation.

Factor	PCA loading Varimax rotation				PCA loading Quartimax rotation				Canonical loading			
	Component 1	Rank	Component 2	Rank	Component 1	Rank	Component 2	Rank	Component 1	Rank	Component 2	Rank
Percentage variation	32		18						52.58		22.34	
Al/Cl	0.06	14	0.22	8	0.06	13	0.22	7	0.0		0.0	
Ba/Cl	0.32	5	0.06	11	0.32	5	0.06	11	-121.2	2	422.7	2
Br/Cl	0.10	9	0.36	1	0.10	4	0.36	1	0.0		0.0	
Ca/Cl	0.42	2	-0.22	8	0.43	2	-0.21	8	2.1		6.9	
F/Cl	0.10	9	0.36	1	0.10	9	0.36	1	0.0		0.0	
Fe/Cl	-0.01	16	0.05	12	-0.02	14	0.05	12	0.0		0.0	
HCO <sub>3</sub> /Cl	0.45	1	-0.04	13	0.45	1	-0.03	13	0.0		-0.4	7
K/Cl	0.24	8	0.24	7	0.23	8	0.24	6	-3.4	4	-18.2	4
Mg/Cl	0.37	3	-0.24	7	0.38	3	-0.24	6	0.3	8	-2.8	5
Mn/Cl	-0.01	16	0.30	5	-0.02	14	0.30	3	-612.7	1	1433.5	1
NO <sub>3</sub> /Cl	-0.07	13	0.36	1	-0.07	12	0.36	1	0.0		0.0	
Na/Cl	0.29	6	0.24	7	0.29	6	0.25	5	0.8	7	0.6	6
SO <sub>4</sub> /Cl	0.09	11	-0.14	10	0.09	10	-0.14	10	0.0		0.0	
Si/Cl	0.36	4	-0.02	14	0.36	4	-0.02	14	1.9	6	0.0	
Sr/Cl	0.25	7	0.16	9	0.25	7	0.16	9	99.5	3	-564.0	3
Zn/Cl	-0.08	12	0.35	4	-0.08	11	0.35	2	0.0		0.0	
pH	0.02	15	0.28	6	0.02	14	0.28	4				

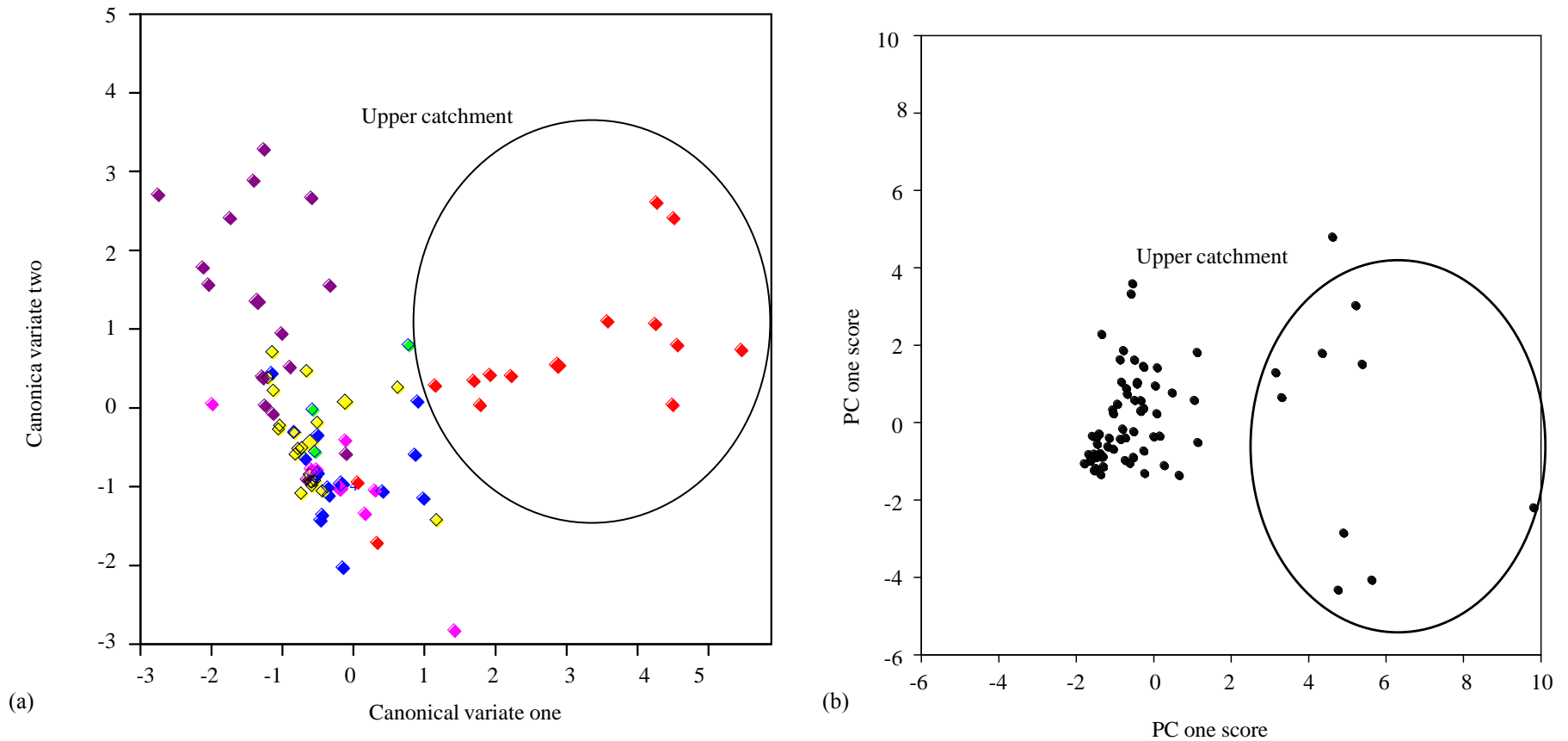


Figure 3.8. (a) Plot of canonical variate one vs canonical variate two; and (b) principle component analyses biplot of principle component one and principle component two. Symbols represent groundwater collected from the upper catchment (♦); mid-catchment (◆); lower catchment (◇); Manobalai piezometers (◆); lower catchment piezometers (◆); and springs (◆).

numerical analyses of hydrochemical data showing no benefit over visual analyses in the identification of groundwater groups in this case.

### **3.2.1. Upper catchment groundwater**

Local groundwater systems recharge on a topographic high and discharge on the adjacent topographic low, with solutes therefore acquired from chemical weathering of locally occurring minerals (e.g., Domenico and Schwartz 1990). Hierarchical cluster analysis indicated samples from the upper catchment were placed into two groups: one which had Na-HCO<sub>3</sub> facies; and one which had Mg-HCO<sub>3</sub> (Figure 3.6). Site Four (19/01/2009), the Yarraman Gauge Seep and Wybong Bridge (06/06/2009) were also in these groups (Table 3.3). Rocks in the Narrabeen Group are dominated by quartz, with major accessory minerals such as feldspar and plagioclase constituting up to 5 % and 10 % of rock volumes (Bai and Keene 1996). The basanite, hawiite and mugearite rocks of the Liverpool Range Volcanics which intrude and cap the Narrabeen Group sandstone are relatively high in Na, K, Mg, and Fe (Schön 1985; Scheibner 1998). Silicate weathering of both the Narrabeen Group and the Liverpool Range Volcanics produces the HCO<sub>3</sub> dominated groundwater seen in groups one and two, with weathering of locally occurring minerals in both groups possible sources of Na and Mg (Bai and Keene 1996; Appelo and Postma 2005).

Different cations dominated group one and two, with group one dominated by Na and group two by Mg. This indicated localised differences in the predominance of Na and Mg containing minerals in the north-east and north-west of the catchment respectively. The chemistry of both groundwater bodies was indicative of localised groundwater systems, with solutes acquired between recharge on the Liverpool Ranges and discharge in the upper Wybong Creek valley. Although spatially separate from samples collected from the upper catchment, the HCO<sub>3</sub> dominated groundwater samples from Site Four (19/01/2009), the Yarraman Gauge Seep and Wybong Bridge (06/06/2009) was consistent with silicate weathering of the Narrabeen Group which also occurs in the lower catchment. Localised groundwater flow systems are, therefore, also likely to occur at these sites.

Table 3.3 (a). Parameters for groundwater bodies as depicted in Figure 3.7., with hydrochemical parameters for the group, samples in each group, TDS ( $\text{mg L}^{-1}$ ), water bearing zones (AHD) and static water level (SWL, AHD). N/A indicates water bearing zone information not available and/or SWL unable to be measured due to the presence of groundwater pumps.  $n$  indicates the number of samples used to describe each parameter.

Group	Hydrochemical parameter	$n$	Mean $\pm$ SD	Sample site	Sample date (DD/MM/YYYY)	TDS ( $\text{mg L}^{-1}$ )	Water bearing zone (AHD)	SWL in relation to water bearing strata (m)
One	Facies	6	$\text{Na-HCO}_3$	Ether's #1	25/04/2006	695	N/A	N/A
	$^{87}\text{Sr}/^{86}\text{Sr}$	1	0.705640	Ether's #1	21/07/2006	615	N/A	N/A
	$\delta^{35}\text{S}$	1	15.881	Ether's #2	21/06/2007	655	N/A	N/A
	$\delta^{18}\text{O}$	1	-6.2418	Ether's #2	21/07/2007	799	N/A	N/A
	$\delta^2\text{H}$	1	-38.9735	Site Four	19/01/2009	241	187	-1.6
	$\text{C}^{14}\text{age}$	1	8 770	Wybong Bridge	06/06/2007	842	134	-1.3
Two	Facies	6	$\text{Mg-HCO}_3$	Ether's #1	21/07/2008	764	N/A	N/A
	$^{87}\text{Sr}/^{86}\text{Sr}$	1	0.703480	Queen Street	22/07/2006	1061	N/A	N/A
	$\delta^{35}\text{S}$	0	N/A	Queen Street	21/07/2008	1030	N/A	N/A
	$\delta^{18}\text{O}$	4	$-5.2310 \pm 0.3072$	Wicks Cuan Creek	21/07/2006	680	N/A	N/A
	$\delta^2\text{H}$	4	$-33.2442 \pm 1.6943$	Wick Cuan Creek	27/03/2009	634	N/A	N/A
	$\text{C}^{14}\text{age}$	0	N/A	Yarraman Gauge Seep	05/07/2007	500	N/A	0
Three	Facies	7	$\text{Na-Mg-HCO}_3$	Roach's #1	22/07/2006	1453	203.3	-2.0
	$^{87}\text{Sr}/^{86}\text{Sr}$	3	$0.705804 \pm 0.001509$	Woodlands Bore	21/07/2006	1035	N/A	N/A
	$\delta^{35}\text{S}$	2	$9.3105 \pm 3.6621$	Wybong Bridge	25/04/2006	1140	134	-1.2
	$\delta^{18}\text{O}$	2	$-6.7172 \pm 0.8824$	Yarraman Bore	17/07/2008	1810	33	108.6
	$\delta^2\text{H}$	2	$-41.6340 \pm 3.8670$	Springs Spring	27/03/2009	673	N/A	N/A
	$\text{C}^{14}\text{age}$	3	$7 493 \pm 9 721$	Dip Paddock Spring	27/03/2009	686	N/A	N/A
Four	Facies	10	$\text{Mg-Cl-HCO}_3$	Wybong Bridge	21/07/2008	1250	134	-0.3
	$^{87}\text{Sr}/^{86}\text{Sr}$	5	$0.704980 \pm 0.001500$	Rossgole #2	24/03/2009	614	N/A	N/A
	$\delta^{35}\text{S}$	2	$15.1785 \pm 1.9212$	Coffin Gully	24/03/2009	850	N/A	N/A
	$\delta^{18}\text{O}$	4	$-5.1040 \pm 1.0275$	Robert's House	25/04/2006	2803	149.6	N/A
	$\delta^2\text{H}$	4	$-32.5815 \pm 6.3846$	Robert's House	23/07/2006	2582	149.6	N/A
	$\text{C}^{14}\text{age}$	0	N/A	PAH-039	24/03/2009	2636	N/A	N/A
				Rockhall North	06/06/2007	1683	N/A	N/A
				Rockhall North	17/07/2008	1905	N/A	N/A
				Site Two Deep	19/01/2009	7277	179.0	0.1
				Yarraman well	17/07/2008	2053	136.4	-0.9

Table 3.3 (b). Parameters for groundwater bodies as depicted in Figure 3.7., with hydrochemical parameters for the group, samples in each group, TDS ( $\text{mg L}^{-1}$ ), water bearing zones (AHD) and static water level (SWL, AHD). N/A indicates water bearing zone information not available and/or SWL unable to be measured due to the presence of groundwater pumps.  $n$  indicates the number of samples used to describe each parameter. S indicates springs or seeps.

Group	Hydrochemical parameter	$n$	Mean $\pm$ SD	Sample site	Sample date (DD/MM/YYYY)	TDS ( $\text{mg L}^{-1}$ )	Water bearing zone (AHD)	SWL in relation to water bearing strata (m)
Five	Facies	9	Na-Mg-Cl-HCO <sub>3</sub>	Roach's #2	22/07/2006	1453	197.4	9.3
	<sup>87</sup> Sr/ <sup>86</sup> Sr	2	0.705613 $\pm$ 0.000892	Roach's #1	21/07/2008	1588	203.3	4.4
	$\delta^{35}\text{S}$	3	17.9320 $\pm$ 9.4507	TSR Seep	05/07/2007	252	N/A	0
	$\delta^{18}\text{O}$	2	-3.0654 $\pm$ 0.5691	Dart's Pivot	21/07/2008	1119	N/A	N/A
	$\delta^2\text{H}$	2	-20.8874 $\pm$ 1.7230	Woodlands Windmill	21/07/2008	1877	N/A	N/A
	$\text{C}^{14}\text{age}$	0	N/A	Googe's Well	21/07/2008	927	N/A	N/A
				Rockhall Riverflats	06/06/2007	2114	N/A	N/A
				Rockhall Old hayshed	06/06/2007	1683	138.0	3.1
				Rockhall Old hayshed	17/07/2008	1905	138.0	4.0
Six	Facies	7	Na-Cl	Robert's #1	25/04/2006	6676	N/A	N/A
	<sup>87</sup> Sr/ <sup>86</sup> Sr	4	0.708194 $\pm$ 0.00145	BFC TSR Deep	25/04/2006	4778	141.0	2.2
	$\delta^{35}\text{S}$	1	6.355	PAH-08	24/03/2009	5151	105.0	50.1
	$\delta^{18}\text{O}$	5	-5.4539 $\pm$ 0.7348	Site One	19/02/2008	1418	184.2	2.2
	$\delta^2\text{H}$	5	-33.6751 $\pm$ 5.8533	Site One	16/07/2008	890	185.0	1.2
	$\text{C}^{14}\text{age}$	2	12 765 $\pm$ 16 397	Site Four	16/07/2008	347	171.0	12.4
				Whip Well	01/05/2009	224	S	S
Seven	Facies	33	Na-Mg-Cl	Robert's #1	02/06/2007	5728	N/A	N/A
	<sup>87</sup> Sr/ <sup>86</sup> Sr	7	0.707246 $\pm$ 0.001284	Robert's House	02/06/2007	3198	149.6	16.9
	$\delta^{35}\text{S}$	7	19 $\pm$ 4.9	Robert's House	29/07/2008	3717	149.6	19.5
	$\delta^{18}\text{O}$	7	-5.1419 $\pm$ 0.6479	Site Two Shallow	19/02/2008	5897	170.6	7.4
	$\delta^2\text{H}$	7	-33.0336 $\pm$ 2.6422	Site Two Shallow	15/07/2008	5521	179.0	-1.0
	$\text{C}^{14}\text{age}$	10	2 519 $\pm$ 4 144	Site Two Shallow	19/01/2009	6968	179.0	0.1
				Site Two Deep	19/02/2008	5181	162.6	14.9
				Site Two Deep	15/07/2008	4343	179.0	0.4
				Site Three	19/02/2008	4570	186.3	2.5
				Site Three	16/07/2008	4573	192.0	-3.2

Table 3.3 (c). Parameters for groundwater bodies as depicted in Figure 3.7., with hydrochemical parameters for the group, samples in each group, TDS ( $\text{mg L}^{-1}$ ), water bearing zones (AHD) and static water level (SWL, AHD). N/A indicates water bearing zone information not available and/or SWL unable to be measured due to the presence of groundwater pumps.  $n$  indicates the number of samples used to describe each parameter. S indicates springs or seeps.

Group	Hydrochemical parameter	$n$	Mean $\pm$ SD	Sample site	Sample date (DD/MM/YYYY)	TDS ( $\text{mg L}^{-1}$ )	Water bearing zone (AHD)	SWL in relation to water bearing strata (m)
Seven	Facies	33	Na-Mg-Cl	Site Six	15/05/2009	1830	165.0	3.5
	$^{87}\text{Sr}/^{86}\text{Sr}$	7	$0.707246 \pm 0.001284$	Site Eight Shallow	15/05/2009	2631	156.5	2.3
	$\delta^{35}\text{S}$	7	$19 \pm 4.9$	Site Eight Fractured	15/05/2009	2498	154.5	4.2
	$\delta^{18}\text{O}$	7	$-5.1419 \pm 0.6479$	Dry Creek Road Seep	05/06/2007	4589	S	S
	$\delta^2\text{H}$	7	$-33.0336 \pm 2.6422$	CALM-02	24/03/2009	13601	N/A	N/A
	$\text{C}^{14}\text{age}$	10	$2519 \pm 4144$	CGN-092	24/03/2009	12805	N/A	N/A
				CGN-148	24/03/2009	4770	N/A	N/A
				CGN-155	24/03/2009	7064	N/A	N/A
				PAH-025	24/03/2009	4155	N/A	N/A
				BFC TSR Deep	06/06/2007	4754	141	10.5
				BFC TSR Deep	17/07/2008	5629	141	8.4
				BFC TSR Shallow	24/03/2009	6745	145	9.1
				Rockhall Riverflats	23/07/2006	1509	N/A	N/A
				Rockhall Riverflats	06/06/2007	2087	N/A	N/A
				Rockhall Hayshed	06/06/2007	2571	126	17.8
				Rockhall Hayshed	17/07/2008	2506	126	18.6
				Frenchies	25/04/2006	4294	119	-4.8
				Frenchies	06/06/2007	5411	119	-4.8
				Frenchies	21/07/2008	3286	119	-3.1
				Hannah's	22/07/2006	5179	146	15.4
				Hannah's	16/07/2008	6248	146	17.3
				Morgan's	25/04/2006	8511	177	4.0
				Morgan's	06/06/2007	8484	177	2.2

Isotopes can give important information on groundwater flow paths, with  $^{87}\text{Sr}/^{86}\text{Sr}$  in groundwater the same as the rock from which it was sourced (e.g., Bullen and Kendall 1998), and the degree of  $\delta^{18}\text{O}$  and  $\delta^2\text{H}$  enrichment indicating the extent to which water evaporates along a flow path (Gonfiantini *et al.* 1998). The  $^{87}\text{Sr}/^{86}\text{Sr}$  signatures for both the upper catchment groundwater bodies were 0.703480 – 0.705640 (Table 3.3), with these signatures indicative of groundwater sourcing Sr from the weathering of volcanic rocks in the area (Gingelet *et al.* 2007). Enrichment of  $^{18}\text{O}$  and  $^2\text{H}$  was greater (i.e. less negative) in group two than in group one, indicating that groundwater in group two is more exposed to evaporation at some point along its flow path. No clear  $^{14}\text{C}$  age occurred for any groundwater bodies (Figure 3.9), with unreliable  $^{14}\text{C}$  ages due to a lack alternative dating methods by which  $^{14}\text{C}$  dates could be calibrated and due to fracture flow in the catchment affecting  $^{14}\text{C}$  dates (Cook 1999). The degree of evaporative enrichment is also difficult to extrapolate from these data, given the small number of samples analysed for isotopes. Isotopic data in this case only indicates groundwater samples in groups one and two are different but not why.

Piezometric surfaces indicate groundwater flow direction on the condition that groundwater flows horizontally, and that SWLs in bores and piezometers represent a single aquifer (e.g., Domenico and Schwartz 1990). The dominance of the subgroups by Na in the western, and Mg in the eastern upper catchment indicated two separate but localised groundwater systems in this area. The localised conditions mean that a piezometric surface may have indicated realistic flow directions. The occurrence of only two bores per subgroup, however, limited the creation of this. Information on water bearing zones was also limited within the state groundwater database (NSW DNR

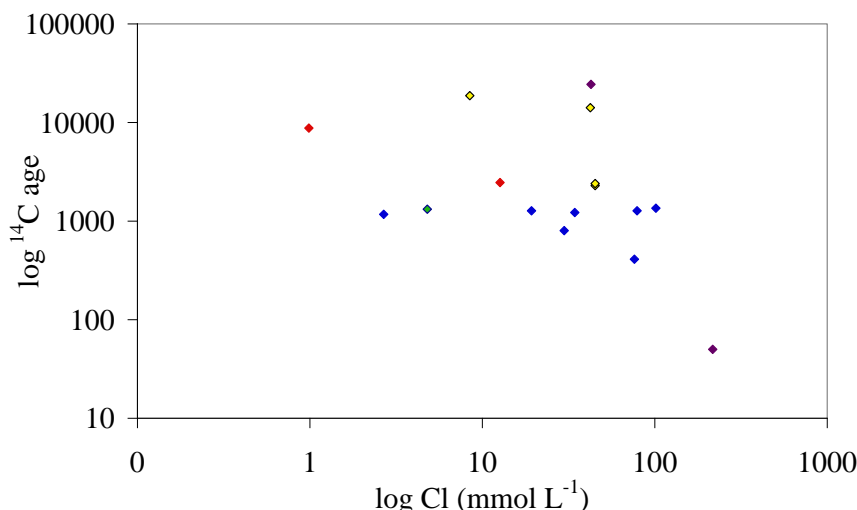


Figure 3.9. Uncorrected  $^{14}\text{C}$  dates for upper catchment groundwater (◆); mid-catchment groundwater (◆); lower catchment groundwater (◆); Manobalai piezometers (◆); and lower catchment piezometers (◆).

2005), and the measurement of water heights was prevented due to groundwater pumps installed within the bores in this part of the catchment. Groundwater flow regimes in the upper catchment were, therefore, not able to be described beyond a conceptual model where localised Na dominated groundwater systems recharge at isolated topographic highs in the north-west of the catchment, while Mg dominated localised groundwater systems recharge on the topographic highs in the north-east. The topographic highs for the localised systems in both the north-east and north-west of the catchment occur in the Liverpool Ranges.

### **3.2.2. Lower catchment groundwater**

Intermediate and regional groundwater systems are recharged at a number of topographic highs and discharged at the major topographic low (e.g., Stuyfzand 1998). The groundwater chemistry of discharging intermediate and regional systems is not necessarily related to the geology of discharge sites (Chambers *et al.* 1996; Uliana *et al.* 2007), with abrupt changes in groundwater chemistry along flow paths indication of groundwater discharge from these systems (e.g., Love *et al.* 1994). Group three represented groundwater samples dominated by Na, Mg and HCO<sub>3</sub>, with these samples collected from different sub-catchments in the mid and lower catchment (Table 3.3). The other four groups which represented groundwater bodies in the lower catchment were also comprised of groundwater samples collected from these areas, with groups partitioned according to Cl-HCO<sub>3</sub> co-dominance, and dominance by Na and/or Mg. Groundwater samples collected from bores screened into the same aquifer, such as Site Four and Site Two, which were screened into alluvium; and Hannah's and Roach's #1 which were screened into the Narrabeen Group; did not necessarily belong to the same groundwater group. The significant difference in chemistry between groundwater samples collected from the same aquifer indicates the occurrence and/or mixing of groundwater bodies with different solute sources, and therefore different spatial extents, within the same aquifer. The dominance of groundwater by Cl in many mid-lower catchment groups is anomalous with silicate weathering of the alluvium and the silica dominated Narrabeen Group aquifers the groundwater was sampled from, and is indication of groundwater discharge from intermediate and/or regional groundwater systems.

Groundwater discharged from regional groundwater bodies is typically saline and Na-Cl dominated (Genereux and Jordan 2006), with water evolving from Ca-HCO<sub>3</sub> to Na-Cl facies with increasing distance down flow paths (Eugster 1984; Jankowski and

Jacobson 1989). The Narrabeen Group occurs throughout the Wybong Creek catchment, with most groundwater samples in the mid and lower catchment yielded from bores screened into this aquifer or into alluvium derived from weathering of the Liverpool Volcanics or Narrabeen Group. Chemical weathering of these silicate dominated materials produces groundwater with  $\text{HCO}_3$ -dominated solutes. The dominance of Cl in many samples, and differing  $^{87}\text{Sr}/^{86}\text{Sr}$ , and  $\delta^{35}\text{S}$  signatures than occurs in the upper catchment, indicated that groundwater in the lower catchment has not evolved from groundwater sourced in the Narrabeen Group nor the Liverpool Range Volcanics. Dominance by Cl instead indicated solutes in many mid-lower catchment samples were acquired from another source. Cl dominated groundwater is known to occur in the Permian strata which underlie the Narrabeen Group and Liverpool Range Volcanics (Kellett *et al.* 1987). Cl dominated salt stores may also occur in the regolith (e.g., Ruprecht and Schofield 1991), with groundwater also evolving to Cl dominance with increasing distance down flow paths due to the precipitation of  $\text{HCO}_3$  and  $\text{SO}_4$  minerals (e.g., Eugster 1984; Jankowski and Jacobson 1989).

Valleys act as groundwater discharge regions with the major topographic low of a catchment receiving discharge from local, intermediate, and regional groundwater systems (e.g., Domenico and Schwartz 1990). Two samples (Dart's Pivot and Roach's #2) had  $\text{HCO}_3$ -Cl facies in the mid-catchment area, with all other  $\text{HCO}_3$ -Cl samples occurring at the top of the basalt-capped sandstone escarpments (Rossgole #2, Coffin Gully, Dip Spring, Springs Spring), within the gravel alluvium of Wybong Creek (Wybong Bridge, Rockhall Riverflats, Rockhall Hayshed, Yarraman Well) or as groundwater seeps (TSR Seep). Although the two  $\text{HCO}_3$ -Cl dominated groundwater samples from the mid-catchment area may represent groundwater evolving from  $\text{HCO}_3$  to Cl dominated facies, mixing of water bodies with Cl and  $\text{HCO}_3$  facies may also give rise to water dominated by these anions, with further geochemical investigation required in order to isolate which of these is more likely.

The potential for groundwater discharge is indicated by hydraulic heads rising above the water-bearing strata in an aquifer and by the occurrence of springs (Freeze and Cherry 1979), with discharge typically occurring in catchment valleys (e.g., Domenico and Schwartz 1990). Discharging and pressurised groundwater in the lower Wybong Creek catchment was indicated by SWLs generally above the level of water-bearing strata in all non-alluvial aquifers (Table 3.3). Static water levels were instead below water-bearing strata in the alluvial aquifer on most sample dates, which indicates the alluvial aquifer can be recharged by Wybong Creek (Praamsa *et al.* 2009). A

number of permanent and ephemeral springs and groundwater seeps occurred in the mid-catchment area, with springs indicating points where groundwater is pressurised to the extent that it is forced to the Earth's surface. Springs in this area were both fresh (e.g. Whip Well) and saline (e.g. Dry Creek Road Seep). In addition, one of two salt scalds that occur in the Wybong Creek catchment also occurred in the mid-catchment area of Wybong Creek, with this possibly indicating saline groundwater discharge (Morgan and Jankowski 2004). The incidence of both saline, and fresh ( $<500 \text{ mg L}^{-1}$ ) springs and groundwater in the mid-catchment area indicates that this area is possibly a site where groundwater discharge from localised, intermediate and/or regional groundwater systems occurs.

Local, intermediate and regional groundwater systems will develop in areas of hummocky terrain similar to that which occurs across the Wybong Creek catchment, with discharge of all these systems possible in the major topographic low of a catchment (Domenico and Schwartz 1990). The mid-catchment area of Manobalai is not the lowest point in the catchment, however, with Wybong Creek itself incised approximately 20 m below the regolith surface where saline seeps and springs occur. Discharge of all groundwater systems in the Manobalai area rather than at lower points in the catchment may occur due to vertical groundwater flow, with a number of mechanisms by which vertical flow occurs.

Recharge and discharge may be vertical in areas where the hydraulic conductivity of a unit is higher than that of the unit above (Domenico and Schwartz 1990). This is almost certainly the case in the Wybong Creek catchment where smectitic clays occur above fractured Narrabeen Group sandstones and conglomerates on both the escarpments and in the Wybong Creek valley. Discharge may also occur in the mid-lower catchment area due to strata in the catchment dipping north and west (Brunton and Moore 2004), whereas the surface topography decreases from north to south. The dipping of beds in the opposite direction to the topographic drive causes groundwater to flow up-dip (Domenico and Schwartz 1990). This cannot be proven in the Wybong Creek catchment, although strata dip north and west while topography dips south. Vertical flow may also occur due to fracturing and faulting, with deep fractures connecting the Permian Coal Measures to the Narrabeen Group sandstones and conglomerates in the lower catchment (Umwelt Environmental Consultants 2006). The conceptual model of a saline regional groundwater system in the Permian Coal Measures being forced to flow up-dip and discharge via fractures in the Narrabeen

Group adjacent to locally derived fresh groundwater systems is consistent with observations in the catchment.

#### **4. Conclusions**

Most outcropping rock in the Wybong Creek catchment is fractured sandstones and conglomerates of the Narrabeen Group. The termination of many bores within this formation indicates that it is an important aquifer within the catchment, with the termination of many bores within the alluvium in the mid-lower catchment indicating this is also an important aquifer. Regional groundwater systems are known to occur within the Permian Coal Measures, however, this groundwater is not utilised within the catchment.

Numerical analyses provided no added benefit in the grouping of groundwater samples despite using many more major and minor ions than visual analyses. Visual and numerical analyses of groundwater samples indicated that groundwater can be divided into two groups, constituting groundwater systems in the upper and lower catchment. Groundwater flow in the upper catchment occurs as localised systems which recharge on isolated topographic highs in the Liverpool Ranges and discharge in adjacent topographic lows. A number of groundwater samples from the lower catchment were also placed in the upper catchment groundwater group. This was due to the similar groundwater chemistry of these and upper catchment groundwater samples, and indicated localised groundwater flow at these sites.

Chloride dominated groundwater in the lower catchment did not source solutes from chemical weathering of the Narrabeen Group. Saline and Na-Cl dominated springs, scalds and seeps in the mid-catchment are instead indicative of discharge from intermediate and/or regional groundwater systems. Abrupt and significant changes in groundwater chemistry within the alluvium and fractured Narrabeen Group were also indication of intermediate and/or regional groundwater systems. Groundwater discharge and recharge within the alluvium and fractured Narrabeen Group was likely to occur as vertical groundwater flow due to fracturing and higher hydraulic conductivity of these formations than the smectitic clays occurring above. This vertical groundwater flow makes it difficult to predict groundwater flow paths. The dipping of strata and topography in opposite directions, indicates groundwater recharging in the Liverpool Ranges may be forced to flow up dip before discharging into the fractured Narrabeen Group. Solutes occurring in this groundwater may be acquired from the deeper Permian Coal Measures in the mid-lower catchment area between recharge and discharge, with

further geochemical investigation necessary to identify the source of solutes to the groundwater described.

The findings of this research were in contrast to Kellett *et al.*'s (1987) work which found HCO<sub>3</sub> dominated groundwater was sourced from the weathering of the Triassic Narrabeen Group. The Cl dominated groundwater could not be related to any of the surficial aquifers in the catchment, with further research required in order to corroborate Kellett *et al.*'s (1987) findings that solutes in this groundwater group are sourced from to the Wittingham Coal Measures. The research presented in this chapter was limited by a lack of data on the geology of the catchment and long term groundwater height data. A detailed description of the aquifers could not be undertaken, therefore, with only a conceptual understanding of confining layers and flow directions within the aquifers described. Further research is required in order to clarify the conceptual models put forward in this chapter, specifically the extent of groundwater bodies. This can be done by conducting tracer studies and pumping tests, with further dating of groundwater in addition to the initial <sup>14</sup>C dates presented also useful for this purpose.



---

## **Chapter Four**

### Surface and groundwater geochemistry of Wybong Creek



## 1. Introduction

The Wybong Creek catchment lies within the upper Hunter Valley, New South Wales, and contains award winning vineyards and cattle growing operations. The high solute concentration in Wybong Creek is a salinity hazard to crops (Rhoades *et al.* 1992; Ayers and Westcot 1994), with irrigation using saline surface water causing vine mortality to at least one vineyard within the catchment (Yarraman). Groundwater is an important solute source to Wybong Creek, as indicated by permanent river flows during drought conditions and sudden increases in salinity independent of tributaries (Chapter Two). The Permian Coal Measures have been suggested as a source of saline groundwater to the Hunter catchment by Kellett *et al.* (1987) and Creelman (1994). Other sources of salinity must also be considered within the catchment, however, with evapoconcentration of groundwater, and mobilisation of salt stores from within the regolith both means by which salinisation occurs within New South Wales (e.g., Bradd *et al.* 1997), Australia (e.g., Salama *et al.* 1993), and indeed the world at large (e.g., Jacobsen and Adams 1958). This research was therefore conducted in order to constrain the source of salinity to the Wybong Creek catchment and prevent further salinisation within this and other catchments in this important agricultural region.

### 1.1. Origin of solutes in groundwater

Solutes are acquired along groundwater flow paths as a result of water-rock interactions such as chemical weathering and cation exchange. Weathering reactions are commonly identified using ion ratios, conservative tracers and reactive tracers. Molar Cl/Br and Na/Cl ratios, for example, are commonly used to identify halite as a source of solutes to groundwater (e.g., Davis *et al.* 1998; Kloppmann *et al.* 2001; Cartwright and Weaver 2005). Ratios of  $^{87}\text{Sr}/^{86}\text{Sr}$  indicate the dominant source of Sr, with the proportion of  $^{87}\text{Sr}$  to  $^{86}\text{Sr}$  in groundwater the same as the mineral the Sr was weathered from, regardless of temperature, chemical speciation or biological processes which might occur (Bullen and Kendall 1998; Ingraham *et al.* 1998). Cation exchange can instead be indicated by Ca/Na and Mg/Na ratios, with increases in Mg/Na and Ca/Na ratios occurring when groundwater percolates through clayey materials due to Na replacing Ca and Mg on the exchange sites of clays (Appelo and Postma 2005).

Saline groundwater can also arise when salt stores created by evapoconcentration and/or evapotranspiration of rainwater are dissolved, and when groundwater evapoconcentrates along flow paths (e.g., Herczeg *et al.* 1992; Cartwright *et al.* 2006). The evaporitic history of water is commonly indicated by the enrichment of  $^{18}\text{O}$  relative

to  $^{16}\text{O}$ , and  $^2\text{H}$  to  $^1\text{H}$ , which are reported as  $\delta^{18}\text{O}$  and  $\delta^2\text{H}$  when analyses are normalised to the standard Vienna Standard Mean Oceanic Water (VSMOW) (e.g., Kendall and Caldwell 1998). Similar  $\delta^{18}\text{O}$  and  $\delta^2\text{H}$  signatures between groundwater and rainfall indicate groundwater that has recharged with little or no evaporation. Enrichment of the heavier water isotopes instead indicates removal of the lighter water isotopes due to evaporation, with groundwater undergoing evaporation at recharge, discharge, or some other point along its flow path.

Groundwater solutes may be acquired via rainfall, cation exchange and chemical weathering, however, the mixing of two or more groundwater bodies also causes changes to solute concentrations. Groundwater mixing can be tracked using tracer studies in areas where groundwater moves fast enough to be tracked within study time frames. Geochemical modelling is instead used to elucidate groundwater flow paths and identify endmembers in areas where flow paths cannot be easily traced, and where knowledge gaps in experimental or field data occur, but further sampling and data gathering is not feasible (e.g., Turner and Barnes 1998). Ratios of  $^{87}\text{Sr}/^{86}\text{Sr}$  are particularly useful in mixing models, and indicate how two endmembers might mix to give rise to a water body with a composition intermediary of the endmembers (Kendall and Caldwell 1998). Two-component mixing models such as these indicate how saline groundwater might mix with saline surface water as occurs in the Wybong Creek catchment, allowing for the identification of likely endmembers.

## **1.2. The Hydrogeology of the Wybong Creek catchment**

Five hydrochemical subgroups occur in the lower Wybong Creek catchment, with these representing intermediate and/or regional groundwater bodies dominated by Na-Cl and co-dominated by  $\text{HCO}_3$  and Mg (Chapter Three). Groundwater in groups five, six and seven were dominated by Cl type facies and had the highest salinity. These samples occurred in bores and piezometers screened into sandstone/conglomerate and alluvium in the southeast of the catchment, with solute concentrations up to one third of seawater in piezometers CGN-092 ( $12\ 805\ \text{mg L}^{-1}$ ) and CALM-02 ( $13\ 691\ \text{mg L}^{-1}$ ). Bores PAH-039 (group four) and PAH-025 (group five) were screened within the Newcastle Coal Measures and instead had Na-Cl- $\text{HCO}_3$  and Na-Mg-Cl- $\text{HCO}_3$  facies, and solute concentrations of  $2636 - 4155\ \text{mg L}^{-1}$  (Chapter Three). Regional groundwater systems occur in the Permian Coal Measures, which includes the Newcastle Coal Measures, with these hypothesised to be the source of salinity to the Wybong Creek catchment (Kellett *et al.* 1987; Creelman 1994). Differing hydrochemical facies and solute

concentrations between groundwater yielded from alluvium, fractured Narrabeen Group rocks and the Newcastle Coal Measures, however, indicated that saline groundwater in piezometers was not directly sourced from the Newcastle Coal Measures.

### 1.3. Aims

The aim of this chapter was to identify the source of solutes to surface and groundwater in the Wybong Creek catchment. This was achieved by meeting the following objectives:

1. To identify chemical weathering reactions occurring along groundwater flow paths;
2. To identify the affects of cation exchange on solute concentrations in groundwater bodies; and
3. To identify the affects of evaporation on solute concentrations in groundwater bodies.

## 2. Materials and methods

Groundwater was sampled from as many bores (25), piezometers (17), and springs (seven) as possible within the Wybong Creek catchment (Figure 4.1). The sampling of surface water and analyses of O and H isotopes are described in Chapter Two (Section 2.2). Sampling of groundwater, and analyses of cations, anions, and Sr, S, and C isotopes is instead described fully in Chapter Three (Section 2.4). Saturation indices were calculated using PHREEQC Interactive version 2.13.2.1727 and the PHREEQC.dat database.

### 2.1. Sources of Ca and Mg to groundwater

A mixing model was created in order to evaluate whether groundwater sampled from regolith attained Ca and Mg through cation exchange and/or other reactions in the regolith (Eq. 4.1). Groundwater samples selected for the purposes of the model were from Sites Three (saline) and Four (fresh), with Site Two (mixed) occurring down gradient of both sites and therefore receiving groundwater which is likely to have interacted with the regolith. Magnesium and Ca were used interchangeably in the following equations (e.g., Appelo and Postma 2005; Hiscock 2005):

$$C_{Mg,mix} = f_{saline} \cdot C_{Mg, saline} + (1-f_{saline}) \cdot C_{Mg,fresh} \quad (4.1)$$

where  $C_{Mg, mix}$  was the Mg concentration ( $\text{mmol L}^{-1}$ ) in the mixed (Site Two Shallow and Deep) groundwater;  $f_{saline}$  was the fraction of saline groundwater from the saline endmember (Site Three) based on Cl concentrations ( $\text{mmol L}^{-1}$ );  $C_{Mg, saline}$  was the mean

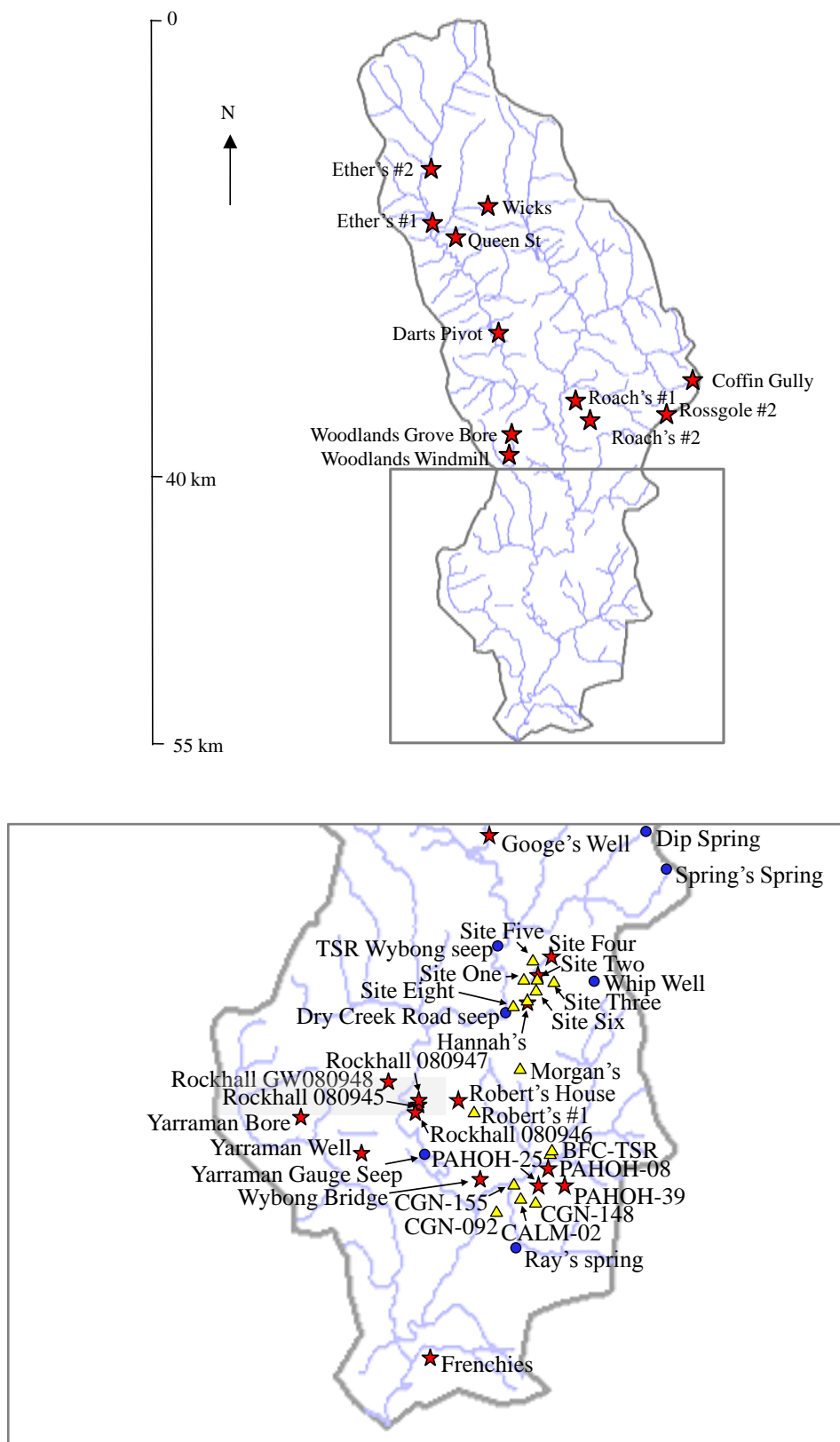


Figure 4.1. Groundwater sampling locations within the Wybong Creek catchment, including springs (●), bores (★), and piezometers (▲), where bores are screened into a number of water-yielding layers and piezometers are screened into a single water-yielding layer.

Mg concentration ( $\text{mmol L}^{-1}$ ) in the saline groundwater (Site Three); and  $C_{\text{Mg}, \text{fresh}}$  was the mean Mg concentration ( $\text{mmol L}^{-1}$ ) in the fresh groundwater (Site Four). The Mg concentration in Site Two groundwater sourced from reactions in the regolith, including cation exchange, was then calculated using Eq. 4.2:

$$C_{\text{Mg}, \text{react}} = C_{\text{Mg, sample}} - C_{\text{Mg, mix}} \quad (4.2)$$

where  $C_{\text{Mg, sample}}$  was the Mg concentration measured in samples from Site Two.

## 2.2. Two-component mixing models

Mixing models were created in order to test how two groundwater endmembers with known solute concentrations might conservatively mix to create a mixed water body. The model was used courtesy of Marc Norman (Research School of Earth Sciences, The Australian National University) as follows (Eq. 4.3):

$$(F_{(M,\text{one})} \times C_{(M,\text{one})}) + ((1 - F_{(M,\text{one})}) \times C_{(M,\text{two})}) \quad (4.3)$$

where  $F$  is the fraction of endmember one or two ( $M$ ) in the mixture and  $C$  is the concentration of the ion in each endmember. An expanded version of this equation was used for modelling the mixing of  $^{87}\text{Sr}/^{86}\text{Sr}$  (Eq 4.4):

$$\frac{\left( F_{(^{87}\text{Sr}/^{86}\text{Sr},\text{one})} \times C_{(^{87}\text{Sr}/^{86}\text{Sr},\text{one})} \times C_{(\text{Sr},\text{one})} + (1 - F_{(\text{Sr},\text{one})}) \times C_{(^{87}\text{Sr}/^{86}\text{Sr},\text{two})} \times C_{(\text{Sr},\text{two})} \right)}{\left( (F_{(\text{Sr},\text{one})} \times C_{(\text{Sr},\text{one})}) + (1 - F_{(\text{Sr},\text{one})}) \times C_{(\text{Sr},\text{two})} \right)} \quad (4.4)$$

Mixing curves were calculated for a range of possible endmembers and plotted to compare with the measured compositions of surface and groundwater samples.

## 3. Results and discussion

The following discussion will progress through a number of lines of evidence as to the source of solutes to surface and groundwater in the Wybong Creek catchment. Water-rock interaction will be discussed first, then evidence for evapoconcentration and cation exchange. Hypothetical mixing models will be presented finally, before a synthesis of all the lines of evidence is presented and a conclusion as to the source of solutes is reached. Raw data for all groundwater samples as presented in the Appendix for Chapter Three (Tables A3.2 – A3.5), while surface water chemistry is instead presented in the Appendix for Chapter Two (Tables A2.4 – A2.5 and A2.7).

### 3.1. Water-rock interaction

Ratios of  $^{87}\text{Sr}/^{86}\text{Sr}$  in groundwater are the same as those in the mineral that the Sr was sourced from, with ion ratios additional means of identifying the weathering reactions which have lead to particular solutes in groundwater (e.g., Bullen and Kendall

1998; Casanova *et al.* 2001). Groundwater from the upper catchment had  $^{87}\text{Sr}/^{86}\text{Sr}$  ratios similar to Tertiary Basalt and basalts in the New England Fold belt, ranging from 0.703442 – 0.706244 (Figure 4.2; Table 4.1). These samples also plotted along a 1:1 line of cations versus  $\text{HCO}_3^-$ , and had TDS concentrations ranging from 615 to 719 mg L<sup>-1</sup> (Figure 4.3). The production of one mole of  $\text{HCO}_3^-$  to one mole of  $\text{Na}^+ + \text{Ca}^+ + \text{Mg}^+ + \text{K}^+$ , and  $^{87}\text{Sr}/^{86}\text{Sr}$  ratios similar to basalts indicates solutes sourced from silicate weathering (e.g., Roy *et al.* 1999; Appelo and Postma 2005), with the Liverpool Ranges therefore indicated as a source of solutes to surface and groundwater in the upper catchment. The additional dominance of Na and Mg can be linked to the occurrence of basinite, hawaiite and alkali olivine basalts within the Liverpool Ranges, with these rocks typically high in Na and Mg (Scheibner 1998). The similarity between  $^{87}\text{Sr}/^{86}\text{Sr}$  in surface water in the upper and lower catchment to groundwater indicates that much of the  $\text{HCO}_3^-$  and Sr in Wybong Creek was acquired from groundwater that discharges from the upper catchment, with the slight increase in  $^{87}\text{Sr}/^{86}\text{Sr}$  in lower catchment surface water indicating an alternate source of Sr with higher  $^{87}\text{Sr}/^{86}\text{Sr}$  in this stretch of the Creek.

Degassing and evapoconcentration causes the precipitation of  $\text{HCO}_3^-$ , Ca and/or Mg ions from solution, causing greater proportions of Na-Cl in the remaining groundwater (e.g., Eugster 1984; Jankowski and Jacobson 1989). Such degassing and evapoconcentration may have caused the Na-Mg-Cl-HCO<sub>3</sub> dominated groundwater from the Newcastle Coal Measures to evolve to the saline, Na-Cl dominated water seen

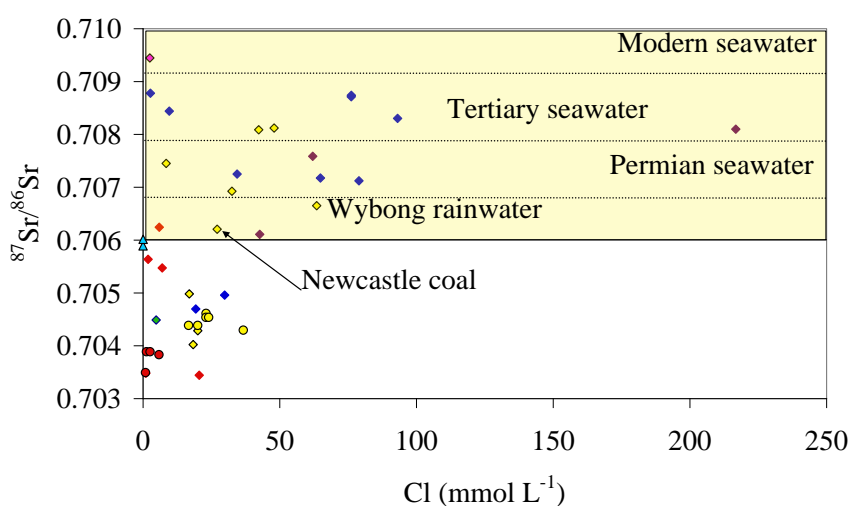


Figure 4.2.  $^{87}\text{Sr}/^{86}\text{Sr}$  ratios relative to Wybong Creek surface and groundwater samples and  $^{87}\text{Sr}/^{86}\text{Sr}$  signatures of possible solute sources to Wybong Creek. The yellow coloured region indicates marine  $^{87}\text{Sr}/^{86}\text{Sr}$  signatures. Symbols indicate groundwater from the upper catchment (♦); mid-catchment piezometers (◆); lower catchment (◇); Manobalai (◆); lower catchment piezometers screened into clays (◆); and springs (◆). Symbols for surface water samples from the upper catchment (●); mid-catchment (●); lower catchment (●); and rainwater (▲), are also shown.

Table 4.1.  $^{87}\text{Sr}/^{86}\text{Sr}$  signatures of possible salt sources occurring in Wybong Creek catchment.

Salt source		$^{87}\text{Sr}/^{86}\text{Sr}$ (%)	References (and contained therein)
Aeolian dust	Great Sandy Desert (Western Australia)	0.722-0.74	(Gingeles <i>et al.</i> 2007)
	Precambrian	0.715	(Gingeles <i>et al.</i> 2007)
	Palaeozoic	0.719	(Gingeles <i>et al.</i> 2007)
	Modern (Lake Eyre)	0.709-0.732	(Revel-Rolland <i>et al.</i> 2006)
Seawater	(Modern)	0.070917 - 0.70923	(Miller <i>et al.</i> 1993; Bricker <i>et al.</i> 1994; Douglas <i>et al.</i> 1995)
	(Tertiary)	0.7079	(Douglas <i>et al.</i> 1995)
	Permian	0.7068	(Faure 1986)
	(Phanerozoic)	0.70912	(Harrington and Herczeg 2003)
Rainwater	(Palaeozoic)	0.7099	(Musgrove and Banner 1993)
		0.7088-0.7200	(Bricker <i>et al.</i> 1994)
		0.7109	(Douglas <i>et al.</i> 1995)
Sandstone	(Murray)	0.704-0.706	(Douglas <i>et al.</i> 1995)
	(Tertiary)	0.703-0.705	(Douglas <i>et al.</i> 1995)
	(New England Fold Belt)	0.703-0.705	(Gingeles <i>et al.</i> 2007)
Basalt	Precambrian Shield	0.725-0.745	(Harrington and Herczeg 2003)
	Stripa Granite (Sweden)	0.74056-0.75360	(Harrington and Herczeg 2003)
	Bangemall Basin (Western Australia)	0.725-0.814	(Harrington and Herczeg 2003)
	Permian Granite (New England Fold Belt)	0.7127	(Gingeles <i>et al.</i> 2007)
Other	Yilgarn Block (Western Australia)	0.86-0.96	(Gingeles <i>et al.</i> 2007)

in the Narrabeen Group and in the alluvium. Pedogenic carbonate has been observed at the 72 km sample site, with carbonate layers such as these thought to have formed through degassing of groundwater in other parts of the Hunter Valley (Hamilton 1992). Most Wybong Creek surface and groundwater samples were super-saturated with calcite and dolomite, indicating that carbonate precipitation is causing decreased proportions of Ca, Mg and HCO<sub>3</sub> relative to Na and Cl in water across the catchment (Figure 4.4). Saline and Cl dominated groundwater had marine  $^{87}\text{Sr}/^{86}\text{Sr}$  signatures of 0.707246 – 0.708194, as opposed to the 0.706206 signature of the single sample which represented the Newcastle Coal Measures (Figure 4.2). The difference in  $^{87}\text{Sr}/^{86}\text{Sr}$  signatures of Na-Cl dominated groundwater and groundwater sampled from the Newcastle Coal Measures indicates that the solutes in groundwater with Na-Cl (group six) and Na-Mg-Cl (Group Seven) facies were not sourced from the Newcastle Coal Measures. Chloride dominated water instead has a marine source of solutes, despite carbonate precipitation causing increased proportions of Cl in Wybong Creek surface and groundwater.

Rainwater acquires solutes from the sea and therefore has many geochemical signatures similar or identical to marine water (Appelo and Postma 2005), with marine signatures in Wybong Creek groundwater either due to solute sourced from rainfall or marine accession. Ratios of Cl/Br differ between rainwater and marine water (Davis *et al.* 1998), however, offering a means of distinguishing solutes sourced from these

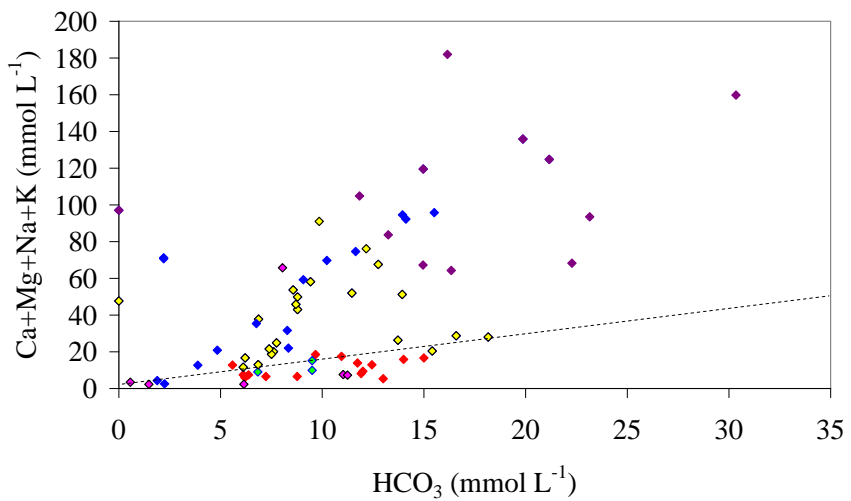
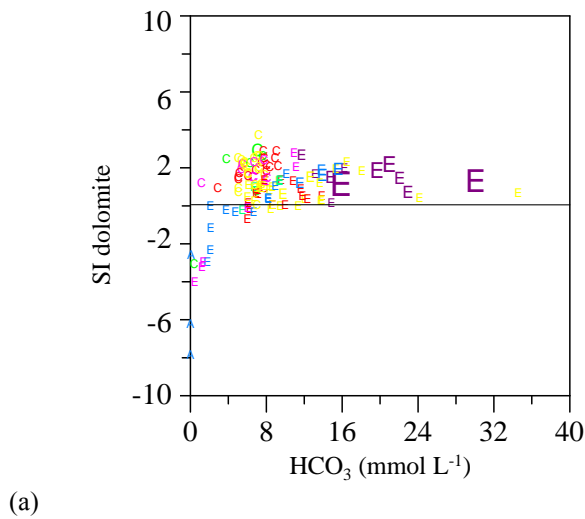
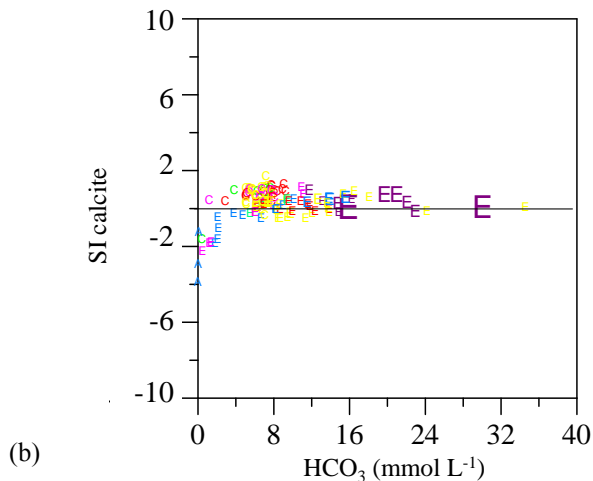


Figure 4.3. Major cation concentrations as a function of  $\text{HCO}_3$  concentration, with 1:1 Cation/ $\text{HCO}_3$  concentrations indicated by the dashed line. Symbols indicate groundwater from the upper catchment (♦); mid-catchment piezometers (◆); lower catchment (◇); Manobalai (◆); lower catchment piezometers screened into clays (◆); and springs (◆). Symbols for surface water samples from the upper catchment (●); mid-catchment (●); lower catchment (●); and rainwater (▲), are also shown.



(a)



(b)

(a) Dolomite; and (b) calcite saturation indices for surface and groundwater samples in the Wybung Creek catchment as a function of  $\text{HCO}_3$  concentration ( $\text{mmol L}^{-1}$ ). Symbols indicate surface and groundwater samples as described for Figure 4.3 and are scaled to the concentration of total dissolved solids (TDS).

endmembers. Ratios of Cl/Br indicated that solutes in piezometers were partially sourced from halite dissolution (Figure 4.5). Another endmember was indicated by samples plotting above the halite dissolution zone, however, it was unclear whether the other endmember was marine water, rainwater, or both. Signatures of  $\delta^{34}\text{S}_{\text{SO}_4}$  were between 6.7 – 28.8, with possible marine and rainwater endmembers not distinguishable using these or Na/Cl ratios (Figure 4.5; Table 4.2). Rainwater must be evaporated many times over in order to become saline, however, with groundwater which has become saline due to the evapoconcentration of rainwater being significantly more enriched in  $^{18}\text{O}$  and  $^2\text{H}$  than marine water. Rainwater and marine can therefore be distinguished despite their similar geochemical signatures through the analyses of  $\delta^2\text{H}$  and  $\delta^{18}\text{O}$ .

### 3.2. Evapoconcentration

Surface water and groundwater can be evaporated significantly as it flows through catchments (e.g., Dimmock *et al.* 1974; Cartwright *et al.* 2004), with some hyper-saline surface water bodies in Australia formed almost entirely through the evapoconcentration of rainwater (e.g. Jankowski and Jacobson 1989; Petrides *et al.* 2006). The evaporation of water is indicated by enrichment of  $^{18}\text{O}$  and  $^2\text{H}$  and depletion of  $^{16}\text{O}$  and  $^1\text{H}$  relative to a local meteoric water line (LMWL; Clark and Fritz 1997). No relationship between solute concentration and  $^{18}\text{O}$  and  $^2\text{H}$  enrichment occurred in groundwater sampled from the Wybong Creek catchment (Figure 4.6). Samples from Whip Well and Site Four, for example, were enriched relative to the approximate LMWL created from three rainwater samples in this study, and relative to the Melbourne (MMWL) and global meteoric water lines (GMWL), with salinities of 223 and 105 – 366 mg L<sup>-1</sup> respectively. Water from Site Two and Hannah's, however, had salinities of 5540 – 6960 and 5204 – 6130 mg L<sup>-1</sup> respectively, and fell on or closer to the meteoric water lines than Whip Well and Site Four samples. No relationship existed between bore depth and evaporation either, with deep bores such as Yarraman Bore at a depth of -39 m Australian Height Datum (AHD) and shallower bores such as Queen Street with a depth of 236 AHD, both falling on the approximate LMWL. The lack of correlation between solute concentration and evaporation indicates that evaporation of rainwater is not directly causing saline groundwater formation or large increases in groundwater salinity such as occurs in central Australia (e.g., Jankowski and Jacobson 1989; Petrides *et al.* 2006), and in Victoria (Cartwright *et al.* 2004), with an absence of a correlation between depth and isotope enrichment further indicating that recharge is rapid and occurs with little evaporation (Gonfiantini *et al.* 1998).

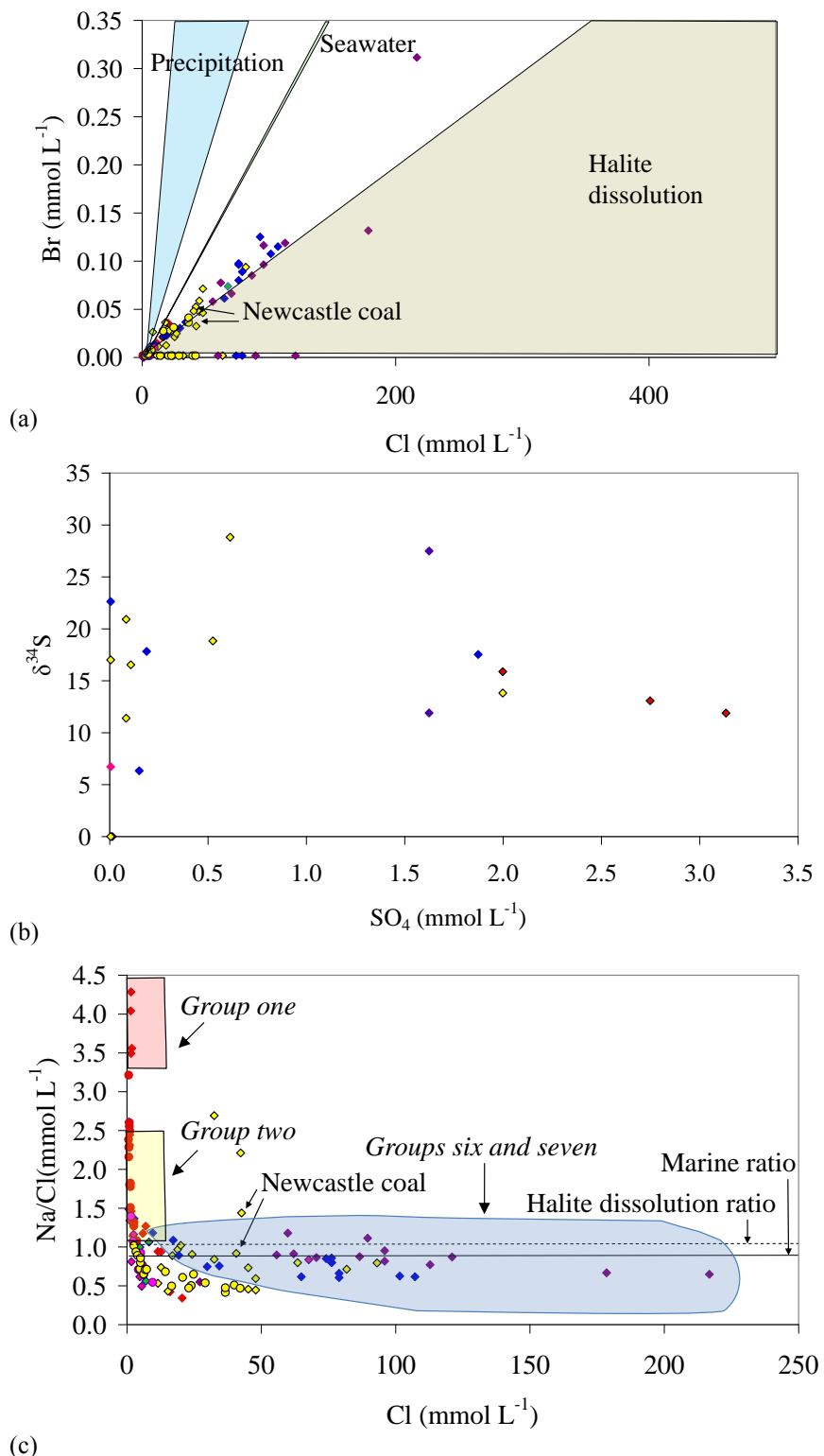


Figure 4.5. (a) Concentrations of Br as a function of Cl ( $\text{mmol L}^{-1}$ ) for Wybong Creek surface and groundwater samples. Ratios of Br/Cl for different solute sources taken from Davis *et al.* (1998); (b) Concentrations of  $\text{SO}_4$  as a function of  $\delta^{34}\text{S}$ ; and (c) Na/Cl ratios for surface and groundwater samples collected from the Wybong Creek catchment, with groups described in Chapter Three. Ratios of Na/Cl in marine water and halite taken from Drever (1997). Symbols indicate groundwater from the upper catchment (♦); mid-catchment piezometers (◆); lower catchment (◇); Manobalai (◆); lower catchment piezometers screened into clays (◆); and springs (◆). Symbols for surface water samples from the upper catchment (●); mid-catchment (●); lower catchment (●); and rainwater (▲), are also shown.

Table 4.2. Ranges in  $\delta^{34}\text{S}$  of sulfur and sulfur containing substances which could be acting as salt sources to Wybong Creek.

Salt source	Details	$\delta^{34}\text{S}$ (‰)	Reference
Seawater	Modern ( $\delta^{34}\text{S}_{\text{SO}_4}$ )	+21	(Clark and Fritz 1997)
	Cambrian	+30	(Claypool <i>et al.</i> 1980)
	Triassic-Jurassic	+16 ± 1.5	(Claypool <i>et al.</i> 1980)
	Late Permian	+10.5 ± 1.0	(Claypool <i>et al.</i> 1980)
	Mesozoic	+10 – +20	(Faure 1986)
Marine evaporites (Gypsum)	Lower Cretaceous	+14	(Chivas <i>et al.</i> 1991)
	Mid-Miocene	+22	(Chivas <i>et al.</i> 1991)
	Modern	+20.99	(Chivas <i>et al.</i> 1991)
Coal	Quaternary sediment (South Australia)	+15.3	(Chivas <i>et al.</i> 1991)
	Tertiary sediment (Victoria, Australia)	+21.8	(Chivas <i>et al.</i> 1991)
	Marine	-16	(Smith <i>et al.</i> 1982)
	High Sulfur (Freshwater depositional environment with subsequent marine incursion, Australian, Organic S > 1% Total S)	+4.6 – +20	(Smith <i>et al.</i> 1982)
Shales	Low Sulfur (Freshwater depositional environment, Australian, Organic S < 1% Total S)	+4.6 – +7.3	(Smith <i>et al.</i> 1982)
	Gas produced from combustion of coal	-3 – +3	
		-40 – +16	(Clark and Fritz 1997)
Biogenic Pyrite		<-50 – +5	(Clark and Fritz 1997)
Igneous rocks		-5 – +18	(Clark and Fritz 1997)

Saline groundwater in the lower Wybong Creek catchment had isotopic and chemical signatures similar to marine water, with halite dissolution contributing to solute concentrations. The lack of  $\delta^2\text{H}$  and  $\delta^{18}\text{O}$  enrichment relative to TDS concentration indicates evapoconcentrated rainwater is not a source of saline water to the catchment. The poor relationship between  $^{87}\text{Sr}/^{86}\text{Sr}$  in groundwater sampled from the Newcastle Coal Measures and saline groundwater from the mid-lower catchment indicated that these too are not the source of the marine influenced saline water to the catchment. Salt stores formed by the complete removal of rainwater by evaporation, however, may exist within the regolith or deeper strata. The mobilisation of this salt by present day rainwater would then give rise to saline groundwater without an evaporitic signature similar to that seen in this study, with different solute concentrations attributed to differing degrees of dilution.

Saline groundwater may be sourced from the Wittingham Coal Measures. These occur beneath the Newcastle Coal Measures, contain halite efflorescences, and were inundated by marine water (Kellett *et al.* 1987). In saline regions of the Hunter Valley groundwater within the Wittingham Coal Measures contains Na-Cl-HCO<sub>3</sub> or Na-Cl dominated groundwater with mean TDS concentrations of 5700 mg L<sup>-1</sup> (Creelman 1994). Sodium and Cl occur at concentrations of up to 2400 and 3500 mg L<sup>-1</sup> respectively within the Na-Cl dominated groundwater of the Wittingham Coal

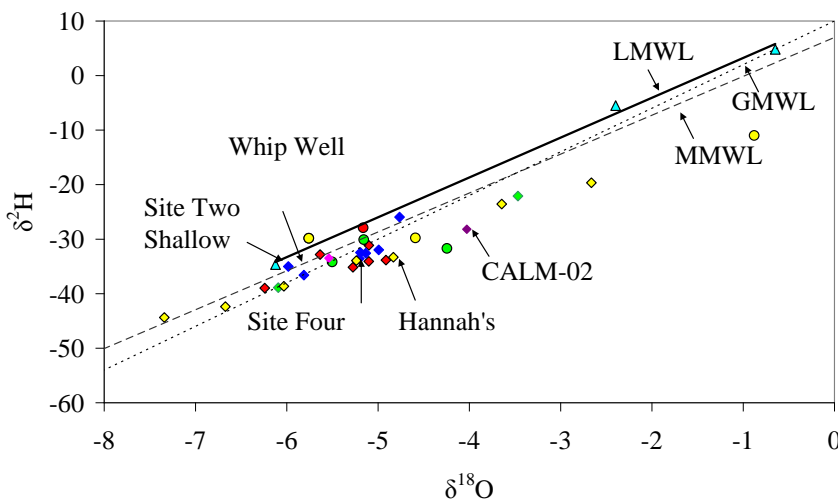


Figure 4.6. Values for  $\delta^2\text{H}$  and  $\delta^{18}\text{O}$  of surface and groundwater samples in the catchment relative to the approximate local (LMWL), Melbourne (MMWL), and GMWL. Symbols indicate groundwater from the upper catchment (◆); mid-catchment piezometers (◆); lower catchment (◆); Manobalai (◆); lower catchment piezometers screened into clays (◆); and springs (◆). Symbols for surface water samples from the upper catchment (●); mid-catchment (●); lower catchment (●); and rainwater are also shown (▲).

Measures at the Mount Arthur Mine (AGE 2006), which lies within 20 km of the Lower Wybong Creek catchment. Concentrations of Na and Cl are lower within the Wittingham Coal Measures at the Bengalla Coal Mine, 12 km from the lower Wybong catchment, at up to 760 and 1170 mg L<sup>-1</sup> respectively (Mackie Martin and Associates 1993). Sodium and Cl concentrations are up to 4290 and 2913 mg L<sup>-1</sup> respectively in groundwater which is identified as sourcing from a marine and halite influenced endmember in this study. The similar hydrochemical facies, marine influence, and similar Na and Cl concentrations within the halite containing Wittingham Coal Measures indicates these are a likely source of saline groundwater to the lower Wybong Creek catchment.

The Wittingham Coal Measures lie at least 300 m below the Earth's surface in the mid-catchment area, beneath both the Narrabeen Group and the Newcastle Coal Measures. Deep fracturing occurs in this part of the Sydney Basin (Tadros 1993; Scheibner 1998), with a number of lineaments, faults and fractures indicated in the mid-catchment area (Chapter Three; Leary and Brunton 2003). Fractures and/or faults would provide means of saline groundwater discharge into overlying aquifers, with vertical groundwater flow from the Wittingham Coal Measures to surficial aquifers occurring throughout the Hunter Valley (Kellett *et al.* 1987; Creelman 1994). Groundwater discharge from the Wittingham Coal Measures to the Hunter Rivers occurs via faults also occurs, with discharge measured at 14 L s<sup>-1</sup> (AGC 1984).

Another alternative source of salinity to the Wybong Creek catchment is a sedimentary brine. These occur in sedimentary basins in other regions of the world, have marine signatures, and have solute concentrations of up to 400 000 mg L<sup>-1</sup> (e.g., Banner *et al.* 1989; Kreitler 1989; Ranganathan and Hanor 1989; Musgrove and Banner 1993). Sedimentary brines are only hypothesised to occur in the Sydney Basin, however, and while they cannot be discredited as a source of solutes to the Wybong Creek catchment they have not been clearly identified anywhere within the region (Patchett and Langford 2005). The Wittingham Coal Measures are, therefore, not the only possible source of Na-Cl dominated water to the Wybong Creek catchment. They are the most likely, however, given the current geological and hydrochemical results.

### 3.3. Cation Exchange

Groundwater and surface water in the upper catchment sourced Mg from the chemical weathering of minerals in the Liverpool Ranges, however, Mg was also co-dominant in groundwater sampled from piezometers screened into regolith in the lower catchment (Chapter Three). Magnesium increased concurrently with Na in groundwater sampled from piezometers and most other water bodies in the catchment, while Ca increased concurrently with Na concentrations in groundwater collected from piezometers and surface water samples (Figure 4.7). Sodium dissolved in groundwater reacts with the exchangeable divalent cations on clay's exchange sites, causing saline water to evolve from Na-Cl facies to Na-Ca/Mg-Cl facies (Appelo and Postma 2005), and eventually resulting in Ca/Mg-Cl dominated groundwater (Eq. 4.5):



where X is the exchange site on the regolith material.

The increase of Ca with Na in groundwater sampled from piezometers screened into clays but not bores, indicated either chemical weathering reactions or cation exchange reactions within the regolith were affecting Ca concentrations. Conservative mixing of groundwater is indicated by points on a Piper plot falling along a straight line parallel to the SO<sub>4</sub>/Cl, while points plotting perpendicular to this line indicate cation exchange is likely to be causing increasing Ca and Mg concentrations with increasing Na (Figure 4.8; Appelo and Postma). Groundwater in lower catchment piezometers plotted perpendicular to the SO<sub>4</sub>/Cl line and therefore source Ca from cation exchange reactions, as opposed to water in the upper catchment which largely acquires Ca through chemical weathering. Magnesium instead increases with increasing Na concentrations in surface water samples, groundwater from bores and groundwater from piezometers,

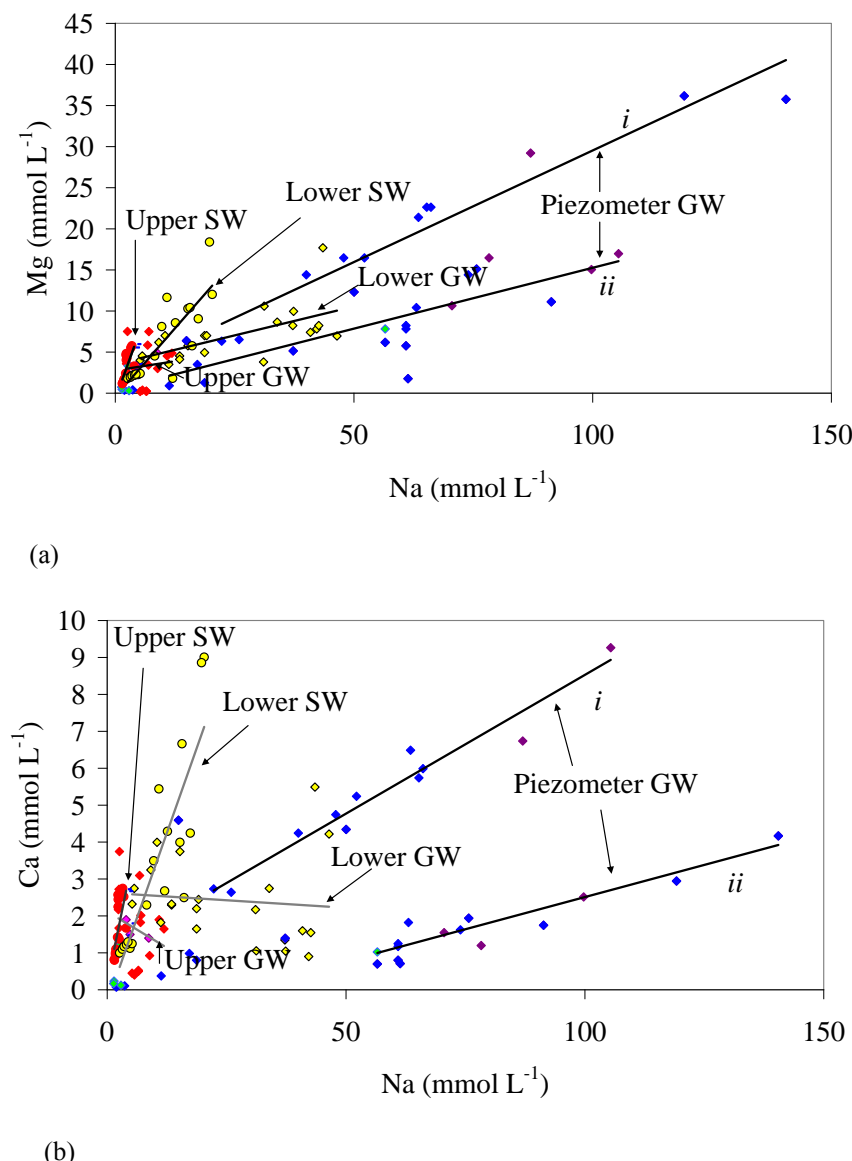


Figure 4.7. (a) Mg vs Na ( $\text{mmol L}^{-1}$ ) ; and (b) Ca vs Na ( $\text{mmol L}^{-1}$ ) in surface water (SW) and groundwater (GW) sampled from the Wybung Creek catchment. Symbols indicate groundwater from the upper catchment (◆); mid-catchment piezometers (◆); lower catchment (◆); Manobalai (◆); lower catchment piezometers screened into clays (◆); and springs (◆). Symbols for surface water samples from the upper catchment (●); mid-catchment (●); lower catchment (●); and rainwater (▲), are also shown.

indicating that both chemical weathering and cation exchange are resulting in the Mg-Na hydrochemical facies seen in the catchment.

Cation exchange causes an increase of one mole Mg and Ca in the soil solution for every two moles of Na exchanged from the clay surface (Jarvie *et al.* 1997). Two cation exchange trends occurred within groundwater from lower catchment piezometers. For every mmol of Na in solution in the high Mg group (group *i*),  $0.2333x + 6.2338 \text{ mmol L}^{-1}$  of Mg was exchanged into solution (Figure 4.7). In the high Ca group (group *i*)  $0.072x + 1.2442 \text{ mmol L}^{-1}$  of Ca was exchanged into solution, with the exchange of both Ca and Mg totalling  $16 \text{ meq kg}^{-1}$ . In the low Mg and low Ca groups (groups *ii*),

$0.0768x + 7.5589$  mmol of Mg, and  $0.0348x - 0.9738$  mmol of Ca respectively were exchanged into solution, totalling  $13.4 \text{ meq kg}^{-1}$ . Samples from group *i* plotted perpendicular to the groundwater mixing line on the piper diagram (Figure 4.8). This indicated that the different proportions of Ca and Mg in groups *i* and *ii* were due to cation exchange on group *i*, while the different proportions of Ca and Mg in group *ii* were due to groundwater mixing.

The trend of increasing Ca and Mg concentrations along groundwater flow paths was investigated further using samples from bores and piezometers screened into regolith in the mid-catchment area. Groundwater at Sites Two Deep and Shallow and Site Three were assumed to be part of the same groundwater body, with groundwater evolving from Na-Cl facies at Sites Three and Four to Na-Cl-Mg facies along the flow path to Site Two. Between 48 and 64 mol % of Mg occurring in Site Two groundwater was sourced from reactions occurring in the regolith between Sites Three and Two. The remaining 36 – 52 % of Mg at Site Two was already present in Site Three groundwater before it arrived at Site Two (Table 4.3). Similar calculations for Ca indicated between 73 and 78 % of this ion were sourced from reactions in the regolith. These results are further evidence that cation exchange plays an important role in the solute composition of groundwater in the catchment.

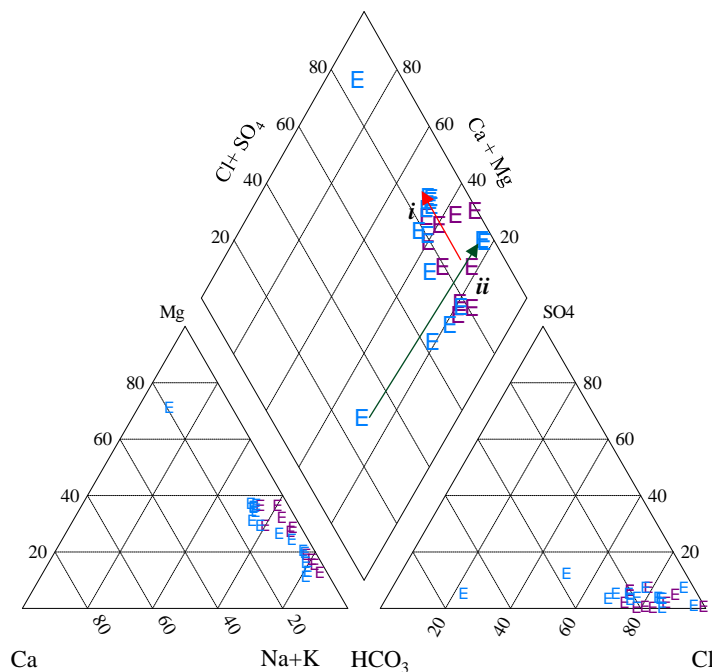


Figure 4.8. Piper diagram showing mixing ( $\longrightarrow$ ) and cation exchange ( $\longrightarrow$ ) trends for groundwater sampled from Manobalai piezometers (♦) and lower catchment piezometers (◆).

Table 4.3. Ca and Mg concentrations estimated as being sourced from chemical reactions in the regolith at Manobalai and groundwater flow from Sites Three and Four to Site Two.

Site	Date (DD/MM/YYYY)	Ca (mg L <sup>-1</sup> )			Mg (mg L <sup>-1</sup> )		
		Ground-water	Reactions	Cation exchange (%)	Ground-water	Reactions	Cation exchange (%)
Two Shallow	19/02/2008	230	180	78	550	350	64
	15/07/2008	210	161	77	400	203	51
Two Deep	19/02/2008	190	138	73	400	193	48
	15/07/2008	170	129	76	350	187	53

### 3.4. Two-component mixing models

Two-component groundwater mixing models test how two packages of water, or endmembers, might theoretically mix on a conservative basis to give rise to a mixed water body with particular proportions and ion concentrations (e.g., Turner and Barnes 1998), such as when one water body mixes with another. Saline groundwater discharge from Tertiary formations is hypothesised to be caused by dissolution of aeolian dust deposits in a number of catchments in south-eastern Australia (Gunn and Richardson 1979; Revel-Rolland *et al.* 2006). None of the mixing curves based on the  $^{87}\text{Sr}/^{86}\text{Sr}$  ratio of aeolian dust from the Lake Eyre basin, the primary dust source in Australia (Bricker *et al.* 1994), resulted in the ratios which occur in surface and groundwater samples from the Wybung Creek catchment (Figure 4.9). Mixing curves based on a sandstone endmember were also dissimilar to groundwater samples from the catchment. Mixing curves modelled using parameters from Wybung Creek surface water samples as the low salinity endmember and parameters from an ideal and optimised high salinity endmember were instead closest to Wybung Creek samples when the high salinity endmember had a marine  $^{87}\text{Sr}/^{86}\text{Sr}$  signature of 0.708700, similar to signatures seen in Hannah's and Site Three.

Different proportions of Sr to Na, Cl and TDS concentrations were tested for the 0.708700 endmember, based on the proportions seen in Wybung Creek groundwater and elsewhere in Australia (Figure 4.10). A mixing model can be created, for example, with a Sr concentration of 50 mg L<sup>-1</sup>. If these Sr concentrations represented 0.007 % of TDS, similar to proportions seen in Site Three groundwater, a TDS of 714 286 mg L<sup>-1</sup> would result (Table 4.4). This is unrealistically saline when compared to brines in central Australia which have a TDS of 300 000 mg L<sup>-1</sup> (Domenico and Schwartz 1990), with solute concentrations only as high as 400 000 mg L<sup>-1</sup> in a select few sedimentary

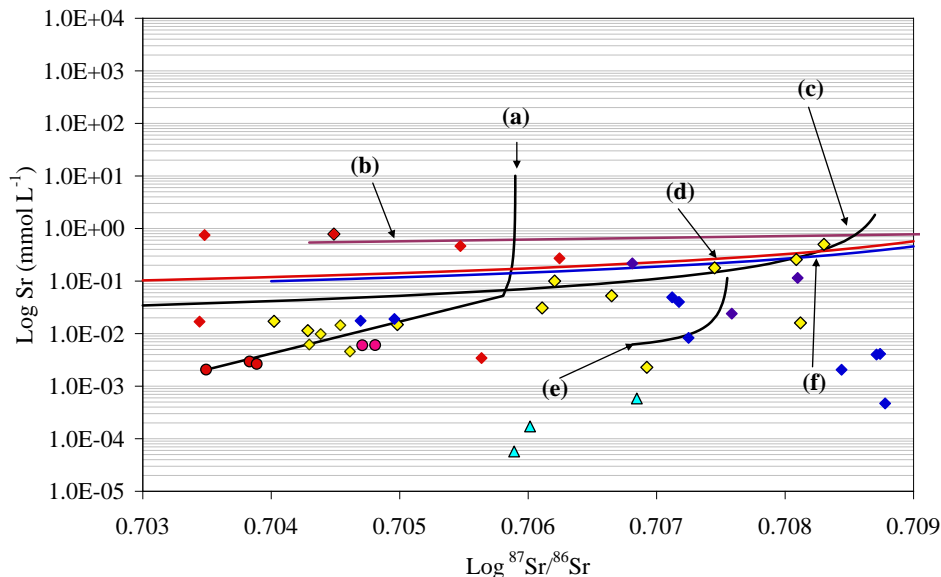


Figure 4.9.

Two-component mixing curves between possible endmembers in the Wybong Creek catchment based on  $^{87}\text{Sr}/^{86}\text{Sr}$  and Sr concentration ( $\text{mmol L}^{-1}$ ), with  $^{87}\text{Sr}/^{86}\text{Sr}$  values for endmembers described in Table 4.1. M. Norman at The Australian National University provided the equations by which these mixing models were calculated. (a) Hypothetical saline groundwater ( $^{87}\text{Sr}/^{86}\text{Sr} = 0.7059$ ,  $\text{Sr} = 10.04 \text{ mmol L}^{-1}$ ) and 11 km sample point surface water ( $0.7035$ ,  $0.002 \text{ mmol L}^{-1}$ ); (b) Great Sandy Desert dust ( $0.7220$ ,  $1.14 \text{ mmol L}^{-1}$ ) and 60 km sample point surface water ( $0.7043$ ,  $0.006 \text{ mmol L}^{-1}$ ); (c) Hypothetical brine ( $0.7090$ ,  $3.42 \text{ mmol L}^{-1}$ ) and hypothetical surface water ( $0.7030$ ,  $0.03 \text{ mmol L}^{-1}$ ); (d) Hypothetical brine ( $0.7087$ ,  $1.83 \text{ mmol L}^{-1}$ ) and hypothetical surface water ( $0.7030$ ,  $0.03 \text{ mmol L}^{-1}$ ); (e) Sandstone ( $0.7109$ ,  $0.09 \text{ mmol L}^{-1}$ ) and 60 km sample point surface water ( $0.7043$ ,  $0.006 \text{ mmol L}^{-1}$ ); and (f) Hypothetical brine ( $0.7087$ ,  $8.56 \text{ mmol L}^{-1}$ ) and 11 km sample point surface water ( $0.7035$ ,  $0.002 \text{ mmol L}^{-1}$ ). Symbols indicate groundwater collected from the upper catchment (♦); mid-catchment (◆); lower catchment (◇); Manobalai (◆); lower catchment piezometers (◆); springs (◆); surface water collected from the upper catchment (●); mid-catchment (●); lower catchment (●); and rainwater (▲), are also indicated.

brines (Ahmed *et al.* 2009). A Sr concentration of  $50 \text{ mg L}^{-1}$  is realistic, however, if it represents a higher proportion of TDS, with the most realistic hypothetical endmember in this study having a Sr concentration of  $50 \text{ mg L}^{-1}$  and Sr concentrations constituting 0.1 % of TDS. Saline groundwater similar to this occurs in Morgan's piezometer, which is screened into clay in the lower catchment.

Ratios of Na/Cl, Sr/Na, and Sr/Cl were also tested for the optimised endmember, with mixing lines falling close to saline groundwater samples in the lower Wybong Creek catchment (Figure 4.10). The modelled high salinity endmember was closest to Wybong Creek samples with TDS concentrations of  $50\,000 \text{ mg L}^{-1}$ . The most likely endmember indicated by groundwater geochemistry was the Wittingham Coal Measures, however, which have a mean TDS concentration of  $5700 \text{ mg L}^{-1}$  (Creelman 1994). This does not dislodge the Wittingham Coal Measures as the main source of Na-Cl dominated water to Wybong Creek, as the initial dissolution of halite contained within the coal would give rise to total salinities much higher than  $5700 \text{ mg L}^{-1}$  before

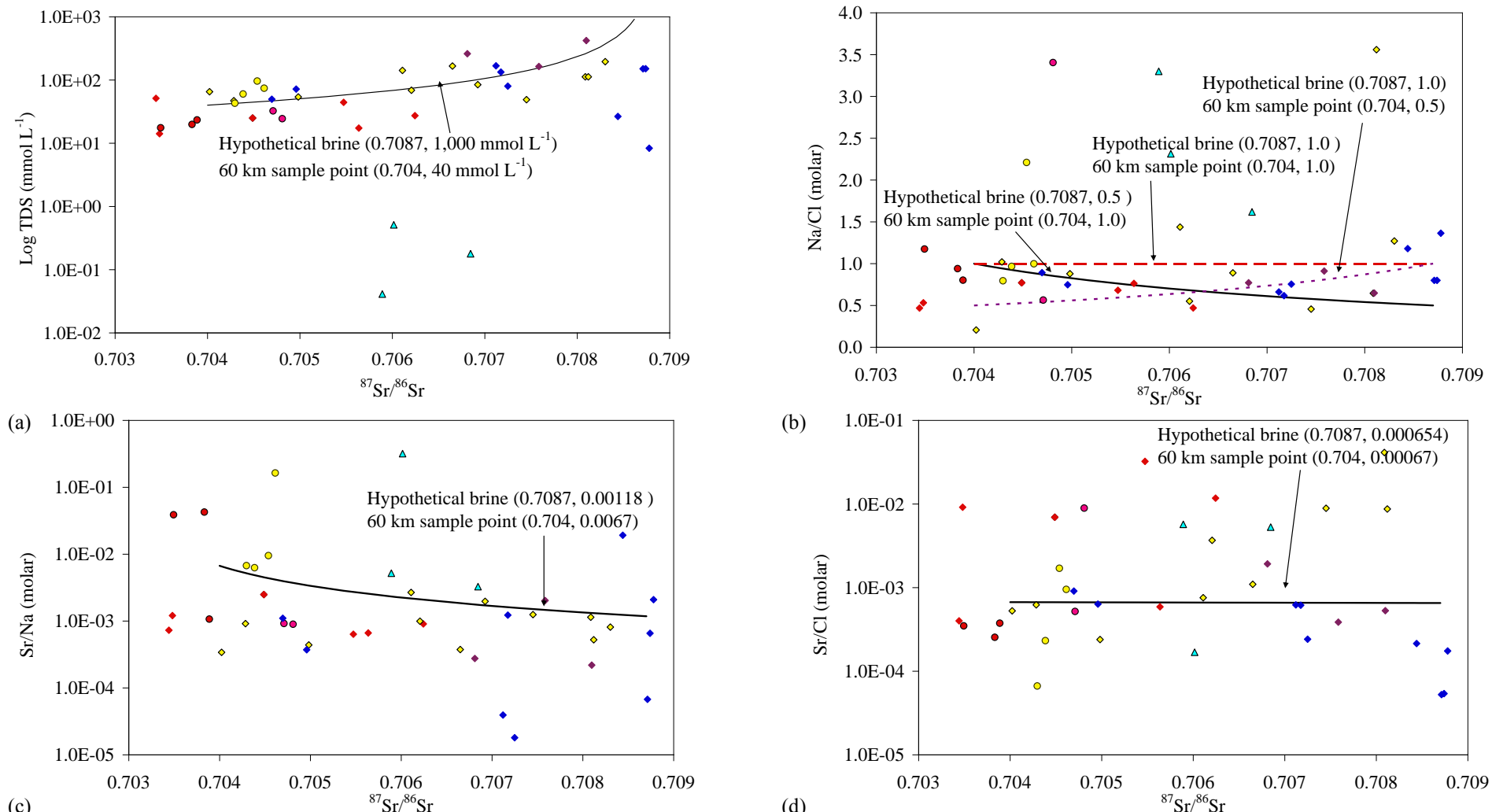


Figure 4.10. Mixing curves between the  $^{87}\text{Sr}/^{86}\text{Sr}$  of 0.0708700 end-member and 60 km sample point surface water based on (a) ( $^{87}\text{Sr}/^{86}\text{Sr}$ , TDS); (b) ( $^{87}\text{Sr}/^{86}\text{Sr}$  and molar Na/Cl ratios); (c) ( $^{87}\text{Sr}/^{86}\text{Sr}$ , molar Sr/Na ratios); and (d) ( $^{87}\text{Sr}/^{86}\text{Sr}$ , Molar Sr/Cl).

Table 4.4. Parameters for two saline groundwater sites from the Wybong Creek catchment and for hypothetical, optimised  $^{87}\text{Sr}/^{86}\text{Sr}$  end-members.

Parameter	Unit	Hannah's (n = 2)	Site Three (n = 2)	Optomised end-member
$^{87}\text{Sr}/^{86}\text{Sr}$		0.708303	0.708712	0.708700
Sr	(mg L <sup>-1</sup> )	2.0	0.4	50
	(mmol L <sup>-1</sup> )	0.02	0.004	0.57
Sr	(% mass of TDS)	0.04	0.009	0.1
TDS	(mg L <sup>-1</sup> )	5700	4600	50000
Na + Cl	(% mass of TDS)	80	90	84
Cl	(mg L <sup>-1</sup> )	3000	2700	30894
	(mmol L <sup>-1</sup> )	84	76	871
Na	(mg L <sup>-1</sup> )	1600	1400	11106
	(mmol L <sup>-1</sup> )	69	61	483
Sr/Cl	(molar)	0.0006	0.0001	0.00065
Cl	(% mass of TDS)	52	59	62
Na	(% mass of TDS)	28	31	22
Na/Cl	(molar)	0.52	0.52	0.55
Sr/Na	(molar)	0.001	0.0003	0.0012

mean concentrations are reached. The results from the two component mixing models presented here are consistent with saline groundwater in the Wybong Creek catchment being sourced from the Wittingham Coal Measures, with other endmembers such as aeolian dust and sandstone discounted as possible sources.

### **3.5. Synthesis**

The Wittingham Coal Measures were deposited during the Early Permian, with saline groundwater discharge from these deposits more than 300 million years later at first seeming unlikely. Other phenomena occur within the catchment, however, which indicate mobilisation of fluids from and within the coal measures. Oil-like sheens were seen in groundwater collected from Yarraman Well, GW080947, and Frenchies (GW040960), though groundwater from the Wybong Creek catchment was not analysed for hydrocarbons. The smell of samples from Sites One to Four at Manobalai was, in addition, not inconsistent with coal. Oil shows and slicks sourced from Permian coal are common throughout the Sydney Basin and occur within the Narrabeen Group (Faiz *et al.* 2006). Coal reached peak maturity during as late as the Early Cretaceous (Tadros 1993), with migration of oil from the coal into the Narrabeen Group occurring as a result of thermal maturation (Ahmed *et al.* 2009). Oil shows in modern times indicate that liquids which were previously trapped are being mobilised from formations previously sealed for hundreds of millions of years, with this providing evidence for the mobilisation of saline groundwater from the Wittingham Coal Measures.

Saline, Na-Cl dominated groundwater arises abruptly in the mid-catchment area of Wybong Creek, with results presented here indicating the Wittingham Coal Measures are the most likely source of Cl dominated water to the catchment. The Wittingham Coal Measures are buried in excess of 400 m in the mid-catchment area, however, beneath the Newcastle Coal Measures and the Narrabeen Group. These strata dip under the Liverpool Ranges in the north of the catchment, while the topography dips to the south. This structure potentially provides the means by which groundwater recharging in the Liverpool Ranges can flow up dip and through the Wittingham Coal Measures (Chapter Three). The movement of saline groundwater from the Wittingham Coal Measures to the surface at specific points within the catchment requires deep and connected fractures to run from the Earth's surface down into these coal measures, with these fractures acting as a conduit for saline groundwater to discharge (Figure 4.11). Though geological mapping in the Wybong Creek catchment itself is limited, deep and

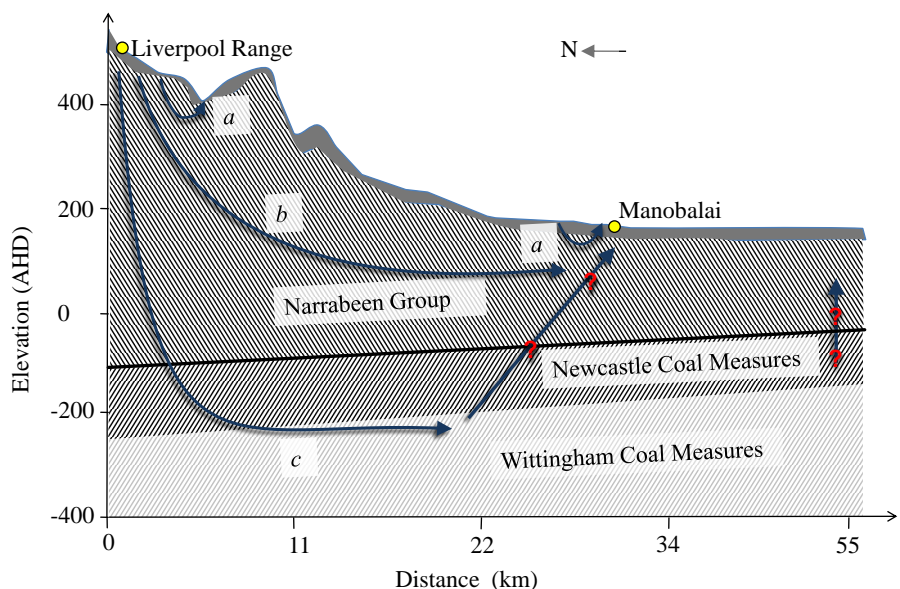


Figure 4.11. Conceptual model of groundwater flow in the Wybong Creek catchment depicting (a) local; (b) intermediate; and (c) regional groundwater systems. Hypothetical fracture flow directions are indicated by (?).

frequent fracturing and faulting is noted in geological reports, with some of these vertical faults connecting the Narrabeen Group to the deeper Permian Coal Measures (Leary and Brunton 2003; Brunton and Moore 2004; Umwelt Environmental Consultants 2006). Groundwater dominated by Na-Cl is discharged from the Wittingham Coal Measures via the Mt Ogilvie fault just east of the Wybong Creek catchment and causes abrupt increases to surface and groundwater salinity in other parts of the Hunter Valley, with discharge via a fault in Big Flat Creek in the south-eastern part of the Wybong Creek catchment also giving rise to abrupt increases in salinity (Creelman 1994). The Wittingham Coal Measures contains groundwater with marine signatures, halite efflorescences and solute concentrations similar to those seen in saline groundwater in the catchment, with fracturing known to connect the Permian Coal Measures to the Narrabeen Group, and groundwater discharge from the Wittingham Coal Measures causing salinity in other parts of the Hunter Valley. Saline groundwater discharge from the Wittingham Coal Measures via fractures and/or faults is, therefore, the most likely source of saline, Na-Cl dominated groundwater to the Wybong Creek catchment.

#### 4. Conclusions

Groundwater in the upper Wybong Creek catchment was dominated by Na-Mg and HCO<sub>3</sub>, similar to surface water in the upper and lower catchment. Ratios of <sup>87</sup>Sr/<sup>86</sup>Sr in groundwater were similar to that of the Tertiary basalt occurring in the area and indicated silicate weathering, with HCO<sub>3</sub>, Na and Mg sourced from weathering of

the hawaiite, mugearite and olivine basalt occurring in the Liverpool Range Volcanics. Increasing proportions of Cl occurred in HCO<sub>3</sub> dominated groundwater with increasing distance down catchment until the Manobalai area in the mid-catchment. Groundwater was largely dominated by Na-Cl from Manobalai south, with the Na-Mg dominated facies seen in groundwater within piezometers screened into regolith the result of cation exchange. Groundwater dominated by Na-Cl could not be sourced from the silica dominated Narrabeen Group occurring at the Earth's surface, nor from the Liverpool Range Volcanics capping and intruding the Narrabeen Group.

Halite dissolution was identified as a source of solutes to the saline Na-Cl dominated water in the mid-lower catchment, with δ<sup>34</sup>S and <sup>87</sup>Sr/<sup>86</sup>Sr indicating a marine solute source. Evapoconcentration of rainwater was discounted as the source of solutes to groundwater, as saline groundwater samples were no more enriched in <sup>18</sup>O and <sup>2</sup>H than fresher surface and groundwater samples. This indicates that marine water and halite dissolution are contributing solutes to the catchment, with the halite containing, marine-influenced groundwater of the Wittingham Coal Measures >300 m below the Earth's surface the most likely source of saline, Na-Cl dominated groundwater to the Wybong Creek catchment. Recharge of regional groundwater bodies, such as the Wittingham Coal Measures, occurs on the major topographic high of one or several catchments, with discharge in the mid-catchment area possible if topography and stratigraphy dip in opposite directions and cause groundwater to flow up dip. The occurrence and mobilisation of saline groundwater from the Wittingham Coal Measures in modern time requires that they have been sealed for millions of years, with oil shows throughout the Sydney Basin and oil-like sheens on groundwater in the Wybong Creek catchment indicating that liquids are being mobilised from previously sealed formations.

Discharge of saline groundwater from the Permian Coal Measures indicates that salinity in the Wybong Creek catchment is a largely natural occurrence, and differs from the dryland salinity that is typically identified within Australia. The poor geological knowledge of the Wybong Creek catchment was a serious limitation to a more precise understanding of saline groundwater flow. Further research which identifies the faults and fractures which allow saline groundwater to move to the Earth's surface is required, with a focus on point source discharge from these conduits required for salinity mitigation and management strategies in the catchment. Long-term studies which identify changes in groundwater height and salinity over time would indicate whether anthropogenic activity was exacerbating the primary salinity that occurs in the

catchment. Analyses for hydrocarbons are necessary in order to constrain these as a constituent of groundwater in the Wybong Creek catchment. If they are present, they could be used as a geochemical tracer to identify groundwater discharge from the coal measures in other parts of the Hunter Valley.



---

## **Chapter Five**

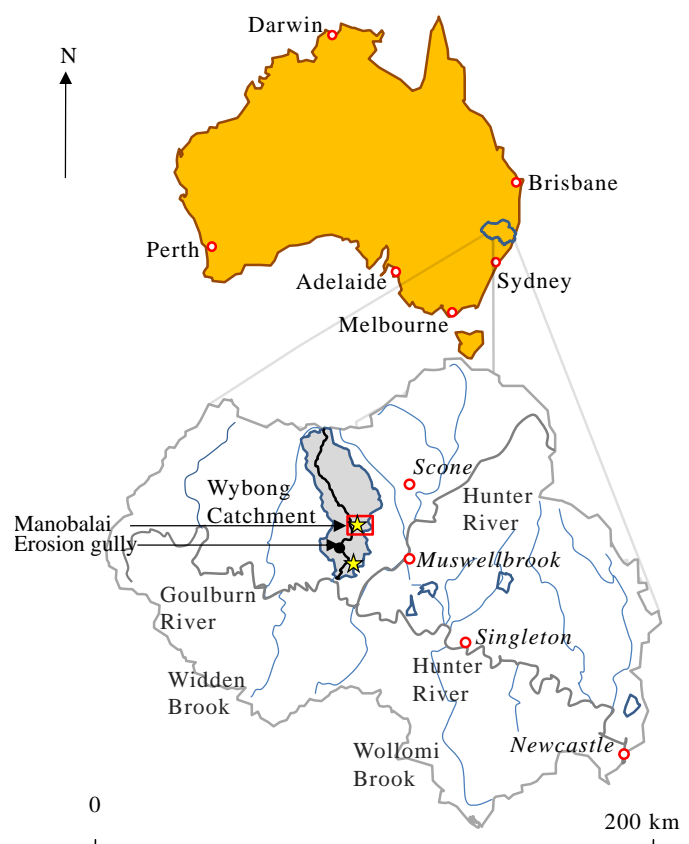
### Causes of salinity at the Manobalai field site



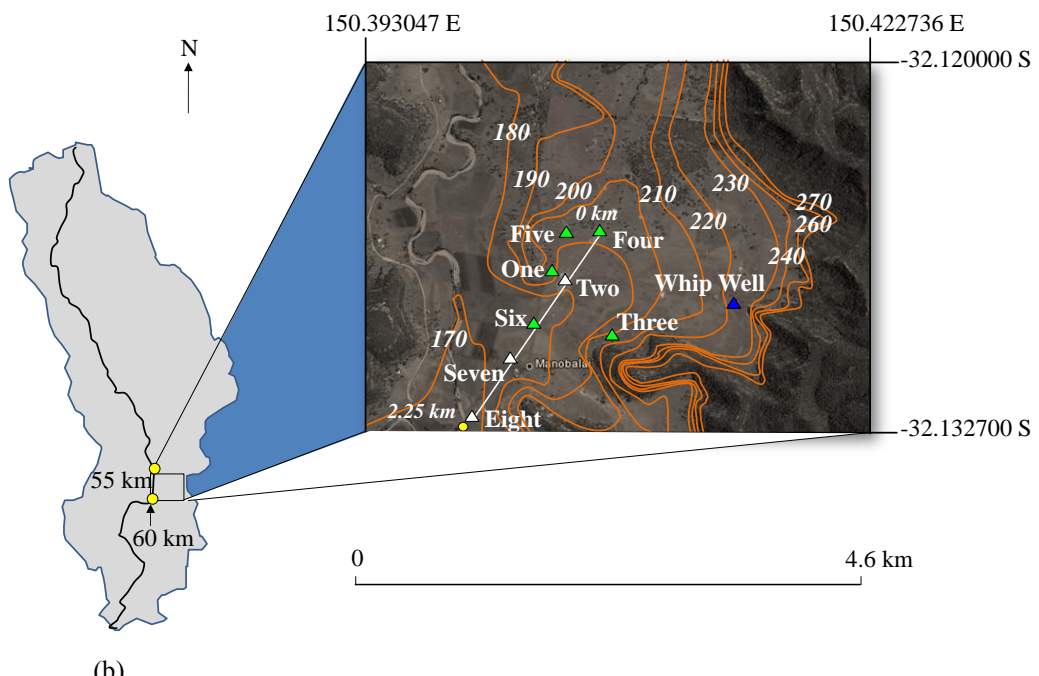
## 1. Introduction

Wybong Creek has been identified as causing increased salinity, sodicity and chlorinity to the Goulburn River which it flows into (Figure 5.1), with the Goulburn River in turn feeding the Hunter River (Creelman 1994). Research on salinity within the Wybong Creek catchment is limited. The Liverpool Ranges form the northern boundary of Wybong Creek, however, with research on the Liverpool Plains indicating dryland salinity arises due to increased groundwater recharge, rising water tables and dissolution of salts from the subsoil (Ringose-Voase *et al.* 2003). Salinity outbreaks in the Liverpool Plains are associated with alluvial landforms (Ringose-Voase *et al.* 2003), and also occur at the breaks of slope (Greiner 1998). Salinity and especially Cl concentrations in surface and groundwaters in the Wybong Creek catchment increase rapidly from the mid-catchment area to the lower catchment (Chapters Two and Three). The occurrence of salinity in the mid-catchment area indicates either a significant salt store within the regolith or a discharging saline groundwater body. Regolith and groundwater sampling was undertaken at the locality of Manobalai in order to identify whether salt stores within the regolith or groundwater discharge was the cause of salinity in the mid-catchment area.

Soil salinisation is perhaps the oldest form of environmental degradation afflicting human civilization (Jacobsen and Adams 1958). As much as 42 % of the Australian continent is estimated to suffer from salinisation (Northcote and Skene 1972), which is most often cited as being human induced and in the form of dryland salinity (e.g., Coram *et al.* 2001). Dryland salinity is related to the naturally high evaporation and/or inadequate regolith infiltration occurring in many Australian catchments, which causes the salts arriving in catchments with dust and rainwater to increase in concentration and form significant salt stores within the regolith over hundreds to thousands of years (Gunn and Richardson 1979; Summerell *et al.* 2006). Deforestation within these catchments causes a decrease in evapotranspirative water use, which in turn causes an increase in groundwater recharge (e.g., Coram *et al.* 2001). Salinisation is then caused when rising groundwater intercepts salt stores in the regolith, with discharging saline groundwater leading to salinised surface water and soils. Examples of such dryland salinity are found in Western Australia (e.g., Engel *et al.* 1987; Ruprecht and Schofield 1991a; Salama *et al.* 1993), South Australia (e.g., Allison *et al.* 1990; Jolly *et al.* 2000; Leaney 2000), and New South Wales (Bradd *et al.* 1997).



(a)



(b)

Figure 5.1.

(a) The location of the Manobalai and erosion gully sampling sites within the Wybong Creek catchment, the Hunter Valley, and Australia. The location of salt scalds within the Wybong Creek catchment are indicated by yellow stars ( $\star$ ); and (b) Location of regolith and groundwater sample sites within the Manobalai area relative to surface water sample sites (●) in the Wybong Creek catchment. Single piezometers are indicated by ( $\blacktriangle$ ), while bore and/or piezometer nests are indicated by ( $\triangle$ ). Numbers in italics indicate elevation as determined by Google Earth, with topographic contours shown in orange.

Significant research has been conducted on the occurrence of human induced salinisation in Australia. Primary salinity, whereby saline water and soils occur independent of human activity, is noted less often within the literature. This is despite much of Australia being prone to primary salinity, with this occurring in deeply weathered and poorly draining catchments that have arid – semi-arid climates (Salama *et al.* 1998; Peck and Hatton 2003; Summerelle *et al.* 2006). Salinity outbreaks within eastern Australia are also related to fractured rock aquifers. These are hypothesised to have acquired salts via aeolian accession throughout the Tertiary (Gunn and Richardson 1979), with saline groundwater seeps commonly occurring at the break of slope beside fractured outcrops (Northcote and Skene 1972; Greiner 1998; Cresswell and Herczeg 2004). Saline groundwater is also a result of rainwater evapoconcentration (Jankowski and Jacobsen 1989), chemical weathering (Hardie and Eugster 1970), and dissolution of marine salts (e.g. Kellett *et al.* 1987; Creelman 1994). Ion to Cl ratios and  $^{87}\text{Sr}/^{86}\text{Sr}$  signatures of groundwater reflect the geochemical source of solutes, while  $\delta^{18}\text{O}$  and  $\delta^2\text{H}$  instead reflect the evapotranspiration history of water (e.g., Eugster and Hardie 1975; Davies and McDowall 1996; Drever 1997; Bullen and Kendall 1998). Analysis of groundwater using these techniques enables the cause of salinity and sources of solutes to catchments to be elucidated.

Dust deposits which contain entrained salts are cited as a source of salinity in a number of catchments (Abuduwaili *et al.* 2008; Jolly *et al.* 2001). Dust deposits are insinuated through the identification of interstratified illite and smectite; kaolinite to illite ratios; from the presence of weathering products foreign to an area (Cattle *et al.* 2002); peaks in dust particle size (Walker *et al.* 1988); and  $^{87}\text{Sr}/^{86}\text{Sr}$  ratios in regolith material which is anomalous with the area (Gingelet *et al.* 2007). The identification of dust deposits is not unequivocal, however, with authigenic carbonate mistakenly labelled as dust deposits in the Liverpool Plains (Radke 1994). Ion distributions within the soil profile resulting from the leaching of aerially deposited salts, however, may enable the identification of aeolian accession as a salinisation process. Profiles of ions within regolith show monotonically increasing concentrations with increasing depth as a result of leaching (e.g., Johnston 1987a), with salt bulges also occurring in the subsoil as a result of biological cycling (Jobbágy and Jackson 2001). Though lateral and vertical groundwater flow destroy leaching patterns and bulges by washing away the salts contained within soil solutions (Johnston 1987b; Chen *et al.* 2002; Summerell *et al.* 2006), the absence or destruction of leaching patterns may then allow for the identification of groundwater as a solute source to the regolith.

## 1.2. Aim

To meet the aim of isolating whether solutes were sourced from salt stores within the regolith or were pre-existing in groundwater at Manobalai, the following objectives were addressed:

1. To characterise regolith chemistry according to sample depth, landform, and texture;
2. To identify minerals acting as sources of solutes to the regolith and groundwater;
3. To identify geomorphological factors controlling salt occurrence in the area; and
4. To correlate solute occurrence within the regolith to either aeolian deposition or groundwater.

## 2. Materials and methods

The selection of sites within the Manobalai field site is presented first in the following materials and methods, followed by regolith sample collection and piezometer installation. The methods for soil quality and soil chemistry are also presented. Groundwater sampling and analyses are instead described with detail in Chapter Three.

### 2.1. Site selection

Manobalai is a locality occurring in the mid-catchment area of Wybong Creek and has a surface area of 43.2 km<sup>2</sup> (Figure 5.1). Regolith, largely comprised of alluvium and some colluviums, covers 13.3 km<sup>2</sup> of this surface area, with the rest composed of Narrabeen Group sandstone and conglomerate escarpments and outcrops (Figure 5.2). Saline regolith (sodosols) occurs within alluvial landforms (Figure 5.3), and is associated with the Sandy Hollow soil landscape series (Kovac and Lawrie 1991). Chocolate coloured smectitic clays derived from olivine-rich basalt cap the forested sandstone escarpments which rise approximately 300 m above Manobalai, and also occur in a narrow (<500 m) margin along the floodplain of Wybong Creek. These smectitic clays are associated with the Merriwa soil landscape series. A 2.5 km<sup>2</sup> area within the 13.3 km<sup>2</sup> of regolith was selected for sample collection (Figure 5.3). The sample sites in this study occurred within a large paddock permanently grazed by cattle. This paddock contained the Manobalai salt scald, located on the valley floor between the outcrops and escarpments. This salt scald was the upper-most of two salt scalds occurring in the Wybong Creek catchment.

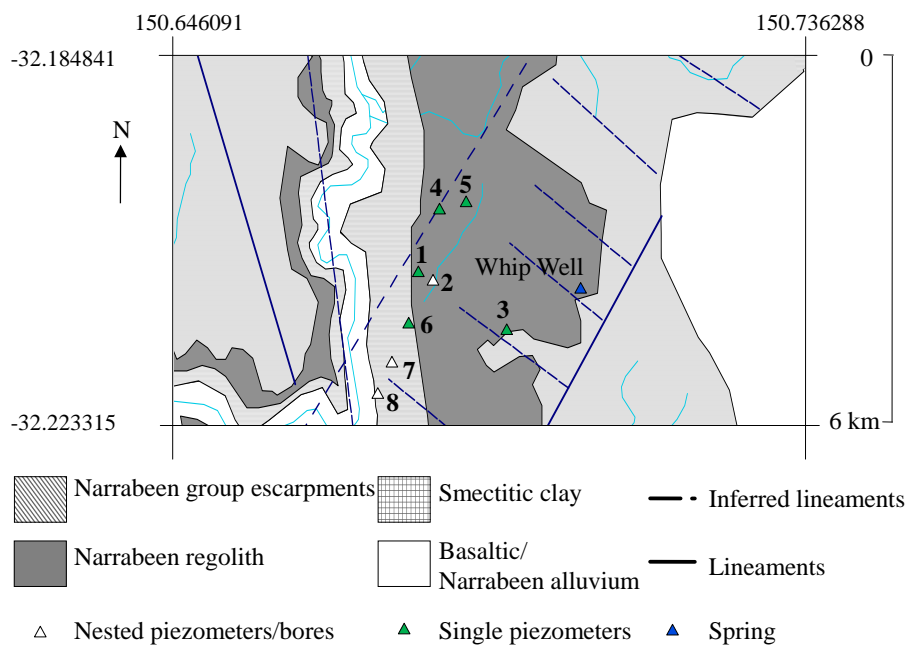


**Figure 5.2.** Lineaments (—) and inferred lineaments (.....) at the Manobalai field site. Grey indicates regolith; cross-hatching indicates the Liverpool Range Volcanics; diagonal lines indicate Narrabeen Sandstone escarpments; and white the Wybong Creek watercourse. Triangles indicate nested piezometer and/or bores ( $\Delta$ ), single piezometers/bores ( $\blacktriangle$ ), and a spring ( $\blacktriangleup$ ). Adapted from Leary and Brunton (2003).

Regolith samples from Sites One to Five were collected from regolith comprised of the Sand Hollow soil landscape series on the 8<sup>th</sup> and 9<sup>th</sup> of January 2008. Sites One to Five within the sample area were selected according to landform, with Sites One, Three and Five located at the breaks of slope, Four in a drainage depression 600 m topographically up-gradient of the salt scald and Two within the salt scald (Figure 5.2). Samples from Sites Six to Eight were collected on the 25<sup>th</sup> and 26<sup>th</sup> of March 2009. These sites were located down gradient of Site One – Five and in smectitic regolith of the Merriwa soil landscape series, with Site Six occurring between Hannah's groundwater monitoring bore and the salt scald, Site Seven at Hannah's bore, and Site Eight occurring topographically down-gradient of all other sites, on the bank of Wybong Creek.

## 2.2. Regolith sample collection

Sites were sampled using a mechanical auger equipped with a tungsten-carbide drill bit, without the use of water or drilling fluid, in order to minimise contamination. Augers were pulled up every 0.25 – 1.00 metres for sample collection. Contaminating regolith from shallower regolith layers was scrapped clean of the samples. Regolith descriptions and field textures were recorded on site according to Northcote's % clay (Northcote 1979), whereby soil samples were formed into a hand bolus to determine

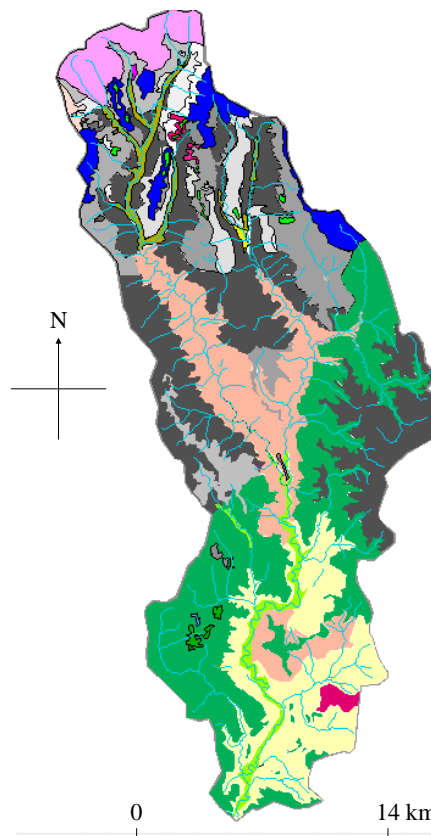


Figure 5.3. Soil landscape series' of the Wybong Creek catchment.  
Adapted from Kovac and Lawrie (1991) and  
McInnes-Clarke (2002).

RG – Rossgole	Tertiary olivine basalt. Local relief 60 – 120 m; slopes 2 – 7 %. Black earths on steeper slopes; eucrazems on less steep slopes.
AH – Ant Hill	Tertiary olivine basalt. Local relief 100 – 180 m, slopes 5 – 15 %. Black earths on mid-lower slopes; red clays on upper slopes; brown clays on mid-slopes; grey clays in poorly drained watercourses; eucrazems on well drained slopes.
Aha – Ant Hill: outcrops	Similar to Ant Hill, but with minor cropping occurring on gently sloping benched areas.
CB – Coober Bulga	Tertiary olivine basalt. Local relief < 600 m; slopes > 33%. Red eucrazems and black earths on steeper slopes; black earths and prairie soils on less steep slopes.
CE – Cranbourne	Tertiary olivine basalt. Local relief to 30 m; slopes 0 – 7 %. Black earths on steeper slopes; eucrazems on the plateau.
ER – Erin	Tertiary olivine basalt. Local relief 0 – 70 m; slopes 1 – 8 %. Black earths on upper and lower slopes.
YM – Yarramoor	High energy narrow floodplains and low terraces of the Liverpool Ranges.
WP – Wappinguy	Permian and Jurassic quartz and lithic sandstone, shale, conglomerate and siltstone; local relief 40 – 80 m, slopes 15 %. Red solodic regoliths with yellow, brown and grey solodic regoliths on mid-lower slopes; siliceous and earthy sands, gleyed solos, red earth eucrazem intergrades, and occasional prairie regoliths on lower slopes. Red and yellow eucrazems have moderate-high salinity.
SY – Sandy Hollow	Quaternary colluvium derived from sandstone, conglomerate and shale. Relief 20 – 40 m, slopes to 10 %. Yellow and red solodic regoliths on mid-upper slopes; Siliceous and earthy sands on lower slopes. High salinity in sodic regoliths.
CR – Castle Rock	Permian sandstone and conglomerate. Local relief 40–80 m; slopes 1 – 5 %. Stony solodic soils on flat slopes and alluvial soils in drainage lines.
GG – Galla Gilla	Tertiary olivine basalt. Local relief 50 – 200 m; slopes > 33 %. Lithosols on steeper slopes; black earths/eucrazems on side slopes.
LP – Lees Pinch	Triassic sandstone. Relief 100 – 300 m, slopes 10 – 30 %. Shallow siliceous sands, shallow loams. Some yellow and brown earths, yellow and grey solos on the breaks of slope. Yellow podzolic regoliths and earthy sands on upper slopes. Low-high salinity.
MP – Munghorn Plateau	Triassic sandstone and shale. Relief 20 – 60 m, slopes 2 – 10 %. Siliceous sands on crests; sandy yellow earths on lower slopes; yellow solos on drainage lines.
MW – Merriwa	Alluvial and gently undulating rises up to 12 m above the stream bed. Alluvial soils, chernozems, prairie soils, grey clays, and black earths on second terraces.

soil texture (Appendix Five: Table A5.1). Samples were collected in labelled resealable plastic bags and stored in ice boxes for transport.

Three pedogenic carbonate samples were collected from an erosion gully incised into smectitic clay which represented the Merriwa soil landscape series. This erosion gully was situated 12 km south Manobalai, adjacent to the 72 km surface water sampling site (Figure 5.4). The carbonate layer occurred approximately three metres below the regolith surface. Approximately 200 mm of regolith was chipped away from the exposed carbonate surface using a pick axe, before samples representing layers from the top 100 mm of carbonate, the middle 700 mm of carbonate, and the bottom 1500 mm of carbonate were collected (Figure 5.4). Samples were stored in plastic bags prior to preparation for isotope analysis.

### 2.3. Piezometer and bore installation

Five piezometers and two bores were installed along a 2.2 km transect of the valley floor at the locality of Manobalai, with three additional piezometers installed at the break of slope and on the edge of outcrops (Figure 5.2). A total of eight sites were

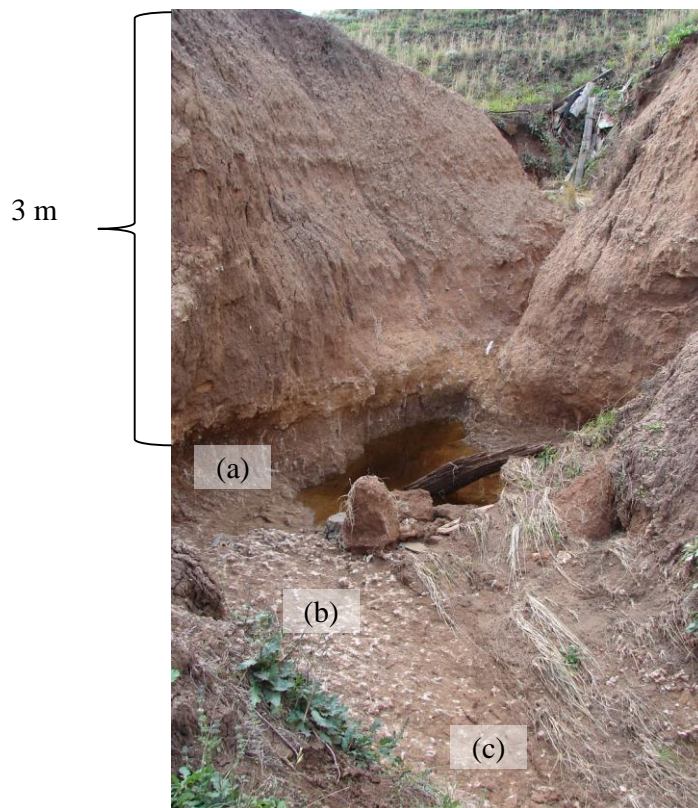


Figure 5.4. The erosion gully adjacent to the 72 km surface water sample site, 12 km south of Manobalai, from which carbonate samples were attained for radio-carbon dating. Layers from which samples were collected from were the: (a) top layer (100–200 mm below the carbonate layer's surface); (b) middle layer (750 mm below the carbonate layer's surface); and (c) bottom layer (1500 mm below the carbonate layer's surface).

established including a site with nested piezometers (Sites Eight); and two sites where a piezometer was nested with a bore ('Hannah's' bore with the piezometer at Site Seven; and Site Two Deep bore with the Site Two Shallow piezometer). Piezometers were installed at the break of slope of Narrabeen Group outcrops (Sites One and Five) and on the side of the escarpment at the eastern limit of the Manobalai area (Site Three). Piezometers were sited within and surrounding the salt scald in order to ascertain groundwater flow paths in relation to the salt scald.

All piezometers but Site Eight Fractured were installed in unconsolidated regolith material. Drilling occurred to the depth of the shallower water table at Site Two Shallow, to just above hard rock at Site Two Deep, through the hard rock to an oxidised and weathered fracture at Site Eight Fractured, and to the depth of hard rock (refusal) at all other sites (Table 5.1). Drilling for all but Site Eight Fractured occurred without the use of water or drilling fluid, in order to minimise contamination. Site Eight Fractured was instead sunk into hard rock with a diamond tipped drill bit, using quick-mud for lubrication. The groundwater monitoring bore (Hannah's) located at Site Seven was installed prior to this study, and is screened into fractured conglomerate between 27 and 30 m (NSW DNR 2005).

Lengths of polyvinylchloride (PVC) pipe measuring 50 mm in diameter were inserted into each of the holes created by augering, with connections between lengths of pipe glued together using PVC pipe cement. Pipes were sealed at both ends with PVC caps. Slot lengths of between 0.5 and 2.0 m were cut into the PVC pipe and screened with 75 µm nylon mesh (Table 5.1). Piezometers at Sites One, Three, Five, and Six – Eight were packed with 2 mm blue metal (gravel) to the top of the screen, which was then sealed with bentonite before the remainder of the hole was back-filled using regolith from the surrounding area. Perched water tables were intercepted 2 – 8 m below the Earth's surface at Sites Two Deep and Four, with groundwater discharge from these perched water tables and the lack of grouting equipment preventing piezometers from being properly sealed at greater depths. Bores were therefore created at these sites, with 2 mm gravel packed along their entire length (15 – 16 m). The bores were then sealed with bentonite 0.5 m below the regolith surface. Bores and piezometers were capped at the surface with PVC caps.

Table 5.1. Parameters for \*bores and piezometers installed at the Manobalai field site, with elevations presented in Australian Height Datum (AHD).

Site	Latitude	Longitude	Elevation (top of collar, AHD)	Elevation (top of hole, AHD)	Depth of hole (m)	Collar height (m)	Drilled width (m)	Screened interval (m)	Depth of gravel pack (m)
One	-32.12324	150.40262	187.27	186.61	2.38	0.66	0.125	2.0	2.0
*Two Deep									
09/01/08 – 23/03/2009	-32.12365	150.40329	180.76	180.22	15.65	0.53	0.125	2.0	15.5
23/03/2009						0.00			
Two Shallow	-32.12365	150.40328	180.72	180.17	8.60	0.55	0.125	2.0	8.4
Three	-32.12535	150.40491	194.34	193.89	5.40	0.45	0.125	2.0	2.0
*Four									
09/01/08 – 23/03/2009	-32.12201	150.40454	188.96	188.38	16.50	0.58	0.125	2.0	16.3
23/03/2009						0.00			
Five	-32.12217	150.40334	193.03	192.46	2.75	0.57	0.125	2.0	2.0
Six	-32.12343	150.40264	177.48	177.00	11.97	0.48	0.125	0.5	0.5
Seven	-32.12559	150.40264	171.42	171.00	8.16	0.42	0.125	1.5	1.5
Eight Shallow	-32.13125	150.39590	164.25	163.50	7.20	0.75	0.125	1.5	1.5
Eight Fractured	-32.13125	150.39590	164.25	163.50	9.78	0.75	0.125	1.5	1.5

### **2.3.1. Surveying**

The relative height datum (RHD) for bores and piezometers was measured using an Ashtech<sup>©</sup> Differential Global Positioning System (DGPS), with a lack of benchmarks in the area preventing the calibration of elevations to Australian Height Datum (AHD).

Bores and piezometers at Sites One and Two were resurveyed in by a professional surveyor (Rod Gleeson, Department of Water and Energy New South Wales, September 2008), with the elevations previously measured by DGPS then calibrated to the surveyed absolute elevations. Elevations stated in this chapter are therefore in AHD.

### **2.3.2. Groundwater sampling and analyses**

Sampling and analysis of water quality parameters and the analyses of cation, anion, and isotope concentrations is described fully in Chapter Three (Sections 2.1.2 – 2.2.2), with charge balances for all groundwater samples presented in the following results below 15 % (Appendix Three: Tables A3.3 – A3.6). The evaporation calculation presented in Section 3.3.2.1. was conducted using PHREEQC Interactive version 2.13.2.1727.

## **2.4. Regolith interpretation**

Regolith landforms were interpreted using field observations, the geographic information system (GIS) MapInfo, and Google Earth satellite imagery. The bounds of the Manobalai Site were chosen using the regolith landform map thus produced.

## **2.5. Soil quality measurements**

Soil quality measurements were conducted as follows.

### **2.5.1. Total soil moisture**

Regolith samples were removed from the sealed plastic bags in which they were transported within a week, with the moisture content of the soils measured according to the Australian Standard™ Method of testing soils for engineering purposes, number AS 1289.2.1.1 – 2005. Samples measuring 40 g were accurately weighed into pre-weighed tins, and placed in a Qualtex oven at 105 °C for >24 hours until constant weight was achieved. Tins were covered and cooled before samples were weighed again. Total moisture (%) was calculated as (Eq. 5.1):

$$\frac{\text{Wet soil} - \text{dry soil}}{\text{dry soil}} \times 100 \quad (5.1)$$

### 2.5.2. Regolith dispersivity

The degree of soil dispersivity was determined using the Emerson test as described in the Australian Standard™ Method of testing soils for engineering purposes, number AS 1289.3.8.1-2006. Three samples from Site Two (0.0 – 0.5; 1.0 – 1.5; and 14.5 – 15.5 m) and three samples from Site Six (0.0 – 0.5; 0.5 – 1.0; and 5.0 – 6.0 m) were submersed in distilled water to test for slaking and dispersivity.

## 2.6. Soil:water extracts

Supernatant was formed from all samples by making 1:5 soil to water extracts (Rayment and Higginson 1992). Regolith samples from Sites One to Five were air-dried in an oven at 40 °C until constant weight was achieved. Samples were then ground under acetone, with acetone making grinding easier while also being able to be completely removed from samples through evaporation. Samples were then sieved through a 2 mm sieve. Eight grams of sieved regolith was placed into 50 mL Falcon tubes and 40 mL milli-Q water added after shaking. Samples were then placed on a mechanical shaker for one hour, before being centrifuged for 15 mins at 5000 rpm. Supernatant extracts measuring 10 mL were then removed for cation and anion analyses, prior to the measurement of EC, pH and  $\text{HCO}_3$  concentrations. Turbid samples were filtered through 0.45  $\mu\text{m}$  Millipore® nitrocellulose filters before measurement.

A range of filtered sample extracts were selected for ion analyses based on the findings of the  $\text{EC}_{1:5}$  results, including samples which had the highest, the lowest and those which had average  $\text{EC}_{1:5}$  values relative to other samples in each core. Samples were analysed for cations using an inductively coupled plasma – atomic emission spectrometer (ICP-AES) and for anions using an ion chromatograph (IC) at the Research School of Earth Sciences, The Australian National University. Quality checks on sample analyses were undertaken using by replicating analyses on 10 % of samples. Standard deviations of replicate samples were as high as 150 % (Tables A5.2 – A5.3). Samples were converted from mg of salt per litre of water ( $\text{mg L}^{-1}$ ) to mg of salt per kilogram of oven-dry soil ( $\text{mg kg}^{-1}$ ) according to Eq. A5.1 (Appendix Five).

### 2.6.1. Cation exchange capacity

Two samples from within the salt scald (Site Two Deep) and three from within the smectitic clay (Site Six) were selected for analyses of cation exchange capacity (CEC). Samples selected from Site Two Deep were from the 0.0 – 0.5 m and 1.0 – 1.5 m layers, and represented samples with both low ( $60 \mu\text{S cm}^{-1}$ ) and high ( $1196 \mu\text{S cm}^{-1}$ ) salinities. Cation exchange capacity analysis of the 1.0 – 1.5 m sample was done twice for the

purposes of replication. Samples from Site Six were from depths of 3 – 4 m with an EC<sub>1:5</sub> of 167 µS cm<sup>-1</sup>; 5 – 6 m (183 µS cm<sup>-1</sup>); 6 – 7 m (405 µS cm<sup>-1</sup>); and 7.5 – 9 m (184 µS cm<sup>-1</sup>).

The following CEC method was used for the analyses, and is modified from Greene and Ford (1985) and Rayment and Higginson (1992). All six of the samples selected for measurement of CEC were pretreated for soluble salts. An ethanol-ethanediol reagent composed of 100 mL ethanediol, 36 mL deionised water, and 864 mL ethanol was prepared in order that soluble salts would be removed from the regolith. A volume of 20 mL of the ethanol-ethanediol reagent was added to 2.5 g of air-dried soil in a 50 mL falcon tube. Samples were then shaken for 30 mins, before being centrifuged for 10 mins at 3000 rpm. The supernatant was then drained and discarded, with samples again treated with the ethanol-ethanediol reagent.

A volume of 25 mL ammonium acetate (1M NH<sub>4</sub>OAc) was added to the regolith samples after pre-treatment, with samples shaken for 60 mins using a mechanical shaker. Samples were then centrifuged at 3000 rpm for 10 mins before being decanted into 100 mL volumetric flasks. Ammonium acetate was added to the 100 mL mark. Samples were then analysed for Ca, Mg, K, and Na using an ICP-AES at the Research School of Earth Sciences, The Australian National University.

### **2.6.2. Exchangeable sodium percentage**

Exchangeable sodium percentage (ESP) was calculated as per Eq. 5.2:

$$\text{ESP} = \frac{100 \times \text{Na}}{\text{CEC}} \quad (5.2)$$

where Na is sodium concentration in meq. 100 g<sup>-1</sup>, and CEC is cation exchange capacity in meq. 100 g<sup>-1</sup>.

## **2.7. Regolith mineral content**

Regolith samples from the salt scald (Site Two Deep) were selected for mineral analyses by X-ray diffraction (XRD) and by Scanning Electron Microscope (SEM), in order to isolate the minerals occurring in the regolith. These few samples were analysed due to the inhibiting cost and inconclusive results.

### **2.7.1. X-ray diffraction analyses**

Samples representing depths of 0.0 – 0.5, 0.5 – 1.0, 4.0 – 4.5, and 15.0 – 16.0 m from the Site Two Deep core were prepared for XRD analysis by grinding samples under acetone using an agate mortar and pestle, to a size of <20 µm. Samples were then placed in a McCrone micronising mill with 10 mL ethanol, shaken for 15 mins, and then

poured into a watch glass and dried in an oven at 40 °C. The resulting powder was then placed onto a slide and into a Siemens D501 X-Ray diffractometer.

### **2.7.2. Scanning electron microscopy analyses**

A subsample representing a depth of 1.0 – 2.0 m from the Site Two Shallow core was prepared for SEM by pressing approximately one gram of the sample onto carbon tape, which was then stuck to an aluminium stubb. The sample was then carbon coated before being loaded into a JSM-6400 scanning electron microscope. The sample was analysed for atomic composition using backscattering techniques at the Research School of Biological Sciences, The Australian National University.

### **2.7.3. Carbon dating**

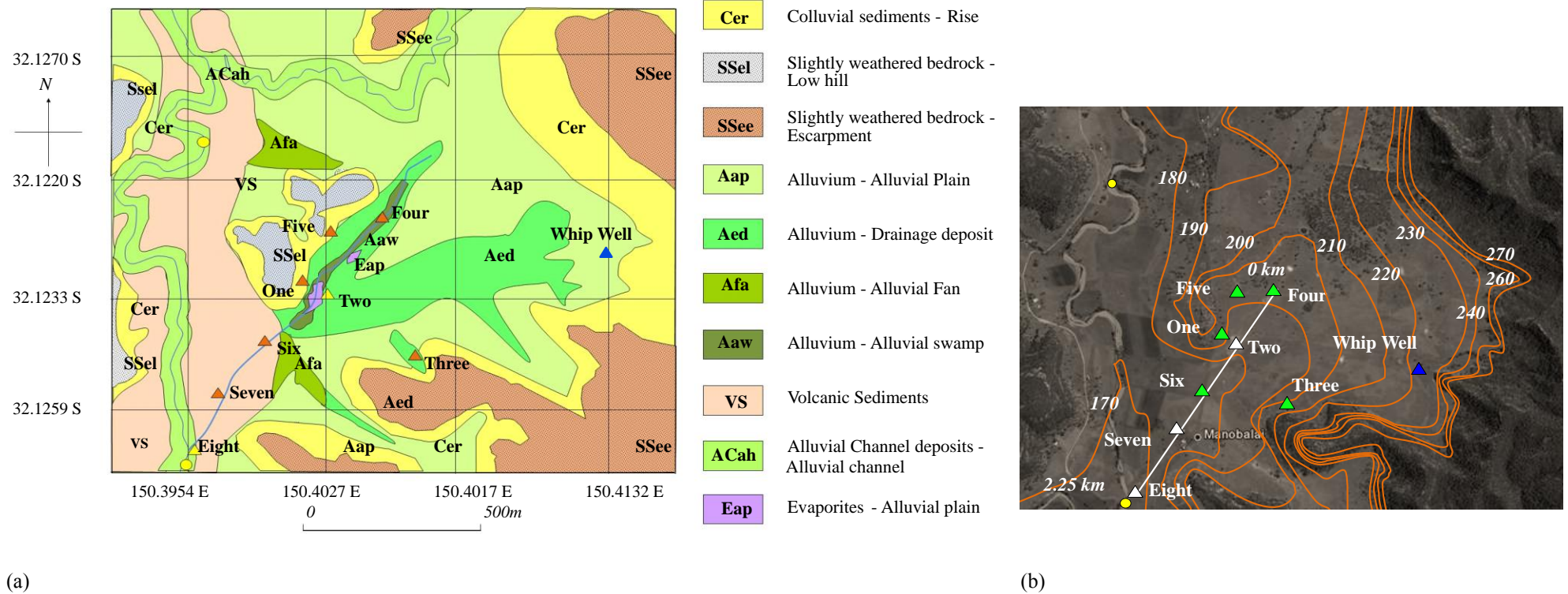
Carbonate subsamples weighing a minimum of two grams were placed in an ultrasonic bath and vibrated until encrusting soil material was removed (approximately one minute). Subsamples were then placed into clean 10 mL test tubes with 0.1 M HCl for 15 mins, in order to remove remaining contaminants. Carbon-14 and carbon-13 concentrations were then measured using a National Electrostatic Corp. (NEC) Single Stage Accelerator Mass Spectrometer (SSAMS) at the Research School of Earth Sciences, The Australian National University.

## **3. Results and discussion**

This results and discussion is split into four sections. The first section discusses the regolith and landform of the Manobalai field site, with the second section then relating landform to regolith chemistry. Groundwater chemistry and how it relates to regolith chemistry is then discussed before a conceptual model of the Manobalai area is presented finally.

### **3.1. Regolith and landform**

Two types of regolith occurred at the Manobalai field site. Regolith at Sites One to Five (i.e. the Sand Hollow soil landscape) was composed of yellow-grey clays, with rounded and sub-rounded quartz sands and gravels which were coloured green, purple and white. Cores collected from Sites Two and Four on the valley floor of Manobalai were composed of interbedded yellow-grey clayey-sands, sandy-clays and medium clays (Figure 5.5), where regolith is defined as a clay when the clay fraction makes up more than 30 % of regolith's weight (Northcote and Skene 1972). Cores collected from the footslopes of the outcrops and escarpments at Sites One, Three, and Five were similarly dominated by yellow-grey sandy clays, with the top layers



(a)

(b)

Figure 5.5. Regolith landform map of the Manobalai field site based on field observations and Google™ Earth satellite imagery, and (b) topographic surface of Manobalai.

Table 5.2. Descriptions of regolith landforms described in Figure 5.5. Regolith descriptions attained during sampling.

Regolith land form	Description
Colluvial sediments – Rise	Brown to red-brown sandy clay loams with vegetation dominated red grass ( <i>Bothriochloa spp.</i> ), with some saffron thistle ( <i>Carthamus lanatus</i> ). Slopes 5 – 9 °.
Slightly weathered bedrock – Low hill	White, weathered sandstone rises up to 20 m high topped with sparse apple box ( <i>Eucalyptus bridgesiana</i> ) and some unidentified approximately one metre high bushes.
Slightly weathered bedrock – Escarpment	Narrabeen Group escarpments rising up to 400 m above the valley floor. Vegetated with various Eucalyptus and <i>Callitris</i> species.
Alluvium – Alluvial plain	Brown to red-brown clays layers interbedded with rounded sands, granules and pebbles, composed of quartz, jasper and chert. Slopes 0 – 5 °. Vegetation dominated by grasses including red grass and kikuyu ( <i>Pennisetum clandestinum</i> ), with some saffron thistle. Several dense stands of <i>Casuarina cunninghamiana</i> and apple box occur.
Alluvium – Drainage deposit	Brown, yellow and grey coarse crumbly clays, clay loams and sandy clays, within a shallow (< 0.3 m) channel. Sparse <i>Juncus acutus</i> .
Alluvium – Alluvial fan	Similar to the alluvial plain description but with poorer sorting of sediments.
Alluvium – Alluvial swamp	Depressional saturated zone, ~ 0 °, with clays ranging from grey to yellow through to brown with black flecks of pyrolusite ( $MnO_2$ ). Clays interbedded with sands and gravels. Vegetation included sparse <i>Juncus acutus</i> and red grasses.
Volcanic sediments	Flat plain (0 – 3 °), bordered by shoots. Vegetation included couch grass ( <i>Chloris truncata</i> ), tall windmill grass ( <i>Chloris ventricosa</i> ), red grass, saffron thistle, kikuyu, and sparse <i>Casuarina cunninghamiana</i> and apple box.
Alluvial channel deposits – Alluvial channel	River channel deeply (20 m) incised Narrabeen Group sandstone and conglomerate, with alluvial deposits largely comprised of basalt cobbles. Little vegetation.
Evaporites – Alluvial plain	Slightly sloping (1 – 2 °) salt scald with some low couch grass and tall windmill grass cover.

composed of sandy-clay loams. Medium-heavy chocolate brown clays instead occurred at Sites Six – Eight (Merriwa soil landscape) further down gradient of Sites One – Five. Thin layers of yellow-grey sandy clays occurred on the bottom of cores from Sites Six – Eight, at the interface between the conglomerate and the chocolate-brown clay. These cores showed little horizontal development, and contained only sparse angular – sub-angular coloured gravels.

The regolith at Sites Two and Four is the result of past alluvial processes at Manobalai. A small Wybong Creek tributary currently turns at a nearly 90° angle towards Wybong Creek, prior to reaching the Manobalai field site. Aeromagnetic

surveys conducted for coal exploration in the area show the paleochannel of this tributary previously flowed along the valley floor of Manobalai (Brunton and Moore 2004). The cores extracted for geological exploration were interpreted by the authors as a floodplain deposit based on this aeromagnetic information. The interbedded sands, gravels and clays observed at Sites Two and Four also indicate a floodplain environment and are consistent with this interpretation of the site (Figure 5.6). Surface water either occurs as overland-flow during storm events or not at all during the current period. The gradual coarsening of regolith from Sites One, Three, and Five instead indicates colluvium, consistent with the location of these sites on the footslopes of the Narrabeen Group outcrops and escarpments.

Soil surveys indicate that the chocolate coloured, clay-rich regolith collected from Sites Six to Eight occurs as floodplain deposits in a narrow strip along Wybong Creek, with these comprised of smectite-rich clays derived from the weathering of the olivine-rich volcanic rocks of the Liverpool Ranges (Kovac and Lawrie 1991). This landform is similar to that which occurs in salinised catchments in the Liverpool Plains, on the other side of the Liverpool Ranges. There low salinity groundwater rises through sands and gravels derived from the weathering of Pillaga sandstone (the Gunnedah formation). This groundwater then intercepts black and grey cracking clays (the Narrabri formation) occurring as shoestrings and lenses above the Gunnedah formation (Ringose-Voase *et al.* 2003), with salinisation occurring due to dissolution of salt stores from this formation. Similar to the Liverpool Plains, smectitic regolith sampled from the Wybong Creek floodplain is derived from the Eocene olivine basalt that makes up the remnants of the Liverpool Shield Volcano (Wellman and McDougall 1974 in: Kellett *et al.* 1987; Kovac 1991), while the weathering of the Narrabeen Group has also produced significant alluvial deposits closer to the escarpments. Unlike the Liverpool Plains, however, where the saline Narrabri formation occurs on top of the coarsely textured Gunnedah formation, smectitic clay in the Wybong Creek catchment occurred as deep and homogenous deposits lying directly on Narrabeen Group saprock in the Wybong Creek floodplain. Alluvium derived from the Narrabeen Group did not occur beneath the thick homogenous smectitic clay, but as a spatially separate unit closer to the Narrabeen Group escarpments.

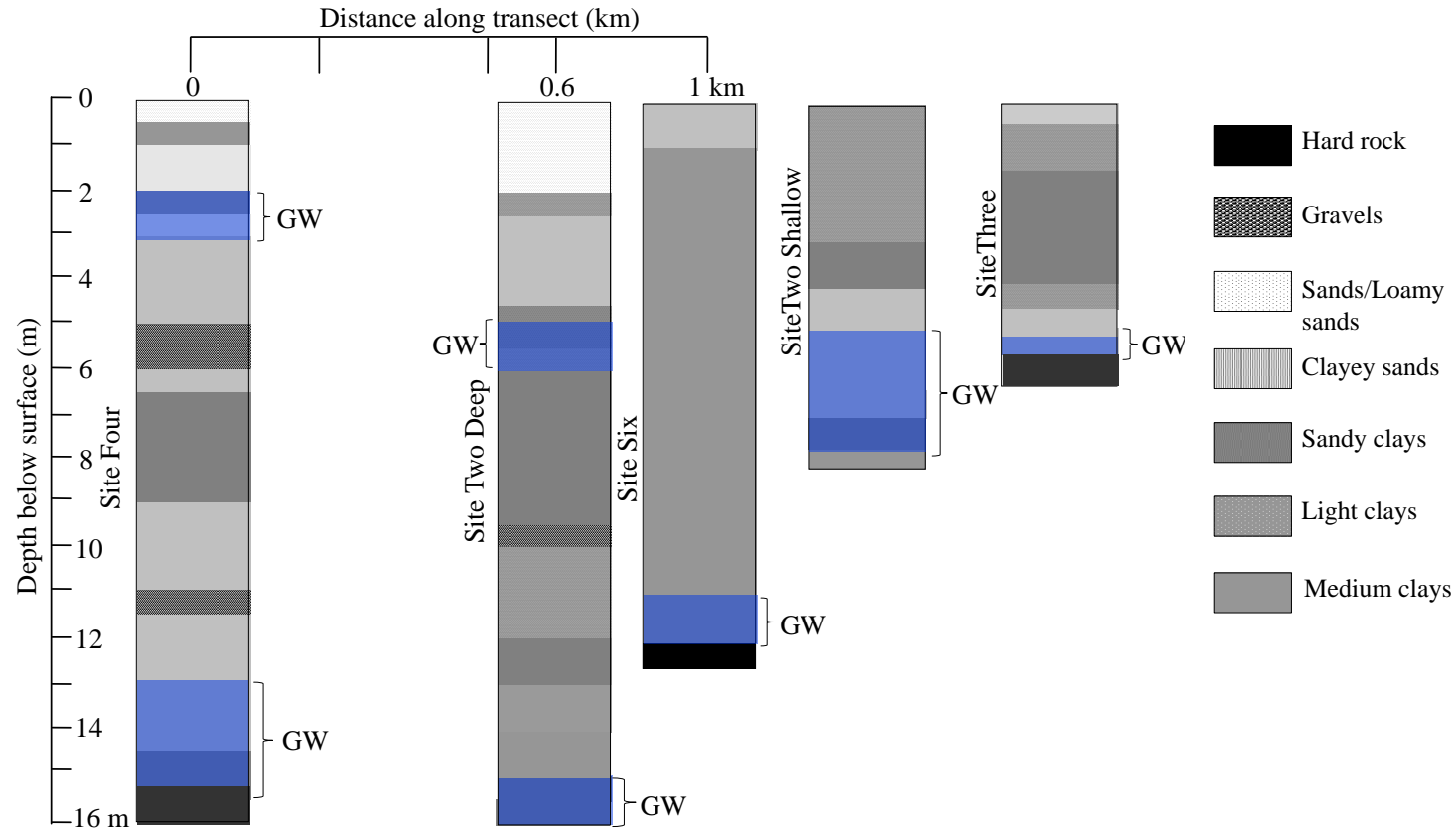


Figure 5.6. Cross-sectional logs of regolith materials occurring in select cores collected from the alluvial fill on the valley floor (Sites Two and Four), the smectitic clay adjacent to Wybong Creek (Site Six), and the colluvial footslopes (Site Three) of the Manobalai field site. Strata yielding groundwater (GW) are indicated in blue.

### **3.2. Soil and regolith chemistry**

The most saline sample collected from Sites One – Five had an EC<sub>1:5</sub> of 1196 µS cm<sup>-1</sup> and occurred in the 1.5 – 2.0 m layer of the Site Two Deep core (Figure 5.7). This was below the 1500 µS cm<sup>-1</sup> level indicating salinity on an EC<sub>1:5</sub> basis (Charman and Murphy 2000). All other samples in the Site Two Deep core had EC<sub>1:5</sub> salinities of 60 – 790 µS cm<sup>-1</sup>. Cores collected from Sites One, Three, Four and Five had EC<sub>1:5</sub> salinities ranging up to 800 µS cm<sup>-1</sup>. Salinity was as high as 1225 µS cm<sup>-1</sup> in the top 0.75 m layer at Site Six and was 1102 µS cm<sup>-1</sup> one metre above the bedrock at Site Seven (Figure 5.7 – 5.9). These results indicate that none of the soils at Manobalai were saline based on EC<sub>1:5</sub> measurements, including those at the Manobalai salt scald.

The quantification of Na and Cl concentrations within a soil is a more accurate measure of salinity than EC<sub>1:5</sub> measurements, with the measurement of Na alone instead indicating the sodicity of a soil (e.g., Oster and Shainberg 2001). Soil and regolith is termed saline when the weight percent of Na and Cl is more than 0.1 % in loams and sandy soils (< 30 % clay), and more than 0.2 % in clay rich (> 30 % clay) soils (Northcote and Skene 1972). Cores collected from Sites One to Five were mostly sandy-clays, with interbedded clayey sands, gravels and clays also occurring (Appendix Five). The highest weight percent of Na and Cl in samples analysed from Sites One to Eight occurred in the 5.5 – 6.0 m and 11 – 12 m layer at Site Two Deep, and in the 10.5 – 11.5 m layer at Site Four (Table 5.3). The weight percent of Na and Cl at these sites was between 0.1 and 0.2, and therefore indicated salinity at levels which could be detrimental to soil structure. While the soils sampled from Manobalai were not saline on an EC<sub>1:5</sub> basis, Na and Cl concentrations were perhaps high enough to indicate salinity in Site Two and Four samples. Such salinity causes decreased soil permeability and slaking, leaving soils hard setting and impenetrable to plant roots (Essington 2004; MacKenzie *et al.* 2004).

Cation exchange capacity (CEC) indicates the degree to which the exchange sites of a regolith sample are taken up by divalent cations, with a decreasing CEC occurring with increasing K and Na content (e.g., Essington 2004). Cation exchange capacity was measured on three samples from Sites Two Deep and three from Site Six. Cation exchange capacity at Site Six ranged from 7.2 – 7.8 meq 100g<sup>-1</sup>, while that in samples from the Site Two Deep core was 0.7 – 2.0 meq 100g<sup>-1</sup> (Table 5.3). The smaller a soil particle is the greater its surface area, with clays having much higher CECs than sands

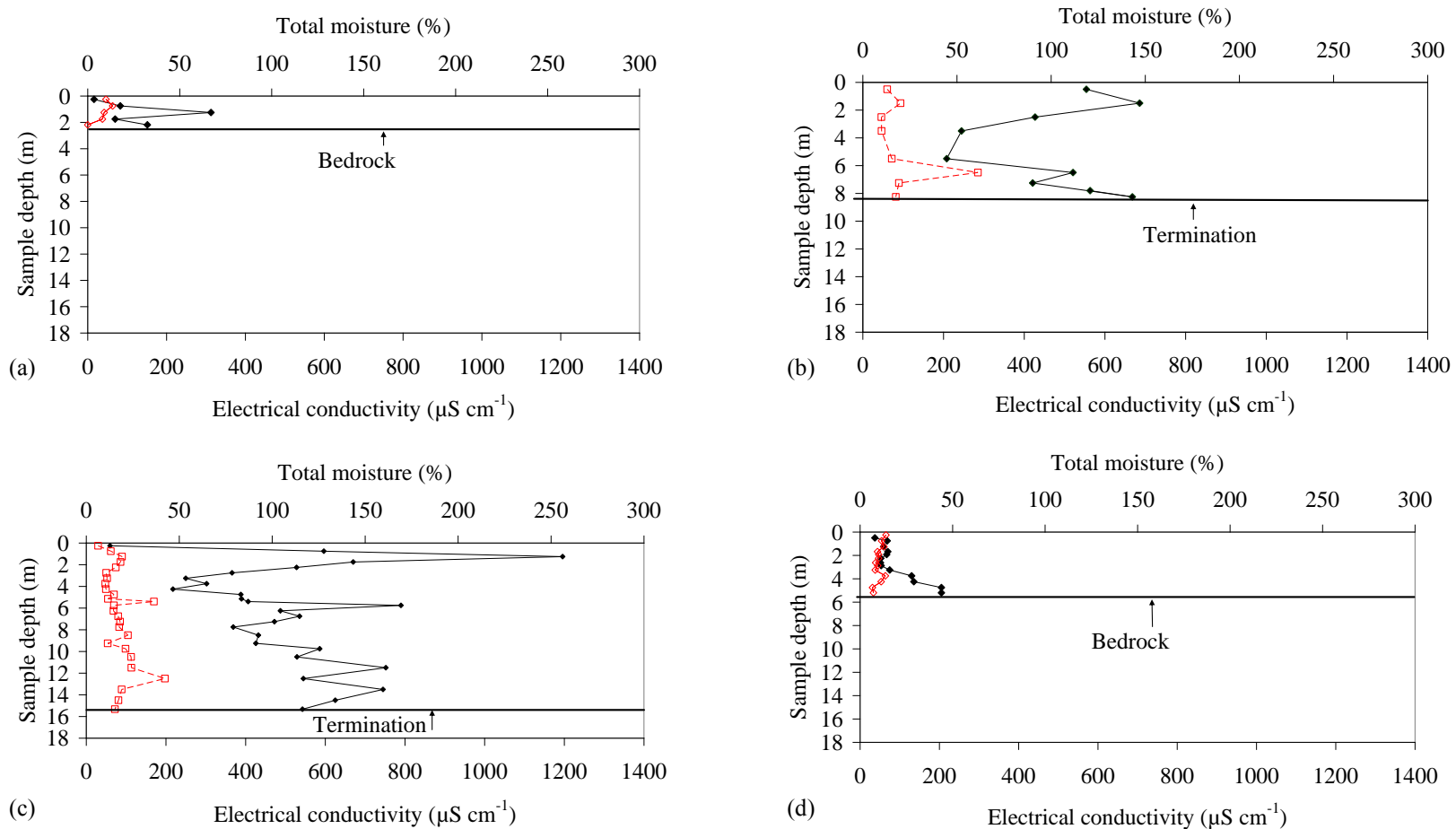


Figure 5.7. EC ( $\mu\text{S cm}^{-1}$ ; ♦) and total moisture (%) (□) versus depth in cores collected from Sites (a) One; (b) Two Shallow; (c) Two Deep; and (d) Three.

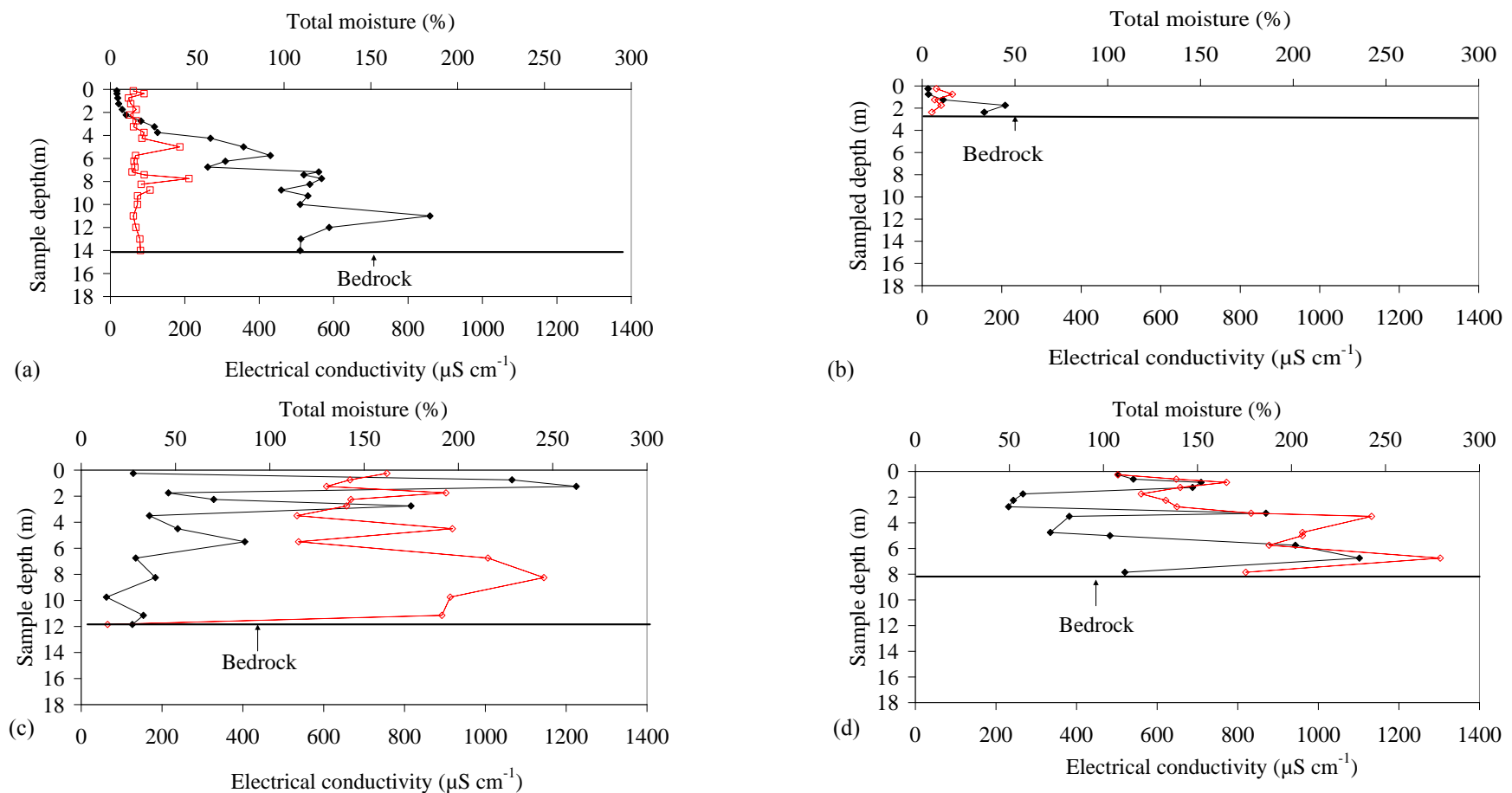


Figure 5.8. EC ( $\mu\text{S cm}^{-1}$ ; ♦) and total moisture (%; □) versus depth in cores collected from Sites (a) Four; (b) Five; (c) Six; and (d) Seven.

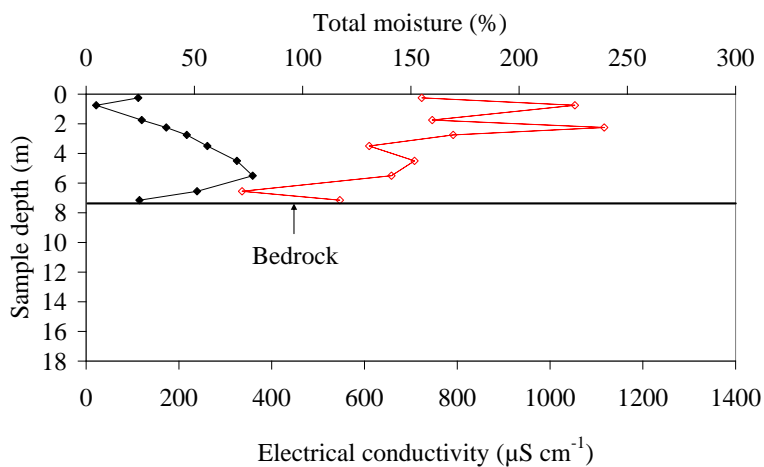


Figure 5.9. EC ( $\mu\text{S cm}^{-1}$ ; ♦) and total moisture (%; □) versus depth in the cores collected from Site Eight Shallow.

(Charman and Murphy 2000). The higher CECs seen at Site Six than at Site Two Deep reflects the higher clay contents at this site. The higher CEC at Site Six also indicates that the regolith at this site has a tendency to coagulate and allow root penetration. Samples with lower CECs also had lower proportions of Na (Table 5.3), with this indicating that CEC was related to surface area of particles, rather than Na concentrations.

The exchangeable sodium percentage (ESP) of a soil indicates the proportion of cation exchange sites filled by Na and thereby the potential dispersiveness of a soil (e.g., Essington 2004). The actual dispersiveness of a soil is instead measured by the Emerson test, whereby soil samples are placed in distilled water and monitored for slaking and dispersion over a number of hours (e.g., MacKenzie *et al.* 2004). The four most saline soil samples from Site Two and the three most saline samples from Site Six were tested for sodicity using the Emerson test, with no dispersivity seen in any of the samples. The maximum ESP of soil samples analysed in this study was 7.6 (Table 5.3). Soils with ESPs above 15 are internationally recognised as being sodic (Essington 2004), while a more sensitive ESP of six denotes sodic soils within Australia (MacKenzie *et al.* 2004). A lack of soil sample dispersivity indicates that Na concentrations were not at levels which are damaging soil structure at the Manobalai site, despite ESPs indicating the proportion of Na was at levels known to cause dispersal and slaking in other Australian soils.

A basic pH promotes sodicity due to  $\text{HCO}_3$ ,  $\text{CO}_3$ , Ca and Mg precipitating out of solution (Essington 2004). Sodium remains in solution and causes both clays and organic matter to become dispersive and form black alkali soils (Thomas 1996). The pH

Table 5.3. Total dissolved solutes (TDS, mg kg<sup>-1</sup>), where the mean ± standard deviation of replicated samples is presented for samples 3, 9, S34 and S26; percent weight Na+Cl of soil weight; the percent Na+Cl of total dissolved solids (TDS, mg L<sup>-1</sup>); exchangeable sodium percentage (ESP); sum of soluble cations (meq. 100 g<sup>-1</sup>); cation exchange capacity (CEC, meq. 100 g<sup>-1</sup>); and pH<sub>1:5</sub> of selected soil samples from Sites Two – Six.

Site	Depth from (m)	Depth to (m)	Composite depth (m)	Sample No.	TDS (mg kg <sup>-1</sup> )	% weight Na+Cl (kg Na+Cl per kg soil)	Na-Cl (% TDS)	ESP	$\Sigma$ Mg,Ca, Na, K (aq) (meq 100 g <sup>-1</sup> )	CEC (meq 100 g <sup>-1</sup> )	pH <sub>1:5</sub>
Two Deep	0.0	0.5	0.25	1	274	0.01	24	7.0	0.34	0.7	7.3
	2.0	1.5	1.25	3	1524 ± 22	0.13 ± 0.00	83 ± 0.9	7.6	2.49	2.0	7.5
	1.5	2.0	1.75	4	1845	0.13	72	10.1	2.86	0.8	7.4
	4.0	4.5	4.25	9	738	0.06	77	N/A	1.54	N/A	7.2
	5.5	6.0	5.75	13	1960	0.17	86	N/A	3.30	N/A	6.5
	6.0	6.5	6.25	14	1357	0.12	86	N/A	2.21	N/A	6.6
	7.5	8.0	7.75	18	943	0.08	85	N/A	1.54	N/A	6.4
	11.0	12.0	11.50	23	2089	0.16	78	N/A	3.34	N/A	7.2
	15.0	16.0	15.50	27	1378	0.12	87	N/A	2.27	N/A	6.5
Two Shallow	0.0	1.0	0.50	28	1430	0.11	78	N/A	2.07	N/A	6.9
	4.0	5.0	4.50	32	620	0.05	73	N/A	1.05	N/A	6.7
	7.0	7.5	7.25	35	1657	0.14	86	N/A	2.77	N/A	6.6
	8.0	8.5	8.25	37	461	0.00	7	N/A	0.60	N/A	6.8
Three	0.0	0.5	0.25	38	829	0.01	12	N/A	1.06	N/A	6.8
Four	0.0	0.25	0.13	53	101	0.00	22	N/A	0.10	N/A	7.4
	5.5	6.0	5.75	64	1834	0.11	58	N/A	4.16	N/A	7.3
	7.0	7.35	7.18	67	2225	0.14	62	N/A	5.20	N/A	7.3
	8.0	8.5	8.25	70	1635	0.12	72	N/A	2.62	N/A	6.8
	10.5	11.5	11.00	74	2170	0.19	88	N/A	3.35	N/A	6.7
	15.2	16.0	15.60	79	187	0.01	32	N/A	0.27	N/A	7.3
Five	0.0	0.5	0.25	80	363	0.01	28	N/A	0.59	N/A	9.0
	0.5	1.0	0.75	81	1553	0.03	22	N/A	2.90	N/A	7.6
	1.0	1.5	1.25	83	88	0.00	4	N/A	0.04	N/A	7.7
Six	0.5	1.0	0.75	S33	4122	0.11	27	N/A	2.0	N/A	8.0
	1.0	1.5	1.25	S20	4880	0.13	27	N/A	2.4	N/A	8.0
	2.5	3.0	2.75	S9	638 ± 251	0.04 ± 0.04	21 ± 7	N/A	1.3 ± 0.5	N/A	8.8
	3.0	4.0	3.50	S34	950 ± 517	0.04 ± 0.05	38 ± 30	5.3	1.0 ± 0.9	7.8	8.8
	5.0	6.0	5.50	S26	1604 ± 10	0.04 ± 0.00	27 ± 0.2	5.1	0.9 ± 0.1	7.2	8.1
	7.5	9.0	8.25	S11	851	0.03	39	7.2	1.0	7.8	9.1

of regolith samples ranged from 5.5 – 8.1 in cores from Sites One – Four, and from 6.8 – 9.2 at Sites Five – Eight, with a slight trend of increasing salinity with decreasing pH (Figure 5.10). The negative relationship between regolith salinity and pH are evidence that Na concentrations in the soil are not related to carbonate precipitation (Thomas 1996). These results corroborate previous findings, with little evidence of saline regolith at Manobalai.

### 3.3. Sources of salinity

Three possible sources of salinity occur within the Manobalai field site. The first source is aeolian salts, which may be washed through the regolith and into groundwater to make it saline. Evapoconcentration of groundwater within the regolith is also a leading contributor to salinity in Australia and is therefore discussed. Evidence for groundwater accession from deeper formations is examined finally.

#### 3.3.1. Aeolian accession

Minerals occurring within a soil profile are attributed to aeolian accession if they cannot be identified as weathering products of rocks in the surrounding geology (e.g., Cattle *et al.* 2002). Quartz was the predominant mineral in all four samples analysed from the salt scald (Site Two) using XRD, with kaolinite, muscovite, and potassium-feldspars occurring in most of the samples (Table 5.4). The quartz grains that made up the coloured sands and gravels occurring in cores collected for this study appear identical to those occurring in the Narrabeen Group. Other minerals such as albite ( $\text{NaSiAl}_3\text{O}_8$ ), orthoclase ( $\text{KAlSi}_3\text{O}_8$ ), and sanidine ( $(\text{K},\text{Na})(\text{Si},\text{Al})_4\text{O}_8$ ) are also common within the

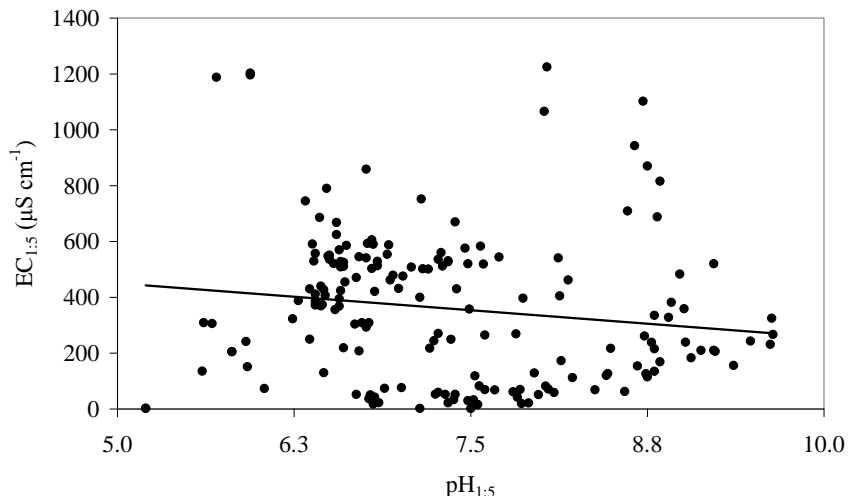


Figure 5.10. Soil salinity ( $\mu\text{S cm}^{-1}$ ) in relation to soil pH of samples from Sites One – Eight at the Manobalai field site.

Narrabeen Group rocks which surround the field site and make up the bedrock (Bai and Keene 1996). There is therefore no evidence of minerals within the regolith which cannot be related to the Narrabeen Group, with no evidence for aeolian dust deposits based on these limited mineralogy results. These results are of limited application, however, due to only a few samples from a single core used for analyses. Other means of identifying aeolian accession to regolith occur, however, and will now be discussed. Rainwater is dominated by  $\text{SO}_4$  and  $\text{HCO}_3$  when it arrives in catchments and evolves to Na and Cl dominated groundwater and/or rivers as a result of carbonate and sulfate precipitation (Eugster and Hardie 1975; Jankowski and Jacobson 1989). Such precipitation would be expected to result in sulfate and carbonate minerals within the shallower layers of the regolith profile, with increasing proportions and dominance of Na and Cl with increasing depth. Carbonate minerals were not identified in any of the four samples from Site Two using XRD analysis and sulfate minerals were only tentatively identified in the sample from 0.5 – 1.0 m below the ground surface (Table 5.4). The pH of solutions below 8.3 indicates that the conditions for carbonate precipitation do not occur (Charman and Murphy 2000), with potential for the formation of pedogenic carbonate at Sites Six – Eight, but not within the alluvium up-gradient. No clear correlation between increasing Na and Cl, and increasing depth occurred at any site (Figures 5.11 – 5.12). The absence of carbonate and sulfate minerals indicates that the production of Na and Cl dominated solutions deeper in the alluvial soil profile was

Table 5.4. Summary of minerals occurring in samples within Site Two Deep, as identified by X-Ray diffraction analyses. Minerals in italics were only tentatively identified. Spectra for these analyses can be found in Appendix for Chapter Five (Figures A5.2 – A5.5).

Depth (m)	Mineral	Empirical formula
0.0-0.5	Quartz	$\text{SiO}_2$
	Potassium-feldspars	$(\text{K},\text{Na})\text{AlSi}_3\text{O}_8$
	Kaolinite	$\text{Al}_2(\text{Si}_2\text{O}_5)(\text{OH})$
0.5-1.0	Quartz	$\text{SiO}_2$
	Sodic-plagioclase	$(\text{Na},\text{Ca})(\text{Al},\text{Si})\text{AlSi}_2\text{O}_8$
	Potassium-feldspars	$(\text{K},\text{Na})\text{AlSi}_3\text{O}_8$
	<i>Portlandite</i>	$\text{Ca}(\text{OH})_2$
	<i>Thenardite</i>	$\text{Na}_2\text{SO}_4$
	<i>Illminite</i>	$\text{FeTiO}_3$
4.0-4.5	Quartz	$\text{SiO}_2$
	Potassium-feldspars	$(\text{K},\text{Na})\text{AlSi}_3\text{O}_8$
	Kaolinite	$\text{Al}_2(\text{Si}_2\text{O}_5)(\text{OH})$
	Muscovite	$\text{KAl}_3\text{Si}_3\text{O}_{10}(\text{OH})_2$
15.0-16.0	Kaolinite	$\text{Al}_2(\text{Si}_2\text{O}_5)(\text{OH})$
	Quartz	$\text{SiO}_2$
	Geothite	$\text{FeO}(\text{OH})$
	Muscovite	$\text{KAl}_3\text{Si}_3\text{O}_{10}(\text{OH})_2$
	<i>Natrolite</i>	$\text{Na}_2(\text{Al}_{1.92}\text{Si}_{2.08})\text{SiO}_{10.04}(\text{H}_2\text{O})_{1.96}$

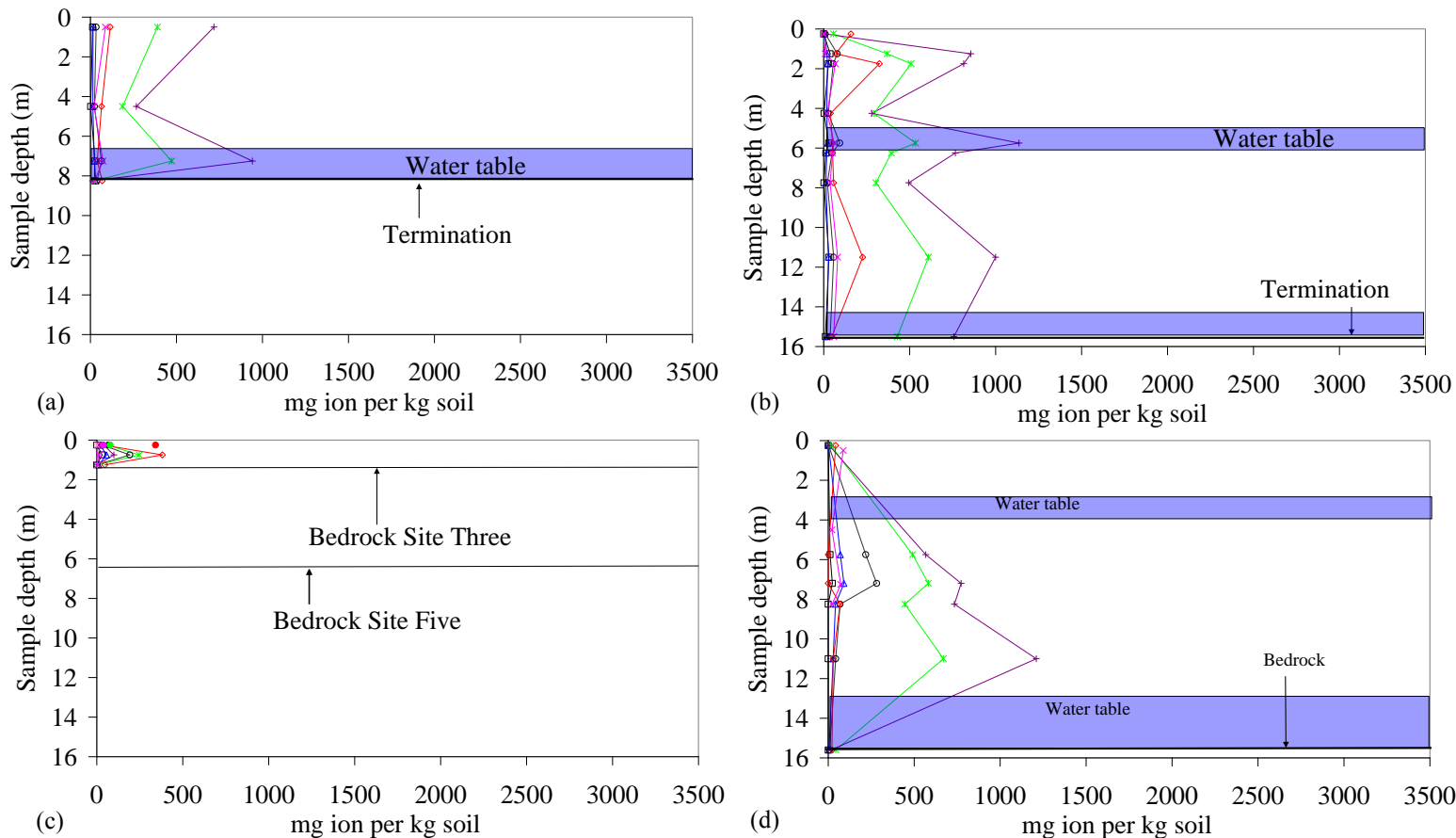


Figure 5.11. Ca (□), K (△), Mg (○), Na (\*),  $\text{HCO}_3$  (◇), Cl (+), and  $\text{SO}_4$  (×) concentrations (mg ion per kg soil) in select samples from soil cores collected from Sites, (a) Two Shallow; (b) Two Deep; (c) Three (points) and Five (lines); and (d) Four. ‘Termination’ indicates terminal drilling depths, with ‘bedrock’ instead indicating drilling was halted when hard rock was intercepted.

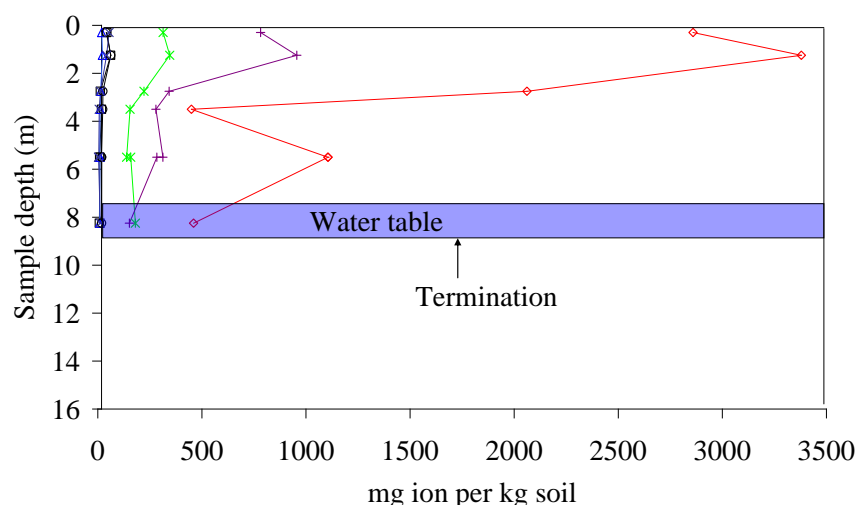


Figure 5.12. Ca (□), K (△), Mg (○), Na (\*), HCO<sub>3</sub> (◇), Cl (+), and SO<sub>4</sub> (×) concentrations (mg ion per kg soil) in select samples from soil cores collected from Site Six. ‘Termination’ indicates terminal drilling depths.

not a result of carbonate and/or sulfate precipitation in shallower layers. Sodium and Cl dominated soil solutions therefore occur by processes not related to direct aeolian accession on Manobalai.

### 3.3.2. Groundwater accession

Solute concentration, soil moisture, and groundwater were all correlated at Manobalai, though sometimes contrastingly at different sites. Total soil moisture was highest at the depth of groundwater interception (Figures 5.7 – 5.9 and Figures 5.11 – 5.12), with differences in regolith textures leading to the large differences in total soil moisture between the alluvial and smectitic clay material. The high total moisture values at Sites Six – Eight reflected the high moisture absorbance of smectitic clays, which can retain up to 670 % of their weight in water before becoming liquid (Odom 1984). The highest moisture contents and soil salinities occurred in the sandiest layers of the soil columns at Sites Two Shallow and Deep, with the highest regolith salinities (2089 mg kg<sup>-1</sup>) just above the layers where groundwater was intercepted (Figure 5.11). Lower salinity regolith layers were instead correlated with the interception of groundwater at Sites Four and Six. These contrasting relationships between regolith salinity and groundwater occurrence were related to the differences in groundwater salinity at the site.

Groundwater salinity at the Manobalai site was highly variable. Groundwater was fresh at Site Four (Table 5.5), with salinities less than 400 mg L<sup>-1</sup> (Rhoades *et al.* 1992). Although the bore and piezometer at Site Two had lower hydraulic heads and were located 600 m topographically down-gradient of Site Four, groundwater at Site Two was moderately – highly saline with salinities in excess of 5000 mg L<sup>-1</sup>. Groundwater

salinity again dropped 300 m topographically down-gradient of Site Two, with salinities of 1721 mg L<sup>-1</sup> occurring at Site Six. The occurrence of the highest Na and Cl concentrations in sandy layers at the same depth where saline groundwater occurs indicates that groundwater transports solutes to the regolith at Site Two. The opposite instead occurs at Site Six and Site Four, where groundwater contains much lower solute concentrations, with this in turn giving rise to regolith with much lower salinities. The results presented here are therefore evidence that groundwater is an important solute transport mechanism at Manobalai, bringing solutes to the sandy layers at salt scald (Site Two) and removing solutes from the regolith at Sites Four and Six. The occurrence of both fresh and groundwater bodies at Manobalai will now be considered.

Abrupt changes in groundwater salinity were seen down the sampling transect at Manobalai (Figure 5.13). Geological structures can cause such abrupt changes in groundwater salinity within catchments (Engel *et al.* 1987; Ringoase-Voase *et al.* 2003). Differences in groundwater salinity between Sites Two and Six were almost certainly caused by a barrier in the form of thick smectitic-clay. This clay arose abruptly between Sites Two and Six, with no evidence of the alluvial regolith at Sites One – Five seen in the Site Six core. The smectitic clay between Sites Two and Six is acting as an impermeable barrier to saline groundwater flowing down-gradient from Site Two, with dolerite dykes in Western Australia impeding the flow of saline water in a similar way (Engel *et al.* 1987).

Differences in hydraulic heads indicate saline groundwater is mounded behind the smectitic clay, which causes impeded flow and therefore much higher hydraulic head at Site Two than Site Six. This groundwater will cause scalding due to capillary rise and evapoconcentration when hydraulic heads approach the regolith surface (e.g. Eugster and Jones 1979; Arad and Evans 1987; Crosbie *et al.* 2007). Mottling of regolith and large (30 mm × 20 mm) flecks of pyrolusite (MnO<sub>2</sub>) were observed at depths within 0.5 m of the regolith surface at Sites Two and Four, and indicated water tables have risen to the regolith surface in the past (Taylor *et al.* 1983). The severity of the scalding at Manobalai is observed to increase in wetter seasons, with the salt scald grassing over substantially during the low-rainfall conditions in this study. The land-holder has observed that the scald at Site Two is completely bare of vegetation when normal rainfall conditions occur (D. Googe, Pers. Comm., 2009). This corroborates the findings

Table 5.5. Chemistry of rain water samples collected from near and within the Wybong Creek catchment and groundwater samples from Manobalai. Samples were not collected from Sites Five and Seven due to an absence of groundwater at these sites. BDL indicates solute concentrations below detection limit, while N/A indicates where the measurement of a parameter was not applicable or where samples were not analysed for a parameter.

Sample type	Name	Date	SWL (m)	TDS (mgL <sup>-1</sup> )	Na (mgL <sup>-1</sup> )	Ca (mgL <sup>-1</sup> )	Mg (mgL <sup>-1</sup> )	K (mgL <sup>-1</sup> )	Cl (mgL <sup>-1</sup> )	SO <sub>4</sub> (mgL <sup>-1</sup> )	HCO <sub>3</sub> (mgL <sup>-1</sup> )	Br (mgL <sup>-1</sup> )	Na/Cl Molar	Cl/Br Molar	<sup>87</sup> Sr/ <sup>86</sup> Sr
Rain water	Denman	7/06/2007	N/A	1.4	0.7	0.2	0.1	0.1	0.4	0.4	1.0	0.0	2.5	6	N/A
		8/06/2007	N/A	0.2	0.1	0.1	BDL	BDL	0.4	0.4	1.0	0.0	0.2	6	N/A
	Muswellbrook	03/09/2007	N/A	7.1	0.6	3.8	0.2	0.1	0.5	1.1	1.0	0.0	1.7	8	0.706015
		22/12/2007	N/A	13	0.67	8.1	0.3	0.3	0.4	2.0	1.0	0.0	2.4	6	N/A
	Wybong	19/01/2008	N/A	22	0.76	10	0.3	0.3	1.2	6.5	1.0	0.0	0.9	18	0.705891
		21/07/2008	N/A	9.2	0.32	0.6	0.3	0.2	0.6	1.0	5.5	0.0	0.8	9	N/A
	Mean		N/A	10.4	0.5	3.8	0.2	0.2	0.6	1.9	1.8	0.0	1.3	9	N/A
Groundwater	Whip Well	26/03/2007	224.0	224	66	5.0	7.4	3.7	88	19	43	0.0	1.2	1767	0.709446
		22/07/2006	162.7	5204	1450	73	253	32	2629	17	742	0.0	0.9	BDL	N/A
	Hannah's	16/07/2008	162.8	6130	1700	65	350	41	3300	42	601	0.1	0.8	744	0.708303
		16/02/2008	185.6	1452	430	32	31	2.8	610	35	295	1.1	1.0	764	N/A
	Site One	15/07/2008	186.4	912	260	15	22	3.1	340	24	237	1.8	1.1	697	0.708440
		19/02/2008	177.9	6247	1500	230	550	37	2700	350	851	0.0	0.8	951	N/A
	Site Two Shallow	15/07/2008	178.0	5540	1200	210	400	28	2800	170	710	6.4	0.6	BDL	0.707121
		20/01/2009	179.1	6960	1460	260	520	34	3600	200	861	8.6	0.6	943	N/A
		19/02/2008	176.8	5327	1100	190	400	27	2800	160	624	4.9	0.6	889	N/A
	Site Two Deep	15/07/2008	179.4	4463	920	170	350	23	2300	120	553	7.1	0.6	1058	0.707174
		20/01/2009	179.1	7277	1520	240	550	40	3800	154	946	9.2	0.6	931	N/A
		16/07/2008	188.8	4855	1400	47	190	31	2700	300	135	7.7	0.7	780	0.708712
	Site Three	20/07/2008	178.4	105	17	3.8	3.3	8.9	22	18	28	0.0	1.1	714	0.708740
		16/07/2008	183.4	366	84	4.2	9.5	6	95	31	115	0.3	1.3	BDL	0.708779
		20/01/2009	185.4	239	44	2.8	8.8	8.2	26	8	137	0.0	2.4	852	N/A
	Site Six	15/05/2009	168.5	1721	395	39	85	12	684	68	413	1.8	0.89	938	0.704696
	Site Eight (S)	15/05/2009	158.8	2712	597	106	158	11	1219	83	509	2.9	0.75	981	0.707249
	Site Eight (F)	15/05/2009	158.7	2477	513	109	154	10	1058	103	505	2.4	0.75	714	0.704959

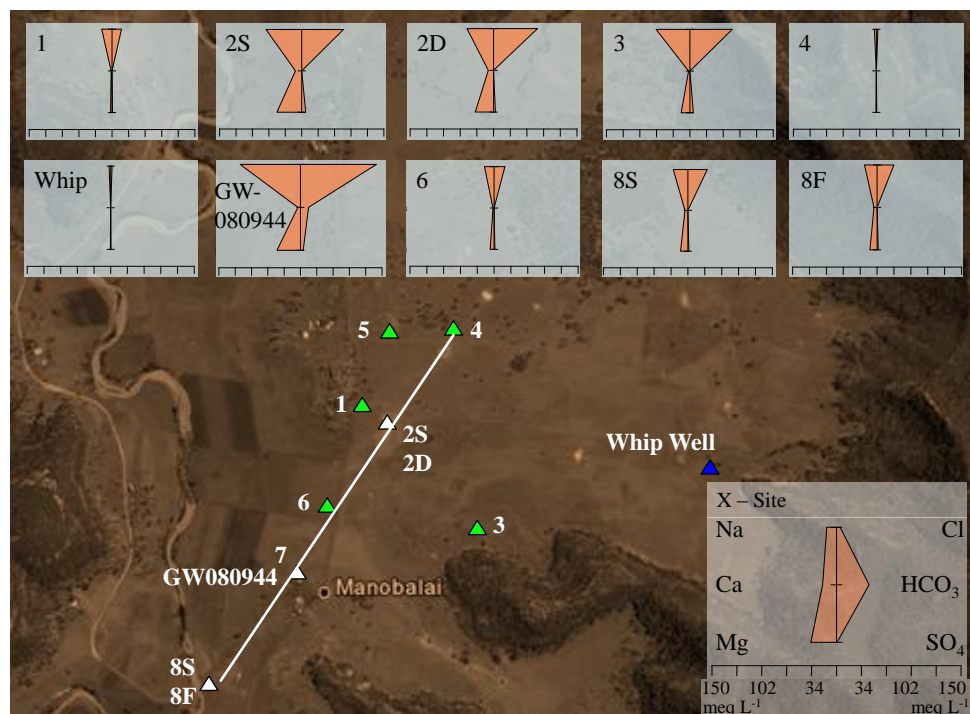


Figure 5.13. Stiff diagrams of representative groundwater samples from Manobalai. Samples collected on 19/02/2008 were from Sites One, Two Deep and Two Shallow; samples collected on 16/07/2008 were from Sites Three and Hannah's; samples from Whip Well were collected on 26/03/2007; and samples collected from Sites Six – Eight were collected on 15/05/2009. Triangles indicate nested piezometer and/or bores ( $\Delta$ ), single piezometers/bores ( $\blacktriangle$ ), and a spring ( $\blacktriangleleft$ ).

presented here, and indicates that salt scalding is likely to exacerbate at Manobalai when increases in recharge bring groundwater close to the regolith surface (e.g., Macpherson and Peck 1987; Armstrong *et al.* 1996).

### 3.3.2.1. Causes of groundwater salinity

Though the change in regolith between Sites Two and Six can explain the changes in groundwater chemistry between these sites, such changes cannot explain the abrupt changes in groundwater salinity at other Manobalai sites. Saline groundwater occurred at Site Two for example, while fresh occurred at Site Four. Bores at both these sites were screened into the same sandy-clay alluvium. In addition, groundwater salinity was at times twice as high in Hannah's bore as in the piezometer at Site Eight Fractured, despite both being screened into fractured conglomerate/sandstone. The causes of such changes in salinity include evapoconcentration of groundwater between sites and mixing of differing groundwater bodies which are discharging into the same aquifer.

Evapoconcentration causes increases in groundwater salinity with increasing distance down flow paths in many parts of south-eastern Australia (e.g., Herczeg *et al.* 1992; Cartwright and Weaver 2005; Petrides *et al.* 2006), but is not the cause of saline groundwater at Manobalai. In order for evaporation to have caused Cl concentrations to

increase from 95 mg L<sup>-1</sup> at Site Four on 15<sup>th</sup> July 2008, to the 2300 mg L<sup>-1</sup> at Site Two Deep, for example, nearly 98 % of the water (54.40 of 55.51 mol H<sub>2</sub>O) would need to evaporate away. Water which had undergone such evaporation would be expected to have similar ion ratios and be significantly enriched in δ<sup>2</sup>H and δ<sup>18</sup>O. Ratios of HCO<sub>3</sub>, SO<sub>4</sub>, Na and TDS to Cl in Site Four groundwater were higher than those in groundwater from Site Two Deep or Shallow (Figure 5.14). This is not conclusive evidence that evapoconcentration between sites has not occurred, due to the precipitation of minerals such as carbonate causing a change in the proportion of ions in solution as water evaporates (e.g. Eugster and Hardie 1975). As previously mentioned, however, carbonate has not been identified within the regolith at Manobalai and the pH of soil/regolith solutions is too low for such precipitation to occur within the alluvium at Sites Two and Four. In addition, the much fresher water at Site Four was more enriched in δ<sup>2</sup>H and δ<sup>18</sup>O and further removed from the approximate local, Melbourne, and global meteoric water lines than groundwater samples from Site Two (Figure 5.15). This indicates that Site Four groundwater had undergone more evaporation than groundwater at Site Two, with the opposite occurring if Site Four groundwater had evapoconcentrated to form Site Two groundwater. The saline groundwater at Site Two is therefore not the product of evapoconcentration along the flow path between Sites Four and Two.

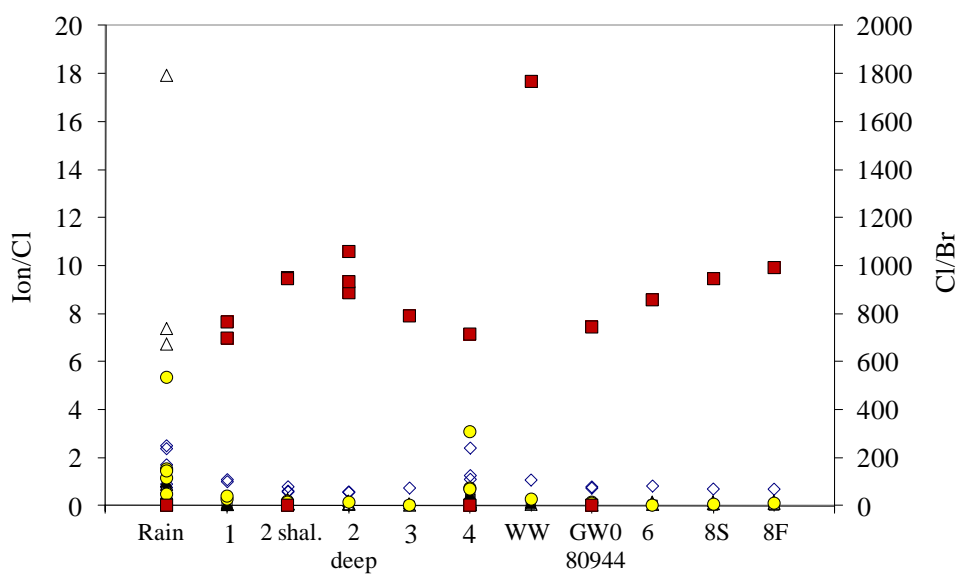


Figure 5.14. Molar ion to Cl ratios of samples collected from Sites One to Four, Whip Well, and the bore Hannah's on 15/07/2008, and for Sites Six to Eight on 15/05/2009. Symbols represent Na/Cl (◇), K/Cl (□), Mg/Cl (△), Ca/Cl (▲), HCO<sub>3</sub>/Cl (●), Cl/Br (■).

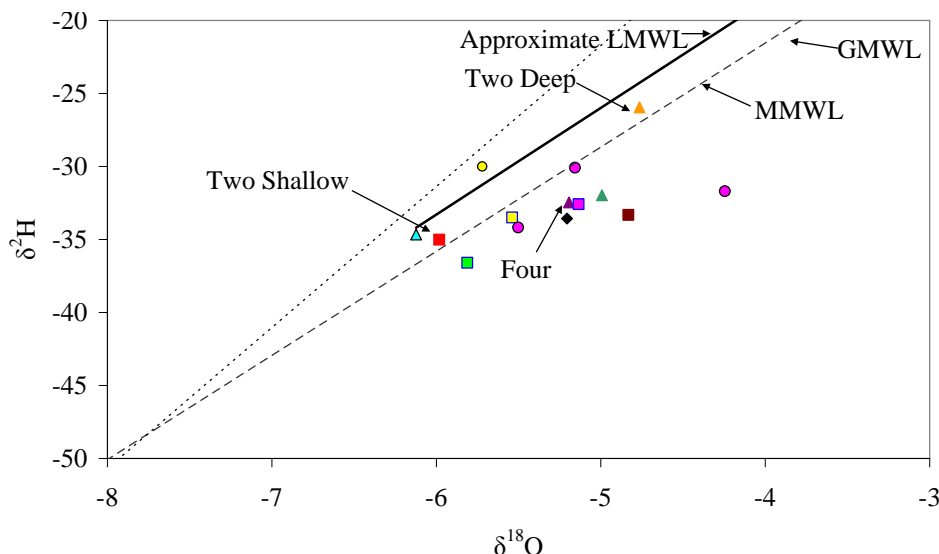


Figure 5.15.  $\delta^2\text{H}$  vs  $\delta^{18}\text{O}$  for groundwater samples collected from Manobalai. Symbols indicate groundwater collected from Sites Two Shallow (■); Two Deep (▲); Three (▲); Four (▲); and Hannah's (■) on 16/07/2008; from Sites Six (□); Eight Shallow (◆); Eight Fractured (■); and Whip Well (□) on 15/05/2009; and rainwater (▲) collected on 22/12/2007; 19/01/2008, and 21/07/2008.  $\delta^2\text{H}$  and  $\delta^{18}\text{O}$  for surface water collected from tributaries (●) in the locality of Manobalai are presented for comparison LMWL indicates the approximate local meteoric water line; MMWL indicates the Melbourne meteoric water line (CSIRO and ANSTO 2004); and GMWL indicates the global meteoric water line (Craig 1961).

Aeolian accession of salts may have caused salt stores to have been built in eastern Australian rock formations, with these leaching out and causing salinity in the valleys below (Gunn and Richardson 1979). Interbedded sandstones and conglomerates of the fractured Narrabeen Group surround the Manobalai field site, and occur as escarpments which rise up to 300 m above the valley floor. Studies on the Narrabeen Group have not identified minerals which could weather to produce Cl through chemical weathering (Bai and Keene 1996), with silicate weathering of the quartz dominated rocks of this group instead leading to HCO<sub>3</sub> dominated facies (Appelo and Postma 2005). Mixed layer illite/smectite deposits occur within the rock (Bai and Keene 1996), with these used as an indication of aeolian accession (Cattle *et al.* 2002). Mixed layer illite/smectite within the Narrabeen Group formed through diagenetic processes (Bai and Keene 1996), however, rather than being deposited as dust from saline catchments in Australia's interior.

Groundwater chemistry at the site was also not consistent with dissolution of dust from within the escarpments. Highly variable solute concentrations occurred in groundwater adjacent to the escarpments at Manobalai, for example, with groundwater at Whip Well and Site Three differing in solute concentration by more than 4000 mg L<sup>-1</sup>. The <sup>87</sup>Sr/<sup>86</sup>Sr ratios of saline groundwater at the Manobalai field site are additional evidence against dissolution of aeolian salt stores, with the 0.706 – 0.709 seen in

groundwater at Manobalai dissimilar to the dust from the interior of Australia, which instead has  $^{87}\text{Sr}/^{86}\text{Sr}$  of 0.722 (Revel-Rolland *et al.* 2006). Ratios of  $^{87}\text{Sr}/^{86}\text{Sr}$  seen in groundwater from Sites One – Four, Whip Well, and Hannah's were instead most similar to marine water (Chapter Four), though groundwater from Sites Six to Eight were similar to the basalts in this area from which the smectitic clay on the Wybong Creek floodplain is derived (Kovac 1991; Gingele *et al.* 2007). With salt stores in the regolith, evapoconcentration, and evolution of saline groundwater within the regolith all discounted as sources of salinity to Manobalai, the alternative source of salinity to the Manobalai field site is discharge from a deeper saline aquifer under the Narrabeen Group. This source of salinity has been discussed previously in the thesis, with no evidence from research within Manobalai existing to discount discharge of saline groundwater from the Wittingham Coal Measures as the source of salinity to this site.

Groundwater discharge from deeper formations is thought to have lead to the formation of pedogenic carbonate in parts of the Hunter Valley (Hamilton 1992). A layer of pedogenic carbonate was identified 12 km south of the Manobalai site, adjacent to the 72 km sample site and Yarraman Gauge. This layer was sampled in order to isolate whether the precipitation of the pedogenic carbonate was caused by CO<sub>2</sub> being respired into the soil by plant roots, downwards transport of CO<sub>2</sub> through rainwater infiltration (Amundson *et al.* 1994), and/or degassing of discharging groundwater (Appelo and Postma 2005). The  $\delta^{13}\text{C}$  values of pedogenic carbonate samples collected for this study ranged from -16 in the top 100 – 200 mm of the carbonate layer, to -15 in the middle 750 mm layer, up to a value of -9 in the bottom 1.5 m layer (Table 5.6). Carbon-14 dates indicate the pedogenic carbonate formed 17 000 – 27 000 years before present, and though  $^{14}\text{C}$  dating is likely to underestimate these ages by up to 3 000 years (Amundson *et al.* 1994), it is of little consequence for the purposes of this discussion as dates still fall in the late Pleistocene.

Table 5.6. Carbon dates for the top, middle and bottom layers of carbonate sampled from an erosion gully adjacent to the 72 km surface water sampling site.

Layer	Sample depth (mm)	$\delta^{13}\text{C}$	$\pm$	Fraction Modern Carbon (fm)	$^{14}\text{C}$ age	$\pm$
Top	100	-16	1	0.0342	27120	270
Middle	750	-15	1	0.1158	17320	110
Bottom	1500	-9	0	0.0348	26980	260

Soil carbonates formed in equilibrium with the atmospheric CO<sub>2</sub> have a δ<sup>13</sup>C value of +3.09 ‰ (Faure 1998); those produced through C3 plant respiration have a value of -24 to -34 ‰; and those produced through C4 plant respiration have a value of -6 to -19 ‰ (Smith and Epstein 1971 in: Gardner 1984). The δ<sup>13</sup>C values of the pedogenic carbonate sampled from the 72 km surface water sample site were closest to those of plants undergoing C4 photosynthesis. Eucalypt (C3) woodland currently dominates forest communities in the area and dominated the valley floors pre-deforestation in the 19<sup>th</sup> and 20<sup>th</sup> centuries (Albrecht 2000). Plant communities in south-east Australia were changing from being dominated by the Casuarina (Casuarinaceae) and Daisy (Asteraceae) families to Eucalypt dominated communities in the late Pleistocene (Kershaw *et al.* 1991), however, with some of members of these families as well as grasses undergoing C4 photosynthesis (Thorn 2004). The pedogenic carbonate in this study formed when plant communities were going through this change (Table 5.6), with the δ<sup>13</sup>C signatures seen in the pedogenic carbonate from the 72 km surface water sample site possibly formed by respiration of CO<sub>2</sub> into the regolith by C4 plants (Thorn 2004). Respiration by C3 plants could also have resulted in the δ<sup>13</sup>C values seen, however, if respired CO<sub>2</sub> mixed with atmospheric CO<sub>2</sub>. There is therefore little evidence within this study as to whether plant communities were related to the formation of the pedogenic carbonate seen at the 72 km sample site. Much more extensive sampling and research than the few samples presented here is required, in order to come to a conclusion with any certainty.

Carbon-14 dates of the top and bottom regolith layers were 27 000 years, with the middle layer having an age of 17 000 years. South-eastern Australia was arid during the Pleistocene, due to the glacial maximum 21 000 BP (Bowler and Wasson 1983). Vegetation was restricted to water courses at this time with lower effective evaporation and less evapotranspiration. This lead to higher groundwater tables and greater runoff (Fried 1993), with increased erosion and dissolution of the salt stored within the regolith (Bowler and Wasson 1983). The pedogenic carbonate at the 72 km sample site may be evidence of higher water tables in the Wybong Creek catchment also, with areas adjacent to fractures in other parts of the Hunter Valley thought to occur as a result of palaeo-groundwater discharge when water tables were higher (Hamilton 1992). The carbonate layer which was 10 000 years younger than the layers above and below may additionally indicate throughflow erosion of a previously occurring layer of regolith (e.g., Beavis 2000), possibly due to this increased groundwater discharge (Table 5.6). These results and discussion can only be presented as hypotheses, however, with

research required on where pedogenic carbonate occurs within the regolith profile, how extensive it is within the Wybong and Hunter catchments, and a range of geochemical and mineralogical analyses required (Radke 1994), in order to come to any conclusions as to the relationship between pedogenic carbonate in the Wybong Creek catchment and groundwater discharge.

### **3.3. Conceptual model of salinity at the Manobalai field site**

Fresh groundwater appears to occur as localised groundwater systems in isolated pockets within Manobalai, with Site Four and Whip Well being good examples of this. Groundwater at Sites One and Three was instead saline and Na-Cl dominated, and arose at specific points on the break of slope on the Narrabeen Group escarpments above the salt scald (Figure 5.16). Hydraulic heads and similar element to Cl ratios indicate that groundwater has a propensity to flow from Sites One and Three down to the salt scald (Table 5.5). South and down gradient of Site Two, this saline groundwater is prevented from flowing into Wybong Creek by smectitic clay at Site Six which acts as a barrier to groundwater flow. Groundwater mounding behind this smectitic clay is likely to be causing the Manobalai salt scald, especially when normal – high rainfall conditions occur in the Wybong Creek catchment. An increase in rainfall in the area is therefore expected to cause a continued rise or sustained high groundwater tables, with scalding at the Manobalai salt scald worsening periodically.

Groundwater sampled from Hannah's monitoring bore (GW080944), which was screened into fractured conglomerate at Site Seven, had similar chemistry to that of Sites One, Two, and Three, which were screened into sandy-alluvium. Site Eight Fractured groundwater was different than that at Hannah's, despite being screened into the same fractured conglomerate. Similar differences occurred between Sites Two and Four, which were screened into sandy-alluvium. Research presented in this chapter did not identify the connectivity or flow paths of groundwater at these sites, however, the similarity of groundwater between sites which have been demonstrated to be hydraulically unconnected (i.e. Hannah's and Site Two) is evidence for discharge of regional groundwater to these sites via fractures. While Site Four and Site Two groundwater has very different salinities, these may in addition indicate different levels of mixing between saline and fresh groundwater bodies, with groundwater at Site Four perhaps occurring as an isolated perched aquifer. Further research which builds on the conceptual model of groundwater flow at Manobalai is required, however, involving the demonstration of groundwater connectivity and flow paths within the site.

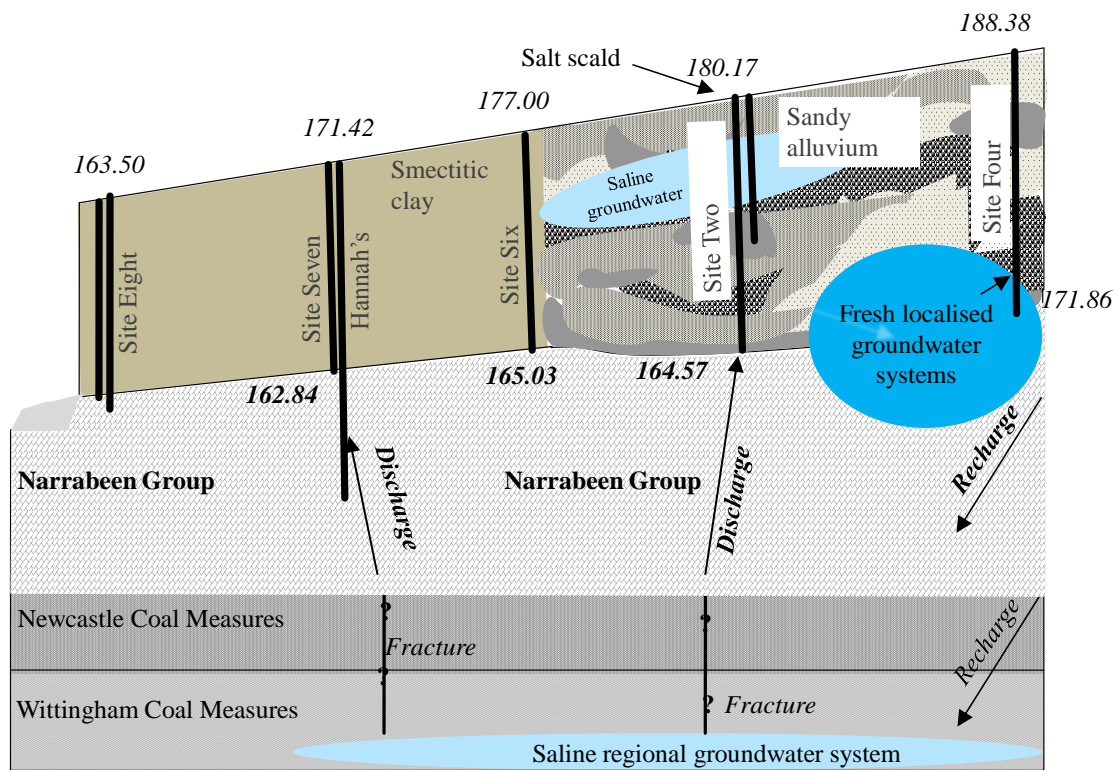


Figure 5.16. Conceptual model of groundwater flow and salinisation along the transect between Sites Four and Site Eight at Manobalai. Arrows indicate flow direction, with elevations of the ground and bedrock surfaces indicated in italics (AHD). Longitudinal profile not to scale.

Black smectitic clays occur as river terraces and in the floodplain of the upper Hunter River (Kovac & Lawrie 1991). Research conducted at the confluence of the Hunter and Goulburn Rivers, downstream of Wybong Creek, found that discharge of regional groundwater from the Wittingham Coal Measures causes salinisation of the alluvial aquifer in this area (Kellett *et al.* 1989), with saline springs and seeps periodically observed at the ground surface (Hamilton 1992). The quantity of water discharged in these seeps is also observed to vary seasonally depending on recharge conditions, in a similar way to salt scalding at Manobalai. Saline soils occur upslope of smectitic-clays in many parts of the Hunter catchment (Kovac & Lawrie 1991), with groundwater mounding behind these possibly causing salt scalding similarly to Manobalai. Groundwater mounding behind dykes, faults and bedrock highs causes regolith and soil salinity in a number of catchments across Australia, with the severity of scalding often dependent on rainfall conditions as seen in the Wybong Creek catchment (Engel *et al.* 1987; Bradd *et al.* 1997; Coram *et al.* 2001; Acworth & Jankowski 2001; Peck & Hatton 2003; Ringrose-Voase 2003).

Research in the Liverpool Plains has found salinisation occurs due to both dissolution of salts from within the regolith and rising water tables (Dyce & Richardson

1997; Ringrose-Voase *et al.* 2003). Poor connectivity occurs between the regional groundwater systems within the fractured rock aquifers of the Liverpool Plains and the alluvial systems above (Ringrose-Voase *et al.* 2003). Salinisation therefore occurs by differing means within the neighbouring Hunter and Liverpool Plains catchments, despite the similarity of the geology and climate. The highly localised nature of salinisation has been noted by a number of authors (e.g. Acworth & Jankowski 2001; Peck & Hatton 2003), with the results presented here reinforcing the imperative for localised studies in ascertaining causes of salinity within even proximal catchments.

The regional extent of groundwater systems makes management of discharge difficult, with changes in hydraulic heads taking sometimes hundreds of years to manifest after a modification of land-use (Coram *et al.* 2001). The planting of trees to decrease recharge to groundwater bodies has been undertaken in a number of Australian catchments (e.g., Salama *et al.* 1993b; George *et al.* 1999), but with limited affect (Coram *et al.* 2001; Peck & Hatton 2003). Tree planting is particularly unlikely to offer a practical means of managing saline discharge in the Hunter Valley, due to the regional extent of the groundwater system causing the salinity. The nature of the salinity problem in the Hunter Valley is such that only limited salinity mitigation measures, such as “living with salt strategies”, can be effectively put in place. The formation of the Hunter River Trading Scheme is an example of such a strategy (New South Wales Office of Water 2010). The limitation of irrigation using both saline and fresh surface and groundwater is another means of preventing further salinisation, with the fresher water in the area diluting and therefore reducing the toxicity of saline groundwater.

#### **4. Conclusions**

Regolith within the Manobalai field site was largely non-saline, though solutes in alluvial samples in the valley floor were dominated by Na and Cl. The most saline samples occurred in samples from various depths at Site Two, Four and Six with cores from the salt scald having salinities ranging from 274 – 2089 mg kg<sup>-1</sup>, and a maximum weight percent of 0.17 % Na and Cl. The occurrence of the salt scald was found to be due to saline groundwater, which was up to 100 times higher in salinity than the regolith on a per weight basis. Pyrolusite within the top layers of the alluvium and increased scalding during wetter periods indicates groundwater moves up and down through the regolith according to recharge conditions. Scalding occurs when groundwater is closest to the surface.

Alluvial fill was derived from the weathering of the Triassic Narrabeen Group that surrounds Manobalai, with the footslopes showing pedological development. Regolith on the Wybong Creek floodplain was instead smectitic clay and derived from the Liverpool Range Volcanics. Saline groundwater arises at specific points at the break of slope and flows down through the coarse sands and silts produced from weathering of the Narrabeen Group to the salt scald. This is in contrast to salinity on the other side of the Liverpool Ranges, where salinity occurs due to dissolution of salts stored in the smectitic clays. Groundwater mounds behind the smectitic clay at Manobalai, which acts as an impermeable barrier to the saline groundwater. This same phenomenon is expected to occur in the lower Wybong Catchment also, with the smectitic clay of the Merriwa soil landscape series occurring adjacent to Wybong Creek and the Sandy Hollow soil landscape series occurring behind it in both the mid and lower catchment areas.

Saline groundwater did not occur at all sites within the Manobalai area. The occurrence of similar saline water in specific bores and piezometers screened into the fractured Narrabeen Group, at the break of slope, and in the valley bottom suggests point source groundwater discharge via fractures and/or faults connected to a saline aquifer. More detailed hydrological research is required to further constrain these findings. These findings have important ramifications in the context of salinity research within Australia, whereby a model of dryland salinity is often assumed and related to salt stores within the regolith, or to evapoconcentration of rainwater and/or groundwater along flow paths. The research presented here indicates that groundwater in the Wybong Creek catchment is instead saline before it is discharged into the regolith and is therefore almost certainly a naturally occurring processes, though further research is required in order to ascertain that human changes to the hydrological cycle have not caused the discharge of regional groundwater into the catchment.

---



---

## **Chapter Six**

The hydrology and hydrogeology  
of Manobalai



## 1. Introduction

Research presented in this thesis has identified saline groundwater discharge as causing abrupt increases to solute concentrations in regolith and surface water in the mid-catchment area of Wybong Creek (Chapter Five). Salinity in Wybong Creek has been observed to fluctuate throughout the day, with this thought to be due to groundwater discharge from confined aquifers adjacent to Wybong Creek responding to loading and unloading events (Chapter Two). Point source increases in salinity within Wybong Creek, in addition, indicate saline groundwater discharge via fractures. The research presented in this chapter is therefore aimed at identifying the physical properties of the aquifers and groundwater flow paths in the mid-catchment locality of Manobalai, to elucidate possible means of limiting saline groundwater flux into Wybong Creek.

The delineation of groundwater flow paths is of particular importance in areas where groundwater transports solutes and/or pollutants to surface water and soils. Despite its importance, such delineation remains a difficult problem within the field of hydrology (e.g., Sandberg *et al.* 2002), and is especially complicated in areas with anisotropic geology and vertical groundwater flow. This is partially due to piezometric surfaces being inaccurate in the identification of groundwater flow paths, due to flow which is not horizontal and at right angles to piezometric contours (e.g., Freeze and Cherry 1979; Domenico and Schwartz 1990). The assessment of vertical groundwater flow and the degree of anisotropy is therefore required in order to accurately identify flow paths within fractured and alluvial aquifers.

Vertical groundwater flow may occur in aquifers which contain fractured and faulted rock (e.g., Cook 1999), and in aquifers composed of interbedded and unconsolidated alluvial sediments. Though groundwater flow via fractures is a common feature of many catchments within Australia (e.g., Jankowski and Acworth 1997; Coram *et al.* 2001; Morgan and Jankowski 2004; Tweed *et al.* 2005), the location and water-bearing capacity of fractures remains difficult to predict (Praamsa *et al.* 2009). The delineation of groundwater flow paths within fractured aquifers is further complicated by spatial changes in fracture permeability and porosity; changes in the connectivity between vertical and horizontal fractures; and changes in fracture geometry (Tweed *et al.* 2005; Praamsa *et al.* 2009). These factors make groundwater flow difficult to predict in fractured aquifers. The analyses of non-reactive groundwater constituents, such as  $^{87}\text{Sr}/^{86}\text{Sr}$ , Cl, and reactive constituents such as  $\delta^{18}\text{O}$  and  $\delta^2\text{H}$  (e.g., Mazor and Nazir 1992; Love *et al.* 1993; Cook 1999; Broers and van der Grift 2004), in addition to

an assessment of the physical properties of an aquifer, such as the degree of fracturing, heterogeneity, and anisotropy, is therefore required in order to properly elucidate groundwater flow paths.

Time-series analyses of hydraulic head changes are of increasing use for understanding the physical properties of an aquifer due to the growing availability of instruments which measure and log changes in hydraulic head simultaneously at spatially separate sites (e.g., Acworth and Brain 2008; Burbey 2009). These highly accurate pressure transducers can detect millimetre scale changes to SWLs at time-steps as small as a second, and provide insight into the factors which control groundwater flow. Hourly changes to hydraulic heads within a bore or piezometer, for example, can indicate the effects of groundwater pumping. Rhythmic hourly changes to hydraulic heads instead indicate an aquifer that is undrained and confined, being loaded and unloaded (Domenico and Schwartz 1990). Phenomena which can cause the loading and unloading of aquifers in this way include atmospheric pressure changes and Earth tides (Acworth and Brain 2008; Burbey 2009). Increasing hydraulic head over days to months instead indicates the response of an aquifer to recharge (Stephenson and Zuzel 1981; Petrides *et al.* 2006), and therefore, the degree to which an aquifer is confined (Arad and Evans 1987; Johnston 1987b; Bourg and Bertin 1993), though deeper confined systems such as regional groundwater bodies may respond to a change in recharge after hundreds to thousands of years (Bowler 1976; Coram *et al.* 2001). Little scientific literature is currently available on time-series analyses of hydraulic heads at a subcatchment – catchment scale, although this is currently an active research area within hydrology (e.g. Acworth and Brain 2008; Burbey 2009). The knowledge provided by such research can provide valuable information on the degree of groundwater connectivity and conditions of groundwater flow, with this an obvious avenue for further research within the field of hydrogeology.

## **1.2. Aims and objectives**

The aim of this chapter was to understand groundwater movements at the Manobalai field site. The following objectives were considered in order to meet this aim:

1. To describe groundwater systems at the Manobalai field site;
2. To isolate factors controlling hydraulic head at Manobalai;
3. To identify groundwater connectivity within the Manobalai area; and

4. To identify whether a relationship exists between changes in Wybong Creek salinity and groundwater discharge from Manobalai.

### 1.3 Background

Research presented in this thesis has shown that important changes in the chemistry of Wybong Creek occur in the mid-catchment area (Chapter Two). Results show groundwater which has high solute and Cl concentrations enters Wybong Creek between the 55 km and 60 km surface water sampling sites. Surface and groundwater within the Wybong Creek catchment became increasingly saline and changed in character from being HCO<sub>3</sub> to Cl dominated downstream of this area. The northern-most, highly saline, Na-Cl dominated bore (Hannah's) also occurs in the mid-catchment area (Chapter Three), with salt scalding occurring less than one kilometre north-east of this bore at the locality of Manobalai. Saline groundwater discharged into Wybong Creek in the mid-catchment area does not acquire the majority of solutes from the regolith, however, but is discharged from a saline aquifer below the Narrabeen Group via fractures in the rock (Chapter Five).

Strata in the Manobalai area generally strike north-south and dip shallowly, though by an unquantified amount, to the west (Leary and Brunton 2003). Escarpments and outcrops are composed of the Narrabeen Group, which includes interbedded layers of the Narrabeen Sandstones and Widden Brook Conglomerate (Figure 6.1).

Groundwater occurs in both the alluvial material adjacent to the Narrabeen Group escarpments, and within the fractured Narrabeen Group which makes up the bedrock below Manobalai. These members are referred to as the Manobalai Alluvium aquifer and fractured Narrabeen Group within this chapter. Distinct lineaments have been delineated using aeromagnetic surveys, and occur in north-east/south-west, east/west and north-north-west/south-south-easterly directions, with the influence of lineaments on the drainage pattern of Wybong Creek probably indicating faults probably occur in the Manobalai area (Leary and Brunton 2003).

### 2. Materials and methods

Detailed sampling and analyses of groundwater samples is described in Chapter Three (Sections 2.1. – 2.2). The installation and surveying in of bores and piezometers is described in Chapter Five (Section 2.3.1), with parameters for these described in Table 6.1.

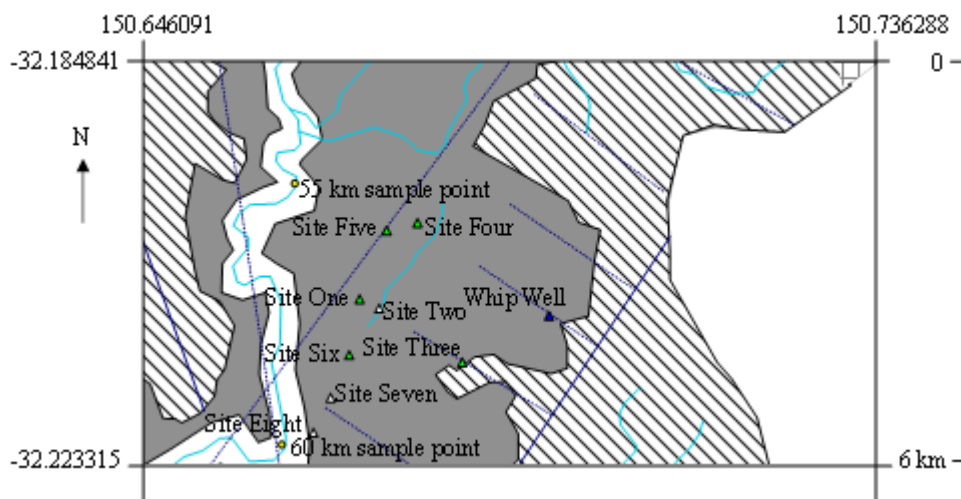


Figure 6.1. Lineaments (—) and inferred lineaments (.....) at the Manobalai field site. Grey indicates regolith; cross-hatching indicates the Liverpool Range Volcanics; diagonal lines indicate Narrabeen Group escarpments; and white the Wybong Creek water course. Triangles indicate nested piezometers and/or bores ( $\Delta$ ), single piezometers/bores ( $\blacktriangle$ ), and a spring ( $\blacktriangledown$ ). Adapted from Leary and Brunton (2003).

## 2.1. Hydrogeologic measurements

Static water levels (SWLs) in piezometers and bores were measured with a dip meter when SWLs had recovered from prior sampling (generally at least a month) and prior to purging, with recovery being when the SWL was similar to levels measured previously. Rising and/or falling-head slug tests were used to measure hydraulic conductivity ( $K$ ). These tests were conducted using both automated and manual measurements, whereby manual measurements were taken at five to 60 second intervals with a dip meter, concurrent with automated measurements by a Schlumberger pressure transducer at five – 30 second intervals.

Groundwater heights were measured hourly and logged by Odyssey pressure data recorders for several months, before these were replaced by Schlumberger pressure transducers. Schlumberger Cera pressure transducers were placed into different piezometers and bores at different times, with these measuring and logging groundwater pressure (i.e. depth of groundwater) and temperature at four hourly increments. Two Schlumberger CTD ‘divers’ measuring electrical conductivity (EC), groundwater pressure, and groundwater temperature were installed within the nested piezometers at Site Eight from March 2009 to May 2009, and moved to the piezometer and bore at Site Two from May 2009 to August 2009. Groundwater depth data from the Schlumberger pressure transducers was calibrated with manual measurements and all pressure transducer readings were corrected for air pressure changes using a Schlumberger Baro

Table 6.1. Parameters for \*bores and piezometers installed at the Manobalai field site, with elevations presented in Australian Height Datum (AHD). Bore collars at Sites Two Deep and Site Four were cut off at the ground on the 23/03/2009 due to damage by livestock.

Site	Latitude	Longitude	Elevation (top of collar, AHD)	Elevation (ground surface, AHD)	Depth of hole (m)	Collar height (m)	Bore/piezo diameter (m)	Screened interval (m)	Depth of gravel pack (m)
One	-32.12324	150.40262	187.27	186.61	2.38	0.66	0.125	2.0	2.0
*Two Deep 09/01/08 – 23/03/2009 23/03/2009	-32.12365	150.40329	180.76	180.22	15.65	0.53	0.125	2.0	15.5
Two Shallow	-32.12365	150.40328	180.72	180.17	8.60	0.55	0.125	2.0	8.4
Three	-32.12535	150.40491	194.34	193.89	5.40	0.45	0.125	2.0	2.0
*Four 09/01/08 – 23/03/2009 23/03/2009	-32.12201	150.40454	188.96	188.38	16.50	0.58	0.125	2.0	16.3
Five	-32.12217	150.40334	193.03	192.46	2.75	0.57	0.125	2.0	2.0
Six	-32.12343	150.40264	177.48	177.00	11.97	0.48	0.125	0.5	0.5
Seven	-32.12559	150.40264	171.42	171.00	8.16	0.42	0.125	1.5	1.5
Eight Shallow	-32.13125	150.39590	164.25	163.50	7.20	0.75	0.125	1.5	1.5
Eight Fractured	-32.13125	150.39590	164.25	163.50	9.78	0.75	0.125	1.5	1.5

diver installed at Site Five, with air pressure data from the Baro diver also used for analyses of time-series data collected in 2009. The CTD instruments were calibrated for EC using 0.01 M KCl ( $1413 \mu\text{S cm}^{-1}$ ) and 0.1 M KCl ( $12\,880 \mu\text{S cm}^{-1}$ ) solutions.

Groundwater was sampled after purging piezometers and bores of at least one well volume, with bailers and pumps used to extract groundwater. Measurements of surface water chemistry, flow, height, and temperature at surface water sampling sites are described in Chapter Two (Section 2.3).

Rainfall data for the Scone SCS weather station was attained from the Australian Bureau of Meteorology (2009). Theoretical Earth tides were modelled using the Tsoft programme (Van Camp and Vauterin 2005). This software was also used to conduct fast Fourier transformations (FFT) of some time-series data, with the removal of noise from the data allowing for more accurate analyses. Cross-correlation analysis was conducted on rainfall and groundwater height data using the statistical software package MiniTab® 15 (2006), with this analysis testing the statistical significance of a relationship between two sets of time-series data. Spectral analyses were conducted using MATLAB 7.4 (2007).

### 2.1.1. Hydraulic conductivity calculations

Pumping tests were not conducted at Manobalai due to time constraints and the impact of saline groundwater on pasture, with the time required for recharge also limiting the use of the Hvorslev method for the measurement of hydraulic conductivity (Appendix Six: Figures A6.1 – A6.3). Hydraulic conductivity ( $K$ ) was calculated using the Bouwer and Rice slug test (Bouwer 1989), with these conducted at Sites One – Four twice, and at Sites Six – Eight once during the study period (Eq. 6.1):

$$K = \frac{r_c^2 \ln(R_e / R_w)}{2L_e} \frac{1}{t} \ln \frac{y_0}{y_t} \quad (6.1)$$

where  $y_0$  = initial depth to water (m);  $y_t$  = displacement at time  $t$  (s);  $t$  = time where  $y_t$  is measured (s);  $r_c$  = radius of casing where the rise of water level is measured (m);  $L_e$  = length of well screen plus any packing materials (m);  $R_w$  = effective radius of piezometer including gravel pack (m); and  $R_e$  = effective distance over which the head displacement dissipates (m). The value of  $\ln(R_e/R_w)$  for fully penetrating piezometers was calculated using Eq. 6.2:

$$\ln \frac{R_e}{R_w} = \left[ \frac{1.1}{\ln(L_w / R_w)} + \frac{C}{L_e / R_w} \right]^{-1} \quad (6.2)$$

where  $C$  is a dimensionless number plotted as a function of  $L_e/R_w$ ; and  $L_w$  = length from bottom of screen to water table. The value of  $\ln(R_e/R_w)$  for partially penetrating piezometers was calculated (Eq. 6.3):

$$\ln \frac{R_e}{R_w} = \left[ \frac{1.1}{\ln(L_w/R_w)} + \frac{A + B \times \ln(h - L_w)/R_w}{L_e/R_w} \right]^{-1} \quad (6.3)$$

where  $h$  = depth from bedrock to water table (m); and  $A$  and  $B$  are dimensionless numbers plotted as a function of  $L_e/R_w$ .

## 2.2. Aquifer modelling

A mathematical model was written in order to identify the possible relationship between increases in salt load in Wybung Creek and groundwater fluxes from fresh and saline groundwater bodies existing within Manobalai. A second model was written in order to assess the semi-diurnal relationship between hydraulic head fluctuations at Manobalai and salinity fluctuations in Wybung Creek. The methods and assumptions by which these models were written are described separately in the following sections.

### 2.2.1. Groundwater fluxes needed to increase Wybung Creek salinity

A model was created in order to identify the quantity and the proportion of saline to fresh groundwater necessary to cause the increase in salt load ( $7.96 \text{ t day}^{-1}$ ) and surface water flow ( $0.14 \text{ m}^3 \text{ s}^{-1}$ ) seen between the 55 and 60 km sample sites on the 18<sup>th</sup> of June 2008 (Table 6.3; Appendix Six). The modelled groundwater bodies discharging into Wybung Creek and the theoretical aquifer these groundwater bodies occurred in had hydrological parameters based on piezometers at the Manobalai site as follows (Table 6.4). The modelled aquifer started between Site Two and Site Four and terminated at a sandstone outcrop south of Manobalai. The height of groundwater above Wybung Creek ( $\partial h$ ) was estimated at 14 m based on measurements of water depth within Site Two and Four bores, with hydraulic conductivity also based on Site Two measurements. Two sets of hydraulic measurements were used to check if the calculated discharge from the modelled fresh groundwater body were realistic. The first set was based on the same parameters as the saline groundwater body, but with different hydraulic conductivity ( $K$ ) values due to textural differences (Table 6.4). The hydraulic gradient ( $\frac{\partial h}{\partial x}$ ) for the second set of hydraulic measurements was based on the assumption that groundwater on the western side of Wybung Creek arises at the break of slope 500 m west of Wybung Creek similar to Site Three.

Table 6.2. Flow at surface water sampling Sites in Wybong Creek on the 5<sup>th</sup> July 2007 and the 18<sup>th</sup> June 2008. Flow analysis is described in Chapter Two (Section 2.4). N/A indicates where flow was not measured.

Site (km)	Flow (m <sup>3</sup> s <sup>-1</sup> )		TDS (mg L <sup>-1</sup> )		Salt load (t day <sup>-1</sup> )	
	2007	2008	2007	2008	2007	2008
11	0.01	0.81	494	353	0.44	24.81
30	0.37	1.38	616	480	19.43	57.17
37	N/A	1.16	572	482	N/A	48.23
48	0.24	0.96	763	531	15.65	43.93
55	N/A	1.08	785	584	N/A	54.65
60	0.38	1.22	750	593	24.33	62.62
72	0.44	1.31	847	661	32.38	74.57
77	0.47	1.97	830	695	33.99	118.09
83	0.80	1.22	823	739	57.00	78.08

Table 6.3. Optimised parameters used to model fresh and saline groundwater flux from Manobalai into Wybong Creek.

	Width of aquifer (m)	Depth of aquifer (m)	Area (m <sup>2</sup> )	K (m s <sup>-1</sup> )	$\delta h$ (m)	$\delta x$ (m)	$v_p$ (m day <sup>-1</sup> )	Q (m <sup>3</sup> day <sup>-1</sup> )	C (mg L <sup>-1</sup> )
Eastern	14	5470	76580	$1.9 \times 10^{-5}$	27.3	2780	$1.6 \times 10^{-3}$	122	4864
Fresh (a)	14	6650	93100	$1.4 \times 10^{-5}$	25.0	500	$5.96 \times 10^{-2}$	5548	1319
Fresh (b)	14	6650	93100	$7.02 \times 10^{-5}$	27.3	2780	$5.96 \times 10^{-2}$	5548	1319

### 2.2.2. Groundwater flux due to increases in hydraulic head

The model written to investigate the possible relationship between the semi-diurnal fluctuations in salinity seen in Wybung Creek (Chapter Two) and daily increases in hydraulic head had two parts. The first part of the model was based on calculations of the amount of groundwater which might be fluxed, and solutes which might be discharged, from Manobalai into Wybung Creek due to increases in hydraulic head. This assumed that the modelled increase in hydraulic head was the same as the maximum daily increase in hydraulic head seen at Site Six, with the resulting quantity of solutes fluxed to Wybung Creek assumed to be the maximum increase in solute flux likely due to daily increases in hydraulic head. Site Six was used as the basis for the model due to smectitic clay preventing flow from sites up-gradient, and Site Six having the largest hydraulic head fluctuations of Sites Six – Eight. Increases in hydraulic head were observed at Sites Six – Eight on the eastern (Manobalai) side of Wybung Creek. Similar changes in hydraulic head were assumed to occur on the western side of Wybung Creek, with groundwater movement assumed to occur by simple Darcian Flow. The quantity of solutes discharged into Wybung Creek from Manobalai as a result of groundwater discharge was (Eqs. 6.4 – 6.6):

$$S = C \times Q \quad (6.4)$$

where  $S$  is the flux of solutes in  $\text{mg day}^{-1}$ ; and  $C$  is the concentration of solutes in the groundwater body ( $\text{mg L}^{-1}$ ) based on solute concentrations at Site Six (Table 6.2). The quantity of groundwater discharged into Wybung Creek ( $Q$ ;  $\text{L day}^{-1}$ ) from Manobalai as a result of increased hydraulic head was calculated using Eq. 6.5:

$$Q = K \times \frac{\partial h}{\partial x} \times W \times H \quad (6.5)$$

where  $Q$  is the discharge of water from aquifers which occur beneath the smectitic clay on the eastern and western side of Wybung Creek ( $\text{m}^3$ ),  $K$  is the hydraulic conductivity based on that at Site Six ( $\text{m s}^{-1}$ );  $\frac{\partial h}{\partial x}$  is the hydraulic gradient running down-hill between Site Six and the 60 km sample site;  $W$  is an assumed aquifer width based on geological structures (i.e. outcrops) at the Manobalai site (m); and  $H$  is the assumed height of the saturated zone in the aquifer (m; Table 6.4).

The second part of this calculation was based on how much saline groundwater would be necessary to cause the diurnal fluctuations in salinity seen in Wybung Creek at the 60 km surface water sample site. The quantity of saline groundwater and the

concentration of saline groundwater needed to increase the concentration of surface water in Wybong Creek by the  $30 \mu\text{S cm}^{-1}$  ( $19.2 \text{ mg L}^{-1}$ ) seen during some months (Chapter Two) was calculated by (Eq. 6.6):

$$C = V \times S \quad (6.6)$$

where  $C$  is the concentration of solutes in Wybong Creek ( $\text{mg L}^{-1}$ ),  $V$  is volume in Wybong Creek based on width, height and length ( $L$ ), and the flux of solutes moving into Wybong Creek is  $S$  in mg (Table 6.4).

### 3. Results and discussion

The following results and discussion are split into three sections. The first focuses on the change in hydraulic heads over time to indicate groundwater connectivity. The second section builds on knowledge deduced using hydraulic head information but uses groundwater chemistry in order to elucidate groundwater connectivity. Modelling of groundwater fluxes from Manobalai is discussed finally. The full suite of hydrochemical data for these analyses is presented as part of the Appendix for Chapter Three (Tables A3.3 – A3.6), with EC, temperature and hydraulic head data compiled on the accompanying DVD.

#### 3.1. Hydraulic head changes

Seven day groundwater hydrographs are presented for different sites at different times in the following discussion, with hydraulic head and at times EC and temperature measured by instruments every four hours. Groundwater hydrographs showed hydraulic head increased and decreased regularly throughout the day in most piezometers and bores installed at Manobalai. Regular hydraulic head changes were up to 23 mm in Site Two Shallow, though Site Three also increased by up to 60 mm on one day (Figure 6.2). Rainfall was not recorded at the Scone SCS weather station during this period.

Table 6.4. Parameters used for the modelling the flux of groundwater from Site Six at Manobalai into Wybong Creek based on fluctuations in hydraulic head.

Parameter	Value
$C_{\text{Site Six}} (\text{TDS mg L}^{-1})$	1721
$C_{60 \text{ km sample point}} (\text{TDS mg L}^{-1})$	19.2
$L (\text{m})$	5 470
$H (\text{m})$	0.017
$W (\text{m})$	18.974
$\delta h (\text{m})$	3.5
$\delta x (\text{m})$	1300
$K (\text{m day}^{-1})$	78.62

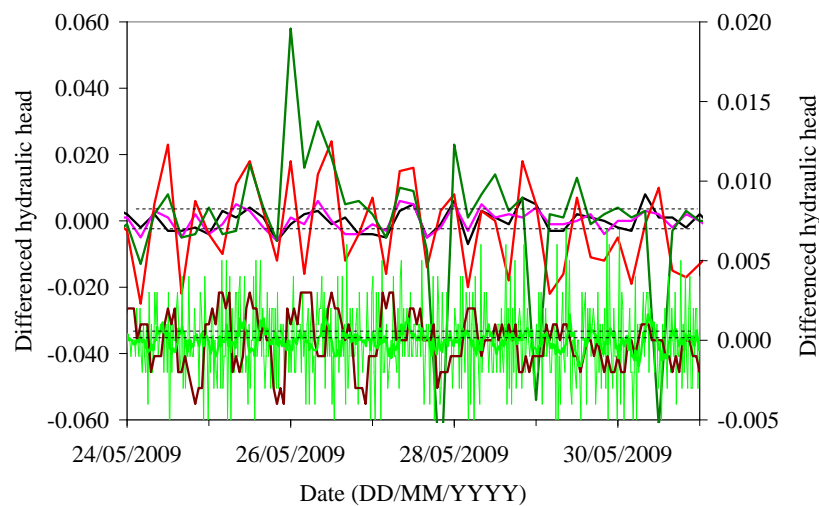


Figure 6.2. Differenced (height at time two – height at time one) groundwater height (AHD) in Site Two Shallow (1° axis; —); Site Three (1° axis; —); Site Eight Shallow (1° axis; —); Site Eight Fractured (1° axis; —); Site Six (2° axis; —); and Hannah’s (2° axis; —), from the 20<sup>th</sup> August to the 27<sup>th</sup> August 2008. Dashed lines indicate the maximum error ( $\pm 0.05\%$ ) on groundwater depth measurements by the Schumberger pressure transducers.

Hydraulic head at Sites Eight Shallow and Eight Fractured fluctuated similarly to Sites Two and Three. Site Six hydraulic head fluctuations were greater than at any other sites monitored, but had a similar seven-point moving average to the hydraulic head seen in piezometers at Site Eight. The changes in hydraulic head at Hannah’s were instead of different periodicity to that seen at other sites. Piezometers at Manobalai were screened into a range of differing substrates, with Sites Eight Shallow and Six screened into smectitic clay; Eight Fractured and Hannah’s into fractured Widden Brook Conglomerate; Site Three into colluvium; and Site Two Shallow into the Manobalai Alluvium (Chapter Five).

The simultaneous increases in hydraulic head measured at Manobalai indicate increased pressure on the aquifers (e.g. Domenico and Schwartz 1990). The increase in pressure at one point would instead cause pressure waves, which would transmit through the aquifers and cause increases in hydraulic head as pressure was dissipated from the source of recharge and/or loading where it originated (e.g., Hegge and Masselink 1991; Timms and Acworth 2005; Xia *et al.* 2007). The similar periodicity and the lack of phase lag between hydraulic head fluctuations at different sites indicates that the aquifers into which these piezometers were screened were all responding to an increase in hydraulic pressure independently of each other, with the cyclical nature of these pressure changes implying that they were caused by loading and unloading of the aquifer. Differences in the elasticity and porosity of aquifer materials, and therefore their response to loading and unloading, is likely causing the differences in the

amplitude of the hydraulic head changes seen at different sites within Manobalai (e.g. Domenico and Schwartz 1990).

Hannah's bore, located adjacent to the piezometer at Site Seven, was screened into fractured conglomerate similar to Site Eight Fractured. Hydraulic head fluctuated differently at these sites, however, with differences occurring both in periodicity and amplitude (Figure 6.2). The response of hydraulic head to pressure changes in fractured aquifers is dependent on fracture geometry (Burbey 2009). The difference in amplitude of the hydraulic head increases and decreases at these sites shows that fractures respond differently to loading, with different fracture geometries occurring. This then implies groundwater at Site Eight Fractured and Hannah's is acquired from different fractures which also have differing hydraulic heads (Cook 1999). Fractures appear to be unconnected within the Narrabeen Group, therefore, with limited and unpredictable groundwater connectivity within this aquifer. Differences in periodicity are more difficult to explain, but may indicate differing and/or interfering phase-lags as a result of differing fracture geometry (Burbey 2009).

Hydraulic head fluctuations in most of the bores and piezometers installed in the alluvium of Sites One – Four were similar in both periodicity and amplitude. Site One showed a smaller degree of groundwater height fluctuations than Site Two Deep for the period it was monitored (July 2008 – December 2008), but fluctuated with similar periodicity. Hydraulic head in Site Two Shallow was similar to that in Site Two Deep, while Site Three was not clearly similar or dissimilar to either (Figure 6.3). Hydraulic head in Sites Four and One were not monitored at this time. The similarity periodicity by which hydraulic head at these sites fluctuated again indicates a similar response to external loading, while differences in amplitude are instead related to the degree to which groundwater is confined at these sites (Acworth and Brain 2008).

The fluctuations in hydraulic head observed at Sites Two Shallow and Four were anti-correlated (Figure 6.3). Changes in hydraulic head due to point source recharge (e.g. Timms and Acworth 2005), or presumably loading, can propagate to other sites within the same aquifer. A change in phase and amplitude of the pressure wave that results from loading and/or recharge occurs with distance and time, and can cause phase lag relationships such as that seen between Site Two Shallow and Site Four. The pressure changes may also be caused by pressure changes being propagated to Site Four from neighbouring aquifers, with the similar periodicity at other sites but phase lags at Site Four indicating wave propagation by a similar force that is farther away.

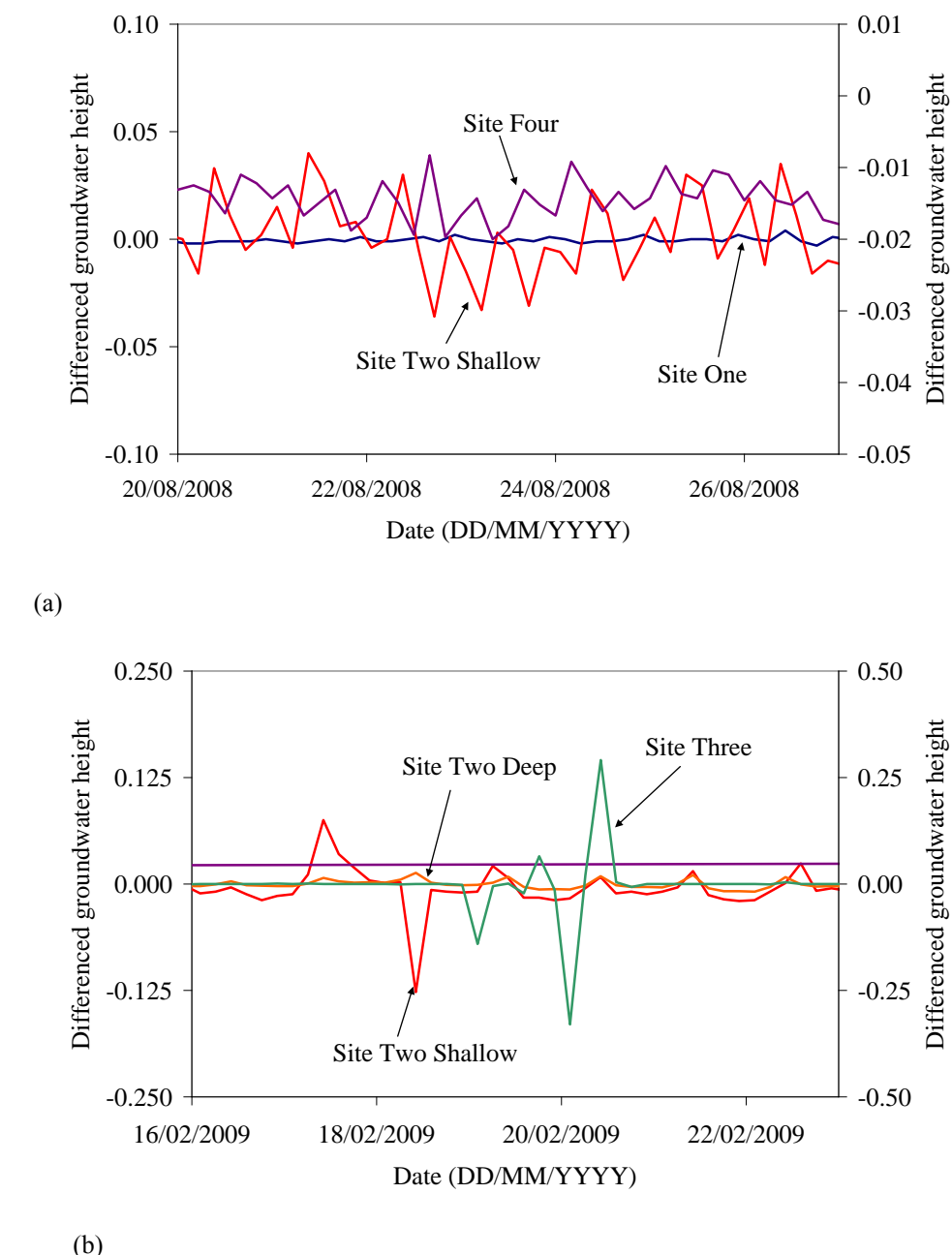


Figure 6.3. Differenced groundwater height (height at time two – height at time one) in Site One ( $1^{\circ}$  axis; blue); Site Two Deep ( $2^{\circ}$  axis; orange); Site Two Shallow ( $1^{\circ}$  axis; red); Site Three ( $2^{\circ}$  axis; green); and Site Four ( $1^{\circ}$  axis; purple), from (a) the 20<sup>th</sup> August to the 27<sup>th</sup> August 2008; and (b) the 16<sup>th</sup> to the 23<sup>rd</sup> February 2009.

The regularity with which hydraulic heads fluctuated at Manobalai indicates that fluctuations were related to a phenomenon or phenomena which affect aquifers every day and with regularity. The gravitational pull of the moon and sun regularly increases and decreases every day, and causes changes in hydraulic head due to a phenomenon termed Earth tides (e.g. Bredehoeft 1967; Burbey 2009), with changes in air pressure (barometric tides) giving rise to similar changes (Domenico and Schwartz 1990). Changes in hydraulic heads as a result of barometric and Earth tides are greatest in fractured aquifers or aquifers confined by plastic clays, due to these materials being

relatively elastic and compressible, with changes in groundwater height occurring when an undrained and confined aquifer is loaded and unloaded (Burbey 2009; Domenico and Schwartz 1990). The possible relationship between Earth Tides, air pressure and aquifers at Manobalai was investigated using the changes in hydraulic head at Site Eight as an example.

Both air pressure and Earth tides can be related to the changes in hydraulic head seen in Site Eight Shallow, but seem less clearly related to the same changes in Site Eight Fractured (Figure 6.4). Hydraulic head at both sites gradually moved out of phase with both air pressure and Earth tides, however, with a good initial correlation which gradually became less well correlated over time. Such phase shifts are known to occur in fractured rock aquifers and are possibly related to the dip and strike of the rock fracture and/or fracture transmissivity and fracture length (Burbey 2009). No clear relationship was identified between air pressure, hydraulic head, and gravity using spectral analyses (Appendix Six: Figure A6.3); nor was any relationship seen between groundwater temperature and hydraulic head (Figure 6.5). The relationship between tides and hydraulic head is questionable, therefore, with more in depth analyses using longer time periods likely required for conclusive results. The changes in hydraulic head are cyclical and must be related to some phenomena which affects the aquifer in a similar cyclical fashion, however, with groundwater pumping discounted as a cause as it does not occur in this area. While the cause of the rhythmic fluctuations in hydraulic head cannot be elucidated, the response of these aquifers to loading and unloading indicates both the Manobalai Alluvium and fractured Narrabeen Group are confined aquifers with undrained boundary conditions, where the increased pressure caused by loading is not dissipated through the aquifer but instead causes groundwater to rise within bores and piezometers.

Increases in hydraulic head were seen at all Manobalai piezometer sites after rainfall, with the exception of Sites Five and Seven where water was never detected. The hydraulic head in Hannah's groundwater monitoring bore (Site Seven), which yielded saline water and was screened into fractured Widden Brook Conglomerate, increased by 40 mm on the day of the rainfall event of 6<sup>th</sup> June 2007 (Figure 6.6). Groundwater height in Eight Shallow responded with an increase of 47 mm; Site Eight Fractured 41 mm; Site Three 30 mm; and Site Two Shallow 210 mm, on the day of and the days following the 26 mm rainfall event recorded at the Scone SCS weather station on the 22<sup>nd</sup> June 2009 (Figure 6.6 – 6.7). A statistically significant relationship between increased hydraulic head and rainfall was identified using cross-correlation analysis,

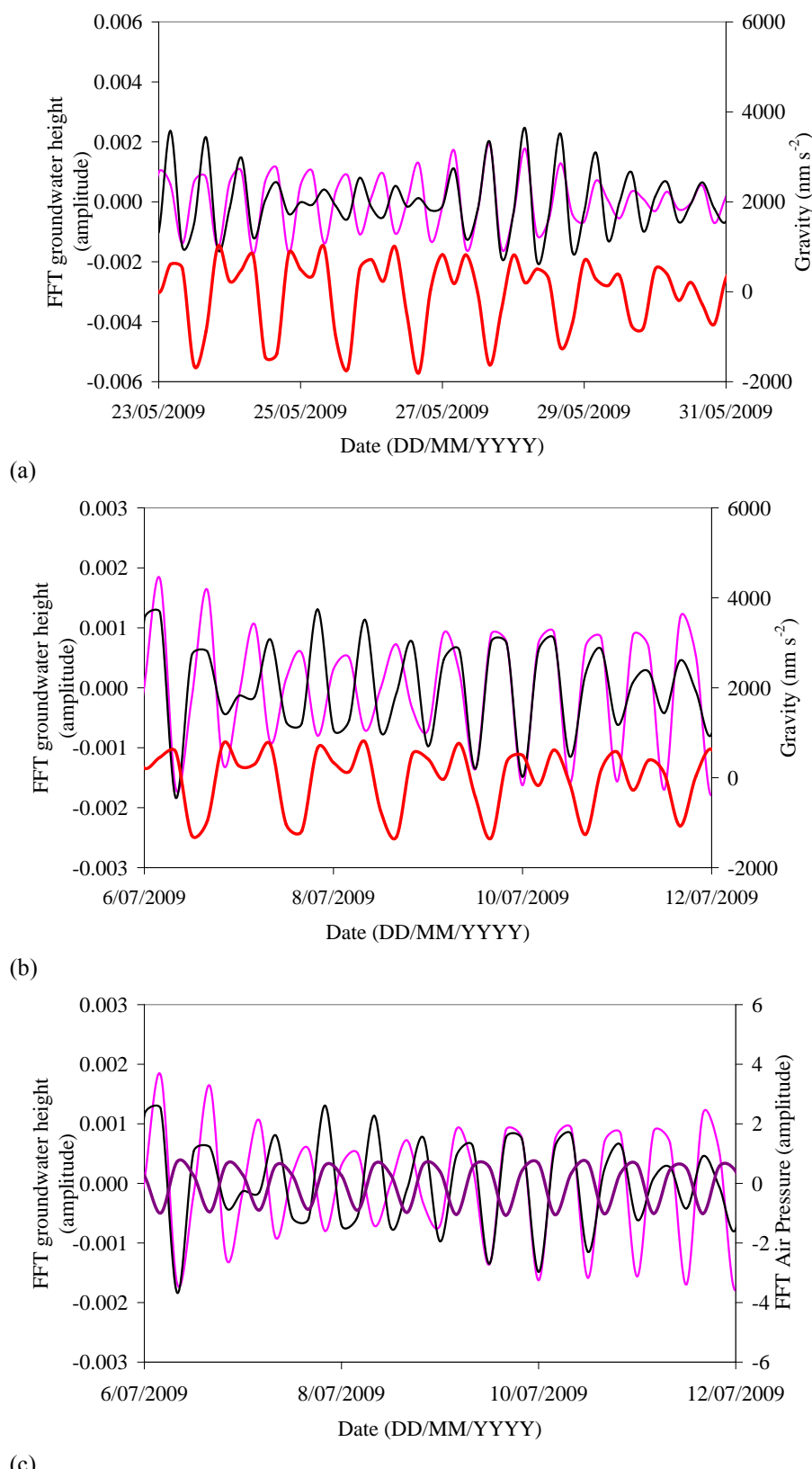


Figure 6.4. Relationships between hydraulic head at Site Eight Shallow (—, AHD); Site Eight Fractured (—, AHD); and theoretical gravity (—, nm s<sup>-2</sup>), and air pressure at Site Five (—, hPa) during (a) May 2009; and (b – c) July 2009, where FFT indicates data was fast Fourier transformed.

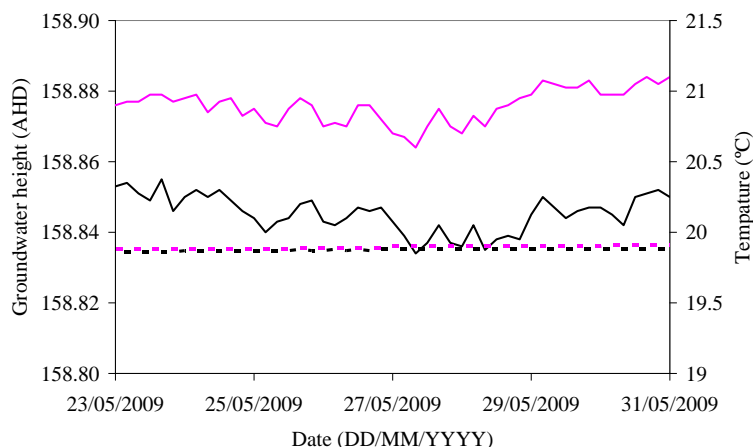


Figure 6.5. Relationships between hydraulic head at Site Eight Shallow (—, AHD), Site Eight Fractured (—, AHD), and and temperature (---) at those sites.

with increases at Sites Two Shallow and Deep occurring 20 and 16 days after rainfall respectively (Figure 6.5; Appendix Six: Tables A6.4 – A6.5). This time lag difference between hydraulic head increases and rainfall at the piezometer/bore nest at Site Two is evidence for differing groundwater flow paths within the regolith. The absence of groundwater in piezometers at Sites Seven and Five instead indicates that rainwater infiltration was not sufficient to cause a detectable increase in groundwater height at these sites, while the increase in hydraulic head above the amount received via rainfall at all other Manobalai sites indicates some combination of direct infiltration by rainwater and lateral groundwater flow.

The different responses of hydraulic heads to rainfall indicate complex flow paths at the Manobalai field site, making the relationship between groundwater height and rainfall difficult to predict. The occurrence of summer-dominated rainfall which is often observed as highly isolated thunderstorms in the Wybung Creek catchment further complicates the delineation of rainfall-recharge relationships. The rapid response of hydraulic head to rainfall does indicate that aquifers are at least partially unconfined, however, and that some degree of localised recharge therefore occurs for both the Manobalai Alluvium and Fractured Narrabeen Group aquifers (Love *et al.* 1993). Results presented here are only preliminary, with groundwater hydrographs covering a number of years necessary to statistically constrain the relationship between rainfall and groundwater recharge (Von Asmuth and Knotters 2004).

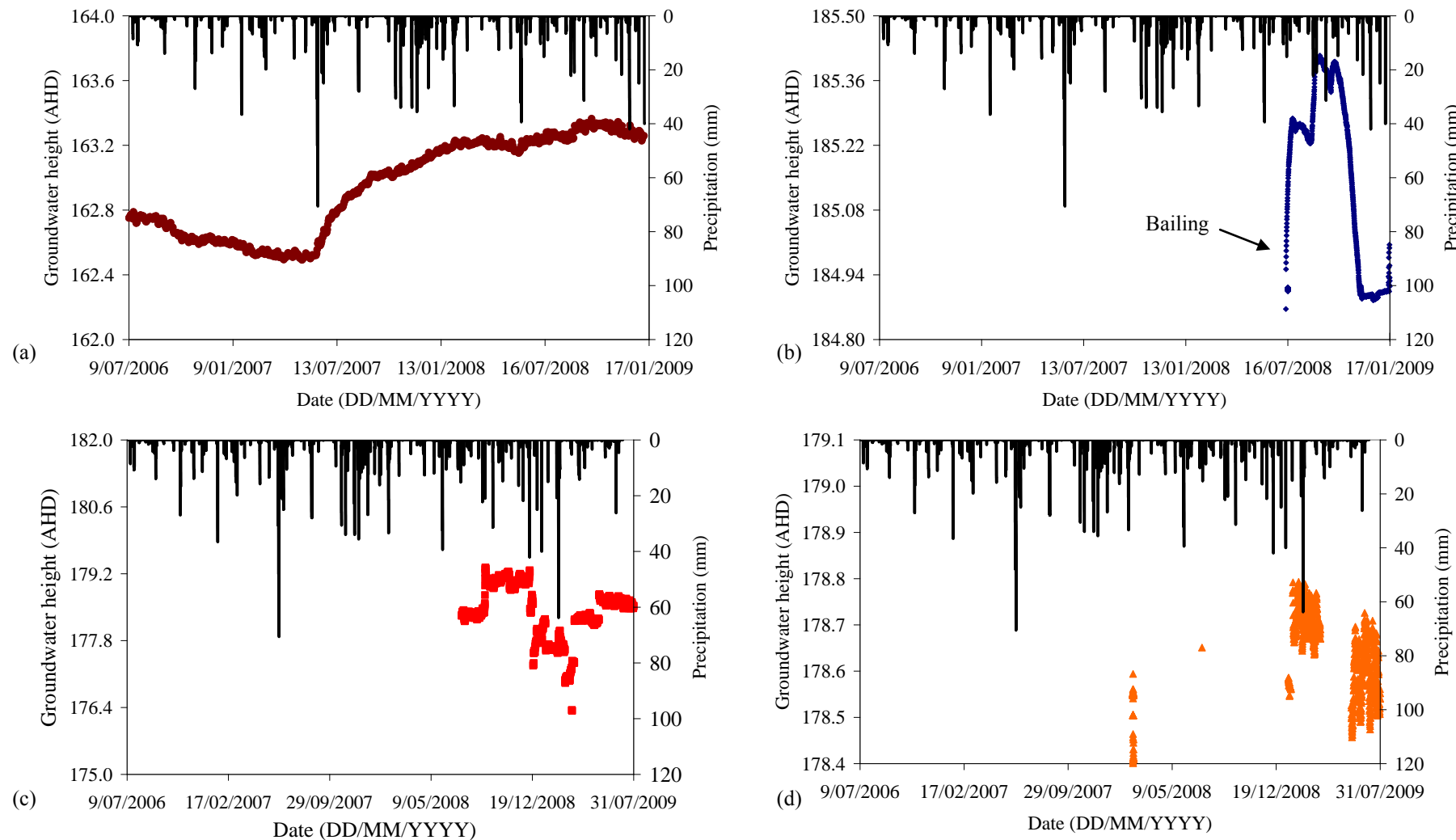


Figure 6.6.

Precipitation at Scone SCS weather station (—) and hydraulic head (Australian height datum) in: (a) Hannah's bore (Fractured Widden Brook Conglomerate; ●); (b) Site One (alluvium; ◆); (c) Site Two Shallow (alluvium; ■); (d) and Site Two Deep (alluvium; ▲). Bailing indicates an increase in groundwater height after purging.

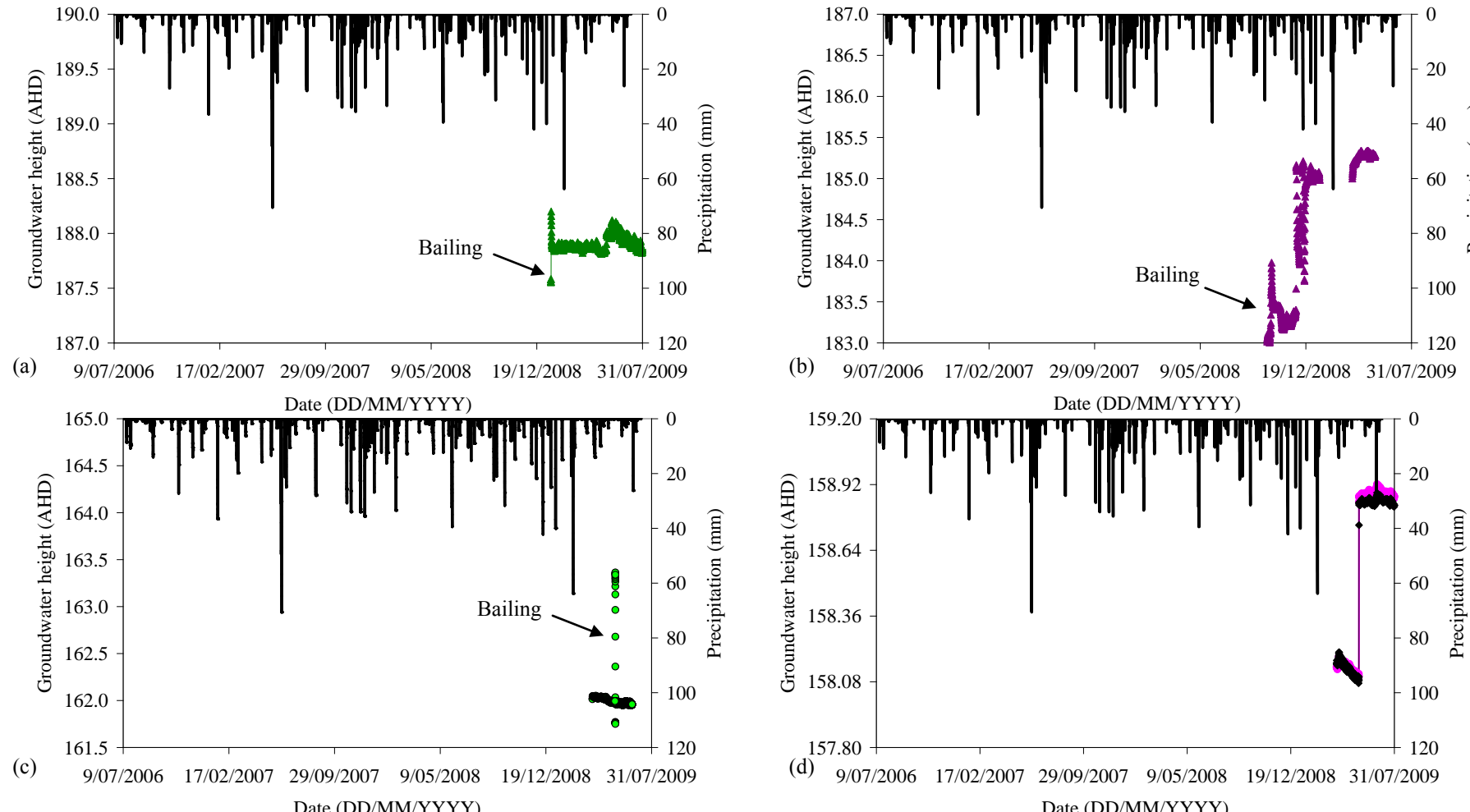


Figure 6.7.

Precipitation at Scone SCS weather station (—) and hydraulic head (Australian height datum) in bores and piezometers at: (a) Site Three (Alluvium; ▲); (b) Site Four (Alluvium; ▲); (c) Site Six (Fractured Narrabeen Group; ●); and (d) Site Eight Fractured (Narrabeen Group; ○) and Shallow (●). Bailing indicates an increase in groundwater height after purging.

Lateral and vertical differences in hydraulic conductivity and/or permeability in aquifer materials indicate anisotropic and/or heterogenous conditions, with anisotropy causing unpredictable vertical groundwater flow within an aquifer (Freeze and Cherry 1979). Some degree of anisotropy with the unconsolidated material at Manobalai has already been identified (Chapter Five), with the smectitic clay above the fractured Narrabeen Group at Sites Six – Eight preventing the horizontal flow of groundwater from the sandy-clay alluvium at Sites One – Five to Wybong Creek. Hydraulic conductivity values also reflected complex flow conditions within Sites One – Five, with hydraulic conductivity in the Site Two Shallow piezometer an order of magnitude faster than the Site Two Deep bore, despite both being screened into what was initially thought to be the same perched aquifer at 6 – 8 m depth (Table 6.5). Static water levels in the Site Two Deep bore and Site Two Shallow piezometer were both higher and lower relative to each other on different dates (Figure 6.8), and almost certainly indicate anisotropy within the aquifer (Domenico and Schwartz 1990).

This anisotropy makes the delineation of groundwater flow paths within the Manobalai field site difficult without groundwater chemistry, with the the degree of heterogeneity and anisotropy at Manobalai difficult to parameterise. Geophysical analyses using techniques such as gamma ray and direct-push EC logging of the holes into which piezometers and bores were sunk at these sites would clearly enable a better understanding of aquifer properties at Manobalai (e.g. Burbey 2009; Brauchler *et al.* 2010). The limited time over which hydraulic head data was collected from sites, the coarse resolution of aquifer materials due to limited regolith sampling, the poor spatial resolution of data due to equipment failure, and the limited number of instruments, also restricts further understanding of aquifer properties at Manobalai using hydraulic head data. Important information can be ascertained using groundwater chemistry, however, which will now be discussed.

### 3.2. Groundwater chemistry

Groundwater chemistry changed abruptly along the 2.2 km transect from Site Four to Site Eight, with increases in salinity from Site Four to Two (Figure 6.8a), decreases between Site Two and Six, increases again to Hannah's Bore, and decreases to Site Eight (Chapter Five). Differences in groundwater salinity between Sites Two and Six occur due to smectitic clay causing a lack of hydraulic connectivity and preventing flow between these sites (Chapter Five). Research presented in this chapter has shown

Table 6.5. Hydraulic conductivity ( $K$ ) measured in bores and piezometers at the Manobalai field site using the Bouwer and Rice slug test (Bouwer 1989). <sup>+</sup> Information sourced from Weight and Sonderegger (2000). Hydraulic conductivity for Sites Five and Seven were not able to be calculated due to the absence of groundwater at these sites. \*Static water level in this piezometer was below the piezometer screen, with  $K$  in this case an (over) estimate of actual  $K$ . Parameters for the calculation of hydraulic conductivity can be found in Tables A6.1 – A6.3. Bore logs for the material extracted to install these bores and piezometers occur in Chapter Five (Figure 5.6).

Site	Date (DD/MM/YYYY)	$K$ (m s <sup>-1</sup> )	(m day <sup>-1</sup> )	Hydraulic conductivity within the range of:	
				Unconsolidated material <sup>+</sup>	Consolidated material <sup>+</sup>
One	14/07/2008	$4.1 \times 10^{-8}$	0.0036	Clay	Shale, siltstone, sandstone, unfractured basalt
Two Deep	14/07/2008	$1.3 \times 10^{-9}$	0.0001	Clay	Shale, siltstone, unfractured basalt
	17/01/2009	$7.6 \times 10^{-6}$	0.6525	Silt/sand	Sandstone, fractured basalt
Two Shallow	14/07/2008	$2.8 \times 10^{-7}$	0.0241	Clay	Shale, siltstone, sandstone, unfractured basalt
	17/01/2009	$7.4 \times 10^{-5}$	6.3644	Silt/sand	Sandstone, fractured basalt
*Three	14/07/2008	$1.1 \times 10^{-7}$	0.0093	Silt	Unfractured basalt,
	17/01/2009	$1.9 \times 10^{-5}$	1.6588	Silt/sand	Sandstone, fractured basalt
Four	14/07/2008	$1.5 \times 10^{-9}$	0.0001	Clay	Shale, siltstone, unfractured basalt
	17/01/2009	$1.4 \times 10^{-5}$	1.1978	Silt/sand	Sandstone, fractured basalt
Six	14/05/2009	$9.1 \times 10^{-4}$	78.9986	Sand	Sandstone
Eight Shallow	14/05/2009	$1.6 \times 10^{-6}$	0.1407	Silt/Clay	Sandstone
Eight Fractured	14/05/2009	$1.0 \times 10^{-5}$	0.8690	Sand/Silt	Sandstone

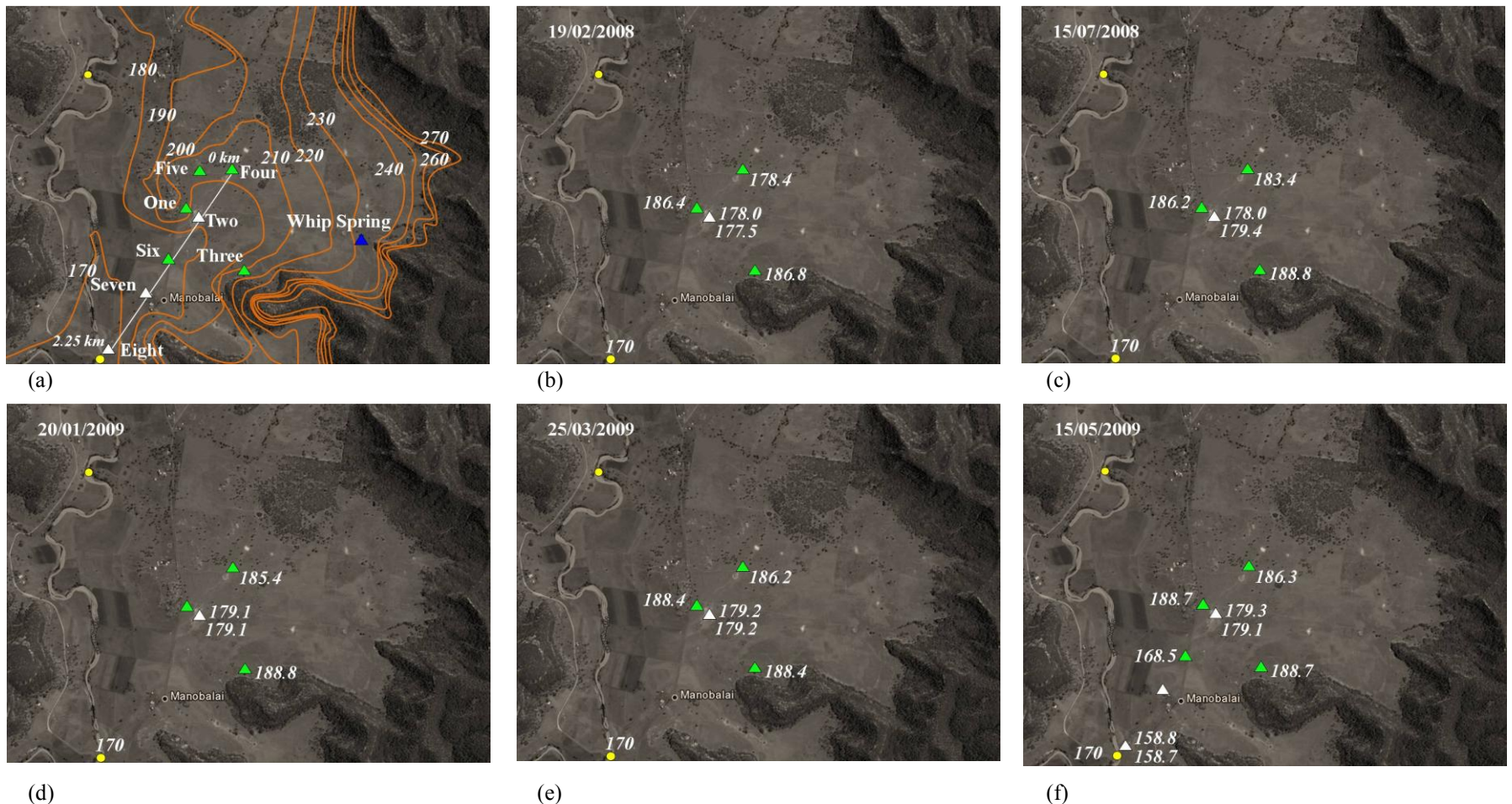


Figure 6.8. (a) Topographic contours at the Manobalai field site (AHD); and hydraulic head (AHD) from recovered bores piezometers at the Manobalai field site on (b) 19/02/2008; (c) 15/07/2008; (d) 20/01/2009; (e) 25/03/2009; and (f) 15/05/2009. Symbols indicate nested piezometers and/or bores ( $\Delta$ ), single piezometers/bores ( $\blacktriangle$ ), and surface water sample sites ( $\circ$ ).

that differences between Hannah's and Site Eight can instead be attributed to a lack of hydraulic connectivity between fractures. Differences in groundwater chemistry between bores and piezometers screened into the same aquifer, such as Sites Two and Four, however, may also be explained by a lack of groundwater connectivity. Differences in salinity at these and other sites are also likely due to the mixing of groundwater bodies (e.g., Tweed *et al.* 2005), localised recharge of aquifers (e.g., Love *et al.* 1993), and/or a lack of hydraulic connectivity, with evidence for each of these addressed in the following discussion.

Similar ion and Sr isotope chemistry was seen in groundwater sampled from Sites Two, Three, and Hannah's. This indicates that groundwater at these sites acquires solutes from a similar source and may therefore be connected in some way (Table 6.6; Figure 6.9), with this solute source likely to be the Wittingham Coal Measures which lie >300 m below Manobalai (Chapter Four). Ratios of  $^{87}\text{Sr}/^{86}\text{Sr}$  in groundwater from Sites Six and Eight Fractured similarly indicated groundwater connectivity and/or a similar source of solutes for these sites (Figure 6.9). Ratios of  $\delta^{18}\text{O}$  indicated differing degrees of evaporation despite similar solute sources, however, with this in turn indicating differing flow paths (Bullen and Kendall 1998). Groundwater from Site Two Deep and Hannah's had the most similar  $\delta^{18}\text{O}$  of groundwater sampled from Manobalai. Groundwater at Sites Six and Eight Shallow was also similar. The variation in  $\delta^{18}\text{O}$  despite similar  $^{87}\text{Sr}/^{86}\text{Sr}$  in most groundwater sampled from Manobalai indicates that many different flow paths exist for groundwater sampled from the site, despite a similar source of solutes.

A large spatial variability in groundwater chemistry can indicate differing degrees of local recharge, whereby existing saline water is diluted by rainfall to differing degrees (e.g., Love *et al.* 1993). The variation in TDS independent of ion proportions and isotopes in most groundwater sampled from Manobalai probably indicates that the saline groundwater discharging into Manobalai is diluted to differing degrees by rainwater within the fractured Narrabeen Group and Manobalai Alluvium. Ion ratios and  $^{87}\text{Sr}/^{86}\text{Sr}$  signatures of this saline groundwater would remain unaltered if low concentration of ions occurred in the diluting water, as occurs with rainfall. This explains the occurrence of fresh but Na-Cl dominated groundwater at Sites Four and Whip Well, with solutes in this Na-Cl dominated groundwater not sourced from silicate weathering of the alluvium at these sites, nor from direct rain accession (Table 6.6).

Table 6.6. Groundwater chemistry and static water level (SWL) within bores and piezometers, the groundwater monitoring bore Hannah's, and the Whip Well spring at the Manobalai field site. N/A indicates that the sample was not analysed for the indicated parameter.

Site	Date	SWL (AHD)	TDS (mg L <sup>-1</sup> )	Na (mg L <sup>-1</sup> )	Ca (mg L <sup>-1</sup> )	Mg (mg L <sup>-1</sup> )	K (mg L <sup>-1</sup> )	Cl (mg L <sup>-1</sup> )	SO <sub>4</sub> (mg L <sup>-1</sup> )	HCO <sub>3</sub> (mg L <sup>-1</sup> )	Na/Cl (molar)	<sup>87</sup> Sr/ <sup>86</sup> Sr
Whip Well One	26/03/09	224.0	223	66	5	7.4	3.7	88	19	43	1.1	0.709446
	19/02/08	186.4	1452	430	32	31	2.8	610	35	295	1.0	0.708440
	15/07/08	186.2	912	260	15	22	3.1	340	24	237	1.1	N/A
Two Shallow	19/02/08	178.0	6247	1500	230	550	37	2700	350	851	0.8	0.707121
	15/07/08	178.0	5540	1200	210	400	28	2800	170	710	0.6	N/A
	20/01/09	179.1	6960	1460	260	520	34	3600	200	861	0.6	N/A
	25/03/09	179.2	N/A	N/A	N/A	N/A	N/A	N/A	N/A	N/A	N/A	N/A
	15/05/09	179.3	N/A	N/A	N/A	N/A	N/A	N/A	N/A	N/A	N/A	N/A
	19/02/08	177.5	5327	1100	190	400	27	2800	160	624	0.6	0.707174
Two Deep	15/07/08	179.4	4463	920	170	350	23	2300	120	553	0.6	N/A
	20/01/09	179.1	7277	1520	240	550	40	3800	154	946	0.6	N/A
	25/03/09	179.2	N/A	N/A	N/A	N/A	N/A	N/A	N/A	N/A	N/A	N/A
	15/05/09	179.1	N/A	N/A	N/A	N/A	N/A	N/A	N/A	N/A	N/A	N/A
	19/02/08	186.8	4573	1400	50	200	32	2701	1.5	135	0.7	0.708740
Three	16/07/08	188.8	4750	1400	47	190	31	2700	15	135	0.7	0.708712
	20/01/09	188.8	N/A	N/A	N/A	N/A	N/A	N/A	N/A	N/A	N/A	N/A
	25/03/09	188.4	N/A	N/A	N/A	N/A	N/A	N/A	N/A	N/A	N/A	N/A
	15/05/09	188.7	N/A	N/A	N/A	N/A	N/A	N/A	N/A	N/A	N/A	N/A
	19/02/08	178.4	105	17	3.8	3.3	8.9	22	18	28	1.1	0.708779
Four	16/07/08	183.4	366	84	4.2	9.5	6.0	95	31	115	1.3	N/A
	20/01/09	185.4	239	44	2.8	8.8	8.2	26	8.0	137	2.4	N/A
	25/03/09	186.2	N/A	N/A	N/A	N/A	N/A	N/A	N/A	N/A	N/A	N/A
	15/05/09	186.3	N/A	N/A	N/A	N/A	N/A	N/A	N/A	N/A	N/A	N/A
	22/07/06	167.4	5204	1450	73	253	32	2629	17	742	0.8	N/A
Hannah's	16/07/08	162.8	6130	1700	65	350	41	3300	42	601	0.7	0.708303
	15/05/09	168.5	1721	395	39	85	12	684	68	413	0.9	0.704696
Eight Shallow	15/05/09	158.8	2712	597	106	158	11	1219	83	509	0.8	0.707249
Eight Fractured	15/05/09	158.7	2477	513	109	154	10	1058	103	505	0.8	0.704959

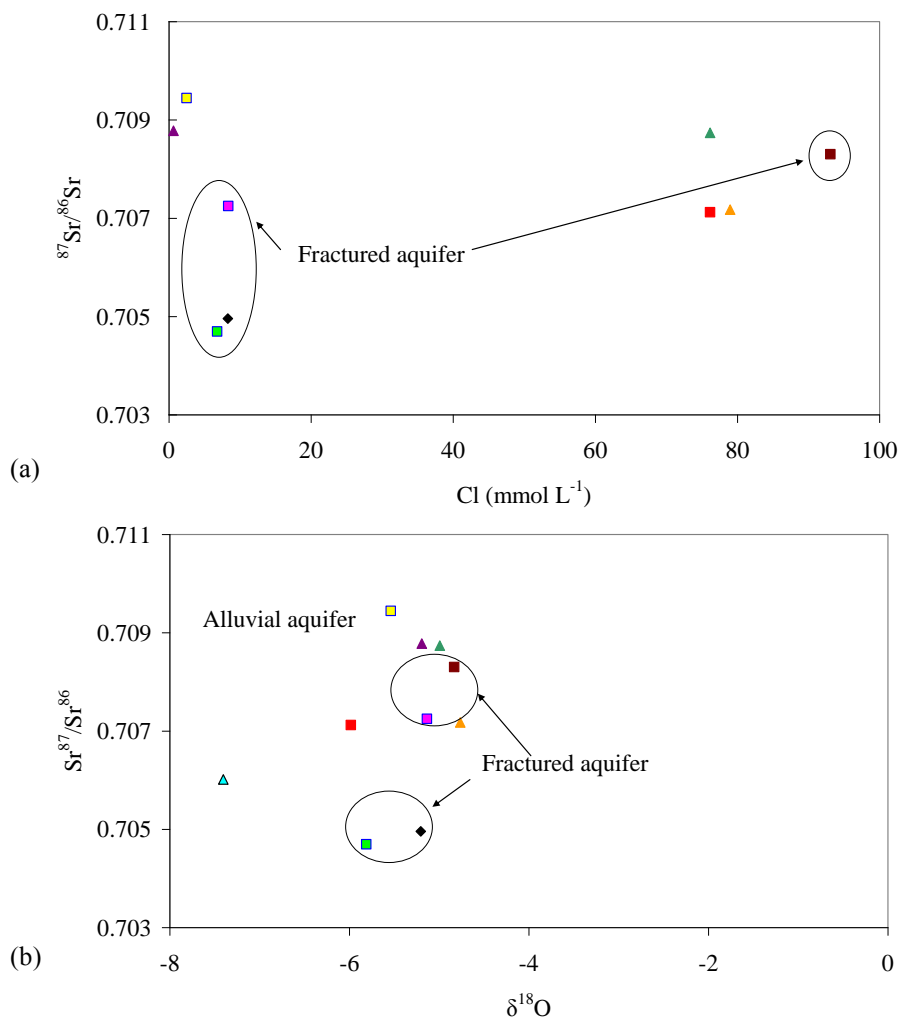


Figure 6.9. (a)  $^{87}\text{Sr}/^{86}\text{Sr}$  vs  $\text{Cl} (\text{mmol L}^{-1})$ ; and (b)  $^{87}\text{Sr}/^{86}\text{Sr}$  versus  $\delta^{18}\text{O}$  for groundwater sampled from Manobalai. Symbols indicate Sites Two Shallow (■); Two Deep (▲); Three (▲); Four (▲); Hannah's (■); Six (□); Eight Shallow (◆); Eight Fractured (■); and Whip Well (□).

Groundwater chemistry is highly variable in younger waters, but becomes increasingly stable as groundwater evolves along a flow path (Stuyfzand 1998). Molar Na/Cl ratios were the same for Sites Three and Two Deep on all dates that groundwater was sampled, with Two Shallow being the same on two of three dates sampled (Table 6.7). The much fresher water at Site Four had different Na/Cl ratios on each sample date, ranging from 1.1 – 2.4, indicating water at this site was either much less chemically evolved than that at Sites Two and Three and/or underwent differing degrees of mixing with locally recharging groundwater on different sample dates. Sites Six, Eight, Hannah's and Whip Well were not sampled regularly enough to ascertain temporal variability. Salinity was highest in groundwater from Sites Two Deep, Shallow, and Hannah's on the last sampling date, though no clear trend could be identified with only three sampling dates. A continuing trend of saline groundwater at Sites Two, Three, and Hannah's indicates that groundwater at these sites is likely to be

largely older and regionally discharging groundwater as opposed to the local and younger groundwater at Whip Well and Site Four. Carbon-14 dates attained for Sites Two Shallow and Three indicate that groundwater recharged 1300 and 410 years before present, while that at Site Four recharged 1170 years before present (Appendix Three: Table A3.6). No clear difference occurs in the age or degree of local versus regional discharge of saline and fresh groundwater at Manobalai based on these  $^{14}\text{C}$  results. The accurate dating of groundwater, however, requires knowledge of fracture geometry, and the use of other geochemical tracers such as  $^3\text{H}$  and  $^{36}\text{Cl}$  to calibrate  $^{14}\text{C}$  dates (Cook 1999). Further research utilising a range of these techniques is therefore required in order to constrain groundwater ages and evolution properly, while continued sampling of groundwater from these sites is also necessary to identify trends of increasing or decreasing salinity.

Temporal variation in EC was monitored using data loggers at Sites Eight Fractured and Shallow from March – May 2009, and at Sites Two Deep and Shallow from May 2009 – August 2009, in order to understand salinity dynamics at these sites. The EC of groundwater in the Site Eight Fractured piezometer increased by  $776 \mu\text{S cm}^{-1}$  for nine days after this piezometer was purged, before plateauing and slowly decreasing with some small EC fluctuations (Figure 6.10). A similar pattern was seen in the Site Two Deep piezometer, where EC gradually increased by  $520 \mu\text{S cm}^{-1}$  for 18 days after it was purged, before plateauing. Electrical conductivity instead increased more gradually after purging of the piezometer at Site Eight Shallow where salinity increased from  $4020 \mu\text{S cm}^{-1}$  up to  $4220 \mu\text{S cm}^{-1}$ , while EC at Site Two Shallow instead fluctuated between  $11\,340 - 11\,980 \mu\text{S cm}^{-1}$  every five to 11 days from May – August 2009. The gradual increase in salinity at Sites Two Deep and Eight Fractured implies recharge from both saline and fresh groundwater bodies, with the fresher groundwater body initially influencing the bore and piezometer. A saline groundwater body then appears to be increasingly influential over time, with the more dense saline water sinking to the bottom of the piezometer where the CTD instruments measured EC, temperature and depth. The more than  $600 \mu\text{S cm}^{-1}$  fluctuation in the Site Two piezometer is more difficult to explain, with changes in salinity independent of rainfall (Figure 6.10). Such patterns may be expected if locally recharging groundwater arrived at Site Two Shallow via different flow paths, with this indicated by research presented. Some flow paths would be longer and others shorter, with this resulting in differing levels of dilution at Site Two on different days as seen here. It is clear from all the data presented in this chapter that salinity is highly dynamic at the Manobalai site. Bores and piezometers

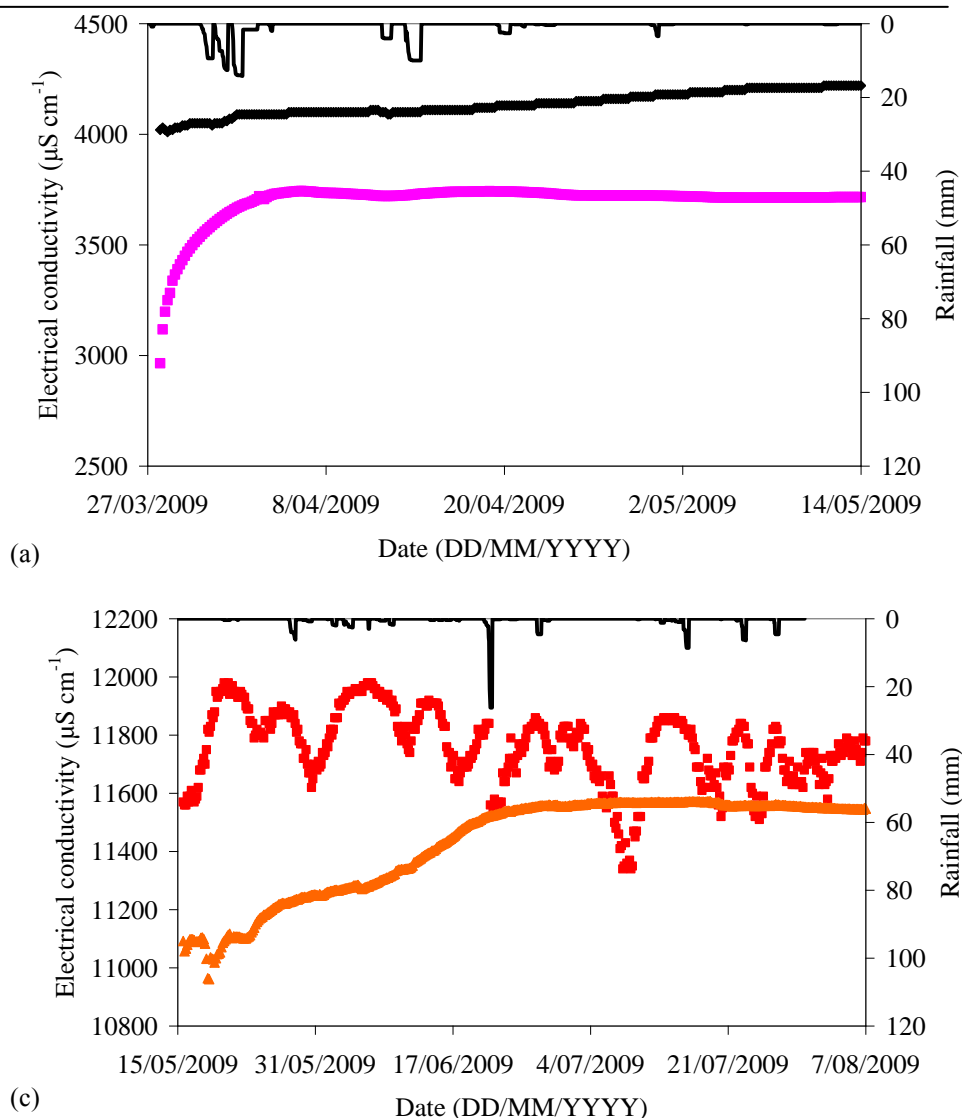


Figure 6.10. (a) Electrical conductivity ( $\mu\text{S cm}^{-1}$ ) in Sites Eight Shallow (◆) and Fractured (■) piezometers in relation to precipitation ( $2^\circ$  axis) between 27/03/2009 – 14/05/2009; and (b) Electrical conductivity in Sites Two Deep (▲) and Shallow (■) in relation to precipitation between 15/05/2009 – 07/08/2009.

were sampled as often as every three months and usually every six months for two years (Table 6.6). Salinity within these sites varied on a day to day basis, however, with much more frequent sampling, using conservative tracers such as isotopes and/or dyes, necessary to understand the complex groundwater flow that occurs.

### 3.3. Surface – groundwater connectivity

Wybong Creek salinity changes from being Na-Mg-HCO<sub>3</sub> to Na-Mg-Cl dominated adjacent to the Manobalai field site, with both flow and solute concentrations increasing along this stretch of the river. Regular fluctuations in Wybong Creek salinity were also recorded adjacent to Manobalai during September, October and November 2007, and in May 2009, with salinity increases and decreases of up to 350  $\mu\text{S cm}^{-1}$  occurring approximately daily (Chapter Two). Salinity fluctuations were hypothesised

as being related to a saline confined aquifer adjacent to the Creek, which was also thought to give rise to the overall increase in salinity and chlorinity between the 55 and 60 km sample sites. Hydraulic head in piezometers screened into saline groundwater bodies presented in this chapter showed similar fluctuations. This suggests that salinity fluctuations in Wybung Creek are a result of Earth tides, which cause changes in the volume of saline groundwater discharged directly into the Creek from a confined aquifer below. Smectitic clay prevents the flow of groundwater from Sites One – Five to Wybung Creek (Chapter Five), and confines the Narrabeen Group aquifer at Sites Six – Eight. Groundwater hydrographs from Sites Six – Eight were therefore selected to investigate the relationship between hydraulic head fluctuations and Wybung Creek salinity, with the maximum depth of piezometers at these Sites at least two metres above the Creek bed.

### 3.3.1. Groundwater flux from Manobalai

Total dissolved solids increased by  $7.96 \text{ t}^{-1} \text{ day}$  between the 55 km and 60 km surface water sample sites on 18/07/2008, of which  $7.12 \text{ t day}^{-1}$  was contributed by the major cations (Na, Mg, Ca, K) and anions ( $\text{HCO}_3^-$ ,  $\text{SO}_4^{2-}$  and Cl). Flow increased by  $0.14 \text{ m s}^{-1}$ . No tributaries occur between these sites, with the increase in salt load and flow attributed to groundwater discharge. A saline and a fresh groundwater body was assumed to be causing the increase in TDS seen between the 55 km and 60 km sample sites, based on observations at Manobalai. The piezometers and bore at Sites One, Two and Three intercepted groundwater which is assumed part of the saline groundwater body, with Site Three groundwater chemistry used as the basis for modelling groundwater input from this groundwater system due to its high salinity and low Mg content indicating little change in groundwater composition due to mixing or chemical reactions within the regolith. Groundwater chemistry from Woodlands Grove Windmill was instead used to model input from the fresh groundwater body, although it was not within Manobalai. This was based on the assumption that its hydrochemistry was not impacted by the Na-Cl dominated regional groundwater body that influences the eastern (Manobalai) side of Wybung Creek. Detailed equations for the calculation of the results presented here can be found in Appendix for Chapter Six (Eqs. A6.1 – A6.6).

Hydrogeochemical inputs from the saline and fresh groundwater bodies were calculated based on Cl inputs, due to the conservative nature of Cl (Eq. A6.2). Different quantities of Cl and proportions of cations and anions to Cl were tested for the saline

and fresh groundwater bodies until the calculated Cl concentrations and proportions of major ion to Cl met the following conditions:

- The Cl contribution from the saline and fresh groundwater bodies calculated using Eq. A6.2 summed to the observed Cl increase between the 55 and 60 km sample sites ( $1.93 \text{ t day}^{-1}$ );
- Solute fluxes to Wybong Creek based on TDS calculated using Eq. A6.3 and Cl calculated from Eq. A6.2 for the saline and fresh groundwater bodies equalled the measured increases between the 55 and 60 km sample sites ( $7.912 \text{ t day}^{-1}$  and  $1.93 \text{ t day}^{-1}$  respectively);
- The quantity of groundwater calculated as being discharged to Wybong Creek was the same as the measured increase between the 55 and 60 km sites;
- The contribution of major cations and anions from the saline and fresh groundwater bodies calculated using Eq. A6.4 were close to the measured increase in major cations and anions between the 55 km and 60 km sample sites, or the discrepancy between measured and calculated values could be attributed to geochemical processes such as redox and/or cation exchange; and
- The values for the hydraulic conductivities ( $k, \text{ m s}^{-1}$ ) of the saline and fresh groundwater bodies using Eqs. A6.5 – A6.8 and salt load ( $S_{TDS}, \text{ t day}^{-1}$ ) calculated in Eq. A6.3 were realistic.

The modelled flux of solutes from the fresh and saline groundwater bodies to Wybong Creek were similar to the increases actually seen. The modelled flux of Ca and Mg was lower than the increase in Mg and Ca seen between the 55 and 60 km sample sites, while the modelled flux of Na and K was higher. This discrepancy can be attributed to cation exchange along the groundwater flow path, which decreases the concentration of monovalent ions such as Na and K in solution, and increases the concentration of Mg and Ca. The low concentrations of  $\text{NO}_3^-$  and  $\text{PO}_4^{3-}$  in Manobalai groundwater indicated fertilizer is not a likely source of K (Table A3.4; Appendix 3). This process has been identified at Manobalai (Chapters Four and Five). The small discrepancy between actual and modelled increases in  $\text{HCO}_3^-$  and  $\text{SO}_4^{2-}$  can be instead attributed to chemical weathering within the regolith.

Calculations indicated that 83 % of the Cl increase between the 55 and 60 km sample sites was sourced from the fresh groundwater body, and 17 % from the saline groundwater body (Table 6.7). Only 7.5 % of the overall increase in TDS seen in Wybong Creek could be attributed to the saline groundwater body. Mean hydraulic conductivities needed to deliver this salt in the quantities calculated and observed, were

between  $1.4 \times 10^{-5}$  and  $1.9 \times 10^{-6} \text{ m s}^{-1}$ , provided that the area of the aquifer was between 98 460 and 76 580 m<sup>2</sup>. Such hydraulic conductivities are typical of sand and silt rich material, and both are consistent with the hydraulic conductivities described earlier in the chapter. The area required is small, and is not consistent with discharge along a 5.5 km wide aquifer. The area required for the model work is instead consistent with fracture flow into the Creek, which would allow for a much smaller total width, and greater aquifer length. The model created to account for the increase in surface water salinity between the 55 and 60 km sample sites had realistic assumptions, with the increase in salinity largely accountable by discharge of relatively fresh groundwater, rather than more saline groundwater. Discrepancies in the real versus modelled increase in solutes were accounted for by the processes of cation exchange, oxidation and reduction.

### 3.3.1. Fluxes to Wybong Creek due to increased hydraulic head

Daily fluctuations in hydraulic head occurred within piezometers at Sites Six – Eight (Figure 6.11). This increase in hydraulic head and therefore hydraulic gradient was investigated as a possible cause of the daily EC fluctuations in Wybong Creek salinity, by creating a simple mathematical model (Section 2.2.2). The effect which an increase in hydraulic head might have on the hydraulic gradient, and therefore groundwater discharge, was estimated based on the maximum increase in hydraulic head seen at Site Six.

The difference between the daily EC maxima and minima at the 60 km sample site was approximately 30 µS cm<sup>-1</sup>, which approximates to around 19.2 mg L<sup>-1</sup>, with increases in hydraulic head at Site Six as much as 17 mm (Figure 6.11). The increase in

Table 6.7. The measured increase in major cations and anions concentration between the 55 km and 60 km sample sites on 18/07/2008, modelled contributions of major cations and anions from the fresh and saline groundwater bodies, and the difference between the modelled contribution from both aquifers and the quantity measured.

	t increase day <sup>-1</sup> between 55 and 60 km sample sites	Contribution (Saline)	Contribution (Fresh)	Contributions (Saline + fresh)	t Difference (Increase - GW contribution)
Na	1.00	0.17	1.11	1.28	0.28
Ca	0.48	0.01	0.31	0.31	-0.17
Mg	0.72	0.02	0.67	0.69	-0.03
K	0.03	0.00	0.29	0.30	0.27
SO <sub>4</sub>	0.25	0.04	0.23	0.27	0.02
Cl	1.93	0.33	1.59	1.93	0.00
HCO <sub>3</sub>	3.5	0.02	3.22	3.24	-0.26
TDS	7.91	0.594	7.32	7.91	0.00
% of TDS		7.51	92.49	100	

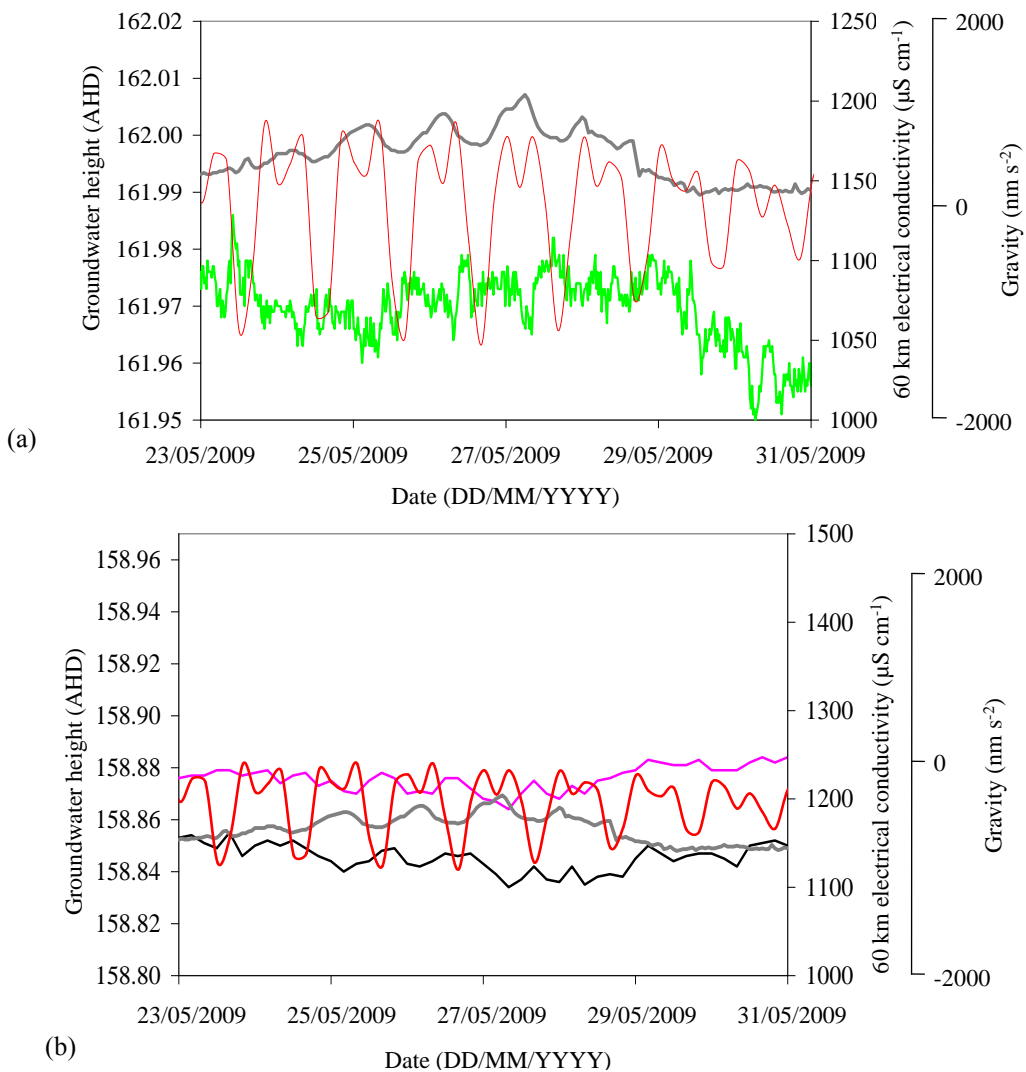


Figure 6.11. Relationships between (a) groundwater height at Site Six (—, AHD), EC at the 60 km sample site (—,  $\mu\text{S cm}^{-1}$ ), and gravity (—,  $\text{nm s}^{-2}$ ); and (b) groundwater height at Site Eight Fractured (—, AHD), Eight Shallow (—), EC at the 60 km sample site and gravity.

groundwater flux to Wybung Creek that would occur as a result of a 20 mm increase in hydraulic head on both the eastern and western side of the creek of the 60 km sample site is  $2.68 \text{ L s}^{-1}$ , assuming that groundwater contributions come from aquifers with the same height, depth, width and hydraulic gradient (Eqs. 6.4 – 6.5). This increase in groundwater flux would cause salinity to increase by  $1.64 \text{ mg L}^{-1}$  (approximately  $2.7 \mu\text{S cm}^{-1}$ ) every second and every metre along the 5.5 km length of Wybung Creek modelled. An increase in salinity of  $1.64 \text{ mg L}^{-1}$  would initially occur at the 55 km surface water sample site, with this increasing up to a total of  $7402 \text{ mg L}^{-1}$  as solutes progressively accumulate in the surface water as it moves down Wybung Creek at up to  $0.743 \text{ m s}^{-1}$ . The actual change in Wybung Creek salinity measured using a MiniSonde 5 was  $30 \mu\text{S cm}^{-1}$  during 23/05/2009 – 31/05/2009 (Figures 6.11 – 6.12), with this

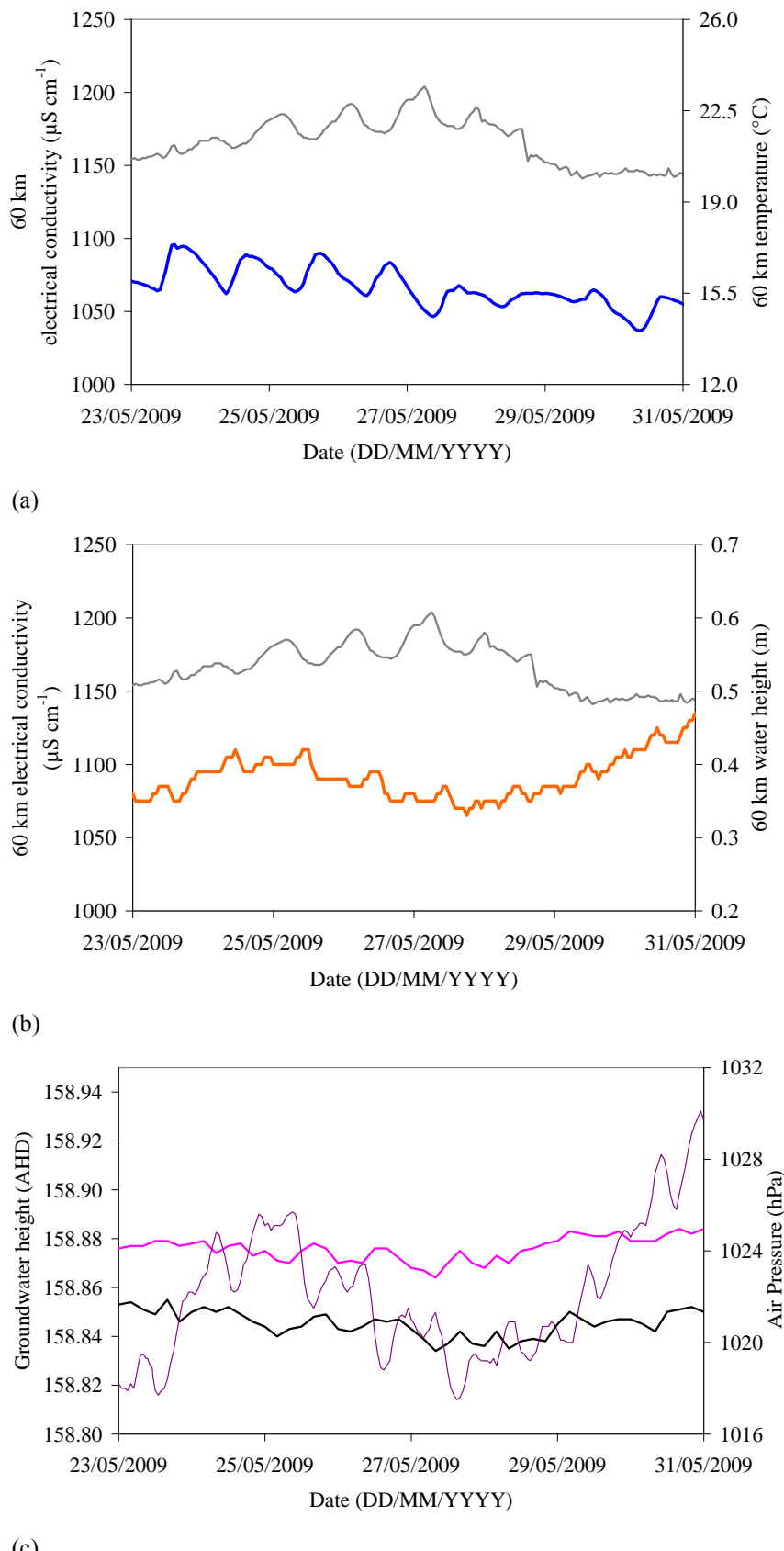


Figure 6.12. Relationships recorded in May 2009 between (a) EC (—,  $\mu\text{S cm}^{-1}$ ) and temperature (—,  $^{\circ}\text{C}$ ) at the 60 km sample site; (b) EC and water height (—, m) at the 60 km sample site; and (c) groundwater height at Site Eight Shallow (—, AHD), Site Eight Fractured (—, AHD), and air pressure (—, hPa).

increase occurring over a number of hours (Chapter Two). Salinity fluctuations of over  $350 \mu\text{S cm}^{-1}$  have been seen within the same day in Wybong Creek (Chapter Two). The increases in diurnal groundwater height at Sites Six and Eight were, therefore not consistent with the increase in Wybong Creek salinity, with the increases in hydraulic head within piezometers also unlikely to reflect an increase of hydraulic head in the aquifer due to the confining smectitic clay. This indicates that the fluctuations in Wybong Creek salinity are related to discharge of solutes from a much smaller area rather than discharge modelled along this 5.5 km stretch of river.

Point source increases of salinity were seen in Wybong Creek and related to groundwater discharge via fractures (Chapter Two), with some changes to Wybong Creek depth occurring with increases in salinity during May 2009 (Figure 6.12). The changes in permeability and porosity caused by cyclical loading and unloading cause an increase in hydraulic head and a decrease in groundwater flow through pores and fractures. This forces groundwater into piezometers and causes an increase in groundwater height, but also appears to decrease saline groundwater flow into Wybong Creek, and cause a decrease in salinity. Temperature fluctuations are not consistent with this discharge, with some indication that loading of the aquifer may be related to air pressure in addition to gravity (Figure 6.12). While fluctuations in Wybong Creek salinity and groundwater height can be related to loading and unloading of the aquifers in the mid-catchment area, and modelling indicates a high degree of surface groundwater connectivity via fractures which connect saline groundwater directly to the Creek, further research is required in order to further constrain the relationship beyond the correlative one shown here, to one which more directly shows cause and effect. This is possible through geophysical techniques which may, for example, measure fracture geometry or response to loading, and which can isolate fracture extents and connectivity.

#### **4. Conclusions**

Two major aquifers occur within the Manobalai field site: the Manobalai Alluvial aquifer; and the fractured Narrabeen Group aquifer. Changes in hydraulic head within the Narrabeen Group aquifer occurred every day, however, changes were of differing amplitude and periodicity. These differences indicate that fractures were not connected, with differences in fracture geometry giving rise to both different periodicity and amplitude in hydraulic changes at these two sites. A similar periodicity in hydraulic head changes as Sites One – Three instead indicated a similar response to a similar

forcing, though a phase lag in hydraulic head fluctuations between Sites Two and Four instead indicated that pressure changes were propagated through the aquifer to Site Four rather than originating at that site. Hydraulic head changes were found to be due to aquifers responding to loading and unloading events, with increases in hydraulic head occurring when increased loading forced groundwater upwards in bores and piezometers. Hydraulic head fluctuations also indicated confined conditions and undrained boundary conditions.

Hydraulic heads in all piezometers and bores increased soon after rainfall, indicating unconfined conditions occurred to some degree. A difference in the relationship between hydraulic head increases and rainfall between the bore and piezometer installed at Site Two indicated these responses were complex, however, with groundwater arriving at sites via a number of different flow paths. Heterogenous and likely anisotropic conditions occur in the Manobalai Alluvium, causing unpredictable vertical and horizontal groundwater flow. The poor hydraulic head and salinity relationships between the bore and piezometer nested into the alluvium at Site Two are particularly good evidence for this complexity.

The two northern-most groundwater sampling sites (Site Four and Whip Well) had the freshest groundwater, with saline water occurring at Sites Two, Three, and Hannah's. Groundwater chemistry indicates solutes can be related to the Wittingham Coal Measures, with abrupt changes in chemistry within the Manobalai site consistent with groundwater discharge via fractures and/or faults connected to this formation and dilution by a locally recharging fresh groundwater body. Further research characterising the faults, fractures, and the geology of the Manobalai area in general is necessary in order to further constrain groundwater flow paths, with tracer tests such as fluorescent dyes and  $^3\text{H}$  possible avenues for further research. Analyses of radio-isotopes such as  $^{36}\text{Cl}$  and  $^3\text{H}$  in addition to the  $^{14}\text{C}$  data collected for this study would also enable groundwater to be dated and recharge histories to be better understood, while reactive transport modelling would enable the evolution of groundwater chemistry along flow paths to be better understood.

Increases in Wybong Creek salinity at the 60 km sample site occurred with similar periodicity to hydraulic head changes seen in piezometers installed adjacent to Wybong Creek. Changes in Wybong Creek salinity could not be related to an increase in groundwater discharge due to increases in hydraulic head. Salinity changes are instead likely to be related to groundwater discharge directly into Wybong Creek whereby

decreased loading of the fractured Narrabeen Group aquifer causes an increase in fracture porosity and allows more groundwater to flow into Wybong Creek.

The modelled groundwater discharge from the fresh and saline groundwater bodies which occur at Manobalai can be linked to increases in salinity between the 55 and 60 km surface water sample sites. The model indicated less than ten percent of the total increase in TDS between the 55 and 60 km surface water sample sites was related to discharge from the saline groundwater body. Further research on surface and groundwater connectivity at the Manobalai field site is clearly necessary. Changes to surface water salinity due to loading of neighbouring aquifers, in particular, have not been previously identified in the literature, with research on changes to groundwater discharge, fracture porosity and surface-groundwater connectivity at this site necessary in order to bring the results presented here beyond more than correlated observations.

---

## **Chapter Seven**

Conclusions on the origin of solutes and  
the processes causing salinisation in the  
Wybong Creek catchment



The aim of this thesis was to identify sources of solutes and processes leading to salinisation in the Wybong Creek catchment. This aim was met by addressing a number of smaller aims, with these addressed within chapters on surface water chemistry in Wybong Creek; the aquifers, rock types and groundwater bodies in the catchment; the source of solutes to these groundwater bodies; sources of salinity to the regolith; and hydrology and hydrogeology on a sub-catchment scale. The main points and conclusions from these chapters are discussed in the following sections.

### **7.1. Sources of salinity to Wybong Creek**

*Aim:* To investigate solute sources and hydrological processes affecting solute concentrations in Wybong Creek.

*Summary points:*

- Wybong Creek was dominated by Na-Mg-HCO<sub>3</sub> in the upper catchment and was dominated by Cl in the lower catchment;
- Abrupt increases in EC and Cl concentrations between the 55 and 60 km sample sites indicated a change in the geochemical environment of this area;
- The increase in EC and Cl between the 55 and 60 km sample sites was due to groundwater discharge into a 20 m long pool in Wybong Creek, 70 m upstream of the 60 km sample site;
- The fluctuating EC at the 60 and 72 km sample sites indicated saline groundwater occurred within a confined aquifer(s) adjacent to Wybong Creek;
- There was no clear relationship between surface water evaporation and salinity; and
- The relationship between aeolian deposition on and solute flux from the Wybong Creek catchment (i.e. input to output ratios) was similar to other catchments which suffer from dryland salinity.

*Conclusion One.*

The increase in solute concentration in the mid-catchment area of Wybong Creek was due to the discharge of a saline, Cl dominated groundwater body.

## **7.2. Aquifers and groundwater bodies in the Wybong Creek catchment**

*Aim:* To understand the extent and interconnectedness of groundwater systems or bodies occurring in the Wybong Creek catchment and the aquifers in which they occur.

*Summary points:*

- Localised groundwater systems occur in the upper catchment with recharge occurring in the Liverpool Ranges and discharge occurring in the upper Wybong Creek valley, with these groundwater systems dominated by  $\text{HCO}_3^-$  and either Na or Mg;
- Intermediate and/or regional groundwater systems occur in the mid-lower Wybong Creek catchment, with Cl dominated groundwater solutes unable to be sourced from chemical weathering of the Narrabeen Group, Liverpool Range Volcanics or the alluvium;
- Vertical groundwater flow is indicated by unpredictable changes to groundwater chemistry in the Wybong Creek catchment;
- Vertical groundwater flow occurs partly due to the occurrence of materials with high hydraulic conductivity underlying clays with low hydraulic conductivity and fractured rock aquifers in many, if not all parts of the Wybong Creek catchment. The dipping of sedimentary beds in the opposite direction to topography and deep fractures are also likely to give rise to some components of vertical flow; and
- The occurrence of both permanent and ephemeral fresh, brackish and saline springs in the mid-catchment area of Manobalai indicates mixing of local and regional groundwater bodies which discharge in this area.

*Conclusion Two.* Groundwater in the upper Wybong Creek catchment occurs as localised groundwater systems, with recharge occurring in the Liverpool Ranges and discharge occurring in the upper Wybong Creek Valley.

*Conclusion Three.* Intermediate and/or regional groundwater systems occur in the lower Wybong Creek catchment, with vertical groundwater flow making it difficult to predict groundwater flow paths.

---

### 7.3. Surface and groundwater geochemistry of Wybong creek

*Aim:* To identify the source of solutes to surface and groundwater in the Wybong Creek catchment.

*Summary points:*

- Cation to  $\text{HCO}_3$  and  $^{87}\text{Sr}/^{86}\text{Sr}$  indicated solutes in upper catchment groundwater, and in surface water from Wybong Creek was sourced from silicate weathering of the Liverpool Range Volcanics;
- Groundwater sourced from the Newcastle Coal Measures had different hydrochemical facies and  $^{87}\text{Sr}/^{86}\text{Sr}$  than saline Na-Cl dominated water in piezometers, indicating solutes were not sourced from the Newcastle Coal Measures;
- Ratios of Na/Cl and Cl/Br indicated halite dissolution was an important source of solutes to Cl dominated groundwater, while  $\delta^{34}\text{S}$  and  $^{87}\text{Sr}/^{86}\text{Sr}$  indicated groundwater also had marine signatures;
- The enrichment of  $^2\text{H}$  and  $^{18}\text{O}$  was not correlated to increased TDS concentrations in Wybong Creek groundwater, indicating that groundwater did not have a marine geochemical signature due to evapoconcentration of rainwater, with groundwater instead acquiring solutes between recharge and discharge;
- Sr isotopes and geochemical modelling based on  $^{87}\text{Sr}/^{86}\text{Sr}$  indicated that solutes were not likely to be sourced from aeolian accession or weathering of sandstone; and
- The marine influenced and halite containing Wittingham Coal Measures are the most likely source of Cl dominated groundwater to the Wybong Creek catchment, with topographic drive and vertical groundwater flow a means by which groundwater may flow up dip and discharge via fractures into the Narrabeen Group sandstones and conglomerates, and alluvium in the mid – lower catchment.

*Conclusion Four.* Silicate weathering in the upper catchment produced  $\text{HCO}_3$ , Mg, and Na dominated surface and groundwater.

---

*Conclusion Five.* The Cl dominated groundwater in the mid-lower Wybong Creek catchment had a marine origin and likely originated from the Wittingham Coal Measures.

*Conclusion Six.* Cation exchange within alluvial clay in the lower catchment caused Mg and Ca to be exchanged for Na and the Na-Cl dominated groundwater in this aquifer to be altered to Na-Mg-Cl facies.

#### **7.4. Salinisation at the Manobalai field site**

*Aim:* To isolate whether groundwater discharging in the Manobalai area acquired solutes from salt stores within the regolith or was saline before it discharged at Manobalai.

*Summary points:*

- Regolith samples were not saline on an EC<sub>1:5</sub> or percent weight Na and Cl basis, with one or two samples having ESP values indicative of saline soils, and none showing slaking or dispersal.
- A lack of sulfate and carbonate bearing minerals in the alluvial regolith indicates that aeolian deposition was not the source of Na-Cl dominated solutes to groundwater in the Manobalai area;
- Differences in the chemistry of fresh and saline groundwater indicated evapoconcentration could not have resulted in the saline groundwater seen at Manobalai;
- Saline groundwater arises at specific points on the break of slope and/or on the valley floor and occurs in the coarsest layers within the regolith;
- Smectitic clay acts as an impermeable barrier to the saline, Na-Cl dominated groundwater that discharges into Manobalai, causing saline groundwater to mound and the formation of the salt scald when groundwater heights are close to the surface; and
- The occurrence of saline and fresh groundwater in both the fractured Narrabeen Group and Manobalai Alluvium aquifers indicates discharge of local, intermediate and/or regional groundwater systems.

*Conclusion Seven.* Salinisation at the Manobalai field site was due to discharge of saline groundwater from an intermediate and/or regional groundwater body not salt stores in the regolith.

### **7.5. The hydrology and hydrogeology of Manobalai**

*Aim:* To understand groundwater movements at the Manobalai field site.

*Summary points:*

- Hydraulic heads in most bores and piezometers increase and decrease regularly throughout the day in response to loading events, with a lack of pressure propagation through the aquifer indicating a lack of connectivity between many of the bores and piezometers at the sites;
- Hydraulic heads in piezometers at the site respond to recharge events either immediately or within a few weeks, with hydraulic heads in piezometers screened into the fractured Narrabeen Group aquifer also responding to loading and unloading caused by Earth tides;
- Anisotropic and heterogenous conditions exist within both the fractured Narrabeen Group aquifer and Manobalai Alluvium, with different hydraulic heads occurring within the bore and piezometer screened into the alluvium at Site Two, and within the bores and piezometers at Hannah's and Site Eight Fractured;
- Modelling of groundwater fluxes into Wybong Creek indicated the increase in surface water salinity between the 55 and 60 km sample sites is mostly due to discharge from the fresh groundwater body, with some also from the saline groundwater body; and
- Changes to Wybong Creek salinity at the 60 km sample site adjacent to Manobalai could not be linked to the changes in hydraulic head which occur as a result of aquifer loading and unloading, and are instead likely related to direct discharge from the fractured Narrabeen Group aquifer into the Creek.

*Conclusion Eight.* Groundwater flow at Manobalai is complex, with anisotropy and groundwater discharge via fractures causing vertical and unpredictable groundwater flow.

*Conclusion Nine.* Groundwater recharge from rainfall in both the alluvium and fractured Narrabeen Group aquifers, and loading of the fractured Narrabeen Aquifer, causes hydraulic heads to increase. These changing loadings appear to be causing the daily, cyclical changes in salinity seen in the Salt Pool at the 60 km Site.

## **7.6. Conclusion – Origins of solutes and salinisation processes in the Wybong Creek catchment**

There are two main sources of solutes to surface and groundwater in the Wybong Creek catchment. Solutes in the upper catchment are largely sourced from chemical weathering of the locally occurring Liverpool Range Volcanics, while those in the lower catchment most likely arise due to discharge of regional groundwater and dissolution of halite from within the Wittingham Coal Measures. These Permian Coal Measures and the Narrabeen Group sandstones and conglomerates dip below the Liverpool Ranges, with groundwater recharging in the Liverpool Ranges possibly forced to flow up dip due to topographic drive. This provides a mechanism by which saline regional groundwater from the Wittingham Coal Measures has the potential to discharge via fractures in the mid-lower Wybong Creek catchment.

Aridity is an important factor contributing to salinity in the catchment, with decreased regolith salinity and increased surface water salinity during the low flow conditions which occur during droughts. Geology is the most important factor contributing to salinity in the catchment, however, with groundwater discharge from the Wittingham Coal Measures giving rise to the saline and Na-Cl dominated surface water delivered into the Goulburn and Hunter Rivers by Wybong Creek. This is in contrast with other catchments in Australia which largely suffer from secondary salinisation processes whereby salinity is brought about by dissolution of salt stores within the regolith and/or changes to the hydrological cycle. The primary salinity that occurs in the Wybong Creek catchment is, therefore, unusual in coastal Australian catchments.

The sustainability of farming in the Wybong Creek catchment depends on the limitation of saline surface and groundwater for irrigation use to prevent further soil/regolith salinisation. Irrigation using Wybong Creek surface water should, therefore, only occur during high-flow or flood events, with the use of groundwater limited to all but a few bores in the upper catchment. Groundwater pumping would lower water tables at the Manobalai field site and alleviate scalding. Salinisation is a natural process occurring in the catchment, however, with the absence of erosion and/or slaking soils at Manobalai indicating that the current non-intensive farm practices occurring at the site

are likely sustainable with the salt scald independently recovering during drought periods.

Saline soils occur upslope of smectitic-clays in many parts of the Hunter catchment. Salinisation of the alluvial aquifer in the Goulburn and Hunter floodplains downstream of Wybong is related to groundwater discharge from the Wittingham Coal Measures, with groundwater mounding in alluvial aquifers behind the smectitic clay possibly causing salt scalding similarly to Manobalai. The regional extent of the Wittingham Coal Measures makes management of discharge difficult, with changes in hydraulic heads taking sometimes hundreds of years to manifest after a modification of land-use. The planting of trees to decrease recharge to groundwater bodies has been undertaken in a number of Australian catchments, but with limited affect. Tree planting is particularly unlikely to offer a practical means of managing saline discharge in the Hunter Valley, due to the regional extent of the groundwater system causing the salinity. The nature of the salinity problem in the Hunter Valley is such that only limited salinity mitigation measures, such as “living with salt strategies”, can be effectively put in place. The formation of the Hunter River Trading Scheme is an example of such a strategy. The limitation of irrigation using both saline and fresh surface and groundwater is another means of preventing further salinisation, with the fresher water in the area diluting and therefore reducing the toxicity of saline groundwater.

The hydrogeochemical information presented in this thesis can be built on in a number of ways. Groundwater recharge will be better understood if dating is conducted using a variety of tracers such as radioactive isotopes and/or CFC-12. The use of tracers such as radioactive isotopes and/or dyes would also allow for a better understanding of groundwater flow paths, with only a poor understanding of groundwater flow within the fractured Narrabeen Aquifer and alluvium possible in this study. Research on the geology of the catchment is necessary, particular in terms of identifying geological structures such as faults, with the lack of this knowledge a serious limitation to the research presented here.

The identification of the Wittingham Coal Measures as the source of salinity to the Wybong Creek catchment occurred through a process of deduction, whereby other possible solute sources were excluded by differing lines of evidence. Groundwater samples were not attained from the Wittingham Coal Measures in this study, though knowledge from previous research in the Hunter Catchment indicated groundwater from this formation was likely to be the source of salinity to the catchment. Sampling of

---

groundwater from the Wittingham Coal Measures can only improve the outcomes of research into salinity in the Wybong Creek catchment, with this another avenue for future research in the catchment.

---

## References



- Abuduwaili J, Gabchenko MV, Junrong X (2008) Elolian transport of salts—A case study in the area of Lake Ebinur (Xinjiang, Northwest China). *Journal of Arid Environments* **72**, 1843-1852.
- Abbot WE, Glengarry, JP (1880) 'Ringbarking and its effects'. Royal Society of New South Wales, Sydney.
- Acworth RI, Brain T (2008) Calculation of barometric efficiency in shallow piezometers using water levels, atmospheric and earth tide data. *Hydrogeology Journal* **16**, 1469-1481.
- Acworth RI, Broughton A, Nicholl C, Jankowski J (1997) The role of debris-flow deposits in the development of dryland salinity in the Yass River catchment, New South Wales, Australia. *Hydrogeology Journal* **5**, 22-37.
- Acworth RI, Jankowski J (2001) Salt source for dryland salinity—evidence from an upland catchment on the Southern Tablelands of New South Wales. *Australian Journal of Soil Research* **39**, 39-59.
- Albrecht G (2000) 'Rediscovering the Coquun: Towards an environmental history of the Hunter River.' (Hunter Catchment Management Trust: Branxton).
- Ahmed M, Volk H, George SC, Faiz M, Stalker L (2009) Generation and expulsion of oils from Permian coals of the Sydney Basin, Australia. *Organic geochemistry* **40**, 810-831.
- Allison GB, Cook PG, Barnett P, Walker GR, Jolly ID, Hughes MW (1990) Land clearance and river salinisation in the western Murray Basin, Australia. *Journal of Hydrology* **119**, 1-20.
- Amundson R, Wang Y, Chadwick O, Trumbore S, McFadden L, McDonald E, Wells S, DeNiro M (1994) Factors and processes governing the <sup>14</sup>C content of carbonate in desert soils. *Earth and Planetary Science Letters* **125**, 385-405.
- Appelo CAJ, Postma D (2005) 'Geochemistry, groundwater and pollution.' (A.A. Balkema Publishers: New York).
- Arad A, Evans R (1987) The hydrogeology, hydrochemistry, and environmental isotopes of the Campaspe river aquifer system, north-central Victoria, Australia. *Journal of Hydrology* **95**, 63-86.
- Armstrong ASB, Rycroft DW, Tanton TW (1996) Seasonal movement of salts in naturally structured saline-sodic clay soils. *Agricultural Water Management* **32**, 15-27.
- Australasian Groundwater and Environmental Consultants Pty LTD (2006) Groundwater impact assessment Mt Arthur South Pit extension project (Umwelt Australia Pty Ltd: Location unknown).
- Australian and New Zealand Environment and Conservation Council (ANZECC), Agriculture and Resource Management Council of Australia and New Zealand (ARMCANZ) (2000) 'Australian and New Zealand guidelines for fresh and marine water quality, volume 1: The guidelines.' (Australian Water Association: Artarmon).
- Australian Bureau of Meteorology (2009) Climate statistics for Australian Locations: Monthly Climate Statistics, Scone (Philip Street).  
[http://www.bom.gov.au/climate/averages/tables/cw\\_061089\\_All.shtml](http://www.bom.gov.au/climate/averages/tables/cw_061089_All.shtml). Downloaded 30<sup>th</sup> April 2009. (Australian Bureau of Meteorology: Sydney).
- Australian Bureau of Statistics (2006) 'Year book Australia'.  
<http://www.abs.gov.au/AUSSTATS/abs@.nsf/ProductsbyCatalogue/54C4B6E54C0C737DCA2570B000368DFD?OpenDocument>. Downloaded on 5<sup>th</sup> September 2007 (Australian Bureau of Statistics: Canberra).
- Australian Department of Agriculture Fisheries and Forestry and Australian Department of Environment and Heritage (2007) 'National action plan for salinity and water quality'.  
<http://www.napswq.gov.au/publications/salinity.html>. Downloaded on 29<sup>th</sup> May 2007 (Australian Government: Canberra).
- Australian Groundwater Consultants (1984) 'Effects of mining on groundwater resources in the Hunter Valley. Volume 1'. (Australian Department of Resources and Energy: Canberra).

- Ayers RS, Westcot DW (1994) 'Water quality for agriculture'. (Food and Agriculture Organization of the United Nations: Rome).
- Bachu S (1995) Flow of variable-density formation water in deep sloping aquifers: Review of methods of representation with case studies. *Journal of Hydrology* **164**, 19-38.
- Bachu S, Michael K (2002) Flow of variable-density formation water in deep sloping aquifers: Minimizing the error in representation and analysis when using hydraulic-head distributions. *Journal of Hydrology* **259**, 49-65.
- Bai GP, Keene JB (1996) Petrology and diagenesis of Narrabeen Group sandstones, Sydney Basin, New South Wales. *Australian Journal of Earth Sciences* **43**, 525-538.
- Banner JL, Wasserburg GJ, Dobson PF, Carpenter AB, Moore CH (1989) Isotopic and trace element constraints on the origin and evolution of saline groundwaters from central Missouri. *Geochimica et Cosmochimica Acta* **53**, 383-398.
- Beale G, Gilmore R, Simons M, Realica S, Nanadakumar N (2000) 'NSW coastal rivers salinity audit: Predictions for the Hunter Valley Issue 1.' (Centre for Natural Resources: Wagga Wagga).
- Beale G, Miller M, Barnett P, Summerell G, Gilmore R, Hoey D (2004) 'NSW coastal salinity audit: Salinity in the Sydney South Coast, Hunter and North Coast regions.' (Centre for Natural Resources: Wagga Wagga).
- Beavis S (2000) Structural controls on the orientation of erosion gullies in mid-western New South Wales, Australia *Geomorphology* **33**, 59-72.
- Bohlke JK, de Laeter JR, De Bievre P, Hidaka H, Peiser HS, Rosman KJR, Taylor PDP (2005) Isotopic compositions of the elements, 2001. *Journal of Physical and Chemical Reference Data* **34**, 57-67.
- Bottomley DJ, Gregoire DC, Raven KG (1994) Saline groundwaters and brines in the Canadian Shield: Geochemical and isotopic evidence for a residual evaporite brine component. *Geochimica et Cosmochimica Acta* **58**, 1483-1498.
- Bourg ACM, Bertin C (1993) Biogeochemical processes during the infiltration of river water into an alluvial aquifer. *Environment Science and Technology* **27**, 661-666.
- Bouwer H (1989) The Bouwer and Rice slug test - An update. *Ground Water* **27**, 304-309.
- Bowler JM, Wasson RJ (1983) Glacial age environments of inland Australia. In 'Late Cainozoic palaeoclimates of the Southern Hemisphere'. (A.A. Balkema: Swaziland).
- Bradd JM, Milne-Home WA, Gates G (1997) Overview of factors leading to dryland salinity and its potential hazard in New South Wales, Australia. *Hydrogeology Journal* **5**, 51-67.
- Brauchler R, Hu R, Vogt T, Al-Halbouni D, Henrichs T, Ptak T, Sauter M (2010) Cross-well slug interference tests: An effective characterization method for resolving aquifer heterogeneity. *Journal of Hydrology Article in press*.
- Bredehoeft JD (1967) Response of well-aquifer systems to Earth tides. *Journal of Geophysical Research* **72**, 3057-3087.
- Bricker OP, Pačes T, Johnson CE, Sverdrup H (1994) Weathering and erosion aspects of small catchment research. In 'Biogeochemistry of small catchments'. (Eds. Moldan B, Černý J) pp. 85-105. (John Wiley & Sons Ltd.: Chichester).
- Bridgman H (1998) Particulate air pollution and meteorology in the Upper Hunter Valley. In 'Geotechnical engineering and engineering geology in the Hunter Valley'. (Eds. Fityus S, Hitchcock P, Allman M, Delaney M). (Australian Geomechanics Society: Newcastle).
- Broers HP and van der Grift B (2004) Regional monitoring of temporal changes in groundwater quality. *Journal of Hydrology* **296**, 192-220.

- Brunton JS, Moore AM (2004) 'The Ridgeland coal drilling programmes, 2001 and 2003, Hunter Coalfield, New South Wales: Geological Survey report No. GS 2004/123'. (Department of Mineral Resources: Maitland).
- Bullen TD, Kendall C (1998) Tracing of weathering reactions and water flowpaths: A multi-isotope approach. In 'Isotope tracers in catchment hydrology'. (Eds. Kendall C, Bullen TD) pp. 611-646. (Elsevier Science B.V.: Amsterdam).
- Burbey TJ (2009) Fracture characterization using Earth tide analysis. *Journal of Hydrology* **380**, 237-246.
- Cartwright I, Hannam K, Weaver TR (2007) Constraining flow paths of saline groundwater at basin margins using hydrochemistry and environmental isotopes: Lake Cooper, Murray Basin, Australia. *Australian Journal of Earth Sciences* **54**, 1103-1122.
- Cartwright I, Weaver TR (2005) Hydrogeochemistry of the Goulburn Valley region of the Murray Basin, Australia: Implications for flow paths and resource vulnerability. *Hydrogeology Journal* **13**, 752-770.
- Cartwright I, Weaver TR, Fifield LK (2006) Cl/Br ratios and environmental isotopes as indicators of recharge variability and groundwater flow: An example from the southeast Murray Basin, Australia. *Chemical Geology* **231**, 38-56.
- Cartwright I, Weaver TR, Fulton S, Nichol C, Reid M, Cheng X (2004) Hydrogeochemical and isotopic constraints on the origins of dryland salinity, Murray Basin, Victoria, Australia. *Applied Geochemistry* **19**, 1233-1254.
- Casanova J, Négrel P, Kloppmann W, Aranyossy JF (2001) Origin of deep saline groundwaters in the Vienne granitic rocks (France): Constraints inferred from boron and strontium isotopes. *Geofluids* **1**, 91-101.
- Cattle SR, McTainsh GH, Wagner S (2002) Aeolian dust contributions to soil of the Namoi Valley, northern NSW, Australia. *Catena* **47**, 245-264.
- Chambers LA, bartley JG, Herczeg AL (1996) Hydrogeochemical evidence for surface water recharge to a shallow regional aquifer in northern Victoria, Australia. *Journal of Hydrology* **181**, 63-83.
- Charman PEV, Murphy BW (2000) 'Soils: Their properties and managements'. (Oxford University Press: Oxford).
- Chebrotev II (1955) Metamorphism of natural waters in the crust of weathering – 2. *Geochimica et Cosmochimica Acta* **8**, 137-170.
- Chen XY, Lintern MJ, Roach IC (2002) 'Calcrete: Characteristics, distribution and use in mineral exploration'. (Cooperative Research Centre for Landscape Environments and Mineral Exploration: Canberra).
- Chivas AR, Andrew AS, Lyons WB, Bird WI, Donnelly TH (1991) Isotopic constraints on the origin of salts in Australian playas. 1. Sulphur. *Palaeogeography, Palaeoclimatology, Palaeoecology* **84**, 309-332.
- Clark ID, Fritz P (1997) 'Environmental isotopes in hydrogeology'. (CRC Press: New York).
- Claypool GE, Holser WT, Kaplan IR, Sakai H, Zak I (1980) The age curves of sulfur and oxygen isotopes in marine sulfate and their mutual interpretation. *Chemical Geology* **28**, 199-260.
- Commonwealth Scientific and Industrial Research Organisations - Land and Water (CSIRO) and Australian Nuclear Science and Technology Organisation (ANSTO) (2004) 'Global network of isotopes in precipitation'. <http://isohis.iaea.org>. Downloaded on November 16<sup>th</sup> 2007 (CSIRO: Sydney).
- Cook PG (1999) 'A guide to regional groundwater flow in fractured rock aquifers'. (CSIRO Land and Water: Glen Osmond).

- Coram JE, Dyson PR, Houlder PA, Evans WR (2001) 'Australian groundwater flow systems contributing to dryland salinity'. (Bureau of Rural Sciences: Canberra).
- Craig H (1961) Isotopic variations in meteoric waters. *Science* **133**, 1702-1703.
- Creelman RA (1994) 'The geological and geochemical framework for assessing salinity in the Hunter valley'. (R.A. Creelman and associates: Epping).
- Cresswell RG, Herczeg AL (2004) 'Groundwater flow systems and salinity in the valleys around Jamestown, South Australia: Geochemical and isotopic constraints.' (CSIRO Land and Water: Canberra).
- Crosbie RS, Hughes JD, Friend J, Baldwin BJ (2007) Monitoring the hydrological impact of land use change in a small agricultural catchment affected by dryland salinity in central NSW, Australia. *Agricultural Water Management* **88**, 43-53.
- Dafny E, Burg A, Gvirtzman H (2006) Deduction of groundwater flow regime in a basaltic aquifer using geochemical and isotopic data: The Golan Heights, Israel case study. *Journal of Hydrology* **330**, 506 - 524.
- Davis JC (1973) 'Statistics and data analysis in geology'. (John Wiley & Sons: New York).
- Davis SN, Whittemore DO, Fabryka-Martin J (1998) Uses of chloride/bromide ratios in studies of potable water. *Ground Water* **36**, 338-350.
- Dimmock GM, Bettenay E, Mulcahy MJ (1974) Salt content of the lateritic profiles in the Darling Range, Western Australia. *Australian Journal of Soil Research* **12**, 63-69.
- Domenico PA, Schwartz FW (1990) 'Physical and chemical hydrogeology'. (John Wiley & Sons: New York).
- Douglas GB, Gray CM, Hart BT, Beckett R (1995) A strontium isotopic investigation of the origin of suspended particulate matter (SPM) in the Murray-Darling River system, Australia. *Geochimica et Cosmochimica Acta* **59**, 3799-3815.
- Drever JI (1997) 'The geochemistry of natural waters'. (Prentice-Hall: Upper Saddle River).
- Eggleton RA (2001) 'The regolith glossary'. (Cooperative Research Centre for Landscape Evolution and Mineral Exploration: Canberra).
- Engel R, McFarlane DJ, Street G (1987) The influence of dolerite dykes on saline seeps in south-western Australia. *Australian Journal of Soil Research* **25**, 125-136.
- Essington ME (2004) 'Soil and water chemistry: An integrative approach'. (CRC Press: London).
- Eugster HP (1984) Geochemistry and sedimentology of marine and nonmarine evaporites. *Swiss Journal of Geosciences* **77**, 237-248.
- Eugster HP, Hardie LA (1975) Saline lakes. In 'Lakes: Chemistry, geology and physics'. (Ed. A Lerman). (Springer-Verlag: New York).
- Eugster HP, Jones BF (1979) Behaviour of major solutes during closed brine evolution. *American Journal of Science* **279**, 609-631.
- Evans KA, Watkins DC, Banwart SA (2006) Rate controls on the chemical weathering of natural polymimetic material. II. Rate-controlling mechanisms and mineral sources and sinks for element release from four UK mine sites, and implications for comparison of laboratory and field scale weathering studies. *Applied Geochemistry* **21** (2), 377-403
- Faure G (1986) 'Principles of isotope geology'. (John Wiley & Sons, Inc: New York).
- Faure G (1998) 'Principles and applications of geochemistry'. (Prentice Hall: New Jersey).

- Fontes JC, Matray JM (1993) Geochemistry and origin of formation brines from the Paris Basin, France 2. Saline solutions associated with oil fields. *Chemical Geology* **109**, 177-200.
- Faiz M, Saghafi A, Sherwood N, Wang I (2006) The influence of petrological properties and burial history on coal seam methane reservoir characterisation, Sydney Basin, Australia. *International Journal of Coal Geology* **70**, 193-208.
- Food and Agricultural Organisation of the United Nations (1989) 'Arid zone forestry: A guide for field technicians'. (Food and Agriculture Organization of the United Nations: Rome)
- Faure G (1986) 'Principles of isotope geology'. (John Wiley & Sons, Inc: New York).
- Fetter CW (2001) 'Applied hydrogeology'. (Prentice-Hall, Inc.: Upper Saddle River).
- Franson MAH (Ed.) (2005) 'Standard Methods for the Examination of Water and Wastewater'. (American Public Health Association, American Water Works Association, Water Environment Federation: Washington, USA).
- Freeze RA, Cherry JA (1979) 'Groundwater'. (Prentice-Hall, Inc.: Englewood Cliffs).
- Fried AW (1993) Late Pleistocene river morphological change, southeastern Australia: The conundrum of sinuous channels during the Last Glacial Maximum. *Palaeogeography, Palaeoclimatology, Palaeoecology* **101**, 305-316.
- Gandy CJ, Smith JWN, Jarvis AP (2007) Attenuation of mining-derived pollutants in the hyporheic zone: A review. *Science of the Total Environment* **373**, 435-446.
- Gardner LR (1984) Carbon and oxygen isotope composition of pedogenic CaCO<sub>3</sub> from soil profiles in Nevada and New Mexico, U.S.A. *Isotope Geoscience* **2**, 55-73.
- GEMS/Water (2004) 'Global environment monitoring system'. <http://www.gemstat.org/default.aspx> Downloaded on 14th July 2009 (United Nations Global Environment Monitoring System Water Programme: Burlington).
- Genereux DP, Jordan M (2006) Interbasin groundwater flow and groundwater interaction with surface water in a lowland rainforest, Costa Rica: A review *Journal of Hydrology* **320**, 385-399.
- George RJ, Nulsen RA, Ferdowsian R, Raper GP (1999) Interactions between trees and groundwaters in recharge and discharge areas – A survey of Western Australian Sites. *Agricultural Water Management* **39**, 39-113.
- Gibbs RJ (1970) Mechanisms controlling world water chemistry. *Science* **170**, 1088-1090.
- Gingele F, De Deckker P, Norman M (2007) Late Pleistocene and Holocene climate of SE Australia reconstructed from dust and river loads deposited offshore the River Murray mouth. *Earth and Planetary Science Letters* **255**, 257-272.
- Glen RA, Beckett J (1993) 'Hunter Coalfield Regional 1:100 000 Geology Map.' (Geological Survey of New South Wales: Maitland).
- Gonfiantini R, Fröhlich K, Araguás-Araguás L, Rozanski K (1998) 'Isotopes in groundwater hydrology. In 'Isotope tracers in catchment hydrology'. (Eds. Kendall C, McDonnell JJ) pp. 203-238. (Elsevier, B.V.: Amsterdam).
- Graustein WC, Armstrong RL (1983) The use of Strontium-87/Strontium-86 ratios to measure atmospheric transport into forested watersheds. *Science* **219**, 289-292.
- Green EG, Dietrich WE, Banfield JF (2006) Quantification of chemical weathering rates across an actively eroding hillslope. *Earth and Planetary Science Letters* **242**, 155-169.
- Greene RSB, Ford GW (1985) The effect of gypsum on cation exchange in two red duplex soils. *Australian Journal of Earth Sciences* **23**, 61-74.

- Greenwood EAN, Milligan A, Biddiscombe EF, Rogers AL, Beresford JD, Watson GD, Wright KD (1992) Hydrologic and salinity changes associated with tree plantations in a saline agricultural catchment in southwestern Australia. *Agricultural Water Management* **22**, 307-323.
- Graustein WC, Armstrong RL (1983) The use of Strontium-87/Strontium-86 ratios to measure atmospheric transport into forested watersheds. *Science* **219**, 289-292.
- Greiner R (1998) Catchment management for dryland salinity control: Model analysis for the Liverpool Plains in New South Wales. *Agricultural Systems* **56**, 225-251.
- Güler CG, Thyne GD, McCray JE, Turner AK (2002) Evaluation of graphical and multivariate statistical methods for classification of water chemistry data. *Hydrogeology Journal* **10**, 455-474.
- Gunn RH, Richardson DP (1979) The nature and possible origins of soluble salts in deeply weathered landscapes of Eastern Australia. *Australian Journal of Earth Sciences* **17**, 197-215.
- Hach Company (2009) 'Chemicals, reagents and standards'. (Hach Company: Loveland).
- Hamilton S (1992) 'Ogilvies Hill groundwater study'. ( NSW DWR: Sydney).
- Hardie LA, Eugster HP (1970) The evolution of closed-basin brines. *Mineralogical Society of America Special Paper* **3**, 273-290.
- Harrington GA, Herczeg AL (2003) The importance of silicate weathering of a sedimentary aquifer in arid Central Australia indicated by very high  $^{87}\text{Sr}/^{86}\text{Sr}$  ratios. *Chemical Geology* **199**, 281-292.
- Harrington NM, Herczeg AL, Le Gal La Salle C (2008) Hydrological and geochemical processes controlling variations in  $\text{Na}^+ - \text{Mg}^{2+} - \text{Cl}^- - \text{SO}_4^{2-}$  groundwater brines, south-eastern Australia. *Chemical Geology* **251**, 8-19.
- Hart BT, Bailey P, Edwards R, Hortle K, James K, McMahon A, Meredith C, Swadling K (1990) Effects of salinity on river, stream and wetland ecosystems in Victoria, Australia. *Water Research* **24**, 1103-1117.
- Healthy Rivers Commission (2002) 'Hunter River: Independent inquiry into the Hunter River system'. (Healthy Rivers Commission: Sydney).
- Hegge BJ, Masselink G (1991) Groundwater-table responses to wave run-up: An experimental study from Western Australia. *Journal of Coastal Research* **7**, 623-634.
- Herczeg AL, Barnes CJ, Macumber PG, Olley JM (1992) A stable isotope investigation of groundwater-surface water interactions at Lake Tyrrell, Victoria, Australia. *Chemical Geology* **96**, 19-32.
- Herczeg AL, Dogramaci SS, Leaney FWJ (2001) Origin of dissolved salts in a large, semi-arid groundwater system: Murray Basin, Australia. *Marine and Freshwater Research* **52**, 41-52.
- Herczeg AL, Simpson HJ, Mazor E (1993) Transport of soluble salts in a large, semi-arid basin: River Murray, Australia. *Journal of Hydrology* **144**, 59-84.
- Hoey D, Ahmed M, Littleboy M (2002) Landscape salinisation and management: An Australian perspective. *Agricultural Sciences* **7**, 53-60.
- Hiscock K (2005) 'Hydrogeology: Principles and practice.' (Blackwell Science LTD.: Oxford).
- Hunter Central Rivers Catchment Management Authority (2002) 'Integrated catchment management plan for the Hunter Catchment.' (Hunter Central Rivers Catchment Management Authority: Muswellbrook).
- Ingraham NL, Caldwell EA, Verhagen BT (1998) Arid catchments. In 'Isotope tracers in catchment hydrology'. (Eds. Kendall C, McDonnell JJ) pp. 435-460. (Elsevier, B.V.: Amsterdam).

- Jacobsen T, Adams RM (1958) Sand and silt in ancient Mesopotamian agriculture. *Science* **128**, 1251-1258.
- Jankowski J, Acworth RI (1997) Impact of debris-flow deposits on hydrogeochemical processes and the development of dryland salinity in the Yass River catchment, New South Wales, Australia. *Hydrogeology Journal* **5**, 71-89.
- Jankowski J, Jacobson G (1989) Hydrochemical evolution of regional groundwaters to playas brines in central Australia. *Journal of Hydrology* **108**, 123 - 173
- Jarvie HP, Neal C, Leach DV, Ryland GP, House WA, Robson AJ (1997) Major ion concentrations and the inorganic carbon chemistry of the Humber rivers. *Science of the Total Environment* **194-195**, 285-302.
- Jobbágy EG, Jackson RB (2001) The distribution of soil nutrients with depth: Global patterns and the imprint of plants. *Biogeochemistry* **53**, 51-77.
- Johnston CD (1987a) Distribution of environmental chloride in relation to subsurface hydrology. *Journal of Hydrology* **94**, 67-88.
- Johnston CD (1987b) Preferred water flow and localised recharge in a variable regolith. *Journal of Hydrology* **94**, 129-142.
- Jolly ID, Williamson DR, Gilfedder, M, Walker GR, Morton R, Robinson G, Jones H, Zhang L, Dowling TI, Dyce P, Nathan RJ, Nanadakumar N, Clarke R, McNeill V (2001) Historical stream salinity trends and catchment salt balances in the Murray-Darling Basin, Australia. *Marine and Freshwater Research* **52**, 53-63.
- Jones BF, Hanor JS, Evans WR (1994) Sources of dissolved salts in the central Murray Basin, Australia. *Chemical Geology* **111**, 135-154.
- Jones L, Atkins P (2002) 'Chemistry: Molecules, matter and change.' (Freeman and company: New York).
- Kellett JK, Williams BG, Ward JK (1987) 'Hydrogeochemistry of the Upper Hunter river valley, NSW'. (Bureau of Mineral Resources, Geology, and Geophysics: Maitland).
- Kendall C, Caldwell EA (1998) Fundamentals of isotope geochemistry. In 'Isotope tracers in catchment hydrology'. (Eds. Kendall C, McDonnell JJ) pp. 51-86. (Elsevier Science B.V.: Amsterdam).
- Kershaw AP, D'Costa DM, McEwen Mason JRC, Wagstaff BE (1991) Palynological evidence for quaternary vegetation and environments of mainland southeastern Australia. *Quaternary Science Reviews* **10**, 391-404.
- Kim J-H, Lee J, Cheong T-J, Kim R-H, Koh D-C, Ryu J-S, Chang H-W (2005) Use of time series analysis for the identification of tidal effect on groundwater in the coastal area of Kimje, Korea. *Journal of Hydrology* **300**, 188-198.
- Kloppmann W, Négrel P, Casanova J, Klinge H, Schelkes K, Guerrot C (2001) Halite dissolution derived brines in the vicinity of a Permian salt dome (N German Basin). Evidence from boron, strontium, oxygen, and hydrogen isotopes. *Geochimica et Cosmochimica Acta* **65**, 4087-4101.
- Knight JH, Gilfedder M, Walker GR (2002) 'Impacts of irrigation and dryland development on groundwater discharge to rivers: A unit response approach to cumulative impacts analyses'. (Cooperative Research Centre for Catchment Hydrology: Canberra).
- Kovac M (1991) 'Singleton: Soil landscape series sheet SI 56-1'. (Soil conservation service, New South Wales: Sydney).
- Kovac M, Lawrie JW (1991) 'Soil landscapes of the Singleton 1:250 000 sheet.' (Soil conservation service of New South Wales: Sydney).

- Kramer W, Weatherall G, Offler R (2001) Origin and correlation of tuffs in the Permian Newcastle and Wollombi Coal Measures, NSW, Australia, using chemical fingerprinting. *International Journal of Coal Geology* **47**, 115-135.
- Kreitler CW (1989) Hydrogeology of sedimentary basins. *Journal of Hydrology* **106**, 29-53.
- Leaney FW (2000) 'Groundwater salinisation in the Tintinara area of SA: Results of field investigations, April 2000'. (CSIRO Land and Water: Canberra).
- Leary SP, Brunton JS (2003) 'The north west Hunter exploration programme 2003 Hunter Coalfield NSW: Geological survey report No. GS 2004/238'. (Department of Mineral Resources: Maitland).
- Le Borgne T, Bour O, Paillet FL, Caudal J-P (2006) Assessment of preferential flow path connectivity and hydraulic properties at single-borehole and cross-borehole scales in a fractured aquifer. *Journal of Hydrology* **328**, 347-359.
- Lischeid G, Kolb A, Alewell C (2002) Apparent translatory flow in groundwater recharge and runoff generation. *Journal of Hydrology* **265**, 195-211.
- Love AJ, Herczeg AL, Armstrong D, Stadter F, Mazor E (1993) Groundwater flow regime within the Gambier Embayment of the Otway Basin, Australia: Evidence from hydraulics and hydrochemistry. *Journal of Hydrology* **143**, 297-338.
- MacKenzie N, Jacquier D, Isbell R, Brown K (2004) 'Australian soils and landscapes.' (CSIRO: Collingwood).
- Mackie Martin and Associates Pty Ltd (1993) 'Bengalla coal development area hydrogeological studies'. (Envirosciences Pty Ltd: Newcastle).
- Macpherson DK, Peck AJ (1987) Models of the effect of clearing on salt and water export from a small catchment. *Journal of Hydrology* **94**, 163-179.
- Macumber PG (1992) Hydrological processes in the Tyrrell Basin, southeastern Australia. *Chemical Geology* **96**, 1-18.
- Mahlknecht J, Gráfias-Solis J, Aravena R, Tesch R (2006) Geochemical and isotopic investigations on groundwater residence time and flow in the Independence Basin, Mexico. *Journal of Hydrology* **324**, 283-300.
- Martel AT, Gibling MR, Nguyen M (2001) Brines in the Carboniferous Sydney Coalfield, Atlantic Canada. *Applied Geochemistry* **16**, 35-55.
- Matsubaya O, Sakai H, Torii T, Burton H, Kerry K (1979) Antarctic saline lakes – stable isotopic ratios, chemical compositions and evolution. *Geochimica et Cosmochimica Acta* **43**, 7-25.
- Mazor E, George RJ (1992) Marine airborne salts applied to trace evapotranspiration, local recharge and lateral groundwater flow in Western Australia. *Journal of Hydrology* **139**, 63-77.
- McCaffrey MA, Lazar B, Holland HD (1987) The evaporation path of seawater and the coprecipitation of Br<sup>-</sup> with K<sup>+</sup> and halite. *Journal of Sedimentary Petrology* **57**, 928-937.
- McInnes-Clarke SK (2002) 'Soil landscapes of the Murrurundi 1:100 000 sheet'. (Department of Land and Water Conservation: Gosford).
- McMahon TA (1968) Geographical interpretation of hydrologic characteristics in the Hunter Valley. *Australian Geographer* **10**, 404-407.
- McNeill VH, Cox ME, Preda M (2005) Assessment of chemical water types and their spatial variation using multi-stage cluster analysis, Queensland, Australia. *Journal of Hydrology* **310**, 181-200.
- Meng SX, Maynard JB (2001) Use of statistical analysis to formulate conceptual models of geochemical behaviour: Water chemical data from the Botucatu aquifer in São Paulo state, Brazil. *Journal of Hydrology* **250**, 78-97.

- Meyer WS (1999) 'Standard reference evaporation calculation for inland, south eastern Australia'. (CSIRO, Land and Water: Adelaide).
- Miller EK, Blum JD, Friedland AJ (1993) Determination of soil exchangeable-cation loss and weathering rates using Sr isotopes. *Nature* **362**, 438-441.
- Möller P, Woith H, Dulksi P, Lüders, Erzinger J, Kämpf H, Pekdeger A, Hansen B, Lodemann M, Banks D (2005) Main and trace elements in KTB-VB fluid: Composition and hints to its origin. *Geofluids* **5**, 28-41.
- Morgan K, Jankowski J (2004) Saline groundwater seepage zones and their impact on soil and water resources in the Spicers Creek catchment, central west, New South Wales, Australia. *Environmental Geology* **46**, 273-285.
- Murray-Darling Basin Authority (2009) 'Water: River operations'. [http://www.mdba.gov.au/water/river\\_operations](http://www.mdba.gov.au/water/river_operations). Downloaded on 22nd April 2009 (Murray-Darling Basin Authority: Canberra).
- Musgrove M, Banner JL (1993) Regional groundwater-mixing and the origin of saline fluids: Midcontinent, United States. *Science* **259**, 1877-1882.
- New South Wales Environment Protection Agency (1994) 'Rainfall quality in the upper Hunter Valley' (NSW EPA: Chatswood).
- New South Wales Department of Environment, Climate Change, and Water (2009) 'Salinity audit: Upland catchments of the Murray-Darling Basin'. <http://www.environment.nsw.gov.au/resources/salinity/09153SalinityAudit.pdf> Downloaded on October 11<sup>th</sup> 2010 (NSW DECCW: Sydney).
- New South Wales Department of Natural Resources (2005) 'New South Wales Groundwater Works'. <http://www.waterinfo.nsw.gov.au/gw/index.html> Downloaded on April 10th 2007. (NSW DNR: Sydney).
- New South Wales Department of Water and Energy (2000) 'Wybong Creek @ Wybong Hydroplot V132'. <http://waterinfo.nsw.gov.au/cgi-bin/browNse.epl?site=210040>. Downloaded on 30<sup>th</sup> November 2009. (NSW DWE: Sydney).
- New South Wales Department of Water and Energy (2009) 'New South Wales river water quality'. <http://waterinfo.nsw.gov.au/cgi-bin/browNse.epl?site=210040>. Downloaded on 30<sup>th</sup> November 2009 (NSW DWE: Sydney).
- Northcote KH (1979) 'A factual key for the recognition of Australian soils'. (Rellim Technical Publications: Adelaide).
- Northcote KH, Skene JKM (1972) 'Australian soils with saline and sodic properties'. (CSIRO: Canberra).
- Odom IE (1984) Smectitic clay minerals: Properties and their uses. *Philosophical Transactions of the Royal Society of London. Series A, Mathematical and Physical Sciences* **311**, 391-409.
- Oster JD, Shainberg I (2001) Soil responses to sodicity and salinity: Challenges and responsibilities. *Australian Journal of Soil Research* **39**, 1219-1224.
- O'Shea B, Jankowski J (2006) Detecting subtle hydrochemical anomalies with multivariate statistics: An example from 'homogeneous' groundwaters in the Great Artesian Basin, Australia. *Hydrological Processes* **20**, 4317-4333.
- Papatheodorou G, Lambrakis N, Panagopoulos G (2007) Application of multivariate statistical procedures to the hydrochemical study of a coastal aquifer: An example from Crete, Greece. *Hydrological Processes* **21**, 1482-1495.
- Patchett A, Langford R (2005) 'New South Wales - Deep saline aquifer storage potential'. (CO2CRC/Geoscience Australia: Canberra).

- Petrides B, Cartwright I, Weaver TR (2006) The evolution of groundwater in the Tyrrell catchment, south-central Murray Basin, Victoria, Australia. *Hydrogeology Journal* **14**, 1522-1543.
- Peck AJ, Hatton T (2003). Salinity and the discharge of salts from catchments in Australia. *Journal of Hydrology* **272**, 191-202.
- Poulsen DL, Simmons CT, Le Galle La Salle C, Cox JW (2006) Assessing catchment-scale spatial and temporal patterns of groundwater and stream salinity. *Hydrogeology Journal* **14**, 1339-1359.
- Pigram JJ (1986) Salinity and basin management in Southeastern Australia. *Geographical Review* **76**, 249-264.
- Praamsma T, Novakowski K, Kyser K, Hall K (2009) Using stable isotopes and hydraulic head data to investigate groundwater recharge and discharge in a fractured rock aquifer. *Journal of Hydrology* **366**, 35-45.
- Radke B (1994) 'Quaternary carbonate "dust" deposits associated with springs in the Mendooran-Liverpool Plains area, western slopes, New South Wales'. (Australian Geological Survey Organisation: Canberra).
- Raine A (2000) 'State of the Hunter River'. (Hunter Catchment Management Trust: Branxton).
- Ranganathan V, Hanor JS (1989) Perched brine plumes above salt domes and dewatering of geopressured sediments. *Journal of Hydrology* **110**, 63-86.
- Rayment GE, Higginson FR (1992) 'Australian Laboratory Handbook of Soil and Water Chemical Methods'. (Inkata press: Melbourne).
- Razack M, Dazy J (1990) Hydrochemical characterization of groundwater mixing in sedimentary and metamorphic reservoirs with combined use of Piper's principle and factor analysis. *Journal of Hydrology* **114**, 371-393.
- Rengasamy P, Olsson KA (1991) Sodicity and soil structure. *Australian Journal of Soil Research* **29**, 935-952.
- Revel-Rolland M, De Deckker P, Delmonte B, Hesse PP, Magee JW, Basile-Doelsch I, Grousset F, Bosch D (2006) Eastern Australia: A possible source of dust in East Antarctica interglacial ice. *Earth and Planetary Science Letters* **249**, 1-13.
- Rhoades JD (1996) Salinity: Electrical conductivity and total dissolved solids. In 'Methods of soil analysis part 3: Chemical Methods'. (Eds. Sparks DL, Page AL, Helmke PA, Loepert RH, Soltanpour PN, Tabatabai MA, Johnston CT, Sumner ME). (Soil Science Society of America, Inc.: Madison).
- Rhoades JD, Kandiah A, Mashalli AM (1992) 'The use of saline waters for crop production - FAO irrigation and drainage paper 48'. (Food and Agricultural Organization of the United Nations: Rome).
- Robins L (2004) 'Dryland salinity and catchment management – A resource directory and action manual for catchment managers'. (CSIRO Land and Water: Australia).
- Robinson JB, Helyar KR (1996) Simulating the impact of acidifying farming systems on Australian soils. *Ecological Modelling* **86**, 207-211.
- Rose CW (2004) 'An introduction to the environmental physics of soil, water and watersheds.' (Cambridge University Press: Cambridge).
- Ringrose-Voase AJ, Young RR, Paydar Z, Huth NI, Bernadi AL, Cresswell HP, Keating BA, Scott JF, Stauffacher M, Banks RG, Holland JF, Johnston RM, Green TW, Gregory LJ, Daniells I, Farquharson R, Drinkwater RJ, Heidenreich S, Donaldson SG. (2003) 'Deep drainage under different land uses in the Liverpool Plains catchment.' (NSW Agriculture: Tamworth).

- Roy S, Gaillerdet J, Allègre CJ (1999) Geochemistry of dissolved and suspended loads of the Seine river, France: Anthropogenic impact, carbonate and silicate weathering. *Geochimica et Cosmochimica Acta* **63**, 1277-1292.
- Ruprecht JK, Schofield NJ (1991a) Effects of partial deforestation on hydrology and salinity in high salt storage landscapes. I. Extensive block clearing. *Journal of Hydrology* **129**, 19-38.
- Ruprecht JK, Schofield NJ (1991b) Effects of partial deforestation on hydrology and salinity in high salt storage landscapes. II. Strip, soils and parkland clearing. *Journal of Hydrology* **129**, 39-55.
- Salama RB, Farrington P, Bartle GA, Watson GD (1993a) The chemical evolution of groundwater in a first-order catchment and the process of salt accumulation in the soil profile. *Journal of Hydrology* **143**, 233-258.
- Salama RB, Farrington P, Bartle GA, Watson GD (1993b) Salinity trends in the wheatbelt of Western Australia: Results of water and salt balance studies from Cuballing catchment. *Journal of Hydrology* **145**, 41-63.
- Salama RB, Farrington P, Bartle GA, Watson GD (1993c) The role of geological structures and relict channels in the development of dryland salinity in the wheatbelt of Western Australia. *Australian Journal of Earth Sciences* **40**, 45-56.
- Salama RB, Otto CJ, Fitzpatrick RW (1999) Contributions of groundwater conditions to soil and water salinization. *Hydrogeology Journal* **7**, 46-64.
- Sandberg SK, Slater LD, Versteeg R (2002) An integrated geophysical investigation of the hydrogeology of an anisotropic unconfined aquifer. *Journal of Hydrology* **267**, 227-243.
- Schaefi B, Maraun D, Holschneider M (2007) What drives high flow events in the Swiss Alps? Recent developments in wavelet spectral analysis and their application to hydrology. *Advances in Water Resources* **30**, 2511-2525.
- Scheibner E (1998) 'Geology of New South Wales - Synthesis'. (Geological Survey of New South Wales: Canberra).
- Schön RW (1985) Petrology of the Liverpool Range Volcanics, eastern New South Wales. In 'Volcanism in eastern Australia: With case histories from New South Wales'. (Eds. Sutherland FL, Franklin BJ, Walther AE) pp. 73-85. (Geological Society of Australia, New South Wales division: Sydney).
- Sharma ML (1984) Evapotranspiration from a *Eucalyptus* community. *Agricultural Water Management* **8**, 41-56.
- Shumway RH (1988) 'Applied statistical time series analysis'. (Prentice Hall: Englewood Cliffs).
- Sikdar PK, Chakraborty S (2008) Genesis of arsenic in groundwater of North Bengal Plain using PCA: A case study of English Bazar Block, Malda District, West Bengal, India. *Hydrological Processes* **22**, 1796-1809.
- Singh KP, Malik A, Mohan D, Sinha S (2004) Multivariate statistical techniques for the evaluation of spatial and temporal variations in water quality of Gomti River (India)— A case study. *Water Research* **38**, 3980-3992.
- Simmons CT, Fenstemaker TR, Sharp Jr. JM (2001) Variable-density groundwater flow and solute transport in heterogeneous porous media: Approaches, resolutions and future challenges. *Journal of Contaminant Hydrology* **52**, 245-275.
- Smith JW, Gould KW, Rigby D (1982) The stable isotope geochemistry of Australian coal. *Organic Geochemistry* **3**, 111-131.
- Somerville P, White I, Beavis S, Macdonald B, Welch S (2006) 'Groundwater and stream water interactions in Widden Brook, Upper Hunter Valley, NSW'. (Goldschmidt Conference 2006: Melbourne).

- State Pollution Control Commission of New South Wales (1987) 'Air pollution from coal mining and related developments'. (SPCC NSW: Sydney).
- Stephenson GR, Zuzel JF (1981) Groundwater recharge characteristics in a semi-arid environment of southwest Idaho. *Journal of Hydrology* **53**, 213-227.
- Stonestrom DA, White AF, Akston KC (1998) Determining rates of chemical weathering in soils – solute transport versus profile evolution. *Journal of Hydrology* **209**, 331-345.
- Stuyfzand PJ (1998) Patterns in groundwater chemistry resulting from groundwater flow. *Hydrogeology Journal* **7**, 15-27.
- Suk H, Lee K-K (1999) Characterization of a ground water hydrochemical system through multivariate analysis: Clustering into ground water zones. *Ground Water* **37**, 358-367.
- Sultan M, Yan E, Sturchio N, Wagdy A, Abdel Galil K, Becker R, Manocha N, Milewski A (2007) Natural discharge: A key to sustainable utilization of fossil groundwater. *Journal of Hydrology* **335**, 25-36.
- Summerell GK, Tuteja NK, Grayson RB, Hairsine PB, Leaney F (2006) Contrasting mechanisms of salt delivery to the stream from three different landforms in South Eastern Australia. *Journal of Hydrology* **330**, 681-697.
- Sumner ME, Miller WP (1996) Cation exchange capacity and exchange coefficients. In 'Methods of soil analysis'. (Ed. Bigham JM). (Soil Science Society of America, Inc.: Madison, Wisconsin).
- Tadros NZ (1993) 'The Gunnedah Basin New South Wales'. (New South Wales Department of Mineral Resources: Sydney).
- Taylor RM, McKenzie RM, Fordham AW, Gillman GP (1983) Oxide minerals. In 'Soils: An Australian viewpoint'. (Eds. CSIRO Division of Soils). (CSIRO: Melbourne).
- Thomas GW (1996) Soil pH and soil acidity. In 'Methods of soil analysis part 3: Chemical methods'. (Eds. Sparks DL, Page AL, Helmke PA, Loepert RH, Soltanpour PN, Tabatabai MA, Johnston CT, Sumner ME). (Soil Science Society of America, Inc.: Madison).
- Thorn VC (2004) Phytolith evidence for C4-dominated grassland since the early Holocene at Long Pocket, northeast Queensland, Australia. *Quaternary Research* **61**, 168-180.
- Timms WA, Acworth RI (2005) Propagation of pressure change through thick clay sequences: An example from Liverpool Plains, NSW, Australia. *Hydrogeology Journal* **13**, 858-870.
- Tóth J (1995) Hydraulic continuity in large sedimentary basins. *Hydrogeology Journal* **3**, 4 -16.
- Turner JV, Barnes CJ (1998) Modeling of isotope and hydrogeochemical responses in catchment hydrology. In 'Isotope tracers in catchment hydrology'. (Eds. Kendall C, McDonnell JJ). (Elsevier, B.V.: Amsterdam).
- Tweed SO, Weaver TR, Cartwright I (2005) Distinguishing groundwater flow paths in different fractured-rock aquifers using groundwater chemistry: Dandenong Ranges, southeast Australia. *Hydrogeology Journal* **13**, 771-786.
- Uliana MM, Banner JL, Sharp Jr. JM (2007) Regional groundwater flow paths in Trans-Pecos, Texas inferred from oxygen, hydrogen, and strontium isotopes. *Journal of Hydrology* **334**, 334-346.
- Umwelt Environmental Consultants (2006) 'Anvil Hill project environmental assessment'. (Centennial Hunter Pty. Limited: Toronto).
- Usunoff EJ, Guzmán-Guzmán A (1989) Multivariate analysis in Hydrochemistry: An example of the use of factor and correspondence analyses. *Ground Water* **27**, 27-34.
- Van Camp M, Vauterin P (2005) Tsoft: graphical and interactive software for the analysis of time series and Earth tides. *Computers and Geosciences* **31**, 631-640.

- Von Asmuth JR, Knotters M (2004) Characterising groundwater dynamics based on a system identification approach. *Journal of Hydrology* **296**, 118-134.
- Walker PH, Chartres CJ, Hutka J (1988) The effect of aeolian accessions on soil development on granitic rocks in south-eastern Australia. I. Soil morphology and particle-size distributions. *Australian Journal of Soil Research* **26**, 1-16.
- Weight WD, Sonderegger JL (2000) 'Manual of applied field hydrogeology'. (McGraw-Hill: New York).
- Wetzel RG (2001) 'Limnology: Lake and river ecosystems'. (Academic Press: San Diego).
- Williams WD (1999) Salinisation: A major threat to water resources in the arid and semi-arid regions of the world. *Lakes and Reservoirs: Research and Management* **4**, 85-91.
- Williams WD (2001) Anthropogenic salinisation of inland waters. *Hydrobiologia* **466**, 329-337.
- Xia Y, Li H, Boufadel M, Guo Q, Li G (2007) Tidal wave propagation in a coastal aquifer: Effects of leakages through its submarine outlet-capping and offshore roof. *Journal of Hydrology* **337**, 249-247.



---

## **Appendix for Chapter Two –**

*Identification of solute sources to  
Wybong Creek*



Table A2.1. Cation detection limits and concentrations in blanks. BDL indicates where solute concentrations were below detection limit. N/A indicates samples were not analysed for the ion specified.

	Date (DD/MM/YYYY)	Al <sup>3+</sup> (mg L <sup>-1</sup> )	Ba <sup>2+</sup> (mg L <sup>-1</sup> )	Cd <sup>2+</sup> (mg L <sup>-1</sup> )	Ca <sup>2+</sup> (mg L <sup>-1</sup> )	Fe <sup>3+</sup> (mg L <sup>-1</sup> )	Mg <sup>2+</sup> (mg L <sup>-1</sup> )	K <sup>+</sup> (mg L <sup>-1</sup> )	Si <sup>4+</sup> (mg L <sup>-1</sup> )	Na <sup>+</sup> (mg L <sup>-1</sup> )	Sr <sup>2+</sup> (mg L <sup>-1</sup> )	Mn <sup>2+</sup> (mg L <sup>-1</sup> )	Zn <sup>2+</sup> (mg L <sup>-1</sup> )
Detection Limit		0.01	0.005	0.002	0.005	0.001	0.02	0.05	0.05	0.05	0.001	0.002	0.005
Field blank two	01/06/2007	0.040	0.019	0.0087	0.36	0.12	0.09	BDL	0.08	1.1	0.003	BDL	0.014
Travel Blank	03/07/2007	0.010	BDL	BDL	0.07	BDL	BDL	BDL	BDL	BDL	BDL	BDL	BDL
Field blank one	05/07/2007	0.010	BDL	BDL	BDL	BDL	BDL	0.21	BDL	BDL	BDL	BDL	BDL
Blank 11	16/07/2008	BDL	0.006	N/A	0.08	0.02	0.1	BDL	BDL	1.4	BDL	BDL	0.01
Blank 12	18/07/2008	BDL	0.17	N/A	0.07	BDL	0.03	BDL	BDL	0.08	BDL	BDL	0.03
Blank 13	24/07/2008	BDL	0.006	N/A	0.09	BDL	0.1	BDL	BDL	0.85	0.002	BDL	0.008
Blank 1	28/07/2008	BDL	0.011	N/A	0.7	BDL	0.63	BDL	BDL	0.93	0.004	BDL	0.043

Table A2.2. Anion detection limits and concentrations in blanks. BDL indicates where solute concentrations were below detection limit. N/A indicates samples were not analysed for the ion specified.

	Date (DD/MM/YYYY)	F (mg L <sup>-1</sup> )	Cl (mg L <sup>-1</sup> )	Br (mg L <sup>-1</sup> )	SO <sub>4</sub> (mg L <sup>-1</sup> )	S <sup>2-</sup> (mg L <sup>-1</sup> )	HCO <sub>3</sub> (mg L <sup>-1</sup> )	NO <sub>3</sub> (mg L <sup>-1</sup> )	PO <sub>4</sub> (mg L <sup>-1</sup> )
Detection Limit		0.1	0.5	0.2	0.5	0.005	0.5	0.5	0.02
Field blank two	01/06/2007	BDL	BDL	N/A	BDL	N/A	N/A	BDL	N/A
Travel Blank	03/07/2007	BDL	BDL	N/A	BDL	N/A	N/A	BDL	N/A
Field blank one	05/07/2007	BDL	BDL	N/A	BDL	N/A	N/A	BDL	N/A
Blank 11	16/07/2008	BDL	BDL	BDL	BDL	N/A	N/A	N/A	N/A
Blank 12	18/07/2008	BDL	BDL	BDL	BDL	N/A	N/A	N/A	N/A
Blank 13	24/07/2008	BDL	BDL	BDL	BDL	N/A	N/A	N/A	N/A
Blank 1	28/07/2008	BDL	BDL	BDL	BDL	N/A	N/A	N/A	N/A

Table A2.3 (a). Water quality measurements of surface water samples from upper Wybong Creek surface water sampling sites.N/A indicate measurement was not conducted on this date.

Site	Latitude	Longitude	Date (DD/MM/YYYY)	EC ( $\mu\text{s cm}^{-1}$ )	pH	Temp. ( $^{\circ}\text{C}$ )	Redox (mV)	Flow ( $\text{m}^3 \text{s}^{-1}$ )	Salt load ( $\text{t day}^{-1}$ )	Charge balance (%)
11 km	-31.571819	150.321638	22/04/2006	814	8.0	19.3	110	N/A	N/A	3.3
			21/07/2006	723	8.3	11.4	164	N/A	N/A	-18.4
			01/06/2007	807	8.1	12.8	124	N/A	N/A	3.3
			06/07/2007	491	8.3	13.3	126	0.01	0.4	-4.9
			18/07/2008	517	8.3	11.7	120	0.77	27.8	20.0
			27/03/2009	666	8.3	23.6	N/A	0.30	16.4	N/A
			22/04/2006	863	8.3	19.5	110	N/A	N/A	1.9
			21/07/2006	821	8.0	13.8	172	N/A	N/A	0.7
			01/06/2007	835	8.2	12.4	110	N/A	N/A	0.7
			06/07/2007	689	8.3	12.4	190	0.24	19.4	-6.0
30 km	-32.158043	150.355016	18/07/2008	592	8.3	12.4	110	1.08	57.2	N/A
			27/03/2009	752	8.2	23.7	N/A	0.31	18.1	N/A
			22/04/2006	1160	8.0	19.6	110	N/A	N/A	0.7
			21/07/2006	1023	8.3	13.8	168	N/A	N/A	-0.5
			01/06/2007	1172	8.1	12.3	100	N/A	N/A	3.6
			06/07/2007	686	8.2	13.2	110	N/A	N/A	3.6
			18/07/2008	595	8.4	12.0	110	0.98	48.2	4.8
			27/03/2009	780	8.2	24.0	N/A	0.30	16.7	N/A
			20/01/2009	972	9.0	25.0	N/A	0.08	N/A	N/A
			Wybong upstream Cuan	150.392361						
48 km	-32.854780	150.392479	22/04/2006	1362	8.0	18.6	110	N/A	N/A	1.6
			21/07/2006	1230	8.3	13.6	185	N/A	N/A	-10.6
			01/06/2007	1294	7.9	12.2	122	N/A	N/A	-4.3
			05/07/2007	928	8.1	12.2	103	0.25	15.6	-8.0
			18/07/2008	674	8.5	12.1	110	0.98	43.9	1.0
			20/01/2009	1080	7.7	22.9	N/A	0.07	N/A	-0.1
			27/03/2009	973	8.1	25.3	N/A	0.47	31.6	N/A

Table A2.3 (b). Water quality measurements of surface water samples from lower Wybong Creek surface water sampling sites. N/A indicates measurement was not conducted on this date.

Site	Latitude	Longitude	Date (DD/MM/YYYY)	EC ( $\mu\text{s cm}^{-1}$ )	pH	Temp. ( $^{\circ}\text{C}$ )	Redox (mV)	Flow ( $\text{m}^3 \text{s}^{-1}$ )	Salt load ( $\text{t day}^{-1}$ )	Charge balance (%)
55 km	-32.114433	150.395336	01/06/2007	1463	8.3	13.6	85	N/A	N/A	-1.6
			05/07/2007	996	8.1	12.2	104	N/A	N/A	-8.0
			18/07/2008	740	8.6	12.8	110	1.24	54.7	0.6
			20/01/2009	1277	8.6	27.7	N/A	N/A	N/A	N/A
60 km	-32.131687	150.395744	22/04/2006	2660	7.7	20.2	110	N/A	N/A	-4.9
			21/07/2006	2181	7.8	14.8	202	N/A	N/A	-0.7
			01/06/2007	3290	7.6	12.5	145	N/A	N/A	-1.2
			05/07/2007	1044	8.4	13.5	94	0.37	24.3	-5.8
72 km	-32.167980	150.381028	18/07/2008	804	8.7	13.0	110	1.5	62.6	1.0
			20/01/2009	1757	7.5	22.6	N/A	0.3	N/A	N/A
			27/03/2009	1251	8.3	20.5	N/A	0.29	22.6	N/A
			21/07/2006	3140	6.8	17.7	188	N/A	N/A	N/A
77 km	-32.170238	150.385695	01/06/2007	4080	8.9	10.5	102	N/A	N/A	-0.7
			05/07/2007	1085	8.2	13.0	121	0.68	32.4	-7.9
			18/07/2008	911	8.6	12.0	110	0.8	74.6	0.3
			20/01/2009	1777	8.3	28.0	N/A	0.01	N/A	N/A
83 km	-32.165949	150.385316	27/03/2009	1440	8.3	22.2	N/A	0.29	25.3	N/A
			05/07/2007	1184	8.2	13.3	143	0.48	34.0	-7.9
			19/07/2008	999	8.5	12.9	110	1.7	118.1	0.8
			22/04/2006	4040	8.0	16.2	110	N/A	N/A	-5.2
87 km	-32.205853	150.374567	23/07/2006	3240	8.1	15.6	159	N/A	N/A	-3.7
			01/06/2007	4060	8.2	12.6	127	N/A	N/A	-0.2
			05/07/2007	1475	7.8	13.1	133	0.76	57.0	-4.6
			19/07/2008	1012	8.5	12.7	110	0.97	78.1	-2.1
87 km	-32.205853	150.374567	27/03/2009	1657	8.2	21.4	N/A	0.31	29.7	N/A
			22/04/2006	5270	7.4	16.4	110	N/A	N/A	1.4
			23/07/2006	4750	7.2	9.9	136	N/A	N/A	N/A
			01/06/2007	2180	8.4	17.7	100	N/A	N/A	-2.7
			05/07/2007	1243	7.9	11.9	227	N/A	N/A	-4.6
			18/06/2008	1142	8.5	13.0	110	N/A	N/A	3.0

Table A2.3 (c). Water quality measurements of surface water samples from Wybong Creek and Goulburn River tributaries. N/A indicates measurement was not conducted on this date.

Tributary	Site	Latitude	Longitude	Date (DD/MM/YYYY)	EC ( $\mu\text{s cm}^{-1}$ )	pH	Temp. ( $^{\circ}\text{C}$ )	Redox (mV)	Charge balance (%)
Wybong	Cuan Creek (Rosedale)	-31.582028	150.373595	21/07/2008	773	7.5	19.2	427	2.6
	Cuan Creek (Wybong Confluence)	-32.083569	150.393217	20/01/2009	1306	8.3	22.8	N/A	-0.6
	Happy Valley Creek	-32.113348	150.402108	20/07/2008	1515	8.4	13.2	110	3.8
	Googe's Causeway 2	-32.113358	150.402108	20/07/2008	1029	8.5	12.8	110	26.1
	Manolobai (Site Four SW)	-32.719261	150.241632	20/07/2008	166.9	8.0	15.5	321	5.1
	Big Flat Creek	-32.154543	150.415045	20/01/2009	288.5	8.9	28.5	N/A	N/A
	Giants Creek	-32.171416	150.315642	21/07/2008	11850	8.5	N/A	110	1.4
	Sandy Creek	-32.154846	150.454300	21/07/2008	2650	8.2	9.6	110	2.5
	Spring Creek	-32.155277	150.443306	21/07/2008	5980	8.1	12.8	110	0.9
	Goulburn (Sandy Hollow)	-32.204593	150.342474	21/07/2008	1918	8.5	14.1	110	3.4
	Goulburn (Yarrawa)	-32.244322	150.381236	21/07/2008	1008	8.4	12.5	110	-1.7
					865	8.3	14.2	110	1.7

Table A2.3 (d). Water quality measurements of rainwater samples collected for this study. N/A indicates samples which were collected by HCR-CMA for which the specified parameters were not able to be measured.

Site	Latitude	Longitude	Date (DD/MM/YYYY)	EC ( $\mu\text{s cm}^{-1}$ )	pH	Charge balance (%)
Denman	32.233854	150.410608	07/06/2007	5.0	5.7	-59
Muswellbrook	-32.161054	150.534008	08/06/2007 03/09/2007 22/12/2007 19/01/2008	3.5 N/A N/A N/A	5.8 N/A N/A 7.1	-97 3.4 1.4 0.1
Wybong	-32.203349	150.383871	21/07/2008	33.1	7.1	-12.7
Wollombi	-32.553534	151.55990	25/07/2008 28/07/2008	28.3 25.1	8.9 7.7	5.6 -9.3

Table 2.4 (a). Cation concentrations in surface waters samples from sampling sites in the mid-upper Wybong Creek catchment. BDL indicates solute concentrations below detection limit N/A indicates samples were not collected for cation analyses on this date.

Table A2.4 (b). Cation concentrations in surface waters samples from sampling sites in the lower Wybong Creek catchment. BDL indicates solute concentrations below detection limit. N/A indicates samples were not collected for cation analyses on this date.

Site	Date (DD/MM/YYYY)	Na (mg L <sup>-1</sup> )	Ca (mg L <sup>-1</sup> )	Mg (mg L <sup>-1</sup> )	Fe <sup>2+</sup> (mg L <sup>-1</sup> )	Al (mg L <sup>-1</sup> )	Ba (mg L <sup>-1</sup> )	Mn (mg L <sup>-1</sup> )	K (mg L <sup>-1</sup> )	Si (mg L <sup>-1</sup> )	Sr (mg L <sup>-1</sup> )	Zn (mg L <sup>-1</sup> )	Ni (mg L <sup>-1</sup> )
60 km	22/04/2006	290	172	208	BDL	BDL	BDL	7.90	BDL	BDL	BDL	BDL	BDL
	21/07/2006	224	140	197	0.2	BDL	BDL	5.40	BDL	0.5	BDL	BDL	BDL
	01/06/2007	370	100	140	BDL	BDL	BDL	4.10	14.0	1.2	BDL	BDL	BDL
	05/07/2007	79	46	52	BDL	BDL	BDL	0.1	3.0	6.9	0.3	BDL	BDL
	18/07/2008	60	40	44	0.1	< BDL	0.1	BDL	2.0	8.8	0.3	BDL	BDL
	20/01/2009	N/A	N/A	N/A	N/A	N/A	N/A	N/A	N/A	N/A	N/A	N/A	N/A
	27/03/2009	N/A	N/A	N/A	N/A	N/A	N/A	N/A	N/A	N/A	N/A	N/A	N/A
	21/07/2006	277	107	286	0.2	BDL	BDL	BDL	5.1	4.0	0.8	BDL	BDL
	01/06/2007	350	160	250	BDL	BDL	0.2	BDL	7.3	6.2	1.5	BDL	BDL
	05/07/2007	92	49	54	BDL	BDL	BDL	0.1	3.4	6.8	0.4	BDL	BDL
72 km	18/07/2008	73	44	47	BDL	< BDL	BDL	BDL	2.2	8.3	0.3	BDL	BDL
	20/01/2009	N/A	N/A	N/A	N/A	N/A	N/A	N/A	N/A	N/A	N/A	N/A	N/A
	27/03/2009	N/A	N/A	N/A	N/A	N/A	N/A	N/A	N/A	N/A	N/A	N/A	N/A
	05/07/2007	93	48	55	BDL	BDL	BDL	0.1	3.3	6.7	0.4	BDL	BDL
77 km	19/07/2008	81	47	51	BDL	BDL	BDL	BDL	2.3	7.7	0.3	BDL	BDL
	22/04/2006	360	267	253	BDL	BDL	BDL	BDL	13.0	BDL	BDL	BDL	BDL
	23/07/2006	249	218	283	99.0	BDL	BDL	BDL	11.0	BDL	0.9	BDL	BDL
	01/06/2007	400	170	220	BDL	BDL	0.1	BDL	6.8	9.8	1.7	BDL	BDL
83 km	05/07/2007	110	45	55	0.3	0.1	BDL	BDL	0.2	5.0	7.4	0.4	BDL
	19/07/2008	93	49	53	BDL	BDL	BDL	BDL	2.7	8.0	0.4	BDL	BDL
	27/03/2009	N/A	N/A	N/A	N/A	N/A	N/A	N/A	N/A	N/A	N/A	N/A	N/A
	22/04/2006	467	361	292	0.8	BDL	BDL	BDL	17.0	BDL	BDL	BDL	BDL
87 km	23/07/2006	454	355	447	0.7	BDL	BDL	BDL	12.0	BDL	1.3	BDL	BDL
	01/06/2007	190	92	110	BDL	BDL	0.2	2.1	17.0	0.6	1.5	BDL	BDL
	05/07/2007	120	50	58	0.1	BDL	BDL	0.1	5.7	7.4	0.5	BDL	BDL
	18/06/2008	100	52	56	BDL	BDL	BDL	2.8	7.6	0.4	BDL	BDL	BDL

Table A2.4 (c). Cation concentrations in surface waters samples from sampling sites in Wybong Creek and Goulburn River tributaries. BDL indicates solute concentrations below detection limit. N/A indicates samples were not collected for cation analyses on this date.

System	Site	Date (DD/MM/ YYYY)	Na (mg L <sup>-1</sup> )	Ca (mg L <sup>-1</sup> )	Mg (mg L <sup>-1</sup> )	Fe <sup>2+</sup> (mg L <sup>-1</sup> )	Al (mg L <sup>-1</sup> )	Ba (mg L <sup>-1</sup> )	Mn (mg L <sup>-1</sup> )	K (mg L <sup>-1</sup> )	Si (mg L <sup>-1</sup> )	Sr (mg L <sup>-1</sup> )	Zn (mg L <sup>-1</sup> )	Ni (mg L <sup>-1</sup> )
Wybong	Cuan Ck (Rosedale)	21/07/2008	46	59	49	BDL	BDL	29.0	0.02	0.8	13.0	0.2	0.04	BDL
	Cuan Ck (Wybong Confluence)	20/01/2009	N/A	N/A	N/A	N/A	N/A	N/A	N/A	N/A	N/A	N/A	N/A	N/A
	Happy Valley Ck	20/07/2008	130	53	82	BDL	BDL	BDL	0.03	4.8	5.1	0.5	0.01	BDL
	Googe's Causeway 2	20/07/2008	150	87	190	0.1	BDL	BDL	0.01	1.9	8.7	0.5	0.01	BDL
	Manolobai (Site Four SW)	20/07/2008	17	3.8	3	BDL	0.9	0.1	0.03	8.9	3.2	0.0	0.03	BDL
	Big Flat Ck	21/07/2008	2000	67	330	0.1	0.2	0.1	0.10	17	5.0	5.1	0.02	BDL
Goulburn	Giants Ck	21/07/2008	350	66	140	BDL	BDL	0.1	0.08	13	3.2	1.0	0.05	BDL
	Sandy Ck	21/07/2008	880	110	200	0.1	BDL	0.3	0.20	8	5.4	2.1	0.02	BDL
	Spring Ck	21/07/2008	881	48.0	47	BDL	BDL	0.1	0.01	4.4	7.4	0.8	BDL	BDL
	Goulburn (Sandy Hollow)	21/07/2008	69	39	40	0.2	BDL	BDL	0.02	4.3	5.3	0.4	0.01	BDL
	Goulburn (Yarrawa)	21/07/2008	86	44	47	BDL	BDL	0.1	0.04	3.9	6.5	0.4	0.02	BDL

Table A2.4 (d). Cation concentrations in rainwater samples collected for this study. BDL indicates solute concentrations below detection limit. N/A indicates samples were not collected for cation analyses on this date.

Site	Date (DD/MM/YYYY)	Na (mg L <sup>-1</sup> )	Ca (mg L <sup>-1</sup> )	Mg (mg L <sup>-1</sup> )	Fe <sup>2+</sup> (mg L <sup>-1</sup> )	Al (mg L <sup>-1</sup> )	Ba (mg L <sup>-1</sup> )	Mn (mg L <sup>-1</sup> )	K (mg L <sup>-1</sup> )	Si (mg L <sup>-1</sup> )	Sr (mg L <sup>-1</sup> )	Zn (mg L <sup>-1</sup> )	Ni (mg L <sup>-1</sup> )
Denman	07/06/2007	0.7	0.2	0.1	BDL	BDL	BDL	0.1	BDL	BDL	BDL	BDL	BDL
	08/06/2007	0.1	0.1	BDL	BDL	BDL	BDL	BDL	BDL	BDL	BDL	BDL	BDL
Muswellbrook	03/09/2007	0.6	3.8	0.2	BDL	0.01	BDL	0.1	0.8	BDL	0.04	BDL	0.04
	22/12/2007	0.67	8.1	0.3	BDL	0.01	BDL	0.3	1.5	BDL	0.04	BDL	0.04
	19/01/2008	0.76	10	0.3	BDL	0.03	BDL	0.3	2.3	BDL	0.07	BDL	0.07
Wybong	21/07/2008	0.32	0.6	0.3	BDL	0.03	0.2	BDL	0.2	0.1	BDL	0.15	BDL

Table 2.5 (a). Anion concentrations from Wybong Creek surface water sampling sites in the mid-upper catchment. BDL indicates solute concentrations below detection limit. N/A indicates samples were not collected for cation analyses on this date.

Sample site	Date (DD/MM/ YYYY)	HCO <sub>3</sub> (mg L <sup>-1</sup> )	Cl (mg L <sup>-1</sup> )	F (mg L <sup>-1</sup> )	Br (mg L <sup>-1</sup> )	NO <sub>3</sub> (mg L <sup>-1</sup> )	SO <sub>4</sub> (mg L <sup>-1</sup> )	PO <sub>4</sub> (mg L <sup>-1</sup> )	
11 km	22/04/2006	464	32	BDL	0.2	0.4	7.8	N/A	
	21/07/2006	478	32	BDL	0.2	0.1	0.6	N/A	
	01/06/2007	494	36	0.1	0.2	0.1	8.8	N/A	
	06/07/2007	312	25	BDL	0.2	1.2	18	N/A	
	18/07/2008	179	22	BDL	0.2	0.8	13	0.9	
	27/03/2009	N/A	N/A	N/A	N/A	N/A	N/A	N/A	
	30 km	22/04/2006	474	45	BDL	0.2	0.2	5.9	N/A
37 km	21/07/2006	494	44	BDL	0.2	0.1	0.5	N/A	
	01/06/2007	514	46	0.1	0.2	0.1	8.6	N/A	
	06/07/2007	425	36	BDL	0.2	0.5	19.0	N/A	
	18/07/2008	312	27	BDL	0.2	0.6	0.7	0.7	
	27/03/2009	N/A	N/A	N/A	N/A	N/A	N/A	N/A	
	22/04/2006	548	94	BDL	0.2	0.1	5.9	N/A	
	21/07/2006	557	91	BDL	0.2	0.1	0.4	N/A	
Wybong upstream Cuan Confluence	01/06/2007	567	130	0.2	0.3	0.1	3.1	N/A	
	06/07/2007	376	46	0.1	0.2	0.1	17	N/A	
	18/07/2008	319	27	BDL	0.2	0.4	9.7	0.8	
	27/03/2009	548	94	BDL	0.2	0.1	5.9	N/A	
	20/01/2009	421	N/A	N/A	N/A	N/A	N/A	N/A	
	48 km	22/04/2006	477	182	BDL	0.2	0.1	0.4	N/A
	21/07/2006	75	206	BDL	0.2	0.1	0.2	N/A	
55 km	01/06/2007	497	210	0.1	0.6	0.1	4	N/A	
	05/07/2007	411	150	0.1	0.3	1.4	23	N/A	
	18/07/2008	333	52	BDL	0.2	1.1	11	0.7	
	20/01/2009	N/A	N/A	N/A	N/A	N/A	N/A	N/A	
	27/03/2009	N/A	N/A	N/A	N/A	N/A	N/A	N/A	
	01/06/2007	414	340	0.1	0.8	0.1	6.1	N/A	
	05/07/2007	403	170	BDL	0.2	0.1	25	N/A	
	18/07/2008	338	82	BDL	0.2	0.7	12	0.7	
	20/01/2009	N/A	N/A	N/A	N/A	N/A	N/A	N/A	

Table A2.5 (b). Anion concentrations in of lower Wybung Creek surface water samples. BDL indicates solute concentrations below detection limit. N/A indicates samples were not collected for cation analyses on this date.

Site	Date (DD/MM/ YYYY)	HCO <sub>3</sub> (mg L <sup>-1</sup> )	Cl (mg L <sup>-1</sup> )	F (mg L <sup>-1</sup> )	Br (mg L <sup>-1</sup> )	NO <sub>3</sub> (mg L <sup>-1</sup> )	SO <sub>4</sub> (mg L <sup>-1</sup> )	PO <sub>4</sub> (mg L <sup>-1</sup> )
60 km	22/04/2006	443	736	BDL	0.2	0.7	71	N/A
	21/07/2006	441	507	BDL	0.2	0.1	1	N/A
	01/06/2007	461	880	0.1	2.5	0.1	53	N/A
	05/07/2007	367	170	0.1	0.4	0.9	25	N/A
	18/07/2008	333	91	BDL	0.2	1.0	13	0.7
	20/01/2009	N/A	N/A	N/A	N/A	N/A	N/A	N/A
	27/03/2009	N/A	N/A	N/A	N/A	N/A	N/A	N/A
72 km	21/07/2006	432	848	BDL	0.2	0.1	1	N/A
	01/06/2007	441	1300	BDL	2.9	0.1	35	N/A
	05/07/2007	375	220	BDL	0.4	17.0	29	N/A
	18/07/2008	352	120	0.1	0.3	0.4	13	0.6
	20/01/2009	N/A	N/A	N/A	N/A	N/A	N/A	N/A
	27/03/2009	N/A	N/A	N/A	N/A	N/A	N/A	N/A
	77 km	5/07/2007	373	220	0.1	0.5	1.1	30
83 km	19/07/2008	351	140	BDL	0.4	0.3	14	0.6
	22/04/2006	448	1034	BDL	0.2	0.4	4	N/A
	23/07/2006	430	817	BDL	0.2	0.1	1	N/A
	01/06/2007	413	1300	0.1	3.3	0.1	42	N/A
	05/07/2007	314	240	BDL	0.5	1.4	44	N/A
	19/07/2008	336	180	BDL	0.4	0.2	17	0.6
	27/03/2009	N/A	N/A	N/A	N/A	N/A	N/A	N/A
87 km	22/04/2006	480	1415	BDL	0.2	0.2	71	N/A
	23/07/2006	422	1495	BDL	0.2	0.1	1	N/A
	01/06/2007	311	590	0.1	2.2	0.1	6	N/A
	05/07/2007	312	260	BDL	0.6	1.5	43	N/A
	18/06/2008	349	180	0.1	0.3	0.3	16	0.5

Table A2.5 (c). Water quality parameters of Wybong Creek and Goulburn River tributaries. BDL indicates solute concentrations below detection limit. N/A indicates samples were not collected for cation analyses on this date.

Tributary	Site	Date (DD/MM/ YYYY)	HCO <sub>3</sub> (mg L <sup>-1</sup> )	Cl (mg L <sup>-1</sup> )	F (mg L <sup>-1</sup> )	Br (mg L <sup>-1</sup> )	NO <sub>3</sub> (mg L <sup>-1</sup> )	SO <sub>4</sub> (mg L <sup>-1</sup> )	PO <sub>4</sub> (mg L <sup>-1</sup> )
Wybong	Cuan Ck (Rosedale)	21/07/2008	429	75	BDL	0.2	1.1	3.7	0.8
	Cuan Ck (Wybong Confluence)	20/01/2009	469	N/A	N/A	N/A	N/A	N/A	N/A
	Happy Valley Ck	20/07/2008	387	250	0.1	0.6	0.5	37	0.1
	Googe's Causeway 2	20/07/2008	236	410	0.1	2.1	1.4	10	BDL
	Manolobai (Site Four SW)	20/07/2008	28	22	BDL	0.2	0.1	18	BDL
	Big Flat Ck	21/07/2008	435	3500	BDL	6.9	0.8	430	BDL
	Giants Ck	21/07/2008	537	700	0.1	2.5	0.3	20	0.2
Goulburn	Sandy Ck	21/07/2008	634	1600	0.5	3.0	0.8	190	BDL
	Spring Ck	21/07/2008	321	390.0	0.2	1.6	0.8	0.4	BDL
	Goulburn (Sandy Hollow)	21/07/2008	279	130	BDL	0.3	1.0	25	0.3
	Goulburn (Yarrawa)	21/07/2008	271	170	BDL	0.4	0.4	24	0.3

Table A2.5 (d). Water quality parameters of rainwater samples collected for this study. N/A indicates samples which were collected by HCR-CMA and with some parameters not able to be measured.

Site	Date (DD/MM/YYYY)	HCO <sub>3</sub> (mg L <sup>-1</sup> )	Cl (mg L <sup>-1</sup> )	F (mg L <sup>-1</sup> )	Br (mg L <sup>-1</sup> )	NO <sub>3</sub> (mg L <sup>-1</sup> )	SO <sub>4</sub> (mg L <sup>-1</sup> )	PO <sub>4</sub> (mg L <sup>-1</sup> )
Denman	7/06/2007	N/A	0.4	BDL	BDL	BDL	0.4	BDL
	8/06/2007	N/A	0.4	BDL	BDL	BDL	0.4	BDL
Muswellbrook	03/09/2007	N/A	0.5	BDL	BDL	BDL	1.1	BDL
	22/12/2007	N/A	0.4	BDL	BDL	BDL	2.0	BDL
	19/01/2008	N/A	1.2	BDL	BDL	BDL	6.5	BDL
Wybong	21/07/2008	0.09	0.6	BDL	BDL	BDL	1.0	BDL
Wollemi	25/07/2008	0.18	3.9	BDL	BDL	BDL	0.6	BDL
Wollemi	28/07/2008	0.10	1.0	BDL	BDL	BDL	0.8	BDL

Table A2.6 (a). Parameters used for the calculation of evapoconcentration between surface water sampling sites along Wybong Creek on the 07/07/2007.

Sample site (07/07/2007)	Flow (m sec <sup>-1</sup> )	Distance from previous site (m)	Flow time between sites (s)	Flow time between sites (days)	Evaporation between sites (m)	Average site width (m)	Evaporation between sites (m <sup>3</sup> )	Evaporation between sites (L)
11 km	0.6	11000	18333	0.21	0.0004	5	21.0	21007
30 km	0.8	19000	24201	0.28	0.0050	3	28.7	28738
48 km	0.1	18000	137237	1.59	0.0029	10	535.2	535224
60 km	0.2	12000	56980	0.66	0.0012	8	114.0	113960
72 km	0.3	12000	37060	0.43	0.0008	5	46.3	46325
77 km	0.3	5000	14509	0.17	0.00003	8	12.7	12695
83 km	0.6	6000	9357	0.11	0.00002	4	4.7	4678

Table A2.6 (b). Parameters used for the calculation of evapoconcentration between surface water sampling sites at different sites along Wybong Creek on the 07/07/2007.

Site (07/07/2007)	Flow (m <sup>3</sup> s <sup>-1</sup> )	Flow (L s <sup>-1</sup> )	Flow (L day <sup>-1</sup> )	Evaporation between sites (L)	Measured TDS (mg L <sup>-1</sup> )	TDS increase between sites due to evaporation (mg L <sup>-1</sup> )	Evaporative increase in concentration (%)
11 km	0.01	10.4	896382	2.3	715	-	-
30 km	0.37	365	31542134	0.1	778	6.5	0.84
48 km	0.24	237	20506781	2.6	867	203	23
60 km	0.38	375	32440608	0.4	1821	30	1.7
72 km	0.44	443	38234333	0.1	2363	22	0.93
77 km	0.47	474	40956365	0.0	2318	7	0.32
83 km	0.80	802	69255043	0.0	2539	1.6	0.06

Table A2.7. Isotopic data for rainwater and surface water samples from sites in Wybong Creek.  
 Oxygen and H isotope analyses done by H. Stuart-Williams and C. Keitel. N/A indicates the sample was not analysed for this parameter.

Site name	Date	$\delta^2\text{H}$	$\delta^{18}\text{O}$
Muswellbrook rainwater	03/09/2007	-48.7418	-7.5951
	19/01/2008	-0.6485	4.8024
	22/12/2007	-34.6606	-6.1227
Denman rain	06/06/2007		
Wybong rain	21/07/2008	-5.5118	-2.3968
<hr/>			
11 km	21/07/2006	-27.9084	-5.1627
	05/07/2007	N/A	N/A
30 km	21/07/2006	-24.9658	-3.8168
37 km	21/07/2006	N/A	N/A
48 km	21/07/2006	N/A	N/A
60 km	21/07/2006	N/A	N/A
72 km	21/07/2006	-5.7584	-29.8306
	05/07/2007	N/A	N/A
83 km	23/07/2006	-4.5913	-29.7651
87 km	21/07/2006	-10.9900	-0.87940

---

**Appendix for Chapter Three –**

*Aquifers and groundwater bodies in  
the Wybong Creek catchment*



Table A3.1. Cation detection limits and concentrations in blanks. BDL indicates where solute concentrations were below detection limit. N/A indicates samples were not analysed for the ion specified.

	Date (DD/MM/YYYY)	$\text{Al}^{3+}$ (mg L <sup>-1</sup> )	$\text{Ba}^{2+}$ (mg L <sup>-1</sup> )	$\text{Cd}^{2+}$ (mg L <sup>-1</sup> )	$\text{Ca}^{2+}$ (mg L <sup>-1</sup> )	$\text{Fe}^{3+}$ (mg L <sup>-1</sup> )	$\text{Mg}^{2+}$ (mg L <sup>-1</sup> )	$\text{K}^+$ (mg L <sup>-1</sup> )	$\text{Si}^{4+}$ (mg L <sup>-1</sup> )	$\text{Na}^+$ (mg L <sup>-1</sup> )	$\text{Sr}^{2+}$ (mg L <sup>-1</sup> )	$\text{Mn}^{2+}$ (mg L <sup>-1</sup> )	$\text{Zn}^{2+}$ (mg L <sup>-1</sup> )
Detection Limit	0.01	0.005	0.002	0.005	0.001	0.001	0.02	0.05	0.05	0.05	0.001	0.002	0.005
Field blank two	01/06/2007	0.040	0.019	0.0087	0.36	0.12	0.09	BDL	0.08	1.1	0.003	BDL	0.014
Travel Blank	03/07/2007	0.010	BDL	BDL	0.07	BDL	BDL	BDL	BDL	BDL	BDL	BDL	BDL
Field blank one	05/07/2007	0.010	BDL	BDL	BDL	BDL	BDL	0.21	BDL	BDL	BDL	BDL	BDL
Blank 11	16/07/2008	BDL	0.006	N/A	0.08	0.02	0.1	BDL	BDL	1.4	BDL	BDL	0.01
Blank 12	18/07/2008	BDL	0.17	N/A	0.07	BDL	0.03	BDL	BDL	0.08	BDL	BDL	0.03
Blank 13	24/07/2008	BDL	0.006	N/A	0.09	BDL	0.1	BDL	BDL	0.85	0.002	BDL	0.008
Blank 1	28/07/2008	BDL	0.011	N/A	0.7	BDL	0.6	BDL	BDL	0.93	0.004	BDL	0.043
Blank	20/01/2009	BDL	BDL	N/A	BDL	BDL	BDL	BDL	BDL	0.2	BDL	BDL	BDL
Blank	27/03/2009	BDL	BDL	N/A	0.2	BDL	0.6	0.2	BDL	1.8	BDL	BDL	0.002

Table A3.2. Anion detection limits and concentrations in blanks. BDL indicates where solute concentrations were below detection limit. N/A indicates samples were not analysed for the ion specified.

	Date (DD/MM/YYYY)	F (mg L <sup>-1</sup> )	Cl (mg L <sup>-1</sup> )	Br (mg L <sup>-1</sup> )	SO <sub>4</sub> (mg L <sup>-1</sup> )	S <sup>2-</sup> (mg L <sup>-1</sup> )	HCO <sub>3</sub> (mg L <sup>-1</sup> )	NO <sub>3</sub> (mg L <sup>-1</sup> )	PO <sub>4</sub> (mg L <sup>-1</sup> )
Detection Limit		0.1	0.5	0.2	0.5	0.005	0.5	0.5	0.02
Field blank two	01/06/2007	BDL	BDL	N/A	BDL	N/A	N/A	BDL	N/A
Travel Blank	03/07/2007	BDL	BDL	N/A	BDL	N/A	N/A	BDL	N/A
Field blank one	05/07/2007	BDL	BDL	N/A	BDL	N/A	N/A	BDL	N/A
Blank 11	16/07/2008	BDL	BDL	BDL	BDL	N/A	N/A	N/A	N/A
Blank 12	18/07/2008	BDL	BDL	BDL	BDL	N/A	N/A	N/A	N/A
Blank 13	24/07/2008	BDL	BDL	BDL	BDL	N/A	N/A	N/A	N/A
Blank 1	28/07/2008	BDL	BDL	BDL	BDL	N/A	N/A	N/A	N/A
Blank	20/01/2009	BDL	BDL	BDL	BDL	N/A	N/A	N/A	N/A
Blank	27/03/2009	0.2	2.4	BDL	BDL	N/A	N/A	BDL	BDL

Table 3.3 (a). Water quality data for groundwater sampled from bores. Total dissolved solids (TDS) is the sum of all cation and anion concentrations in the sample. N/A indicates SWL was unable to be measured due to irrigation pumps in the bores.

GW number	Site	Sample date (DD/MM/YYYY)	SWL (AHD)	EC ( $\mu\text{s cm}^{-1}$ )	pH	Temp. (°C)	TDS ( $\text{mg L}^{-1}$ )	Charge balance (%)
GW080595	Ether's #1	25/04/2006	269.0	666	8.0	20	695	12.8
		21/07/2006	261.0	749	8.0	16	615	11.3
		21/07/2008	267.0	914	7.0	19	764	-2.0
No number	Ether's #2	07/06/2007	N/A	752	7.8	16	655	2.8
		21/07/2007	N/A	768	7.5	18	779	15.5
GW038293	Roach's #1	22/07/2006	201.3	2440	7.1	21	1453	13.5
		21/07/2008	207.7	2252	7.4	21	1839	9.6
GW080943	Roach's #2	22/07/2006	206.7	1789	7.5	21	1811	7.0
GW061136	Queen St	22/07/2006	N/A	1228	7.2	19	1061	-26.2
No number	Darts Pivot	21/07/2008	300	1252	7.0	18	1030	-1.2
GW063952	Woodlands Grove Bore	21/07/2008	N/A	1628	7.0	18	1119	-4.0
No number	Woodlands Grove Windmill	21/07/2008	215.0	1380	7.7	14	1035	-2.1
GW017391	Wick's Cuan Ck	21/07/2006	228.2	1950	7.6	16	1877	
		21/07/2008	271.1	799	7.9	11	680	17.1
			N/A	773	7.5	19	634	1.7
GW025789	Googe's Well	21/07/2008	171.1	1364	7.5	19	927	-1.2
GW047877	Robert's House	25/04/2006	N/A	3130	7.6	20	2176	-0.4
		23/07/2006	N/A	5000	7.2	16	2003	-12.8
				5382	6.9	20	3150	-13.8
		02/06/2007	166.5	1740	7.5	22	1759	-2.1
		29/07/2008	169.1	6060	6.9	20	3718	0.3
GW080434	Wybong Bridge	25/04/2006	132.8	1115	7.5	22	1713	-40.0
		06/06/2007	132.7	1019	7.5	19	1260	-17.1
		21/07/2008	133.7	3090	7.3	23	4294	-0.3
GW040960	Frenchies	25/04/2006	114.2	9130	7.2	18	5411	3.2
		06/06/2007	114.2	5920	7.3	17	3286	5.6
		21/07/2008	115.9					-2.6

Table A3.3 (b). Water quality data for groundwater sampled from bores. Total dissolved solids (TDS) is the sum of all cation and anion concentrations in the sample. N/A indicated SWL was unable to be measured due to irrigation pumps in the bores.

GW number	Site	Sample date (DD/MM/YYYY)	SWL (AHD)	EC ( $\mu\text{s cm}^{-1}$ )	pH	Temp. ( $^{\circ}\text{C}$ )	TDS (mg L $^{-1}$ )	Charge balance (%)
GW080946	Rockhall Riverflats	23/07/2006	141.1	2380	7.6	21	1509	6.3
		06/06/2007	138.0	2530	7.6	20	2087	9.6
GW080947	Rockhall North	17/07/2008	137.9	2668	7.4	19	1706	2.1
GW080948	Rockhall Hayshed	06/06/2007	141.4	2790	7.3	20	1683	0.1
GW080945	Rockhall Old Hayshed	17/07/2008	142.4	3330	7.2	20	1905	-1.1
GW080944	Hannah's	06/06/2007	143.8	5950	6.8	21	3533	-2.4
		17/07/2008	144.6	6090	6.9	19	3638	-1.7
GW035173	Yarraman Well	06/06/2007	141.1	3310	7.4	21	2571	-0.2
		17/07/2008	142.0	3590	7.7	19	2506	-0.1
GW200417	Yarraman Bore	22/07/2006	167.4	9000	6.9	21	5204	-0.4
		16/07/2008	162.8	10780	7.1	20	6130	-1.0
GW056645	Rossgole Bore #2	17/07/2008	135.5	3560	7.3	19	2053	-0.9
GW045179	Coffin Gully Bore	27/03/2009	141.6	2945	7.3	20	1810	-17.6
		N/A	2800	6.7	19	1629	-3.2	
		27/03/2009	N/A	4840	6.9	20	2032	-14.3

Table A3.3 (c). Water quality data for groundwater sampled from piezometers. Total dissolved solids (TDS) is the sum of all cation and anion concentrations in the sample.

	Site	Sample date (DD/MM/YYYY)	SWL (AHD)	EC ( $\mu\text{s cm}^{-1}$ )	pH	Temp. ( $^{\circ}\text{C}$ )	TDS ( $\text{mg L}^{-1}$ )	Charge balance (%)
Piezo	Robert's #1	25/04/2006	168.0	7470	7.5	23	6676	-10.5
		02/06/2007	171.0	11600	7.7	21	5728	-8.4
Morgan's		25/04/2006	181.0	6920	7.3	23	8511	-1.4
		06/06/2007	179.2	15250	7.2	19	8484	-7.8
BFC TSR Deep		25/04/2006	143.2	5100	7.8	22	4778	-12.6
		06/06/2007	151.5	7830	7.9	19	4754	6.6
		17/07/2008	149.4	12580	7.7	12	5629	12.7
BFC TSR Shallow		17/07/2008	154.1	7660	8.3	14	6745	-2.9
PAH-039		24/03/2009	155.1	4390	6.6	21	2636	-7.1
PAH-025		24/03/2009	156.3	9310	6.8	21	4155	-14.7
CGN-148		24/03/2009	149.9	11330	6.5	21	4770	5.3
CGN-155		24/03/2009	153.6	18400	6.8	20	7064	-2.9
CALM-02		24/03/2009	142.2	32900	6.9	21	13601	-4.9
CGN-092		24/03/2009	150.5	25400	6.8	21	12805	-6.3
PAH-08		24/03/2009	155.1	7240	7.1	23	5151	-7.5

Table A3.3 (d). Water quality data for groundwater sampled from Manobalai piezometers.

Site	Sample date (DD/MM/YYYY)	SWL (AHD)	EC ( $\mu\text{s cm}^{-1}$ )	pH	Temp. (°C)	TDS ( $\text{mg L}^{-1}$ )	Charge balance (%)
Site One	19/02/2008	186.4	1850	7.3	23	1418	-1.8
	16/07/2008	186.2	1520	7.9	12	890	-1.3
Site Two Shallow	19/02/2008	178.0	11750	7.2	23	5897	-15.0
	15/07/2008	178.0	9230	7.1	18	5521	-1.0
Site Two Deep	19/01/2009	179.1	11590	7.1	21	6968	0.2
	19/02/2008	177.5	8660	7.3	23	5181	-0.4
Site Three	15/07/2008	179.4	7050	7.1	20	4343	-2.2
	19/01/2009	179.1	11120	7.1	25	7283	1.0
Site Four	16/07/2008	188.8	8660	6.5	17	4570	-0.9
	19/02/2008	188.8	8410	7.5	23	4573	-0.1
Site Six	16/07/2008	183.4	562	7.0	21	347	1.8
	19/01/2009	185.4	369	7.8	23	241	6.2
Site Eight Shallow	15/05/2009	168.5	2785	8.4	18	1721	-0.9
	15/05/2009	158.8	4740	8.3	21	2712	0.6
Site Eight Fractured	15/05/2009	158.7	4070	7.7	20	2477	1.1

Table A3.3 (e). Water quality data for groundwater collected from springs. N/A indicates the groundwater sampled was not analysed for the parameter specified.

Site	Sample date (DD/MM/YYYY)	SWL (AHD)	EC ( $\mu\text{s cm}^{-1}$ )	pH	Temp. (°C)	TDS ( $\text{mg L}^{-1}$ )	Charge balance (%)
Dry Creek Road Seep	05/06/2007	155.0	3850	7.7	N/A	4589	2.8
Yarraman Gauge Seep	05/07/2007	144.0	317	7.9	13	500	46.1
TSR Seep	05/07/2007	179.0	380	7.1	12	252	8.9
Whip Well	27/03/2009	225.0	190	6.5	22	224	5.5
Springs Spring	27/03/2009	467.0	1665	8.3	19	1061	-14.1
Dip Paddock Spring	27/03/2009	363.0	2020	7.9	19	1083	-17.7
Ray's Spring	24/03/2009	160.0	329	7.4	27	75	38.6

Table A3.4 (a). Anion concentrations in groundwater sampled from bores. BDL indicates ion concentrations below detection limit.

	Site	Sample date (DD/MM/YYYY)	TDS (mmol L <sup>-1</sup> )	Cl (mmol L <sup>-1</sup> )	HCO <sub>3</sub> (mmol L <sup>-1</sup> )	F (mmol L <sup>-1</sup> )	Br (mmol L <sup>-1</sup> )	NO <sub>3</sub> (mmol L <sup>-1</sup> )	SO <sub>4</sub> (mmol L <sup>-1</sup> )	PO <sub>4</sub> (mmol L <sup>-1</sup> )	0.0002
GW080595	Ether's #1	25/04/2006	15.97	1.4	7.23	BDL	BDL	0.008	0.437	BDL	
		21/07/2006	14.41	1.5	6.20	BDL	BDL		0.300	BDL	
		21/07/2008	20.88	1.0	8.77	BDL	BDL	0.008	4.372	BDL	
No number	Ether's #2	07/06/2007	17.98	1.8	6.38	BDL	BDL		2.123	BDL	
GW038293	Roach's #1	21/07/2006	34.09	1.5	6.11	BDL	BDL	0.013	1.998	0.002	
		21/07/2008	44.30	11.6	12.44	BDL	BDL		1.499	BDL	
GW080943	Roach's #2	22/07/2006	44.89	12.7	9.67	BDL	BDL		3.760	BDL	
GW061136	Queen St	22/07/2006	22.84	2.3	11.74	BDL	BDL		0.387	BDL	
		21/07/2008	22.16	1.6	11.92	0.008	BDL	0.023	0.005	0.011	
No number	Darts Pivot	21/07/2008	27.34	5.9	5.59	0.018	0.006	0.010	2.748	0.002	
GW063952	Woodlands Bore	21/07/2008	25.06	4.8	9.51	0.018	0.005	0.023	0.005	0.008	
No number	Woodlands WM	21/07/2008	41.18	8.2	9.51	0.012	0.009	0.023	7.494	0.008	
GW017391	Wick's Cuan Ck	21/07/2006	15.2	1.0	7.9	BDL	BDL		BDL	BDL	
GW025789	Googe's Well	21/07/2008	14.15	1.0	7.03	0.005	BDL	0.018	0.005	0.008	
GW047877	Robert's House	25/04/2006	57.60	35.4	8.43	BDL	BDL		N/A	0.005	0.007
		23/07/2006	54.11	32.5	8.79	BDL	BDL		N/A	0.005	BDL
		02/06/2007	99.66	48.0	N/A	0.053	0.071		BDL	3.622	BDL
GW080434	Wybong Bridge	29/07/2008	111.13	45.1	11.46	0.058	0.059	0.029	1.998	BDL	
		25/04/2006	56.42	11.5	6.87	BDL	BDL		0.005	BDL	
		06/06/2007	58.34	6.2	6.11	0.005	0.011		0.350	BDL	
		21/07/2008	33.31	12.7	6.85	BDL	BDL		0.008	0.312	0.005
GW040960	Frenchies	25/04/2006	131.94	63.5	9.43	BDL	BDL		0.250	BDL	
		06/06/2007	163.17	81.8	12.75	0.005	0.094		0.187	BDL	
		21/07/2008	100.43	45.1	8.70	0.010	0.048		0.026	0.005	0.112

Table A3.4 (b). Anion concentrations in groundwater sampled from bores. BDL indicates ion concentrations below detection limit. N/A indicates sample was not analysed for this anion.

Site	Sample date (DD/MM/YYYY)	TDS (mmol L <sup>-1</sup> )	Cl (mmol L <sup>-1</sup> )	HCO <sub>3</sub> (mmol L <sup>-1</sup> )	F (mmol L <sup>-1</sup> )	Br (mmol L <sup>-1</sup> )	NO <sub>3</sub> (mmol L <sup>-1</sup> )	SO <sub>4</sub> (mmol L <sup>-1</sup> )	PO <sub>4</sub> (mmol L <sup>-1</sup> )
GW080946 Rockhall Riverflats	23/07/2006	40.37	15.3	6.21	BDL	BDL	1.998		BDL
	06/06/2007	53.59	16.9	15.41	0.017	0.021	BDL	0.005	BDL
	17/07/2008	47.58	18.9	7.61	0.006	0.013	0.011	0.612	0.001
GW080947 Rockhall North	06/06/2007	46.83	20.0	7.51	0.007	0.029	BDL	0.005	BDL
	17/07/2008	53.76	24.3	7.39	BDL	0.026	0.008	0.005	0.006
GW080948 Rockhall Hayshed	06/06/2007	110.64	48.0	8.57	0.042	0.046	BDL	0.031	BDL
	17/07/2008	108.34	42.3	13.93	0.036	0.053	0.040	0.400	0.002
GW080945 Rockhall Old Hayshed	06/06/2007	66.33	18.3	18.16	0.014	0.036	0.006	1.249	BDL
	17/07/2008	67.11	21.2	16.59	0.006	0.028	0.056	0.137	0.001
GW080944 Hannah's	22/07/2006	162.89	74.2	12.16	BDL	N/A	BDL	0.212	BDL
	16/07/2008	195.22	93.1	9.85	0.028	0.125	0.052	0.525	0.007
GW035173 Yarraman Well	17/07/2008	58.86	25.7	7.75	0.008	0.021	0.010	0.107	0.002
GW200417 Yarraman Bore	17/07/2008	48.83	8.5	13.72	0.024	0.026	0.016	0.084	0.005
GW056645 Rossdale Bore No. 2	27/03/2009	42.18	16.02	10.07	0.01	0.02	0.01	0.16	BDL
GW045179 Coffin Gully Bore	27/03/2009	51.40	20.53	13.93	0.01	0.04	0.04	0.19	BDL

Table A3.4 (c). Anion concentrations in groundwater sampled from piezometers. BDL indicates ion concentrations below detection limit. N/A indicates sample was not analysed for this anion.

Site	Sample date (DD/MM/YYYY)	TDS (mmol L <sup>-1</sup> )	Cl (mmol L <sup>-1</sup> )	HCO <sub>3</sub> (mmol L <sup>-1</sup> )	F (mmol L <sup>-1</sup> )	Br (mmol L <sup>-1</sup> )	NO <sub>3</sub> (mmol L <sup>-1</sup> )	SO <sub>4</sub> (mmol L <sup>-1</sup> )	PO <sub>4</sub> (mmol L <sup>-1</sup> )
Robert's #1	25/04/2006	214.41	89.6	14.97	BDL	BDL	0.137	BDL	BDL
Morgan's	02/06/2007	193.94	95.9	N/A	0.012	0.116	0.005	0.005	BDL
	25/04/2006	262.83	121.0	19.87	BDL	BDL	1.124	BDL	BDL
BFC TSR Deep	06/06/2007	260.95	112.8	21.16	0.011	0.119	BDL	1.149	BDL
	25/04/2006	151.00	59.9	13.25	0.000	BDL	BDL	0.300	BDL
BFC TSR Shallow	06/06/2007	143.51	62.1	16.34	0.074	0.078	0.003	0.312	BDL
	17/07/2008	163.75	70.5	22.28	0.018	0.066	0.037	1.624	0.001
PAH-039	17/07/2008	214.84	95.9	11.84	BDL	0.096	BDL	1.624	BDL
	24/03/2009	68.86	27.11	13.84	0.02	0.02	0.49	0.93	BDL
PAH-025	24/03/2009	111.37	40.67	24.25	0.04	0.05	0.92	1.21	BDL
CGN-148	24/03/2009	140.45	55.74	14.96	0.03	0.06	0.05	2.34	BDL
CGN-155	24/03/2009	207.12	86.59	23.15	0.04	0.09	BDL	3.69	BDL
CALM-02	24/03/2009	421.29	216.79	16.16	0.05	0.31	BDL	5.90	BDL
CGN-092	24/03/2009	377.39	178.52	30.35	0.05	0.13	BDL	8.43	BDL
PAH-08	24/03/2009	142.02	42.68	34.64	0.14	0.03	BDL	0.15	BDL

Table A3.4 (d). Anion concentrations in groundwater sampled from bores and piezometers at Manobalai. BDL indicates ion concentrations below detection limit.

Site	Sample date (DD/MM/YYYY)	TDS (mmol L <sup>-1</sup> )	Cl (mmol L <sup>-1</sup> )	HCO <sub>3</sub> (mmol L <sup>-1</sup> )	F (mmol L <sup>-1</sup> )	Br (mmol L <sup>-1</sup> )	NO <sub>3</sub> (mmol L <sup>-1</sup> )	SO <sub>4</sub> (mmol L <sup>-1</sup> )	PO <sub>4</sub> (mmol L <sup>-1</sup> )
Site One	19/02/2008	43.44	17.21	4.84	0.039	0.023	BDL	0.005	BDL
	16/07/2008	26.53	9.59	3.88	0.021	0.014	BDL	0.017	BDL
Site Two Shallow	19/02/2008	185.38	76.16	13.95	BDL	0.080	BDL	0.005	BDL
	15/07/2008	167.73	78.98	11.64	<0.01	0.002	0.013	1.874	0.001
Site Two Deep	19/01/2009	211.18	101.54	14.11	<0.01	0.108	BDL	2.498	BDL
	19/02/2008	159.73	78.98	10.23	BDL	0.089	BDL	0.175	BDL
	15/07/2008	133.82	64.87	9.07	BDL	0.061	0.016	0.005	0.001
Site Three	19/01/2009	221.09	107.18	15.51	BDL	0.115	BDL	1.923	BDL
	16/07/2008	150.77	76.16	2.21	BDL	0.096	0.044	0.187	0.002
Site Four	19/02/2008	151.20	76.19	2.21	BDL	0.098	0.044	0.019	0.002
	16/07/2008	9.57	2.68	1.89	0.016	0.004	BDL	0.150	0.066
Site Six	19/01/2009	5.84	0.73	2.25	BDL	BDL	0.100	BDL	
	15/05/2009	49.55	19.29	6.77	<0.01	0.020	<0.01	0.71	BDL
Site Eight Shallow	15/05/2009	79.79	34.39	8.34	<0.01	0.016	0.07	0.87	BDL
Site Eight Fractured	15/05/2009	71.52	29.85	8.28	<0.01	0.032	0.02	1.07	BDL

Table A3.4 (e). Anion concentrations in groundwater sampled from springs. BDL indicates ion concentrations below detection limit.

Site	Sample date (DD/MM/YYYY)	TDS (mmol L <sup>-1</sup> )	Cl (mmol L <sup>-1</sup> )	HCO <sub>3</sub> (mmol L <sup>-1</sup> )	F (mmol L <sup>-1</sup> )	Br (mmol L <sup>-1</sup> )	NO <sub>3</sub> (mmol L <sup>-1</sup> )	SO <sub>4</sub> (mmol L <sup>-1</sup> )	PO <sub>4</sub> (mmol L <sup>-1</sup> )
Dry Creek Road Seep	05/06/2007	143.58	67.7	8.05	0.058	0.074	0.14	1.624	BDL
Yarraman Gauge Seep	05/07/2007	10.01	1.1	6.15	BDL	0.002	BDL	0.237	BDL
TSR Seep	05/07/2007	6.16	1.7	1.48	BDL	0.002	0.15	0.387	BDL
Whip Well	27/03/2009	6.67	2.48	0.56	0.020	BDL	BDL	0.19	BDL
"Springs Paddock" Spring	27/03/2009	23.62	4.80	11.03	0.020	0.01	0.01	0.16	BDL
"Dip Paddock" Spring	27/03/2009	24.12	5.47	11.25	0.010	0.01	BDL	0.09	BDL
Ray's spring	24/03/2009	3.66	0.70	1.31	<0.01	<0.01	0.01	0.05	<0.001

Table A.3.5 (a). Cation concentrations in groundwater sampled from bores. BDL indicates ion concentrations below detection limit.

Site	Sample date (DD/MM/YYYY)	Na (mmol L <sup>-1</sup> )	Ca (mmol L <sup>-1</sup> )	Mg (mmol L <sup>-1</sup> )	Fe <sup>2+</sup> (mmol L <sup>-1</sup> )	Al (mmol L <sup>-1</sup> )	Ba (mmol L <sup>-1</sup> )	Mn (mmol L <sup>-1</sup> )	K (mmol L <sup>-1</sup> )	Si (mmol L <sup>-1</sup> )	Sr (mmol L <sup>-1</sup> )	Zn (mmol L <sup>-1</sup> )
Detection limit 2 × 10 <sup>-3</sup>	1 × 10 <sup>-4</sup>	8 × 10 <sup>-4</sup>	2 × 10 <sup>-5</sup>	4 × 10 <sup>-4</sup>	4 × 10 <sup>-5</sup>	1 × 10 <sup>-3</sup>	2 × 10 <sup>-3</sup>	1 × 10 <sup>-5</sup>	2 × 10 <sup>-3</sup>	1 × 10 <sup>-5</sup>	8 × 10 <sup>-5</sup>	BDL
GW080595 Ether's #1	25/04/06	5.698	0.399	0.370	0.00537	BDL	BDL	0.00036	0.05371	0.35606	0.00913	BDL
	21/07/06	5.220	0.449	0.206	BDL	BDL	0.00036	0.06394	0.46287	0.06685	0.00076	
	21/07/08	2.479	1.672	2.181	0.00143	0.00074	0.00371	0.00040	0.19694	0.20651	0.00365	0.00029
No number Ether's #2	07/06/07	6.525	0.499	0.235	0.00340	0.00037	0.00109	0.00036	0.17648	0.19583	0.00342	BDL
	21/07/07	6.525	0.524	0.230	0.00018	BDL	0.00393	0.00015	0.17392	0.22788	0.00354	0.00021
GW038293 Roach's #1	22/07/06	8.874	0.923	3.003	BDL	BDL	0.00018	0.10998	0.23500	0.00457	0.00138	
	21/07/08	10.874	1.896	4.526	0.00054	0.00074	0.00124	BDL	0.21484	0.46287	0.07799	0.00064
GW080943 Roach's #2	22/07/06	11.875	1.647	4.855	0.00090	BDL	BDL	0.00109	0.13044	0.27416	0.00571	0.00138
GW061136 Queen St	22/07/06	2.566	1.871	3.744	BDL	BDL	0.00018	0.04092	0.23144	0.00114	0.00138	
	21/07/08	2.349	2.171	3.580	BDL	0.00037	0.00095	0.00042	0.05627	0.42727	0.00262	0.00040
No number Dart's Pivot	21/07/08	6.960	1.821	3.415	0.00036	0.00148	0.00277	0.00082	0.56268	0.27060	0.00479	0.00084
GW063952 WL Bore	21/07/08	4.785	1.497	3.580	0.00036	BDL	0.00028	0.00003	0.03069	0.78332	0.00308	0.01498
No number WL WM	21/07/08	8.700	1.397	4.937	0.00036	BDL	0.00037	0.00309	0.14834	0.74772	0.00582	0.00443
GW017391 Wick's Cuan Ck	21/06/06	2.479	1.347	2.098	BDL	BDL	BDL	0.00512	0.39166	0.00114		
	21/07/08	2.349	1.223	1.728	0.00036	0.00185	0.00036	0.00003	0.00972	0.74772	0.00098	0.00084
GW025789 Googe's Well	21/07/08	3.958	1.896	3.127	0.00018	0.00074	0.00060	0.00004	0.05371	0.42727	0.00468	0.00043
GW047877 Robert's House	25/04/06	6.699	0.524	4.978	BDL	0.00037	BDL	0.00127	0.15857	0.14598	0.00457	BDL
	23/07/06	6.699	0.524	5.308	BDL	BDL	0.00073	0.16881	0.12106	0.00228	BDL	
	2/06/07	37.190	1.347	8.229	0.00161	0.00074	0.00109	0.00164	0.89518	0.28128	0.01484	0.00138
	29/07/08	42.193	0.898	7.817	0.00090	0.00111	0.00095	0.00120	1.07422	0.39166	0.01826	0.00061
GW080434 Wybong Bridge	25/04/06	31.057	2.171	3.785	0.00018	0.00037	BDL	0.00073	0.76730	0.21363	0.00913	0.00290
	06/06/07	40.888	1.198	2.263	BDL	0.00074	0.00007	0.00091	0.92076	0.35250	0.02625	BDL
	21/07/08	5.655	2.745	4.526	0.00072	0.00334	0.00058	0.00087	0.06650	0.42727	0.00810	0.00026
GW040960 Frenchies	25/04/06	46.455	4.217	6.953	0.00179	0.00037	BDL	0.01838	0.53711	0.53408	0.04908	BDL
	06/06/07	43.498	5.489	17.692	0.00967	0.00741	0.00117	0.01256	0.89518	0.67651	0.05250	0.00076
	21/07/08	33.928	2.745	8.640	0.00448	0.00185	0.00095	0.00473	0.51153	0.53408	0.02625	0.00049

Table A.3.5 (b). Cation concentrations in groundwater sampled from bores. BDL indicates ion concentrations below detection limit.

Site	Sample date	Na (mmol L <sup>-1</sup> )	Ca (mmol L <sup>-1</sup> )	Mg (mmol L <sup>-1</sup> )	Fe <sup>2+</sup> (mmol L <sup>-1</sup> )	Al (mmol L <sup>-1</sup> )	Ba (mmol L <sup>-1</sup> )	Mn (mmol L <sup>-1</sup> )	K (mmol L <sup>-1</sup> )	Si (mmol L <sup>-1</sup> )	Sr (mmol L <sup>-1</sup> )	Zn (mmol L <sup>-1</sup> )
GW080946 Rockhall RF	23/07/06	11.222	1.821	3.497	BDL	0.00074	0.00011	0.00983	0.14579	0.18871	0.00913	0.00076
	06/06/07	13.484	2.296	4.526	0.13072	0.10007	0.00095	0.02002	0.14323	0.49848	0.01484	0.00076
	17/07/08	13.484	2.320	4.114	0.00358	0.00519	0.00124	0.01656	0.14323	0.33113	0.01484	0.00063
GW080947 Rockhall North	06/06/07	9.134	3.244	6.172	0.00054	0.00111	0.00015	0.00728	0.11509	0.56969	0.01141	BDL
	17/07/08	10.439	3.992	6.994	0.00179	0.00148	0.00040	0.00003	0.12277	0.49848	0.01370	0.00046
GW080948 Rockhall Hayshed	06/06/07	42.628	1.547	8.229	0.03223	0.00037	0.00080	0.00655	1.30440	0.23500	0.01598	BDL
	17/07/08	40.888	1.597	7.406	0.03331	0.00148	0.00095	0.00764	1.35556	0.25636	0.01712	0.00050
GW080945 Old Hayshed	06/06/07	18.704	2.196	6.994	0.03223	0.00074	0.00066	0.01820	0.13300	0.42727	0.01712	BDL
	17/07/08	19.139	2.445	6.994	0.00054	0.00111	0.00124	0.01220	0.13556	0.39166	0.01940	0.00060
GW080944 Hannah's	22/07/06	63.072	1.821	10.409	BDL	0.00111	0.00005	0.00127	0.81845	0.21007	0.01598	0.00183
	16/07/08	73.946	1.622	14.400	0.00555	0.00445	0.00138	0.00218	1.04864	0.49848	0.02283	0.00061
GW035173 Yarraman Well	17/07/08	15.224	3.743	5.760	BDL	0.00111	0.00047	0.00098	0.12021	0.42727	0.01598	0.00086
GW200417 Yarraman Bore	17/07/08	18.704	1.647	4.937	0.00394	0.00037	0.00604	0.00182	0.99749	0.17803	0.01016	0.00066
GW056645 Rossdale Bore No. 2	27/03/09	6.786	3.094	5.842	BDL	0.00007	<0.00001	0.00002	0.14527	0.00024	0.01348	0.00018
GW045179 Coffin Gully Bore	27/03/09	7.047	2.014	7.488	BDL	0.00010	0.00002	0.09002	0.00022	0.01688	0.00185	

Table A.3.5 (c). Cation concentrations in groundwater sampled from piezometers. BDL indicates ion concentrations below detection limit.

	Sample date (DD/MM/YYYY)	Na (mmol L <sup>-1</sup> )	Ca (mmol L <sup>-1</sup> )	Mg (mmol L <sup>-1</sup> )	Fe <sup>2+</sup> (mmol L <sup>-1</sup> )	Al (mmol L <sup>-1</sup> )	Ba (mmol L <sup>-1</sup> )	Mn (mmol L <sup>-1</sup> )	K (mmol L <sup>-1</sup> )	Si (mmol L <sup>-1</sup> )	Sr (mmol L <sup>-1</sup> )	Zn (mmol L <sup>-1</sup> )
<b>Robert's #1</b>	25/04/2006	99.305	1.248	7.529	BDL	BDL	0.00564	1.09979	0.49848	0.03196	BDL	
	02/06/2007	78.296	1.198	16.458	0.02507	0.00852	0.00117	0.01038	1.09979	0.78332	0.02397	BDL
<b>Morgan's</b>	25/04/2006	104.960	4.641	8.476	BDL	BDL	0.01201	2.09728	0.42727	0.21685	BDL	
	06/06/07	86.995	6.737	29.212	0.01558	0.00852	0.00131	0.01129	1.84151	0.64090	0.21685	0.00122
<b>BFC TSR</b>	25/04/2006	70.205	0.773	5.308	0.00233	0.00185	BDL	0.00400	0.97191	0.26704	0.03196	BDL
	06/06/2007	56.547	0.699	6.172	0.00054	0.00111	0.00138	0.00055	0.86960	0.32401	0.02397	0.00917
	17/07/2008	60.897	0.798	5.760	0.00322	0.25944	0.00182	0.00837	0.81845	0.64090	0.02397	0.00096
<b>BFC TSR</b> Shallow	17/07/2008	91.345	1.747	11.109	BDL	0.02854	0.00371	0.05097	0.66499	0.39166	0.04337	0.00058
	24/03/2009	14.920	4.591	6.377	0.00806	0.00051	0.00005	0.00195	0.460378	0.00005	0.09975	0.00015
<b>PAH-039</b>	24/03/2009	37.277	1.395	5.143	BDL	0.00016	0.00001	0.00119	0.360629	0.00010	0.03994	0.00004
	24/03/2009	50.022	4.342	12.302	0.00734	0.00002	0.00001	0.00153	0.5678	0.00004	0.03844	0.00011
<b>CGN-155</b>	24/03/2009	75.686	1.939	15.100	0.02220	0.00030	0.00032	0.00468	0.782643	0.00003	0.03750	0.00012
	24/03/2009	140.497	4.167	35.754	BDL	0.00000	0.00003	0.00522	1.539709	BDL	0.11476	0.00052
<b>CALM-02</b>	24/03/2009	119.183	2.944	36.165	0.03904	0.00020	0.00001	0.00924	1.524363	BDL	0.05003	0.00015
	24/03/2009	61.332	0.709	1.765	0.00107	0.00012	0.00001	0.00020	0.552454	0.00013	0.03080	0.00016

Table A.3.5 (d). Cation concentrations in groundwater sampled from Manobalai piezometers. BDL indicates ion concentrations below detection limit.

Site	Sample date (DD/MM/YYYY)	Na (mmolL <sup>-1</sup> )	Ca (mmolL <sup>-1</sup> )	Mg (mmolL <sup>-1</sup> )	Fe2+ (mmolL <sup>-1</sup> )	Al (mmolL <sup>-1</sup> )	Ba (mmolL <sup>-1</sup> )	Mn (mmolL <sup>-1</sup> )	K (mmolL <sup>-1</sup> )	Si (mmolL <sup>-1</sup> )	Sr (mmolL <sup>-1</sup> )	Zn (mmolL <sup>-1</sup> )
Site One	19/02/2008	18.704	0.798	1.275	BDL	0.00074	0.00033	0.00455	0.07161	0.46287	0.00137	0.00006
	16/07/2008	11.309	0.374	0.905	BDL	0.00445	0.00146	0.00819	0.07929	0.31333	0.00205	0.00095
Site Two Shallow	19/02/2008	65.246	5.739	22.629	BDL	0.00222	0.00218	0.02184	0.94633	0.53408	0.06848	BDL
	15/07/2008	52.197	5.240	16.458	0.00734	0.01334	0.00371	0.05825	0.71614	0.46287	0.04908	0.00024
Site Two Deep	19/01/2009	63.507	6.487	21.395	BDL	0.00148	0.00393	0.06553	0.86960	0.51272	0.05935	BDL
	19/02/2008	47.847	4.741	16.458	BDL	0.00111	0.00211	0.04187	0.69057	0.42727	0.04793	0.00006
	15/07/2008	40.018	4.242	14.400	0.00197	0.00111	0.00350	0.08373	0.58826	0.39166	0.03995	0.01437
Site Three	19/01/2009	66.116	5.988	22.629	0.00609	0.00148	0.00612	0.09101	1.02306	0.44151	0.05935	BDL
	16/07/2008	60.897	1.173	7.817	0.01755	0.00111	0.00102	0.03276	0.79287	1.31741	0.00399	0.02599
	19/02/2008	60.897	1.248	8.229	BDL	0.00074	0.00080	0.03458	0.81845	1.38862	0.00411	0.02446
Site Four	16/07/2008	3.654	0.105	0.391	0.01970	0.04077	0.00044	0.00619	0.15346	0.39166	0.00047	0.00306
	19/01/2009	1.914	0.070	0.362	0.01791	0.01482	0.00082	0.00248	0.20973	0.17091	0.00048	0.00269
Site Six	15/05/2009	17.203	0.983	3.493	N/A	BDL	0.00020	0.00247	0.31465	0.75304	0.00830	BDL
Site Eight Shallow	15/05/2009	25.955	2.639	6.512	N/A	BDL	0.00054	0.00552	0.29247	0.65779	0.01896	BDL
Site Eight Fractured	15/05/2009	22.294	2.731	6.324	N/A	BDL	0.00144	0.04035	0.26618	0.59202	0.01754	BDL

Table A.3.5 (e). Cation concentrations in groundwater sampled from springs. BDL indicates ion concentrations below detection limit.

Site	Sample date (DD/MM/YYYY)	Na (mmolL <sup>-1</sup> )	Ca (mmolL <sup>-1</sup> )	Mg (mmolL <sup>-1</sup> )	Fe2+ (mmolL <sup>-1</sup> )	Al (mmolL <sup>-1</sup> )	Ba (mmolL <sup>-1</sup> )	Mn (mmolL <sup>-1</sup> )	K (mmolL <sup>-1</sup> )	Si (mmolL <sup>-1</sup> )	Sr (mmolL <sup>-1</sup> )	Zn (mmolL <sup>-1</sup> )
Dry Creek Rd Seep	05/06/2007	56.547	1.023	7.817	BDL	0.00074	0.00058	0.00003	0.35807	0.17447	0.02168	BDL
Yarraman Seep	05/07/2007	1.435	0.235	0.453	0.00179	0.00259	0.00007	0.00003	0.17392	0.24568	0.00228	BDL
TSR Seep	05/07/2007	1.348	0.167	0.741	BDL	0.02446	0.00022	0.00018	0.02046	0.17803	0.00114	BDL
Whip Well Springs Spring	27/03/2009	2.884	0.124	0.305	BDL	0.00102	<0.00001	0.00033	0.09386	0.00002	0.00044	0.00048
Dip Spring Ray's Spring	27/03/2009	2.958	1.235	3.349	BDL	0.00002	0.00001	0.00035	0.04245	0.00025	0.00457	0.00004
	24/03/2009	2.701	1.205	3.324	BDL	0.00031	<0.00001	0.00001	0.04654	0.00015	0.00582	0.00004
	1.040	0.125	0.293	BDL	0.0009	0.0000	0.0013	0.1281	0.0001	0.0015	BDL	

Table A3.6 (a). Isotope concentrations in groundwater sampled from selected bores. O and H isotopes analysed by C. Keitel and H. Stuart-Williams (RSBS, ANU); C isotopes analysed by S. Fallon (RSES, ANU); and Sr isotopes analyses by M. Norman (RSES, ANU). N/A indicates samples were not analysed for this parameter.

GW Number	Site name	Sample date (DD/MM/YYYY)	$\delta^{18}\text{O}$ ‰	$\delta^2\text{H}$ ‰	$^{14}\text{C}$ age (abp)	$\delta^{13}\text{C}$ ‰	$\delta^{34}\text{S}$ ‰	$^{87}\text{Sr}/^{86}\text{Sr}$	$^{87}\text{Sr}/^{86}\text{Sr}$ 2SE
GW080595	Ether's #1	25/04/2006	-5.27	-35.1579	N/A	N/A	N/A	N/A	N/A
		21/07/2006	N/A	N/A	8770	-9	N/A	N/A	N/A
No number	Ether's #2	07/06/2007	-6.24177	-38.9735	N/A	N/A	15.881	0.705637	0.00001
		21/07/2007	N/A	N/A	N/A	N/A	N/A	N/A	N/A
GW038293	Roach's #1	22/07/2006	-5.10102	-34.083	N/A	N/A	N/A	0.705473	0.00001
		21/07/2008	N/A	N/A	N/A	N/A	N/A	N/A	N/A
GW080943	Roach's #2	22/07/2006	-5.10067	-31.1419	N/A	2460	-6	11.891	N/A
GW061136	Queen St	22/07/2006	N/A	N/A	N/A	N/A	N/A	N/A	N/A
No number	Dart's Pivot	21/07/2008	N/A	N/A	N/A	N/A	N/A	N/A	N/A
	Woodlands	21/07/2008	-6.09325	-38.8996	N/A	N/A	13.082	0.706244	0.00001
GW063952	Grove Bore	21/07/2008	N/A	N/A	N/A	N/A	6.721	0.704488	0.00001
No number	Woodlands	21/07/2008	N/A	N/A	N/A	N/A	N/A	N/A	N/A
GW017391	Grove Windmill	06/06/2007	-4.91327	-33.8447	N/A	N/A	N/A	N/A	N/A
	Wick's Cuan Ck	21/07/2008	-5.64	-32.8322	N/A	N/A	N/A	0.703481	0.00001
GW025789	Googe's Well	21/07/2008	-3.47	-22.1057	N/A	N/A	N/A	N/A	N/A
GW047877	Robert's House	25/04/2006	N/A	N/A	N/A	N/A	N/A	0.706924	0.00001
		23/07/2006	-5.23737	-33.9374	N/A	N/A	N/A	N/A	N/A
GW080434	Wybong Bridge	02/06/2007	N/A	N/A	N/A	N/A	N/A	N/A	N/A
		29/07/2008	N/A	N/A	2290	-15	13.82	N/A	N/A
GW040960	Frenchies	25/04/2006	N/A	N/A	N/A	N/A	N/A	N/A	N/A
		06/06/2007	N/A	N/A	N/A	N/A	N/A	17.011	0.706650
		21/07/2008	N/A	N/A	N/A	N/A	N/A	N/A	N/A
		21/07/2008	N/A	N/A	N/A	N/A	N/A	N/A	N/A
					2400	-9			

Table A3.6 (b). Isotope concentrations in groundwater sampled from selected bores. O and H isotopes analysed by C. Keitel and H. Stuart-Williams (RSBS, ANU); C isotopes analysed by S. Fallon (RSES, ANU); and Sr isotopes analyses by M. Norman (RSES, ANU). N/A indicates samples were not analysed for this parameter.

GW Number	Site name	Sample date (DD/MM/YYYY)	$\delta^{18}\text{O}$ ‰	$\delta^2\text{H}$ ‰	$^{14}\text{C}$ age (abp)	$\delta^{13}\text{C}$ ‰	$\delta^{34}\text{S}$ ‰	$^{87}\text{Sr}/^{86}\text{Sr}$	$^{87}\text{Sr}/^{86}\text{Sr}$ 2SE
GW080946	Rockhall Riverflats	23/07/2006	N/A	N/A	N/A	N/A	N/A	N/A	N/A
		06/06/2007	-2.66302	-19.669	N/A	N/A	N/A	0.704982	0.00002
		17/07/2008	N/A	N/A	N/A	N/A	28.823		
GW080947	Rockhall North	06/06/2007	N/A	N/A	N/A	N/A	N/A	0.704285	0.00001
		17/07/2008	N/A	N/A	N/A	N/A	N/A		
GW080948	Rockhall Hayshed	06/06/2007	N/A	N/A	N/A	N/A	N/A	0.708120	0.00001
		17/07/2008	N/A	N/A	N/A	N/A	N/A		
GW080945	Rockhall Old Hayshed	06/06/2007	N/A	N/A	N/A	N/A	N/A	0.708088	0.00001
		17/07/2008	N/A	N/A	14130	-15	N/A		
		22/07/2006	N/A	N/A	N/A	N/A	N/A	N/A	N/A
GW080944	Hannah's	16/07/2008	-4.83	-33.3207	N/A	N/A	18.835	N/A	N/A
		17/07/2008	-3.64	-23.5702	N/A	N/A	16.537	N/A	N/A
GW035173	Yarraman Well	17/07/2008	-7.34	-44.3684	18700	-5	11.4	0.707451	0.00002
GW200417	Yarraman Bore	17/07/2008	N/A	N/A	N/A	N/A	N/A	N/A	N/A
GW056645	Rossgole Bore No. 2	27/03/2009							
GW045179	Coffin Gully Bore	27/03/2009	-5.50228	-34.1796	1320	-10	N/A	0.703442	0.00002

Isotope concentrations in groundwater sampled from selected piezometers. O and H isotopes analysed by C. Keitel and H. Stuart-Williams (RSBS, ANU); C isotopes analysed by S. Fallon (RSES, ANU); and Sr isotopes analysed by M. Norman (RSES, ANU). N/A indicates samples were not analysed for this parameter.

Site name	Sample date (DD/MM/YYYY)	$\delta^{18}\text{O}$ ‰	$\delta^2\text{H}$ ‰	$^{14}\text{C}$ age (abp)	$\delta^{13}\text{C}$ ‰	$\delta^{34}\text{S}$ ‰	$^{87}\text{Sr}/^{86}\text{Sr}$	$^{87}\text{Sr}/^{86}\text{Sr}$
Robert's #1	25/04/2006	N/A	N/A	N/A	N/A	N/A	N/A	N/A
	02/06/2007	N/A	N/A	N/A	N/A	N/A	N/A	N/A
Morgan's	25/04/2006	N/A	N/A	N/A	N/A	N/A	0.766811	0.00001
	06/06/2007	N/A	N/A	N/A	N/A	N/A	N/A	N/A
BFC TSR Deep	25/04/2006	N/A	N/A	N/A	N/A	N/A	N/A	N/A
	06/06/2007	N/A	N/A	N/A	N/A	N/A	0.707585	0.00002
BFC TSR Shallow	17/07/2008	N/A	N/A	N/A	N/A	11.899	N/A	N/A
	17/07/2008	N/A	N/A	N/A	N/A	27.49	N/A	N/A
PAH-039	24/03/2009	-6.03	-38.639	N/A	N/A	N/A	0.706206	0.00002
PAH-025	24/03/2009	N/A	N/A	N/A	N/A	N/A	N/A	N/A
CGN-148	24/03/2009	N/A	N/A	N/A	N/A	N/A	N/A	N/A
CGN-155	24/03/2009	N/A	N/A	N/A	N/A	N/A	N/A	N/A
CALM-02	24/03/2009	-4.03	-28.1794	50	-10	N/A	0.708098	0.00001
CGN-092	24/03/2009	N/A	N/A	N/A	N/A	N/A	N/A	N/A
PAH-08	24/03/2009	-6.67	42.3811	24360	5	N/A	0.706109	0.00001

Table A3.6 (d). Isotope concentrations in groundwater sampled from Manobalai piezometers. O and H isotopes analysed by C. Keitel and H. Stuart-Williams (RSBS, ANU); C isotopes analysed by S. Fallon (RSES, ANU); and Sr isotopes analysed by M. Norman (RSES, ANU). N/A indicates samples were not analysed for this parameter

Site name	Sample date (DD/MM/YYYY)	$\delta^{18}\text{O}$ ‰	$\delta^2\text{H}$ ‰	$^{14}\text{C}$ age (abp)	$\delta^{13}\text{C}$ ‰	$\delta^{34}\text{S}$ ‰	$^{87}\text{Sr}/^{86}\text{Sr}$	$^{87}\text{Sr}/^{86}\text{Sr}$ 2SE
Site One	19/02/2008	N/A	N/A	N/A	N/A	N/A	N/A	N/A
	16/07/2008	N/A	N/A	N/A	N/A	N/A	0.708440	0.00002
Site Two Shallow	19/02/2008	N/A	N/A	N/A	N/A	N/A	N/A	N/A
	15/07/2008	-5.98	-35.0159	1270	-6	17.532	0.707121	0.00001
Site Two Deep	19/01/2009	N/A	N/A	1350	-8	N/A	N/A	N/A
	19/02/2008	N/A	N/A	N/A	N/A	N/A	N/A	N/A
	15/07/2008	-4.76	-25.9564	N/A	N/A	22.624	0.707174	0.00002
Site Three	19/01/2009	N/A	N/A	N/A	N/A	N/A	N/A	N/A
	16/07/2008	N/A	N/A	410	-11	N/A	0.708712	0.00002
Site Four	19/02/2008	-4.99	-31.9713	N/A	N/A	17.825	0.708740	0.00001
	16/07/2008	-5.19	-32.4629	1170	-13	6.335	0.708779	0.0001
Site Six	19/01/2009	N/A	N/A	N/A	N/A	N/A	N/A	N/A
Site Eight Shallow	15/05/2009	-5.81	-36.5964	N/A	-12	N/A	0.704696	0.00001
Site Eight Fractured	15/05/2009	-5.20	-33.5695	1220	-8	N/A	0.707249	0.00001
	15/05/2009	-5.13	-32.5822	800	-6	N/A	0.704959	0.00002

Table A3.6 (e). Isotope concentrations in groundwater sampled from springs. O and H isotopes analysed by C. Keitel and H. Stuart-Williams (RSBS, ANU); C isotopes analysed by S. Fallon (RSES, ANU); and Sr isotopes analysed by M. Norman (RSES, ANU). N/A indicates samples were not analysed for this parameter.

Site name	Sample date (DD/MM/YYYY)	$\delta^{18}\text{O}$ ‰	$\delta^2\text{H}$ ‰	$^{14}\text{C}$ age (abp)	$\delta^{13}\text{C}$ ‰	$\delta^{34}\text{S}$ ‰	$^{87}\text{Sr}/^{86}\text{Sr}$	$^{87}\text{Sr}/^{86}\text{Sr}$ 2SE
Dry Creek Road Seep	05/06/2007	N/A	N/A	N/A	N/A	N/A	N/A	N/A
Yarraman Gauge Seep	05/07/2007	N/A	N/A	N/A	N/A	N/A	N/A	N/A
TSR Seep	05/07/2007	N/A	N/A	N/A	N/A	N/A	N/A	N/A
Whip Well	27/03/2009	-5.54	-33.4921	N/A	N/A	0.709446	0.00002	
"Springs Paddock" spring	27/03/2009	N/A	N/A	N/A	N/A	N/A	N/A	N/A
"Dip Paddock" spring	27/03/2009	N/A	N/A	N/A	N/A	N/A	N/A	N/A
Ray's spring	24/03/2009	N/A	N/A	N/A	N/A	N/A	N/A	N/A

---

## **Appendix for Chapter Five –**

*Causes of salinity at the Manobalai field site*



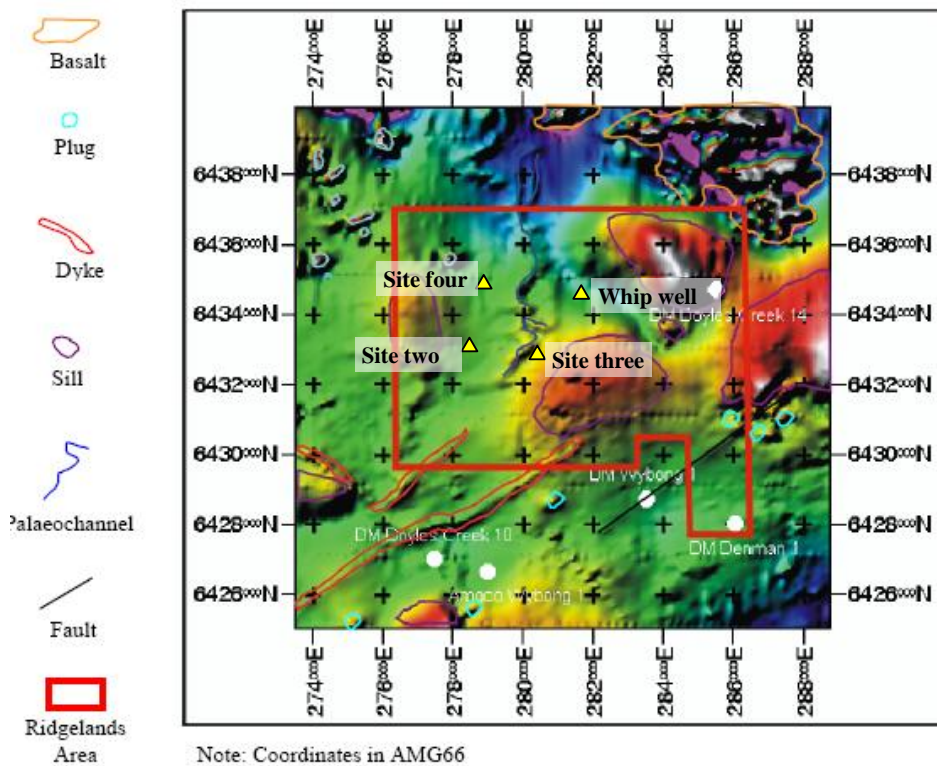


Figure A5.1. Aeomagnetic interpretation of the Manobalai field site (Brunton and Moore 2004). Note mapping coordinates for this image are in AMG66, not GDA94 as per other figures in this thesis.

Soil solute concentrations as a function of oven-dry soil weight were calculated using Eq. A5.1:

$$\text{TDS (mg kg}^{-1}\text{)} = \left( \left( \frac{C}{V} \right) / (125 \times w_a) \right) \times 1 + \left( 1 - \left( \frac{\frac{w_a}{100} \times w_o}{100} \right) \right) \quad (\text{A5.1})$$

where  $C$  is the ion concentration ( $\text{mg L}^{-1}$ ) in the soil-water 1:5 supernatant;  $V$  is the sample volume (L) added to the soil for the 1:5 soil-water extract;  $w_a$  is the weight (g) of air-dry soil in the 1:5 soil-water extract; and 125 converts 8 g of air-dried soil sample to 1 kg of soil. The right hand side of the equation corrects air-dry soil weights to oven-dry soil weights ( $w_o$ ).

Table A5.1 (a). Soil quality measurements of samples from Sites One and Two Deep, where TM indicates total soil moisture (%) and colour is defined based on Munsell's soil colour.

Site	Sample No.	Sample depth (m)	pH <sub>1:5</sub>	TM (%)	EC <sub>1:5</sub> ( $\mu\text{S cm}^{-1}$ )	Soil texture	Soil colour
One	83	0.0-0.5	7.6	9.9	16.0	Medium sandy loam	7.5YR 3/3
	84	0.5-1.0	7.6	13.5	83	Medium coarse sandy clay	2.5YR 3/6
	85	1.0-1.5	5.8	8.9	313	Medium sandy clay and sub-angular conglomerate fragments	2.5YR 3/6
	86	1.5-2.0	7.6	8.0	70	Medium sandy clay and sub-angular conglomerate fragments	N/A
	87	2.0-2.4	5.9	0.0	151	Conglomerate	N/A
Two Deep	1	0.0-0.5	7.3	6.4	60	Sand	10YR 6/2
	2	0.5-1.0	6.8	13.2	596	Loamy sand	10YR 5/2 (10YR 5/6)
	3	1.0-1.5	5.9	19.2	1196	Loamy sand	10YR 5/8 (6/10Y)
	4	1.5-2.0	7.4	18.4	670	Loamy sand	10YR 5/1 (10YR 5/8)
	5	2.0-2.5	6.6	15.9	528	Light clay	10YR 5/4 (10YR 5/1)
	6	2.5-3.0	6.5	10.7	366	Clayey sand	10YR 4/3
	7	3.0-3.5	6.1	11.2	250	Clayey sand	10YR 5/2 (10YR 4/6)
	8	3.5-4.0	6.7	10.2	302	Clayey sand	10YR 5/2 (10YR 4/3)
	9	4.0-4.5	7.2	10.6	218	Clayey sand	10YR 4/3
	10	4.5-5.0	6.3	14.9	388	Clay	10YR 5/4
	11	5.0-5.3	6.4	11.7	390	Clay	10YR 4/2
	12	5.3-5.5	6.8	36.4	406	Clay	10YR 4/4 (6/5GY)
	13	5.5-6.0	6.5	14.9	790	Sandy clay	10YR 4/4 (6/5GY)
	14	6.0-6.5	6.6	14.6	487	Sandy clay	10YR 5/3 (6/5GY)
	15	6.5-7.0	6.6	17.2	535	Sandy clay	7.5YR 5/3
	16	7.3-7.5	7.0	18.2	472	Sandy clay	6/5G (10YR 4/6)
	18	7.5-8.0	6.4	17.7	369	Sandy clay	10YR 4/6
	19	8.0-8.5	7.0	22.4	432	Sandy clay	10YR 5/4
	20	9.0-9.5	6.4	11.5	426	Sandy clay	10YR 6/1
	21	9.5-10.0	6.6	21.1	586	Sandy clay	10YR 4/6
	22	10.0-11.0	6.8	24.1	529	Platey clay	7/10 Y
	23	11.0-12.0	7.2	24.3	752	Silty clay	7/10 Y
	24	12.0-13.0	6.7	42.3	545	Sandy clay	10YR 4/6
	25	13.0-14.0	6.3	19.0	745	Sandy clay	10YR 4/6
	26	14.0-15.0	6.6	17.3	625	Clay	7.5YR 4/6
	27	15.0-16.0	6.5	15.4	543	Sandy clay	10YR 5/6

Table A5.1(b). Soil chemistry for quality measurements of samples from Sites Two Shallow and Three, where TM indicates total soil moisture (%) and colour is defined based on Munsell's soil colour.

Site	Sample No.	Sample depth (m)	pH <sub>1:5</sub>	TM (%)	EC <sub>1:5</sub> ( $\mu\text{S cm}^{-1}$ )	Soil texture	Soil colour
Two Shallow	28	0.0-1.0	6.9	12.9	554	Silty clay	10YR 4/6 (10YR 6/3)
	29	1.0-2.0	6.4	20.0	686	Clay	5Y5/2
	30	2.0-3.0	6.5	9.8	427	Clay	10YR 4/6
	31	3.0-4.0	7.2	10.0	245	Sandy clay	10YR 4/3
	32	4.0-5.0	6.7	15.4	208	Clayey sand	N/A
	33	5.0-6.0	6.5	61.1	521	Clayey sand	N/A
	34	6.0-7.0	6.8	19.2	421	Clayey sand	N/A
	35	7.0-7.5	6.6	17.5	668	Sandy clay	10YR 4/6
Three	36	7.5-8.0	6.5	12.9	563	Clay	
	37	0.00-0.50	6.8	14.0	14.0	Loamy clay	10YR 6/3
	38	0.50-1.00	7.7	11.6	11.6	Sandy clay loam	10YR 4/6
	39	1.00-1.50	8.1	12.9	12.9	Medium clay	10YR 5/6
	40	1.50-1.85	7.9	9.4	9.4	Light clay (sandy clay)	7.5YR 5/8 (7.5YR 7/1)
	41	1.85-2.00	8.1	10.0	10.0	Light clay (sandy clay)	7.5YR 4/6
	42	2.00-2.50	7.4	10.0	10.0	Light clay (sandy clay)	10YR 5/4
	43	2.50-2.75	8.0	8.4	8.4	Light clay (sandy clay)	10YR 6/1
	44	2.75-3.00	7.3	9.5	9.5	Light clay (sandy clay)	5YR 4/6
	45	3.00-3.50	6.6	8.2	8.2	Sandy clay loam	10YR 7.5YR 4/6
	46	3.50-4.00	6.5	13.6	13.6	Sandy clay loam	(10YR 6/2)
	47	4.00-4.50	5.6	11.4	11.4	Silty clay	10YR 6/8 (7/BG)
	48	4.50-5.00	5.8	6.7	6.7	Clayey sand	7.5YR 5/6
	49	5.00-5.40	5.8	7.2	7.2	Clayey sand	10YR 6/2 (10YR 5/8)

Table A5.1 (c). Soil quality measurements of samples from Sites Four and Five, where TM indicates total soil moisture (%) and colour is defined based on Munsell's soil colour.

	Sample No.	Sample depth (m)	pH <sub>1:5</sub>	TM (%)	EC <sub>1:5</sub> ( $\mu\text{S cm}^{-1}$ )	Soil texture	Soil colour
Site							
Four	51	0.00-0.25	6.8	13.2	42	Fine sandy loam	10YR 3/2
	52	0.25-0.50	6.8	19.4	51	Plastic clay	10YR 3/2, 10YR 6/1, Black streaks
	53	0.50-1.00	6.8	10.4	17.2	Clayey sand	10YR 6/2 (10YR 6/1)
	54	1.00-1.50	7.5	11.7	17.7	Clayey sand	10YR 5/3
	55	1.50-2.00	7.9	14.9	19.7	Clayey sand	10YR 4/2
	56	2.00-2.45	7.3	11.3	22.2	Clay	10YR 4/2
	57	2.45-3.00	7.5	14.9	31.9	Clay	10YR 4/2
	58	3.00-3.50	7.8	13.3	42.2	Coarse sandy clay/clayey sand	10YR 6/1 (5YR 5/8)
	59	3.50-4.00	8.0	19.4	82.1	Coarse sandy clay/clayey sand	10YR 6/1 (5YR 5/8)
	60	4.00-4.50	7.5	18.2	118.4	Very coarse sandy clay/clayey sand	7.5 YR 5/8
	61	4.50-5.50	8.5	40.0	126.7	Coarse sandy clay/clayey sand	7.5 YR 5/8
	62	5.50-6.00	7.8	14.5	269.0	Clayey sand/gravels	10YR 6/1 (5YR 5/8)
	63	6.00-6.50	7.5	13.6	358.0	Clayey sand/gravels	7.5YR 4/6
	64	6.50-7.00	7.4	14.1	430.0	Coarse sandy clay	7.5 R 5/8
	65	7.00-7.35	6.7	12.4	309.0	Coarse sandy clay	7.5YR 4/6
	66	7.35-7.50	7.4	19.5	261.7	Coarse sandy clay	10YR 6/1 (7.5YR 5/8)
	67	7.50-8.00	7.3	45.3	560.0	Coarse sandy clay	10YR 6/1 (7.5YR 5/8)
	68	8.00-8.50	7.5	17.7	520.0	Coarse sandy clay	10YR 6/1 (7.5YR 5/8)
	69	8.50-9.00	7.6	22.9	567.7	Coarse sandy clay	
	70	9.00-9.50	7.3	22.9	536.0	Coarse sandy clay	5YR 5/6
	71	9.50-10.50	7.9	15.6	459.3	Very coarse clayey sand	5YR 5/8, 7.5RR 5/6, 7.5RR 4/6
	72	10.50-11.50	7.3	15.6	531.0	Very coarse clayey sand	5YR 4/4
	73	11.50-12.50	7.2	13.2	510.0	Very coarse clayey sand	5YR 4/4
	74	12.50-13.50	6.8	14.7	859.0	Very coarse clayey sand	5YR 4/4
	75	13.50-14.50	6.9	17.0	588.0	Coarse sandy clay	10YR 6/1.(7.5YR 5/8)
	76	14.50-15.50	7.3	17.3	512.0	Conglomerate	10YR 6/1
	77	15.50-16.50	6.8	N/A	510.0	Conglomerate	
Five	78	0.00-0.50	6.9	7.6	14.85	Medium-coarse sandy loam	7.5YR 3/3
	79	0.50-1.00	6.7	16.2	15.7	Sandy clay	10YR 5/8
	80	1.00-1.50	7.3	6.8	52.6	Medium sandy loam	7.5YR 4/3
	81	1.50-2.00	9.2	10.2	208.7	Medium sandy loam	7.5YR 4/3
	82	2.00-2.75	9.4	5.2	156.1	Bedrock	10YR 7/3

Table A5.1 (d). Soil quality measurements of samples from sites Six, Seven and Eight, where TM indicates total soil moisture (%) and colour is defined based on Munsell's soil colour.

Site	Sample No.	Sample depth (m)	pH <sub>1:5</sub>	TM (%)	EC <sub>1:5</sub> ( $\mu\text{S cm}^{-1}$ )	Soil texture	Soil colour
Six	31	0.0 – 0.5	8.0	172	128.7	Sandy gravel	Yellow grey coloured gravel
	33	0.5 – 1.0	8.0	162	1066	Medium clay	Chocolate brown
	20	1.0 – 1.5	8.0	143	1225	Medium clay	Chocolate brown, black flecks
	1	1.5 – 2.0	8.8	130	216	Medium clay	Chocolate brown, black flecks
	25	2.0 – 2.5	8.9	193	328	Medium clay	Chocolate brown
	9	2.5 – 3.0	8.8	143	816	Medium clay	Chocolate brown
	34	3.0 – 4.0	8.8	141	169	Medium clay	Chocolate brown
	28	4.0 – 5.0	8.8	114	239	Medium clay	Chocolate brown
	26	5.0 – 6.0	8.1	197	405	Medium clay	Chocolate brown
	15	6.0 – 7.5	8.8	115	135	Medium clay	Chocolate brown
	11	7.5 – 9.0	9.1	216	184	Medium clay	Chocolate brown
	24	9.0 – 10.5	8.6	245	62	Medium clay	Chocolate brown
	21	10.5 – 11.8	8.7	196	154	Medium clay	Chocolate brown
	38	11.8 - 11.9	8.7	191	127	Medium clay	Chocolate brown
Seven	37	0.0 – 0.5	6.8	108	503	Medium clay	Chocolate brown
	29	0.5 – 0.7	8.1	139	541	Medium clay	Chocolate brown
	5	0.7- 1.0	8.6	165	709	Medium clay	Chocolate brown
	3	1.0 – 1.5	8.8	141	688	Medium clay	Chocolate brown
	2	1.5 – 2.0	9.6	120	267	Medium clay	Chocolate brown
	27	2.0 – 2.5	9.5	133	243	Medium clay	Chocolate brown
	30	2.5 – 3.0	9.6	139	231	Medium clay	Chocolate brown
	6	3.0 – 3.5	8.8	179	870	Medium clay	Chocolate brown
	10	3.5 – 4.0	8.9	243	382	Medium clay	Chocolate brown
	32	4.0 – 4.5	8.8	206	335	Medium clay	Chocolate brown
	7	4.5 – 5.5	9.0	206	483	Medium clay	Chocolate brown
	12	5.5 – 6.0	8.7	188	943	Medium clay	Chocolate brown
	14	6.0 – 7.5	8.7	279	1102	Medium clay	Chocolate brown
	4	7.5 – 8.2	9.2	176	520	Fine sandy gravel	Yellow grey coloured gravel
Eight shallow	17	0 – 0.5	8.2	155	112	Sandy gravel	Yellow grey coloured gravel
	19	0.5 – 1.5	7.9	226	22	Medium clay	Chocolate brown
	16	1.5 – 2.0	8.5	160	120	Medium clay	Chocolate brown
	8	2.0 – 2.5	8.1	239	173	Medium clay	Chocolate brown
	36	2.5 – 3.0	8.5	170	217	Medium clay	Chocolate brown
	22	3.0 – 4.0	8.7	131	261	Medium clay	Chocolate brown
	18	4.0 – 5.0	9.6	152	325	Medium clay	Chocolate brown
	23	5.0 – 6.0	9.0	141	359	Medium clay	Chocolate brown
	13	6.0 – 7.1	9.0	72	239	Medium clay	Chocolate brown
	35	7.1 – 7.2	8.8	117	115	Sandy gravel	Yellow grey, coloured gravel

Table A5.2 (a). Cation concentrations of select regolith samples from the Manobalai field site, with concentrations calculated as described in Eq. A5.1, where the mean of replicate samples is stated  $\pm$  the standard deviation. Ion concentrations below detection limits are denoted by BDL and N/A denotes measurement was either not undertaken or not able to be undertaken.

Site	Depth from (m)	Depth to (m)	Sample no.	Ba (mg kg <sup>-1</sup> )	Ca (mg kg <sup>-1</sup> )	Fe (mg kg <sup>-1</sup> )	K (mg kg <sup>-1</sup> )	Mg (mg kg <sup>-1</sup> )	Mn (mg kg <sup>-1</sup> )	Na (mg kg <sup>-1</sup> )	P (mg kg <sup>-1</sup> )	Sr (mg kg <sup>-1</sup> )
Two Deep	0.0	0.5	1	0.1	BDL	18	6	9	0.2	57	BDL	BDL
	0.5	1.0	3a	0.02	38	BDL	19	81	BDL	374	BDL	0.7
			3b	0.04	39	BDL	19	81	BDL	385	BDL	0.7
			3c	0.02	38	BDL	19	81	BDL	383	BDL	0.7
			3 (mean)	0.03 $\pm$ 0.01	38 $\pm$ 0.3	N/A	19 $\pm$ 0.13	81 $\pm$ 0.3	N/A	381 $\pm$ 6	N/A	0.7 $\pm$ 0.0
	1.5	2.0	4	<0.05	28	BDL	22	56	BDL	541	BDL	BDL
	4.0	4.5	9a	0.27	2.0	BDL	18	27	1.2	297	BDL	0.1
			9b	BDL	30	0.4	13	34	BDL	242	BDL	0.5
			9c	0.18	5.2	7.5	10	14	0.7	128	BDL	0.1
			9 (mean)	0.15 $\pm$ 0.14	12.5 $\pm$ 15.4	2.6 $\pm$ 4.2	14 $\pm$ 4.2	25 $\pm$ 10	0.6 $\pm$ 0.6	222 $\pm$ 86	N/A	0.2 $\pm$ 0.2
Two Shallow	5.5	6.0	13	0.1	13	BDL	24	95	BDL	541	BDL	0.7
	6.0	6.5	14	<0.05	1	BDL	18	48	BDL	396	BDL	0.3
	7.5	8.0	18	<0.05	26	2	13	21	BDL	305	BDL	0.1
	11.0	12.0	23	<0.05	23	BDL	28	59	BDL	620	BDL	0.6
Three	15.0	16.0	27	<0.05	13	BDL	19	38	BDL	433	BDL	0.3
	0.0	1.0	28	0.1	13	39	15	33	0.1	390	BDL	0.3
	4.0	5.0	32	0.1	1	35	14	23	0.3	187	BDL	0.1
	7.0	7.5	35	0.0	26	BDL	23	65	BDL	472	BDL	0.6
	8.0	8.5	37	0.9	23	236	32	38	1.0	22	BDL	0.4
Three	0.0	0.5	38	1.9	19	225	25	68	0.9	77	BDL	0.4

Table A5.2 (b). Cation concentrations of select regolith samples from the Manobalai field site, with concentrations calculated as described in Eq. A5.1, where the mean of replicate samples is stated  $\pm$  the standard deviation. Ion concentrations below detection limits are denoted by BDL and N/A denotes measurement was either not undertaken or not able to be undertaken.

Site	Depth from (m)	Depth to (m)	Sample no.	Ba (mg kg <sup>-1</sup> )	Ca (mg kg <sup>-1</sup> )	Fe (mg kg <sup>-1</sup> )	K (mg kg <sup>-1</sup> )	Mg (mg kg <sup>-1</sup> )	Mn (mg kg <sup>-1</sup> )	Na (mg kg <sup>-1</sup> )	P (mg kg <sup>-1</sup> )	Sr (mg kg <sup>-1</sup> )
Four	0.0	0.3	53	0.2	BDL	22	2	3	0.9	16	BDL	0.4
	5.5	6.0	64	2.6	11.1	404	71	220	0.8	495	BDL	BDL
	7.0	7.4	67	0.8	24.3	373	93	287	2.1	593	BDL	0.6
	8.0	8.5	70	0.5	BDL	220	42	70	2.2	450	BDL	0.7
	10.5	11.5	74	BDL	BDL	1	29	44	1.9	680	BDL	0.1
	15.2	16.0	79	0.4	BDL	24	4	8	0.0	44	BDL	BDL
Five	0.0	0.5	80	1.2	BDL	150	20	33	6.3	61	BDL	0.1
	0.5	1.0	81	1.2	30.8	515	56	193	4.9	249	BDL	0.9
	1.0	1.5	83	0.2	BDL	16	11	BDL	1.2	4	BDL	BDL
Six	0.5	1.0	S33	BDL	44.0	0.3	19	41	BDL	314	BDL	0.6
	1.0	1.5	S20	BDL	61.7	BDL	22	63	BDL	345	BDL	0.9
	3.0	4.0	S34a	0.02	8.3	6.7	6	13	0.18	51	BDL	0.1
			S34b	BDL	27.3	1.5	15	35	BDL	259	BDL	0.5
			S34								BDL	0.3 $\pm$ 0.2
	5.0	6.0	(mean)	0.01 $\pm$ 0.01	17.8 $\pm$ 13.5	4.1 $\pm$ 3.7	11 $\pm$ 6	24 $\pm$ 16	0.09 $\pm$ 0.13	155 $\pm$ 147	BDL	
			S26a	0.05	8.9	11.4	9	18	0.37	138	BDL	0.1
			S26b	0.05	10.4	3.8	10	19	0.35	158	BDL	0.2
7.5	9.0	S26	(mean)	0.05 $\pm$ 0.00	9.6 $\pm$ 1.0	7.6 $\pm$ 5.4	10 $\pm$ 1	18 $\pm$ 1	0.36 $\pm$ 0.01	148 $\pm$ 14	BDL	0.2
		S11	BDL	7.4	8.1		9	18	0.55	180	BDL	0.2

Table A5.3 (a). Anion concentrations of select regolith samples from the Manobalai field site, with concentrations calculated as described in Eq. A5.1, where the mean of replicate samples is stated  $\pm$  the standard deviation. Ion concentrations below detection limits are denoted by BDL and N/A denotes measurement was either not undertaken or not able to be undertaken.

Site	Depth from (m)	Depth to (m)	Sample no.	$\text{HCO}_3$ (mg kg $^{-1}$ )	F (mg kg $^{-1}$ )	Cl (mg kg $^{-1}$ )	Br (mg kg $^{-1}$ )	$\text{NO}_3$ (mg kg $^{-1}$ )	$\text{PO}_4$ (mg kg $^{-1}$ )	$\text{SO}_4$ (mg kg $^{-1}$ )
Two Deep	0.0	0.5	1	159	2.4	9	BDL	12.8	BDL	BDL
	0.5	1.0	3a		0.9	878	2.0	0.7	BDL	37
			3b		0.9	882	2.0	1.2	BDL	64
			3c		0.9	886	1.9	0.5	BDL	37
			3 (mean)		0.9 $\pm$ 0.0	882 $\pm$ 4	2.0 $\pm$ 0.0	0.8 $\pm$ 0.3	BDL	46 $\pm$ 16
	1.5	2.0	4	325	9.2	819	1.6	5.5	BDL	68
	4.0	4.5	9a	40	2.3	284	BDL	BDL	BDL	21
			9b		1.8	543	1.5	BDL	BDL	16
			9c		1.2	200	0.6	2.9	BDL	10
			9 (mean)		1.8 $\pm$ 0.6	343 $\pm$ 179	0.7 $\pm$ 0.7	1.0 $\pm$ 1.7	BDL	16 $\pm$ 5.2
Two Shallow	5.5	6.0	13	51	2.5	1151	2.6	1.7	BDL	61
	6.0	6.5	14	52	2.8	771	1.8	1.2	BDL	52
	7.5	8.0	18	58	2.6	495	BDL	8.0	BDL	37
	11.0	12.0	23	230	5.9	1017	2.3	13.0	BDL	82
Three	15.0	16.0	27	48	2.8	766	1.9	BDL	BDL	58
	0.0	1.0	28	116	3.8	725	1.6	1.8	BDL	88
	4.0	5.0	32	65	2.8	267	BDL	3.3	BDL	21
	7.0	7.5	35	40	3.4	949	2.4	BDL	BDL	73
Three	8.0	8.5	37	69	2.5	12	BDL	BDL	BDL	23
	0.0	0.5	38	342	13.9	19	BDL	BDL	BDL	37

Table A5.3 (b). Anion concentrations of select regolith samples from the Manobalai field site, with concentrations calculated as described in Eq. A5.1, where the mean of replicate samples is stated  $\pm$  the standard deviation. Ion concentrations below detection limits are denoted by BDL and N/A denotes measurement was either not undertaken or not able to be undertaken.

Site	Depth from (m)	Depth to (m)	Sample no.	HCO <sub>3</sub> (mg kg <sup>-1</sup> )	F (mg kg <sup>-1</sup> )	Cl (mg kg <sup>-1</sup> )	Br (mg kg <sup>-1</sup> )	NO <sub>3</sub> (mg kg <sup>-1</sup> )	PO <sub>4</sub> (mg kg <sup>-1</sup> )	SO <sub>4</sub> (mg kg <sup>-1</sup> )
Four	0.0	0.3	53	43	0.9	6	BDL	4.4	BDL	3
	5.5	6.0	64	0	4.0	572	1.3	BDL	BDL	51
	7.0	7.4	67	0	5.1	787	1.8	1.2	BDL	56
	8.0	8.5	70	69	4.4	740	1.8	3.8	BDL	50
	10.5	11.5	74	29	4.9	1227	2.4	28.5	BDL	123
	15.2	16.0	79	22	0.6	15	BDL	5.0	BDL	62
Five	0.0	0.5	80	36	4.0	40	BDL	BDL	BDL	12
	0.5	1.0	81	376	4.4	100	BDL	BDL	BDL	14
	1.0	1.5	83	47	BDL	BDL	BDL	3.1	BDL	5
Six	0.5	1.0	S33	2860	2.2	782	1.6	BDL	N/A	58
	1.0	1.5	S20	3380	2.4	956	2.1	0.6	N/A	46
	3.0	4.0	S34a	450	0.9	49	BDL	BDL	N/A	BDL
			S34b	N/A	2.0	510	1.3	BDL	N/A	15
			S34 (mean)	N/A	1.5 $\pm$ 0.8	279 $\pm$ 326	0.7 $\pm$ 0.9	BDL	N/A	7.4 $\pm$ 10.5
	5.0	6.0	S26a	1105	1.5	313	0.9	BDL	N/A	4.8
			S26b	N/A	1.4	284	0.9	BDL	N/A	3.6
			S26 (mean)	N/A	1.4 $\pm$ 0.1	298 $\pm$ 0.6	0.9 $\pm$ 0.0	N/A	N/A	4.2 $\pm$ 0.9
	7.5	9.0	S11	46	3.2	152	BDL	BDL	N/A	12

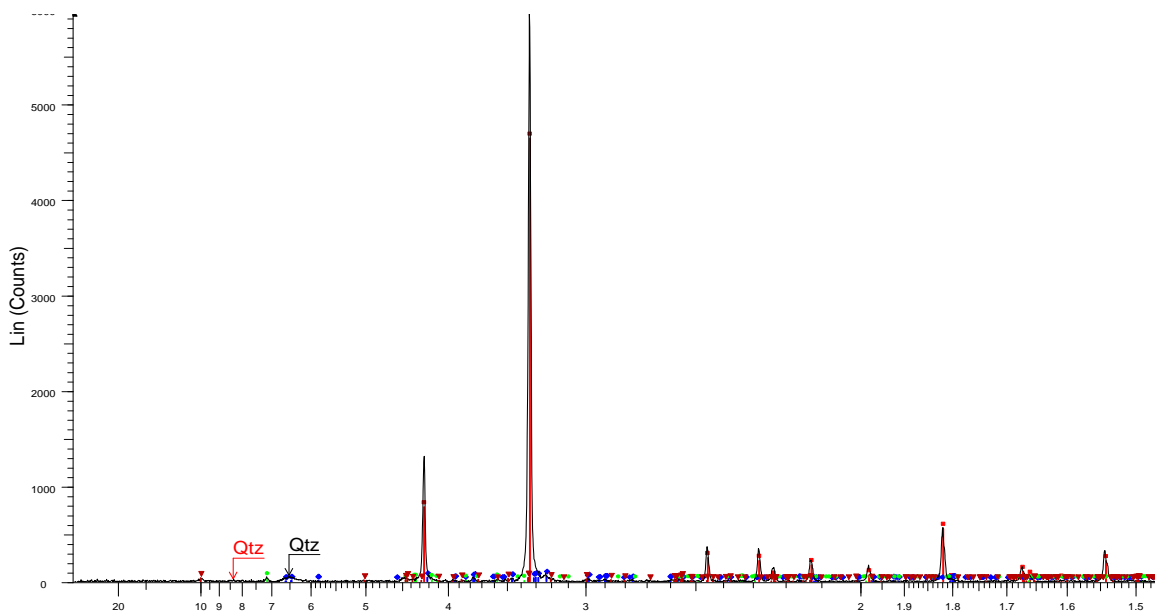


Figure A5.2. X-ray diffractometry results from 0.0-0.5 m at Site Two Deep. Symbols represent (●) Quartz ( $\text{SiO}_2$ ) (●); K-Feldspars; and (●) Kaolinite  $\text{Al}_2(\text{Si}_2\text{O}_5)(\text{OH})$ .

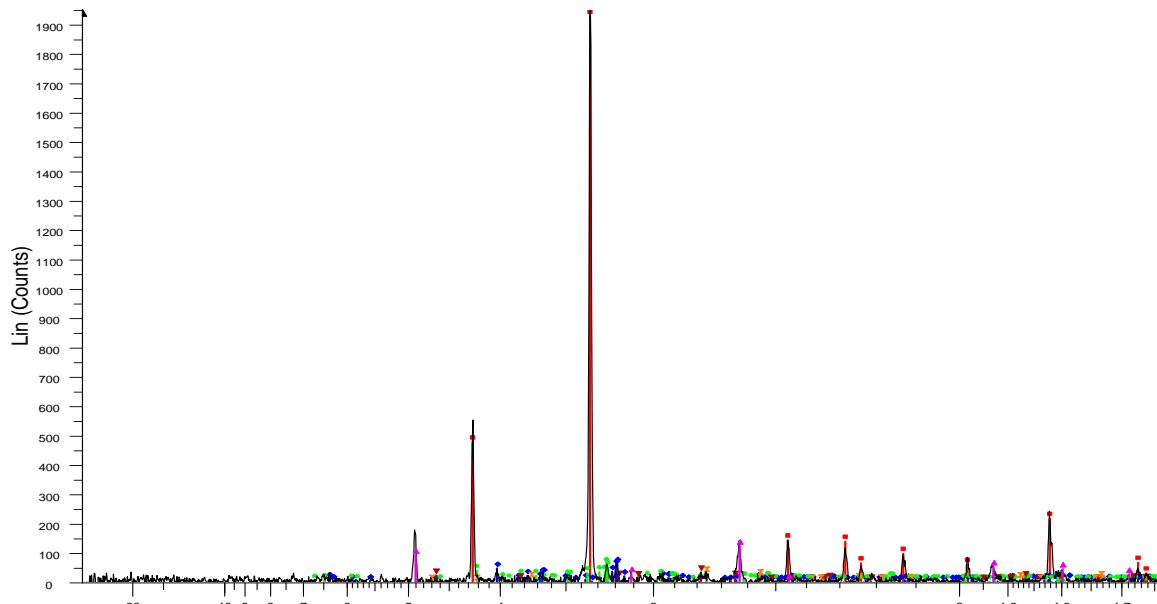


Figure A5.3. X-ray diffractometry results from 0.5-1.0m at Site Two Deep. Symbols represent (●) Quartz ( $\text{SiO}_2$ ); (●) Na-Plagioclase; (●) K-Feldspar; (●) Portlandite ( $\text{Ca}(\text{OH})_2$ ); (●) Thenardite ( $\text{Na}_2\text{SO}_4$ ); and (●) Illminite ( $\text{FeTiO}_3$ ).

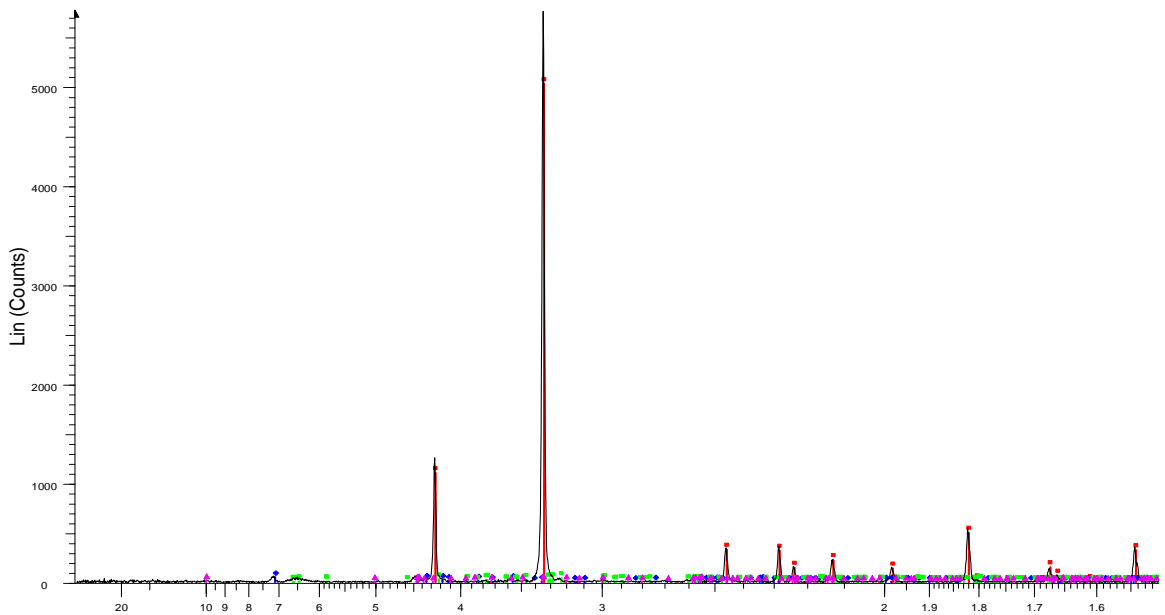


Figure A5.4. X-ray diffractometry results from 4.0-4.5m at Site Two Deep. Symbols represent (●) Quartz ( $\text{SiO}_2$ ) ; (●) K-Feldspars; (●) Kaolinite ( $\text{Al}_2(\text{Si}_2\text{O}_5)(\text{OH})$ ); and (●) Muscovite  $\text{KAl}_3\text{Si}_3\text{O}_{10}(\text{OH})_2$ .

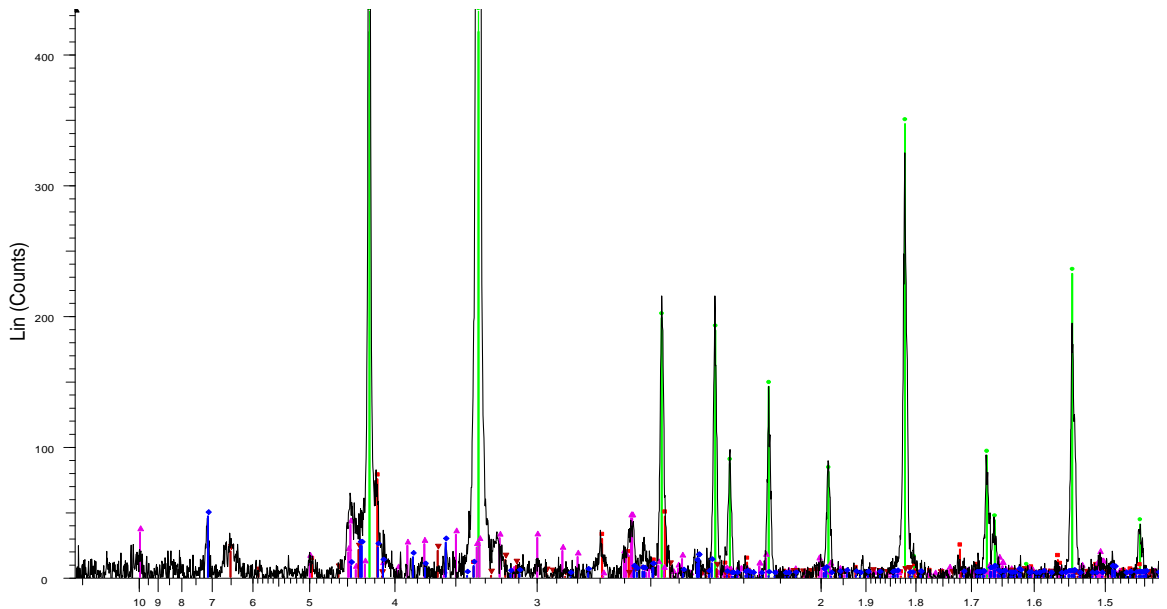


Figure A5.5. X-ray diffractometry results from 15.0-16.0m at Site Two Deep. Symbols represent (●) Kaolinite ( $\text{Al}_2(\text{Si}_2\text{O}_5)(\text{OH})$ ); (●) Quartz ( $\text{SiO}_2$ ) ; (●) Geothite ( $\text{FeO}(\text{OH})$ ); (●) Muscovite  $\text{KAl}_3\text{Si}_3\text{O}_{10}(\text{OH})_2$ ; and (●) Natrolite ( $\text{Na}_2(\text{Al}_{1.92}\text{Si}_{2.08})\text{SiO}_{10.04}(\text{H}_2\text{O})_{1.96}$ ).

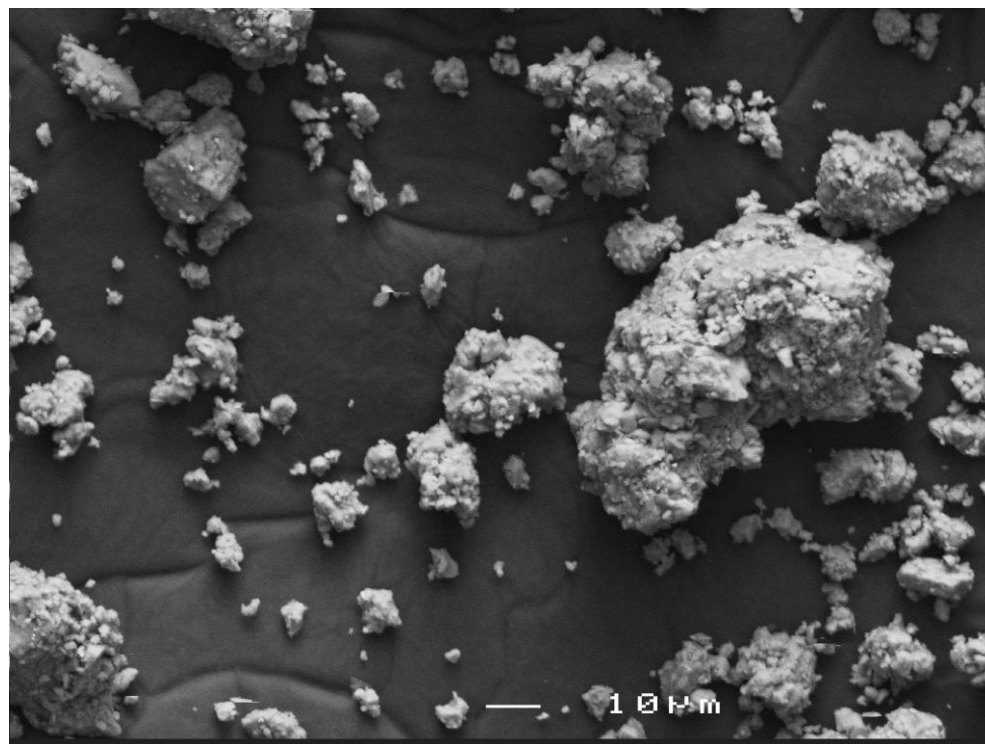


Figure A5.6. SEM image of subsample from the top 0.5m at Site Two Deep. Analyses showed that grains were sand ( $\text{SiO}_2$ ), with muscovite, microcline and illite coating the grains

---

## **Appendix for Chapter Six –**

*The hydrology and hydrogeology of Manobalai*



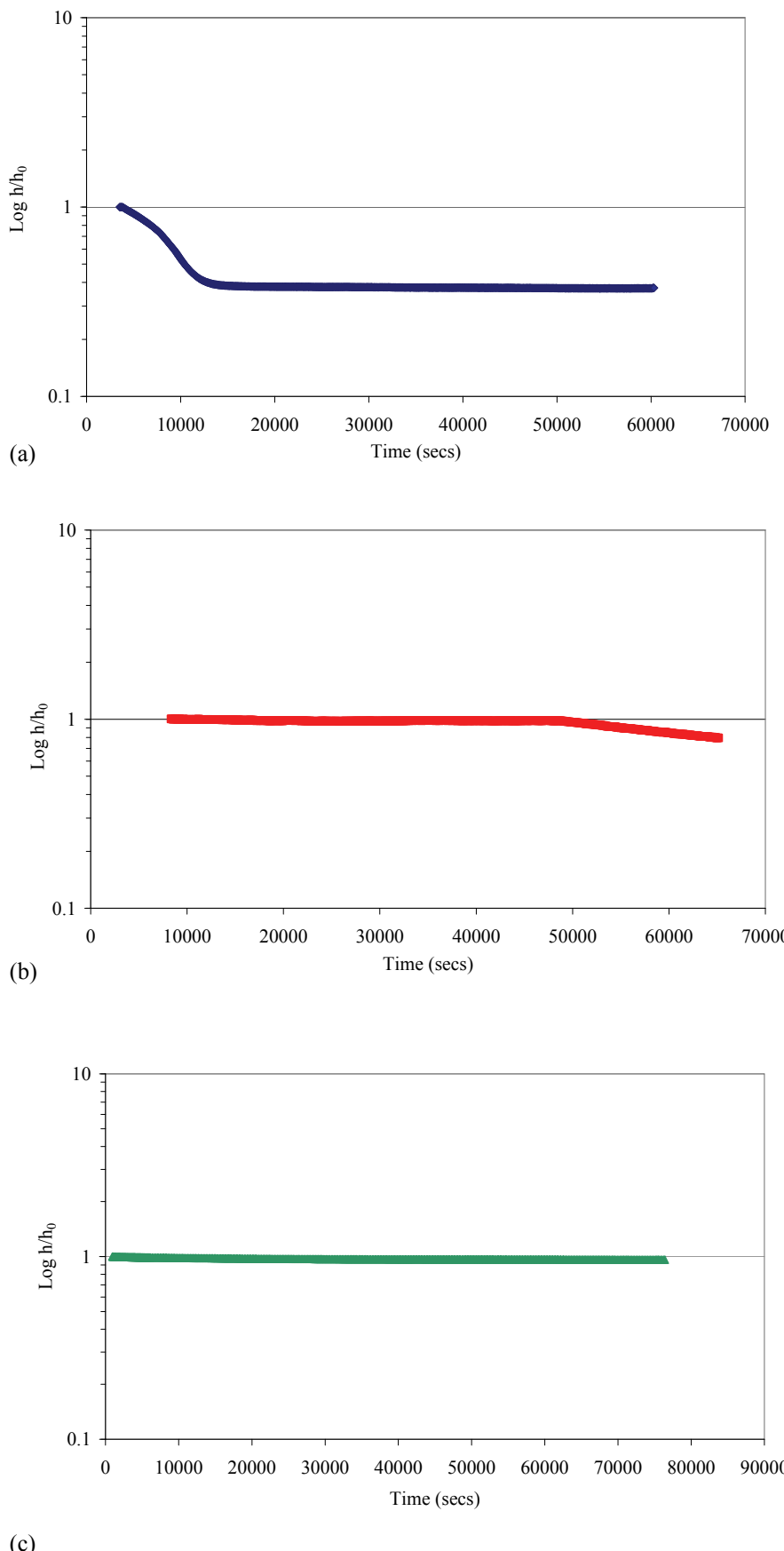


Figure A6.1 Slug test analysis using Hvorslev method for groundwater data on 14/07/2008. Sites depicted are: (a) One; (b) Two Shallow; and (c) Three.

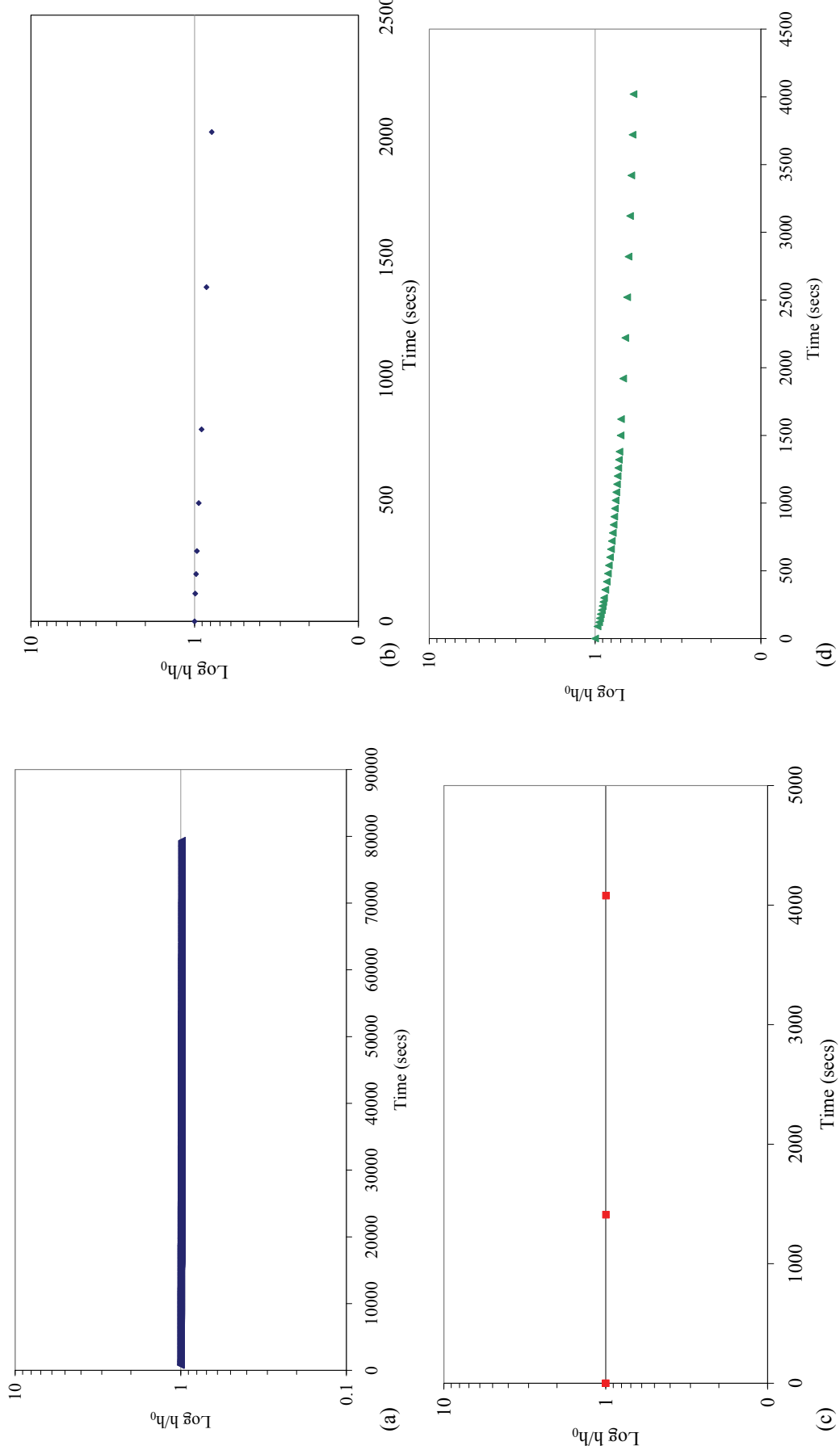


Figure A6.2. Slug test analyses using the Hvorslev method for sites (a) Four (14/07/2008); (b) Two Shallow (18/01/2009); (c) Two Deep (18/01/2009); and (d) Three (18/01/2009).

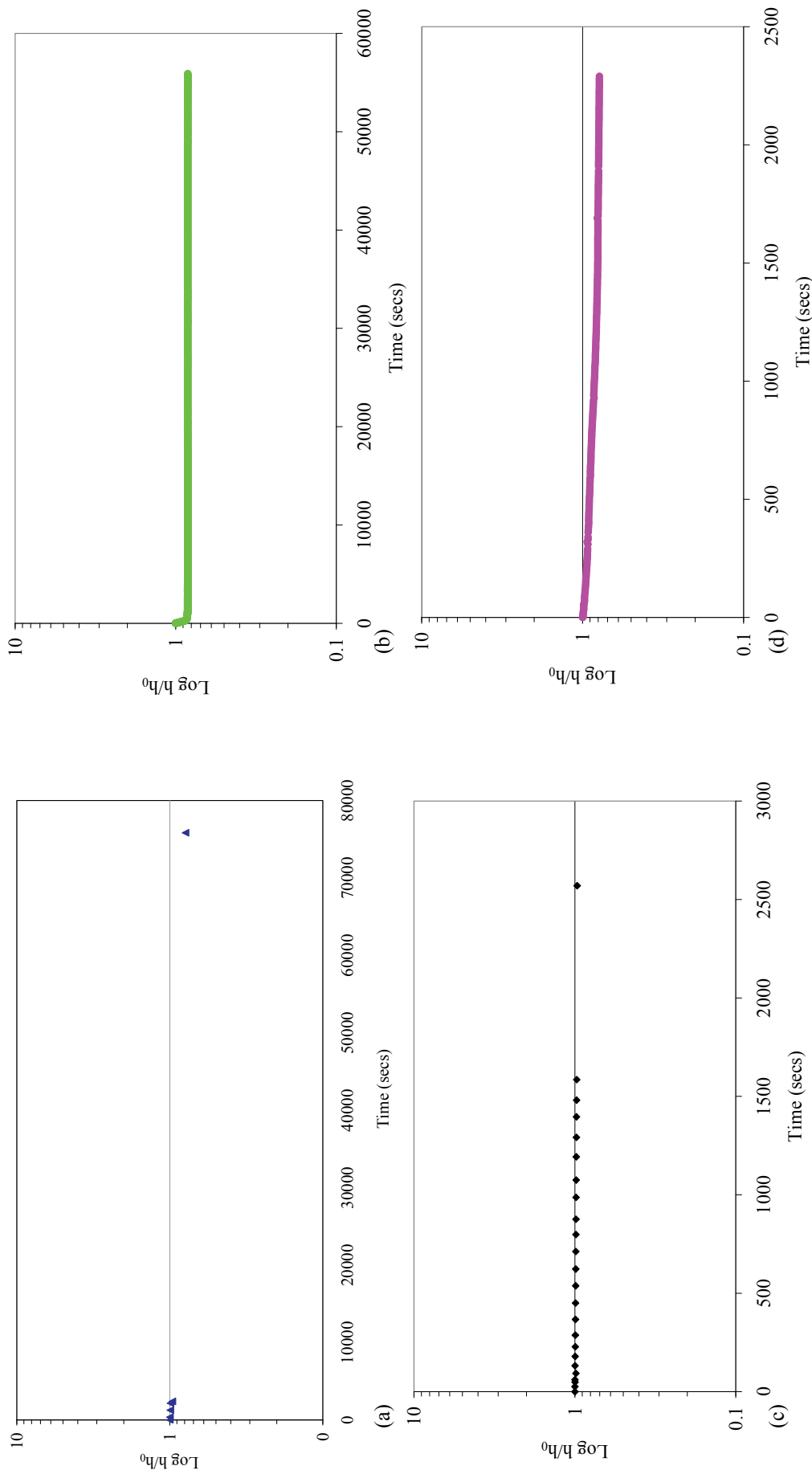


Figure A6.3 Slug test analyses using the Hvorslev method for sites (a) Four (18/01/2009); (b) Six (15/05/2009); (c) Eight Shallow (15/05/2009); and (d) Eight Fractured (15/05/2009).

Figure A6.3

The Cl load ( $S_{Cl}$ , t day $^{-1}$ ) delivered from each of the groundwater bodies was calculated using Eq. A6.2:

$$S_{Cl} = \frac{S_{Cl(60 \text{ km} - 55 \text{ km})}}{100\%} \times \% \text{ } Cl_{(fresh, saline)} \quad (\text{A6.1})$$

where  $S_{Cl(60 \text{ km} - 55 \text{ km})}$  is the measured increase in Cl (t day $^{-1}$ ) between the 55 km and 60 km surface water sample sites, and %  $Cl_{(fresh, saline)}$  is the percent Cl contributed to Wybung Creek from the fresh and saline groundwater bodies.

The calculations made in order to check these assumptions are shown below.

$$S_{TDS} = \frac{100\% \times S_{Cl(fresh, saline)}}{\% Cl_{(fresh, saline)}} \quad (\text{A6.2})$$

where the value of for percentage concentration of Cl relative to TDS (% Cl) for groundwater from Site Three and Woodlands Windmill was taken from Table 6.7, and the Cl load ( $S_{Cl site three, Woodlands}$ ) was calculated using Eq A6.1., and the salt load ( $S_{TDS}$ , t day $^{-1}$ ) was the contribution of solutes from the fresh and saline groundwater bodies.

Using the calculated total salt load ( $S_{TDS}$ , t day $^{-1}$ ) values for Site Three and Woodlands Windmill, and the proportion of major anions and cations relative to TDS measured in groundwater samples from these sites, the contribution of major cations and anions to the increase seen between the 55 km and 60 km sampling points could then be calculated using the values represented in Table 6.7 and Eq. A6.3.

$$S_{M^\pm} = S_{TDS} \times S_{M^\pm} \% \quad (\text{A6.3})$$

where the quantity of the cation or anions contributed to the stretch of water between the 55 km and 60 km sample sites is  $S_{M^\pm}$  (t day $^{-1}$ ), and  $S_{TDS}$  (t day $^{-1}$ ) is the value calculated using Eq. A6.2. The final results of this stage of the calculation are presented in Table 6.7.

After the first three of the four assumptions were met, the specific discharge ( $V_D$ , m sec $^{-1}$ ) necessary to give rise to the solute load delivered from the groundwater bodies represented by Site Three and Woodlands Windmill was calculated using Eq.A6.4 – A6.6:

$$V = \frac{S_{TDS} \times 10^9}{C_{(fresh, saline)}} \quad (\text{A6.4})$$

where the volume of water delivered to Wybung Creek from the fresh and saline groundwater bodies per day was  $V$  (L day $^{-1}$ ), the salt load was calculated in Eq. A6.2, and the concentration of solutes in each aquifer was  $C$  (mg TDS L $^{-1}$ ), with these values based on solute concentrations at Site Three and Woodlands Windmill. Discharge to Wybung Creek was then calculated using Eq. A6.5:

$$Q = \frac{V}{L/m^3} \quad (\text{A6.5})$$

where the discharge was  $Q$  ( $\text{m}^3 \text{ day}^{-1}$ ),  $V$  was calculated in Eq. A6.5, and  $L/m^3$  is a conversion between litres and cubic meters. Specific discharge was then calculated using Eq. A6.6:

$$V_D = \frac{Q}{A} \quad (\text{A6.6})$$

where area was  $A$  ( $\text{m}^2$ ) of the aquifers, which to be consistent with all other calculations needed to be between 76580 and 98460  $\text{m}^2$ . Discharge was calculated using Eq. A6.5. The hydraulic conductivity necessary for each of these aquifers to deliver these salt loads was calculated using Eq. A6.7:

$$K = \frac{V_D}{\left( \frac{dh}{dx} \right)} \quad (\text{A6.7})$$

where the hydraulic conductivity ( $K$ ,  $\text{m sec}^{-1}$ ) was based on the specific discharge calculated Eq A6.7 and measured values of hydraulic gradients  $\left( \frac{dh}{dx} \right)$  for Sites Three and the break of slope on the western side of Wybung Creek.

Table A6.1. Hydraulic conductivity calculated for piezometers at the Manobalai site on the 14<sup>th</sup>-17<sup>th</sup> of July, 2008. Hydraulic conductivity was calculated using the falling-head Bouwer and Rice slug test. All piezometers were fully penetrating with the exception of those indicated with the symbol † which were partially penetrating.

\*Static water level in this piezometer was below the piezometer screen, with K in this case an (over) estimate of the actual K. N/A indicates this constant was not necessary for calculation of K.

Site	$y_0$ (m)	$y_t$ (m)	$t$ (s)	$r_c$ (m)	$L_e$ (m)	$R_w^2$ (m)	$L_e/R_w$	$h$ (m)	$L_w$ (m)	$A$	$B$	$C$	$\ln(-\frac{R_e}{R_w})$ (m s <sup>-1</sup> )	$K$
One	2.1	2.0	57381	0.625	2	0.063	32	0.7	0.70	N/A	N/A	1.0	0.49	$4.1 \times 10^{-8}$
†Two Deep	15.7	15.5	57895	0.625	15	0.063	240	17	1.00	2.0	0.5	N/A	0.44	$1.3 \times 10^{-9}$
†Two Shallow	8.6	3.2	29785	0.625	8	0.063	128	17	6.39	2.0	0.5	N/A	0.24	$2.8 \times 10^{-7}$
Three	6.4	6.2	14841	0.625	2	0.063	32	0.4	*0.63	N/A	N/A	1.0	0.51	$1.1 \times 10^{-7}$
Four	16.2	16.0	41135	0.625	16	0.063	256	1.0	1.01	N/A	N/A	1.5	0.40	$1.5 \times 10^{-9}$

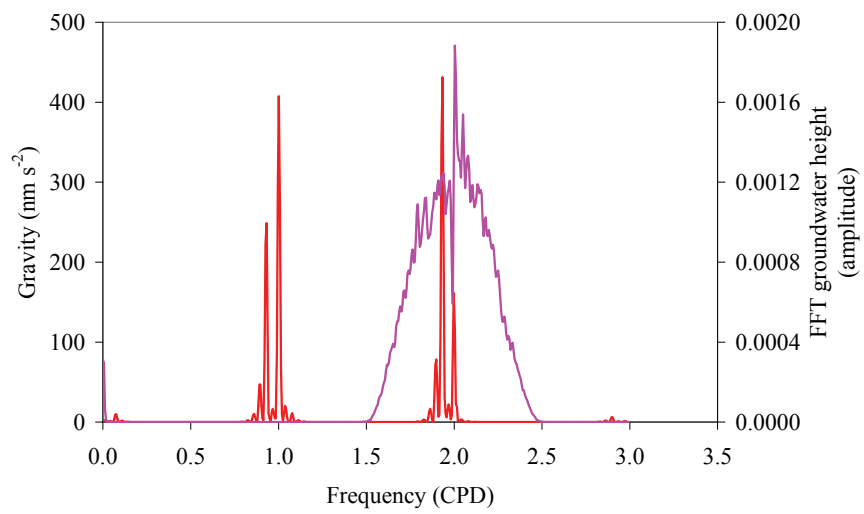
Table A6.2. Hydraulic conductivity calculated for piezometers at the Manobalai site on the 17th-21st of January, 2009. Hydraulic conductivity was calculated using the Bouwer and Rice slug test, with <sup>R</sup> measurements based on a rising head slug test and <sup>F</sup> based on a falling head slug test. All piezometers were fully penetrating with the exception of those indicated with the symbol  $\dagger$  which were partially penetrating. \*Static water level in this piezometer screen, with hydraulic conductivity (K) in this case an (over) estimate of actual K. N/A indicates this constant was not necessary for calculation of K.  $y_0$  = initial depth to water;  $y_t$  = displacement at time t;  $t$  = time where  $y_t$  is measured;  $r_c$  = radius of casing where the rise of water level is measured;  $L_e$  = length of well screen plus any packing materials;  $R_w$  = effective radius of piezometer;  $h$  = depth from bedrock to water table;  $L_w$  = length from bottom of screen to water table; and  $R_e$  = effective distance over which the head displacement dissipates. A, B and C are dimensionless numbers plotted as a function of  $L_e/R_w$ .

Site	$y_0$ (m)	$y_t$ (m)	$t$ (s)	$r_c$ (m)	$L_e$ (m)	$R_w^2$ (m)	$L_e/R_w$	$h$ (m)	$L_w$ (m)	A	B	C	$\ln\left(\frac{R_e}{R_w}\right)$ (m s <sup>-1</sup> )	K (m s <sup>-1</sup> )
<sup>R</sup> $\dagger$ Two Deep	0.6	0.1	1410	0.625	15	0.0625	240	17	0.98	2.0	0.5	N/A	2.2	$7.6 \times 10^{-6}$
<sup>R</sup> $\dagger$ Two Shallow	0.1	7.8	488	0.625	8	0.0625	128	17	6.39	2.0	0.5	N/A	3.0	$7.4 \times 10^{-5}$
<sup>F</sup> Three	2.15	2.82	700	0.625	2	0.0625	32	0.4	*0.63	N/A	1.0	2.0	$1.9 \times 10^{-5}$	
<sup>R</sup> Four	0.02	9.05	2160	0.625	16	0.0625	256	1.01	1.01	N/A	1.5	2.5	$1.4 \times 10^{-5}$	

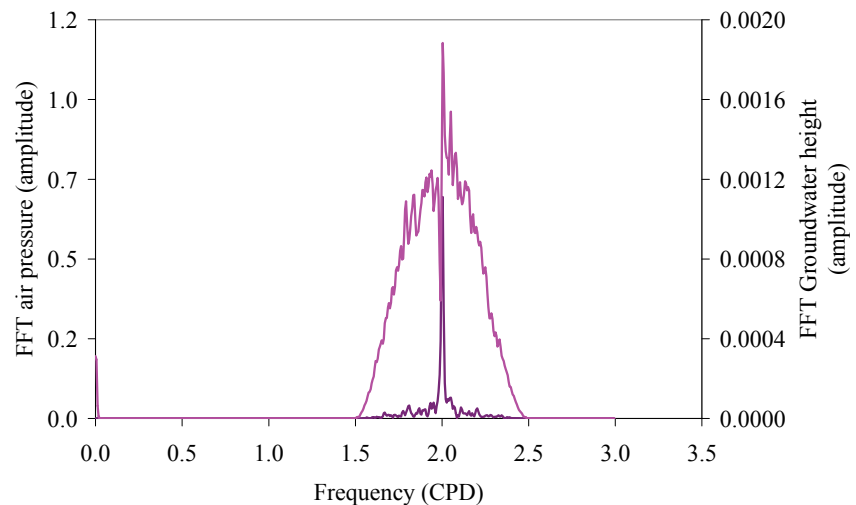
Table A6.3.

Hydraulic conductivity calculated for select piezometers at the Manobalai site on the 14<sup>th</sup> of May 2009. Hydraulic conductivity was calculated using falling-head Bouwer and Rice slug tests. Piezometers were fully penetrating with the exception of that indicated by the symbol † which was partially penetrating. N/A indicates this constant was not necessary for calculation of  $K$ .  $y_0$  = initial depth to water;  $y_t$  = displacement at time  $t$ ;  $t$  = time where  $y_t$  is measured;  $r_c$  = radius of casing where the rise of water level is measured;  $L_e$  = length of well screen plus any packing materials;  $R_w$  = effective radius of piezometer;  $h$  = depth from bedrock to water table;  $L_w$  = length from bottom of screen to water table; and  $R_e$  = effective distance over which the head displacement dissipates. A, B and C are dimensionless numbers plotted as a function of  $L_e/R_{wp}$ .

Site	$y_0$ (m)	$y_t$ (m)	$t$ (secs)	$r_c$ (m)	$L_e$ (m)	$R_w^2$ (m)	$L_e/R_w$	$h$ (m)	$L_w$ (m)	$A$	$B$	$C$	$\ln(\frac{R_e}{R_w})$ (m s <sup>-1</sup> )	$K$
†Six	11.5	1.60	575	0.63	0.5	0.063	7.9	3.40	2.92	1.0	0.5	N/A	0.670	$9.1 \times 10^{-4}$
Eight (Shallow)	7.7	7.62	287	0.63	1.5	0.063	23.8	0.79	0.79	N/A	N/A	2.5	2.541	$1.6 \times 10^{-6}$
Eight (Fractured)	9.4	8.42	570	0.63	1.5	0.063	23.8	0.82	2.85	N/A	N/A	2.5	1.850	$1.0 \times 10^{-5}$



(a)



(b)

Figure A6.4 Spectral analyses of relationships between hydraulic head at the Site Eight Fractured (—), (a) gravity (—); and (b) air pressure (—).

Table A6.4 Correlation coefficients for the relationship between water height in site two shallow and rainfall at the Scone weather station. Results which were significant at the 95% confidence level are indicated in bold.

Lag (days)	Cross-correlation coefficient	Level of significance (95%)
-29	0.003373	0.099015
-28	0.014431	0.099136
-27	0.003050	0.099258
-26	0.026039	0.099381
-25	-0.032831	0.099504
-24	0.002968	0.099627
-23	0.003926	0.099751
-22	-0.020441	0.099875
-21	-0.004459	0.100000
<b>-20</b>	<b>0.108981</b>	<b>0.100125</b>
-19	-0.112542	0.100251
-18	-0.011618	0.100377
-17	-0.005573	0.100504
-16	-0.000343	0.100631
-15	-0.018647	0.100759
-14	-0.016730	0.100887
-13	0.014529	0.101015
-12	0.004612	0.101144
-11	-0.005979	0.101274
-10	0.161289	0.101404
-9	-0.207977	0.101535
-8	-0.044108	0.101666
-7	-0.008473	0.101797
-6	0.011165	0.101929
-5	0.008847	0.102062
-4	-0.000078	0.102195
-3	0.007554	0.102329
-2	-0.004292	0.102463
-1	-0.012408	0.102598
0	0.022921	0.102733
1	0.009696	0.102869
2	-0.009255	0.103005
3	0.025968	0.103142
<b>4</b>	<b>0.128485</b>	<b>0.103280</b>
5	-0.034753	0.103418
6	-0.036828	0.103556
7	-0.036190	0.103695
8	-0.048138	0.103835
9	-0.028111	0.103975
10	-0.008222	0.104116
11	0.010763	0.104257
12	0.009198	0.104399
13	-0.002634	0.104542
14	-0.010444	0.104685
15	0.006863	0.104828
16	0.005163	0.104973
17	0.049011	0.105118
18	-0.016471	0.105263
19	-0.050164	0.105409
20	-0.025025	0.105556
21	-0.005451	0.105703
22	0.002201	0.105851
23	0.102732	0.106000
24	-0.040593	0.106149
25	-0.017261	0.106299
26	-0.057836	0.106449
<b>27</b>	<b>0.238610</b>	<b>0.106600</b>
28	-0.293030	0.106752
29	0.014430	0.106904

Table A6.5 Correlation coefficients for the relationship between water height in site two deep and rainfall at the Scone weather station. Results which were significant at the 95% confidence level are indicated in bold.

Lag (days)	Cross-correlation coefficient	Level of significance (95%)
-27	0.009387	0.108148
-26	0.005494	0.108306
-25	0.006899	0.108465
-24	0.004058	0.108625
-23	0.008354	0.108786
-22	0.036945	0.108947
-21	0.002706	0.109109
-20	0.005401	0.109272
-19	0.006036	0.109435
-18	0.005248	0.109599
-17	0.011299	0.109764
<b>-16</b>	<b>0.110951</b>	<b>0.109930</b>
-15	0.005638	0.110096
-14	0.006037	0.110264
-13	0.007742	0.110432
-12	0.017684	0.110600
-11	-0.021949	0.110770
-10	-0.022048	0.110940
-9	-0.030692	0.111111
-8	0.002106	0.111283
-7	0.002468	0.111456
<b>-6</b>	<b>0.182688</b>	<b>0.111629</b>
-5	0.006559	0.111803
-4	0.011057	0.111979
-3	0.011939	0.112154
-2	0.006706	0.112331
-1	0.004040	0.112509
0	0.013098	0.112687
1	-0.036657	0.112867
2	0.006930	0.113047
3	-0.004297	0.113228
4	0.005418	0.113410
5	0.005998	0.113592
6	-0.007422	0.113776
7	0.000684	0.113961
8	0.053762	0.114146
9	0.011898	0.114332
10	-0.013148	0.114520
11	0.005475	0.114708
12	0.007100	0.114897
13	-0.003986	0.115087
14	0.011334	0.115278
15	0.012822	0.115470
16	0.006169	0.115663
17	0.006648	0.115857
18	0.005397	0.116052
19	0.005480	0.116248
20	0.004204	0.116445
21	0.007924	0.116642
22	0.013997	0.116841
23	0.010871	0.117041
24	0.013968	0.117242
25	-0.173000	0.117444
26	0.001356	0.117647
27	0.105092	0.117851